Luciferase complementation for the determination of arrestin recruitment: Investigations at histamine and NPY receptors

Dissertation

Zur Erlangung des Doktorgrades der Naturwissenschaften (Dr. rer. Nat.)

an der Fakultät für Chemie und Pharmazie der Universität Regensburg

vorgelegt von

Johannes Felixberger

aus Hebertsfelden

2014

Die vorliegende Arbeit entstand in der Zeit von Juni 2010 bis November 2014 unter der Anleitung von Herrn Prof. Dr. Armin Buschauer am Institut für Pharmazie der Naturwissenschaftlichen Fakultät IV – Chemie und Pharmazie – der Universität Regensburg.

Das Promotionsgesuch wurde eingereicht im Dezember 2014.

Tag der mündlichen Prüfung: 30.01.2015

Prüfungsausschuss: Prof. Dr. S. Elz (Vorsitzender)
Prof. Dr. A. Buschauer (Erstgutachter)
Prof. Dr. G. Bernhardt (Zweitgutachter)
Prof. Dr. J. Wegener (Drittprüfer)

für meinen Vater

Danksagung

An dieser Stelle möchte ich mich bei allen bedanken, die zum Gelingen dieser Doktorarbeit beigetragen haben. Mein besonderer Dank gilt:

Prof. Dr. A. Buschauer für die Möglichkeit, dieses interessante und herausfordernde Thema zu bearbeiten, für seine wissenschaftliche Anleitung und die Unterstützung bei der Durchsicht dieser Arbeit.

Prof. Dr. G. Bernhardt für seine Unterstützung und Anregung bei allen experimentellen und fachlichen Problemen und seine konstruktive Kritik bei der Durchsicht dieser Arbeit, sowie die einmaligen Sommerfeste.

Prof. Dr. J. Wegener für die Teilnahme an der Promotionsprüfung als Drittprüfer.

Prof. Dr. S. Elz für die Übernahme des Vorsitzes bei der Promotionsprüfung.

Prof. Dr. T. Ozawa und Dr. M. Tanaka (Department of Chemistry, School of Science, The University of Tokyo, Japan) für die Bereitstellung der Expressionsvektoren zur Etablierung des Arrestin-Rekrutierungs-Assays.

Dr. R. Lane (Faculty of Pharmacy and Pharmaceutical Sciences, Monash University, Melbourne, Australien) für die Hilfe bei der Datenanalyse und der Anwendung des „Operational Model“.

Prof. Dr. J. Schlossmann für die Möglichkeit zur Nutzung des ChemiDoc Imaging Systems sowie des Radioaktivlabors.

Prof. Dr. Roland Seifert (Institute für Pharmakologie, Medizinische Hochschule Hannover) für die Bereitstellung der Baculovirus Stocklösungen und die anregenden Diskussionen über funktionelle Selektivität an GPCRs.

Dr. B. Striegl, Dr. M. Kunze und PD. Dr. A. Strasser für die Bereitstellung der H_1R Liganden.

PD. Dr. A. Strasser für die Durchführung der GTPase Experimente am H_1R und die Hilfe bei der Zusammenstellung der Ligandenauswahl für die Untersuchungen am H_1R.

Dr. A. Spickenreiter, Dr. T. Birnkammer, Dr. P. Baumeister, N. Plank, S. Biselli und Dr. D. Erdmann für die Bereitstellung der H_2R Liganden.

Dr. P. Baumeister, Dr. R. Geyer, Dr. P. Igel, Dr. A. Spickenreiter und Dr. S. Gobleder für die Bereitstellung der H_4R Liganden.

Prof. Dr. Holger Stark (Institute für Pharmazie und medizinische Chemie, Johann Wolfgang Goethe University, Frankfurt am Main) für die Bereitstellung der H_4R Liganden ST-1006 und ST-1012.

Dr. U. Nordemann für die Durchführung der Luciferase-Genreporter Experimente am H_4R.

Prof. Dr. Chiara Cabrele (Institut für Molekularbiologie, Universität Salzburg, Österreich) und S. Dukorn für die Bereitstellung der Peptidliganden.

Dr. M. Keller und Dr. S. Weiß für die Bereitstellung der Y_1R Liganden.

Dr. N. Pluym, K. Kuhn und Dr. P. Baumeister für die Bereitstellung der Y_2R Liganden.

S. K. Jaiswal für die Unterstützung bei der Durchführung der GTPγS Experimente am H_2R und allen andere Forschungs- und Wahlpflichtpraktikanten für die Unterstützung bei der Laborarbeit.

M. Beer-Krön für ihre Hilfsbereitschaft in allen Belangen, die Unterstützung bei der Durchführung der Luciferase-Genreporter Experimente, sowie die phänomenale Bayrisch-Creme und die konstante Versorgung mit Süßigkeiten.

B. Wenzl für die Vorbereitung des Biochemiepraktikums und die Durchführung der Mycoplasmentests.

P. Richthammer für seine Hilfe bei technischen Problemen und der Wartung von Geräten.

E. Schreiber für die Hilfe bei der Zellkultur und die Durchführung der Calcium-Assays.

K. Reindl, U. Hasselmann und S. Heinrich für die Unterstützung bei allen organisatorischen Angelegenheiten.

N. Plank, S. Huber, Dr. U. Nordemann und allen anderen Bürokollegen für die hervorragende Atmosphäre im Büro, die gegenseitige Unterstützung und die Aufheiterung wenn mal wieder nichts funktioniert hat.

P. Baumeister, S. Huber und N. Plank für die Hilfe bei der Korrektur und die fachlichen Unterstützung beim Zusammenschreiben der Doktorarbeit.

Allen derzeitigen und ehemaligen Kollegen für die gegenseitige Unterstützung, die gute Atmosphäre im Labor und die lustigen Feste.

Meiner Familie, meiner Freundin Franziska und allen Freunden für den Rückhalt und die tatkräftige Unterstützung.

Contents

Chapter 1

Introduction

1. Introduction

1.1. G-Protein Coupled Receptors

G-protein coupled receptors (GPCRs) represent the largest and most diverse superfamily of membrane receptors. There are approximately 800 genes in the human genome encoding GPCRs, accounting for roughly 3 % of the transcribed genes.[1-3] Thereof, a large portion comprises chemoreceptors, involved in taste and smell perception, whereas ~360 receptors are targeted by endogenous ligands.[4] The latter GPCRs are one of the most important targets for drug discovery, and currently, approximately 30 % of the marketed drugs are associated with GPCRs.[5] Despite their importance, the majority of these approved drugs addresses only a small fraction of the "drugable" GPCRs, leaving a large untapped potential for future discoveries.[5]

1.1.1. Classification

Today, the common system for the classification of GPCRs follows the so-called GRAFS system introduced by Fredriksson *et al.* in 2003.[4] It divides the GPCR superfamily into five phylogenetic classes, named glutamate, rhodopsin, adhesion, frizzled/taste2 and secretin receptor family.[4] The receptor classification of the International Union of Pharmacology (IUPHAR) is largely consistent with the GRAFS system, containing five classes, class A (rhodopsin), class B (secretin), class C (glutamate) and the Adhesion and Frizzled class (http://www.guidetopharmacology.org/).

Class A (rhodopsin family) is the largest family of GPCRs, containing roughly 670 receptors subdivided into four groups, designated α to δ.[4] The receptors of this class are highly diverse with regard to structure and the nature of their natural ligand, including peptides, small molecules like amines, nucleosides and lipids or odorants in case of the olfactory receptors. Class B (secretin family) is a small family of peptide hormone receptors, including the calcitonin and glucagon receptors. Class C (glutamate family) contains the metabotropic glutamate and GABA receptors, the Frizzled class consists of the ten frizzled receptors, binding the family of Wnt glycoproteins, as well as the smoothened receptor.[6,7] The Adhesion class is the second largest GPCR family. Although it shares similarities with the class B receptors, it is poorly understood.

As the histamine and neuropeptide Y receptors covered in this thesis all belong to the Class A of rhodopsin like GPCRs, the following paragraphs on receptor structure, signaling and regulation will focus solely on this family.

1.1.2. Protein structure

The general architecture of GPCRs can be divided into three parts, the extracellular region, comprised of the N-terminus and the three extracellular loops (ECL1-3), a membrane domain consisting of the seven transmembrane helices and the intracellular region, consisting of the three intracellular loops (ICL1-3) and the C-terminus (cf. Fig. 1-1).[8] In principle, the extracellular domain conveys ligand access and specificity, the transmembrane domain relays the extracellular signal to the intracellular domain that then transduces the signal on to the cellular signaling machinery.[8]

Our understanding of GPCR architecture and function was greatly facilitated by the availability of high-resolution crystal structures. In 2000, Palczewski *et al.* had published the structure of bovine rhodopsin (Fig. 1-1),[9] long before the first structure of a nonvisual GPCR, the β_2 adrenergic receptor was resolved in 2007.[10-13] Since then, improvements in protein engineering and crystallography techniques resulted in an increasing number of solved structures.[8] In 2011, the first structure of an active receptor in complex with the G_α protein gave insight into the mechanisms of receptor-G-protein interaction.[13]

The general 7TM architecture was confirmed by the available crystal structures, with the transmembrane domains arranged in a counter clockwise manner, and an intracellular helix H8 running parallel to the plasma membrane.[14] The available class A receptor structures reveal two distinct types of the extracellular domains, that either occlude the

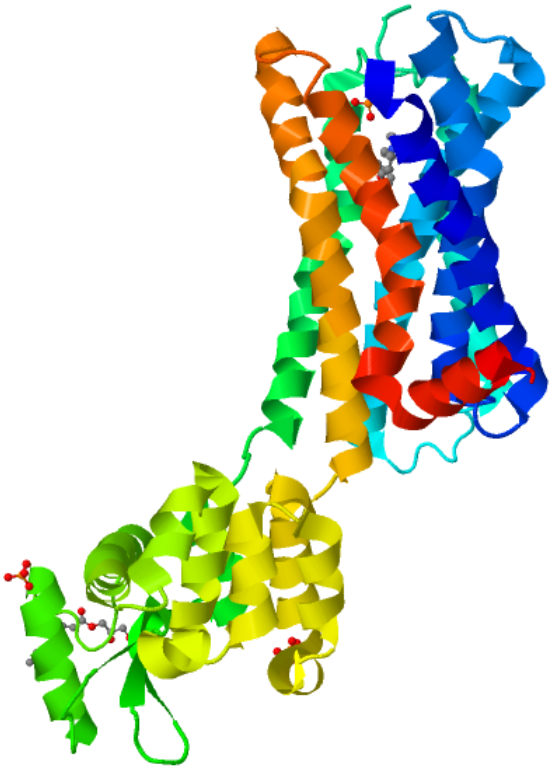

Fig. 1-1: 3D model of the histamine H_1 receptor in complex with doxepin and a T4L insertion into the third ICL. The seven transmembrane helices are depicted in blue (TM1) through red (TM7) (adapted from Shimura *et. al.* 2011).[15]

ligand binding pocket or leave it water accessible.[8,15] In rhodopsin, the N-terminus and the ECL2 fold into β-hairpin loops, forming a lid for the binding pocket.[9] Such a lid is also present in other receptors addressed by lipophilic ligands.[16] In receptors of hydrophilic ligands, the ECL2 structure is diverse, but in most cases, ECL2 is believed to play a role in initial ligand binding and in guiding the ligand to the binding pocket.[8,17] ECL1 and ECL3 are much shorter than ECL2 and generally lack distinct structural features.

By contrast to the extra- and intracellular domains, the transmembrane domains of class A GPCRs show a higher similarity amongst the different receptor structures.[18] Two of the most prominent conserved features are the so-called E(D)R$^{3.50}$Y and NP$^{7.50}$xxY(x)$_{5,6}$F motifs (superscripts according to the Ballesteros–Weinstein numbering[19]). The E(D)R$^{3.50}$Y motif is part of a hydrogen bonding network between TM3 and TM6, the so-called ionic lock, that stabilizes the receptor in its inactive conformation.[14,20] Of the NP$^{7.50}$xxY(x)$_{5,6}$F motif, Asn$^{7.49}$ is part of a hydrogen bonding network between TM1, TM2 and TM7, while the Y(x)$_{5,6}$F submotif constrains the TM7-H8 microdomain.[14] Another feature, with implications on receptor stability, is the conserved disulfide bridge between Cys$^{3.25}$ (inTM3) and a cysteine residue in the ECL2, anchoring the helix near the ligand binding site, thereby limiting conformational flexibility during receptor activation.[9,14]

The intracellular domain of the receptor is responsible for coupling to cellular effectors, like G-proteins, G-protein receptor kinases (GRKs) and arrestins. ICL1 is approximately six amino acids long and contains a helical turn, while ICL2 usually comprises one or two α-helical turns.[8] Most receptors contain an additional short aliphatic helix H8 close to the C-terminus.[8] In the active receptor, ICL2 interacts with the N-terminus of the G-protein[13], and H8 is involved in initial G-protein recruitment. On the other hand, in many GPCRs, ICL3 and the C-terminus are long and intrinsically disordered, containing linear peptide motifs responsible for the formation and specificity of various protein-protein interactions.[8,21]

1.2. G-Protein signaling

The most prominent unifying feature of the GPCR superfamily is the ability to couple to and to activate heterotrimeric G-proteins, although this paradigm was attenuated by the inclusion of receptors like members of the frizzled class, that signal exclusively through other pathways.[22] In their inactive form, the G-proteins are heterotrimers, composed of the G$_\alpha$ subunit that contains the GTPase active site, and the tightly bound G$_{\beta\gamma}$ heterodimer. Agonist-induced conformational changes of the receptor trigger an interaction with the inactive, GDP bound form of the heterotrimeric G-protein, leading to the formation of the so-called ternary complex. Then, the active receptor acts as a guanine-nucleotide exchange factor (GEF) on the G-protein, stimulating the exchange of GDP for GTP by the G$_\alpha$ subunit. The associated conformational changes lead to the release of the heterotrimeric G-protein from the receptor, and, subsequently, to the dissociation of the α subunit from the G$_{\beta\gamma}$ dimer. Subsequently, the G$_\alpha$ subunit and, to a lesser extent, the G$_{\beta\gamma}$ dimer interact with a multitude of signal effector proteins, activating distinct signaling cascades. Upon hydrolysis

of the bound GTP, the G_α subunit is inactivated, leading to its reassociation with the $G_{\beta\gamma}$ dimer.

In mammals, 16 known genes encode different G_α subunits; furthermore there are 5 genes for the G_β subunit and 12 for the G_γ subunit.[23] Receptor specificity of the heterotrimeric G-protein is mainly procured by the G_α subunit, although it has been shown that association with different $G_{\beta\gamma}$ dimers influences receptor coupling.[24] Mutational studies and investigations using G_α chimeras revealed that the extreme C-terminal domain of G_α plays a crucial role in receptor recognition.[24] In the inactive trimeric form of the G-protein, $G_{\beta\gamma}$ functions as a guanine nucleotide dissociation inhibitor (GDI), increasing the affinity of G_α for GDP.[25]

The heterotrimeric G-proteins are grouped into four families, based on sequence homologies and functional similarities of the different G_α subunits. The $G_{\alpha S}$ family includes $G_{\alpha s}$, expressed as long and short splice variants, as well as the olfactory α subunit, $G_{\alpha olf}$.[22] These G_α subunits signal through activation of membrane-bound adenylate cyclases (ACs).[26] The $G_{\alpha i}$ family is composed of the AC inhibiting subunits $G_{\alpha i1}$ $G_{\alpha i2}$ $G_{\alpha i3}$ and $G_{\alpha o}$, furthermore the retinal α subunit, transducing or $G_{\alpha T}$, as well as $G_{\alpha gust}$ and $G_{\alpha z}$.[22,26] The $G_{\alpha q}$ family comprises $G_{\alpha q}$ and $G_{\alpha 11}$ as well as $G_{\alpha 14}$ and $G_{\alpha 15}$, all activating the phospholipases Cβ1-3 (PLCβs).[27] The residual G_α family includes $G_{\alpha 12}$ and $G_{\alpha 13}$, that primarily signal through the small GTPase Rho.[28] In addition to the G_α mediated signaling, it has been demonstrated that the $G_{\beta\gamma}$ dimer, formerly considered a mere negative regulator of G_α, modulates a vast array of signaling effectors.[25] These include canonical G_α pathways involving ACs and PLCs, but also novel $G_{\beta\gamma}$ interaction partners such as kinases or GEFs.[25,26,29-31]

Adenylate cyclases, catalyzing the formation of the second messenger cyclic-adenosine-3',5'-monophosphate (cAMP), represent one of the most important classes of G-protein signaling effectors. There are 9 different mammalian isoforms of membrane-bound ACs, differing in their susceptibility to individual G_α and $G_{\beta\gamma}$ subunits, as well as in G-protein independent regulation mechanisms.[26,32] AC activation leads to a rise in the cytosolic cAMP concentration, that subsequently activates protein kinase A (PKA).[33] The activated PKA modulates via phosphorylation a plethora of downstream effectors, including metabolic enzymes, small G-proteins and, most importantly, the transcription factor cAMP-response element-binding protein (CREB) i.e. inducing the transcription of gene under control of the cAMP response element promoter (CRE).[33,34] In the cell, cAMP levels are carefully controlled by the regulation of its synthesis catalyzed by ACs and its degradation mediated by phosphodiesterases (PDE), both enzymes regulated by PKA in a feedback mechanism.[34]

The phospholipases Cβ, the second main class of G-protein effectors, catalyze the hydrolysis of phosphatidylinositol-4,5-bisphosphate yielding the two second messengers diacylglycerol (DAG) and inositol-1,4,5-trisphosphate (IP_3).[27] The four mammalian isoforms of PLCβ are all activated by the $G_{\alpha q}$ family, but differ in their regulation mechanisms and their susceptibility to different $G_{\beta\gamma}$ dimers.[35] IP_3 mainly acts through activation of the inositolphosphate receptor, a Ca^{2+} channel located primarily in membrane of the endoplasmatic reticulum (ER), resulting in an increase in the intracellular (cytosolic) calcium

concentration.[36] Calcium is a ubiquitous cellular effector that signals through sensors like troponin C (TnC) and calmodulin (CAM), subsequently modulating the activity of various signaling proteins, including Ca^{2+}/calmodulin dependent protein kinases (CAMK), protein kinase C (PKC) and several transcription factors.[37] DAG is the second effector produced by PLCβ that, besides activating PKC, interacts with a separate set of six distinct protein families, sharing a C1 domain for DAG recognition, including protein kinase D (PKD), the DAG kinases and the MRCK family.[38,39]

The broad variety of G-protein signaling is further complicated by the omnipresent crosstalk between convoluted signaling pathways and the influence of the large family of regulators of G-protein signaling (RGS) that modulate G_α activity.[33,35,40] Furthermore, the cellular response to a GPCR mediated signal depends on the tissue specific expression of different isoforms of certain effectors and regulators and even on the formation of site specific signaling scaffolds, so called signalsomes. The latter influence the availability and stoichiometry and, thus, the interaction of the different signaling proteins and second messengers.[25,41]

1.3. Arrestins

Classically, arrestins are considered universal regulators of GPCRs, playing a crucial role in receptor desensitization and trafficking. In addition, there is a growing body of evidence that by interacting with a variety of cell signaling proteins, arrestins act as multifunctional adaptors on their own and mediate distinct, G-protein independent signaling pathways.

1.3.1. Arrestin isoforms

In comparison to the huge, diverse superfamily of GPCRs, arrestins represent a relatively small clan of cytosolic regulatory proteins. The arrestin family comprises 4 isoforms revealing high sequence homology. Arrestin 1 and 4 are exclusively expressed in the retina, where they regulate the activity of the photosensor rhodopsin.[42,43] Contrary to the two visual arrestins, in mammals arrestin 2 and 3, more commonly referred to as β-arrestin 1 and 2, are ubiquitously expressed in almost any tissue and cell type and have been demonstrated to interact with the vast majority of GPCRs.[44] In addition to the classic arrestin proteins, a new family of protein that, despite low overall sequence similarity with β-arrestins, share the overall "arrestin fold" structure, was identified. In mammals, six members of this family, called α-arrestins or arrestin domain containing proteins (ARRDC), named ARRDC 1 – 5 and thioredoxin-interacting protein (Txnip) have been described so far.[43] Their function in mammals is only starting to be elucidated, but they seem to act as versatile adaptors that link GPCRs to E3 ubiquitin ligases and endocytic factors.[45]

The crystal structures of all four members of the arrestin family have been solved and reveal a remarkably similar structure, generally referred to as the arrestin fold.[43] They are

composed of two seven stranded β sandwiches, the N-terminal and C-terminal domains, connected by a hinge region.[46-49] In the inactive conformation, the unstructured C-terminus folds back towards the N-terminal domain, where it forms hydrophobic interactions as well as an ion pair with the so-called polar core, the main phosphate sensor of the molecule.[47,48,50] These interactions, in concert with additional salt bridges within the polar core, constrain the protein in its inactive conformation.[48] The conformational changes associated with the binding of an active, phosphorylated receptor involve a rotation of the N- and C-terminal domain relative to each other.[51] The polar core of the arrestin most likely interacts with the phosphorylated residues of the receptor, thereby exposing the C-terminus of arrestin and giving access to several binding motifs responsible for an interaction with components of the endocytic machinery.[51,52]

1.3.2. Mechanisms of receptor desensitization and trafficking

The most prominent and name giving function of arrestins is their ability to inhibit G-protein signaling by the activated GPCR. A decisive step hereby is the phosphorylation of the ligand-activated receptor by G-protein receptor kinases (GRK) at specific sites in the ECL3 and the C-terminus.[50] There are seven mammalian GRKs, the two "visual" GRKs (GRK 1 and 7) are exclusively expressed in the retina, while four of the other GRKs are ubiquitously expressed and interact with the majority of GPCRs.[53] In its active conformation the receptor is immediately targeted by GRKs, either in a G-protein independent manner or through recruitment by the $G_{\beta\gamma}$ dimer.[43,54] The phosphorylated receptor subsequently recruits arrestins that bind to the cytosolic face of the receptor, thus sterically hindering further interaction of the receptor with the G-protein.[55,56] Furthermore, β-arrestins have been shown to scaffold enzymes such as phosphodiesterases and diacylglycerol kinases involved in the degradation of second messengers.[57,58] In combination, the two effects lead to an effective deactivation of the G-protein mediated signal transduction.[55]

Beyond desensitization, the bound arrestin, serving as essential adaptor, that links the receptor to components of the endocytic pathway and leads to its internalization via clathrin coated pits (CCP), plays a crucial role in receptor trafficking.[43] Hereby, arrestin interacts with clathrin and the adaptor AP2, a protein complex involved in cargo selection for CCPs, via highly conserved binding motifs at its C-terminus, promoting the recruitment of the GPCR-arrestin complex to CCPs.[55,59-61]

After vesicle formation, the fate of the receptor-arrestin complex is determined by the stability of its protein-protein interaction.[55] Accordingly, receptors can be grouped into two classes; class A receptors such as the β_2 adrenergic or dopamine D_1A receptor, preferentially form a transient complex with arrestin and are recycled to the plasma membrane soon after internalization.[62,63] Class B receptors, including neurotensin receptor 1 and vasopressin receptor V_2, on the other hand form a stable complex with arrestin that persists after internalization and serves as a scaffold for several other interaction partners at the endosomes.[43,62] Furthermore, class B receptors are subject to proteasomal degradation instead of recycling to the cell membrane.[64] Class A and B receptors also differ

in their affinities to the arrestin isoforms, while class A receptors exhibit a higher affinity to β-arrestin 2 than to β-arrestin 1 and do not interact with visual arrestin, class B receptors have comparable affinities to both β-arrestin isoforms and also recruit visual arrestin.[43,62] It has been demonstrated that different phosphorylation patterns, especially in the C-terminus of the receptor, are responsible for the stability of the complex and additionally influence arrestin conformations that drive interactions with various components of the ubiquitin-proteasome system.[63,65-67] Ubiquitination of the receptor as well as the accompanying arrestin defines the trafficking itinerary of the internalized receptor and furthermore the formation of distinct endosomal signaling complexes.[55,64,68] Hereby, β-arrestins are pivotal in the sophisticated regulation between assembly and degradation of defined ubiquitination patterns, acting as adaptors of different E3 ubiquitin ligases, like Nedd4 or Mdm2, as well as deubiquitinases like USP20 and 33.[55,69-72]

1.3.3. Arrestin mediated cell signaling

Beyond their function as modulators of G-protein dependent signaling, arrestins interact with a plethora of signaling proteins. Proteomic analyses identified a total of 71 interaction partners of β-arrestin 1 and 167 of β-arrestin 2, thereof 102 proteins interacted with both isoforms, including various proteins involved in cellular signaling and nucleic acid binding.[73] Furthermore, quantitative phosphoproteomics analysis after stimulation of angiotensin II type 1A receptor with an arrestin biased agonist demonstrated arrestin mediated phosphorylation and dephosphorylation of 224 different proteins, including 38 kinases and 3 phophatases.[74] The combination of these findings using sophisticated bioinformatics tools allowed the construction of a kinase network for arrestin mediated signaling, demonstrating that arrestin signaling is far more complex than previously anticipated.[74,75] The function and the physiological consequences of the majority of these interactions is only poorly understood, but there is more detailed information available on the impact of arrestin on certain pathways, especially the MAP kinase network.

There are three major classes of MAPKs in mammals, the extracellular signal regulated kinases, ERK1/2; the c-Jun N-terminal kinase/stress-activated protein kinases (JNK/SAPK); and the p38/HOG1 MAPKs.[76] The cellular function of the different MAPKs is pleiotropic, including regulation of cell cycle progression, growth arrest and apoptosis.[76] The different MAPKs are organized in a series of parallel phosphorylation cascades that are regulated by the spatial coordination of the individual components through scaffolding proteins.[41,77] Arrestins act as GPCR regulated scaffolds for the regulation of all three classes of MAPKs.[76] Especially the arrestin mediated activation of the ERK1/2 cascade was studied in detail. All three components of the ERK cascade, c-Raf1, MEK1/2 and ERK1/2 interact with β-arrestin 2, and receptor induced arrestin conformations strongly increase ERK1/2 binding.[76,78,79] When mediated by class B GPCRs, receptor, arrestin and the components of the ERK cascade form a stable signalsome complex that is crucial for the regulation of ERK.[80] Likewise, the stability of this signalsome complex is tightly regulated by the phosphorylation and ubiquitination pattern of the receptor and the associated arrestin in particular.[64,66,81] Most interestingly, arrestin mediated ERK activation is temporally and

spatially distinct from the canonical G-protein or receptor tyrosine kinase induced activation pattern.[82] G-protein activated ERK is not spatially restricted and readily diffuses into the nucleus, where it influences a multitude of transcription factors.[83] Furthermore, it is rapidly inactivated by MAPK phosphatases, i. e. the ERK signal closely follows the rapid time course of G-protein activation.[76] On the other hand, arrestin activated ERKs, at least when mediated by class B GPCRs, are spatially restricted to the cytosol through the stable signalsome complex that additionally protects ERK from phosphatase inactivation resulting in a long lasting signal.[76,80,84] Thus, these two distinct ERK populations influence different effectors resulting in different G-protein and arrestin mediated ERK signaling.[82,85] Beyond MAPK signaling, arrestins have been demonstrated to regulate signaling through the Src family of nonreceptor tyrosine kinases in a similar manner.[76,86]

The MAPKs and Src pathways are only two out of several physiologically important signaling pathways regulated by arrestins that influence a plethora of cellular functions. Thereby, the spatiotemporal organization through the arrestin signalsome is pivotal for the control of directed physiological responses like chemotaxis and cell migration.[87]

1.4. The concept of biased agonism

In the classic “two state” model, the receptor is regarded as a bimodal switch that can adopt two distinct conformations, whereof the active one interacts with the G-proteins and induces cellular signaling.[88] Ligand binding to the receptor can influence the equilibrium between the two receptor states; agonists shift the equilibrium towards the active conformation, while inverse agonists favor the inactive state and neutral antagonists preserve the unimpaired condition. This model was sufficient to describe ligand activation of the receptor measured through a single readout and allowed the characterization of different compounds by assigning them a single efficacy determining their power to induce the investigated response. This approach elegantly allowed for the generation of structure-activity relationships, useful to guide drug development.

Advances in molecular biology provided recombinant test systems, allowing the independent observation of multiple ligand induced receptor behavior, including activation of different G-proteins, arrestins or other effects like receptor phosphorylation and internalization.[89] This refined methodology revealed discrepancies in the function of certain ligands, when different cellular effectors were analyzed. Findings, like receptor internalization by ligands described as antagonists, differential activation of ACs or PLC through ligands acting on the same receptor or especially the G-protein independent activation of arrestins,[90-93] are incompatible with the existence of a single active state of a receptor.[94,95] This implies that efficacy cannot be regarded as an intrinsic property of the ligand-receptor couple, but has to be considered as a pluridimensional phenomenon depending on the nature of the receptor-effector coupling as well as on the ligand-receptor interaction.[89,96] Therefore, ligands can be functionally biased with multiple different efficacies for the different readouts, i.e. activating only certain receptor states. Since the first recognition of functional selectivity in the mid-1990s,[97] this so called biased agonism

has been demonstrated for an ever growing number of ligands at a multitude of therapeutically relevant GPCR targets,[88] including serotonin receptors,[98,99] opioid receptors,[100] β-adrenoceptors,[92,96,101] dopamine receptors[93,102-104] and the angiotensin type 1A receptor.[105-107]

The observed versatility in signal transduction through GPCRs is incompatible with the existence of a single active conformation of the receptor. According to current understanding, receptors rather exist in ensembles of multiple conformations that interact with various downstream effectors.[89] In this "multistate model", functional selectivity can be explained by the stabilization of distinct ligand specific receptor conformations that selectively interact with only a subset of the cellular effectors.[89,108] GPCRs possess a much higher plasticity than previously anticipated and for several receptors, the existence of multiple conformations was demonstrated by advanced NMR techniques.[108,109] For the β_2 adrenergic receptor, such distinct ligand specific conformation were demonstrated even for functionally closely related ligands.[110,111] Furthermore, it was shown that the interaction of the receptor with G-proteins and arrestins is mediated by different receptor conformations.[112]

1.4.1. Functional selectivity in drug discovery, challenges and opportunities

The general acceptance of functional selectivity at GPCRs poses a new challenge for drug discovery efforts. To address receptor activation, the majority of high throughput screening and drug development programs in industry and academia rely on readout systems based on measurement of easily accessible second messengers, such as Ca^{2+} or cAMP, or directly measuring G-protein activation, for example via binding of radiolabeled GTPγS. While adequate and robust for the characterization of unbiased compounds, this approach falls short to address the putative pluridimensional efficacy of new ligands towards multiple signaling pathways. Therefore, this procedure is prone to errors: ligands producing desired or undesired effects may not be identified. The identification of ligand-specific undesired cellular responses is of particular relevance to prevent the failure of drug candidates at later stages of the development process. Holistic readouts such as label free cell-based assays offer the advantage to address the full plethora of signaling pathways but fail to provide insights into the mode of action of the investigated ligands.[89] A comprehensive characterization of new compound libraries needs to include alternate systems, such as arrestin recruitment or ERK phosphorylation assays, to account for the versatility of GPCR signaling.

So far, there are only a few examples of ligand bias producing a desired effect in patients. Out of 16 investigated β_1-blockers, carvedilol was the only β-arrestin biased agonist at the β_2 adrenoreceptor.[92] Interestingly, carvedilol exhibits a unique beneficial profile in the treatment of chronic heart failure, and although the underlying physiological mechanisms are unclear, these findings point towards the involvement of arrestin

mediated pathways.[89,92,113] The arrestin biased angiotensin II type 1 receptor ligand TRV120027, that is currently in clinical development for the treatment of heart failure, is another example .[107,108] TRV120027 is able to reduce blood pressure, but unlike unbiased agonists, that decrease cardiac performance, it increases cardiac output.[107,114] Opioid μ receptors represent another target for biased ligands.[108] In β-arrestin 2 knockout mice, morphine induced prolonged analgesia with reduced constipation and respiratory depression compared to the wild type animals, suggesting a favorable pharmacological profile of G-protein biased compared to unbiased agonists.[108,115,116] These findings led to the development of TRV130, a G-protein biased agonists causing less gastrointestinal dysfunction and respiratory suppression than morphine at equivalent doses.[100]

Collectively, these findings emphasize the necessity for a full pharmacological characterization of newly developed receptor ligands with regard to alternate signaling pathways to enable a comprehensive analysis of their physiological implications.

1.5. References

1. Lander, E. S.; Linton, L. M.; Birren, B.; International Human Genome Sequencing, C. Initial sequencing and analysis of the human genome. *Nature* **2001**, 409, 860-921.
2. Vassilatis, D. K.; Hohmann, J. G.; Zeng, H.; Li, F.; Ranchalis, J. E.; Mortrud, M. T.; Brown, A.; Rodriguez, S. S.; Weller, J. R.; Wright, A. C.; Bergmann, J. E.; Gaitanaris, G. A. The G protein-coupled receptor repertoires of human and mouse. *Proc. Natl. Acad. Sci. U. S. A.* **2003**, 100, 4903-4908.
3. Gloriam, D. E.; Fredriksson, R.; Schioth, H. B. The G protein-coupled receptor subset of the rat genome. *BMC Genomics* **2007**, 8, 338.
4. Fredriksson, R.; Lagerstrom, M. C.; Lundin, L. G.; Schioth, H. B. The G-protein-coupled receptors in the human genome form five main families. Phylogenetic analysis, paralogon groups, and fingerprints. *Mol. Pharmacol.* **2003**, 63, 1256-1272.
5. Garland, S. L. Are GPCRs still a source of new targets? *J. Biomol. Screen.* **2013**, 18, 947-966.
6. Lagerstrom, M. C.; Schioth, H. B. Structural diversity of G protein-coupled receptors and significance for drug discovery. *Nat. Rev. Drug Discov.* **2008**, 7, 339-357.
7. Schulte, G. International Union of Basic and Clinical Pharmacology. LXXX. The class Frizzled receptors. *Pharmacol. Rev.* **2010**, 62, 632-667.
8. Venkatakrishnan, A. J.; Deupi, X.; Lebon, G.; Tate, C. G.; Schertler, G. F.; Babu, M. M. Molecular signatures of G-protein-coupled receptors. *Nature* **2013**, 494, 185-194.
9. Palczewski, K.; Kumasaka, T.; Hori, T.; Behnke, C. A.; Motoshima, H.; Fox, B. A.; Le Trong, I.; Teller, D. C.; Okada, T.; Stenkamp, R. E.; Yamamoto, M.; Miyano, M. Crystal structure of rhodopsin: A G protein-coupled receptor. *Science* **2000**, 289, 739-745.
10. Rasmussen, S. G.; Choi, H. J.; Rosenbaum, D. M.; Kobilka, T. S.; Thian, F. S.; Edwards, P. C.; Burghammer, M.; Ratnala, V. R.; Sanishvili, R.; Fischetti, R. F.; Schertler, G. F.; Weis, W. I.; Kobilka, B. K. Crystal structure of the human beta2 adrenergic G-protein-coupled receptor. *Nature* **2007**, 450, 383-387.
11. Cherezov, V.; Rosenbaum, D. M.; Hanson, M. A.; Rasmussen, S. G.; Thian, F. S.; Kobilka, T. S.; Choi, H. J.; Kuhn, P.; Weis, W. I.; Kobilka, B. K.; Stevens, R. C. High-resolution crystal structure of an engineered human beta2-adrenergic G protein-coupled receptor. *Science* **2007**, 318, 1258-1265.
12. Rosenbaum, D. M.; Cherezov, V.; Hanson, M. A.; Rasmussen, S. G.; Thian, F. S.; Kobilka, T. S.; Choi, H. J.; Yao, X. J.; Weis, W. I.; Stevens, R. C.; Kobilka, B. K. GPCR engineering yields high-resolution structural insights into beta2-adrenergic receptor function. *Science* **2007**, 318, 1266-1273.
13. Rasmussen, S. G.; DeVree, B. T.; Zou, Y.; Kruse, A. C.; Chung, K. Y.; Kobilka, T. S.; Thian, F. S.; Chae, P. S.; Pardon, E.; Calinski, D.; Mathiesen, J. M.; Shah, S. T.; Lyons, J. A.; Caffrey, M.; Gellman, S. H.; Steyaert, J.; Skiniotis, G.; Weis, W. I.; Sunahara, R. K.; Kobilka, B. K. Crystal structure of the beta2 adrenergic receptor-Gs protein complex. *Nature* **2011**, 477, 549-555.
14. Hofmann, K. P.; Scheerer, P.; Hildebrand, P. W.; Choe, H. W.; Park, J. H.; Heck, M.; Ernst, O. P. A G protein-coupled receptor at work: the rhodopsin model. *Trends Biochem. Sci.* **2009**, 34, 540-552.
15. Shimamura, T.; Shiroishi, M.; Weyand, S.; Tsujimoto, H.; Winter, G.; Katritch, V.; Abagyan, R.; Cherezov, V.; Liu, W.; Han, G. W.; Kobayashi, T.; Stevens, R. C.; Iwata, S. Structure of the human histamine H1 receptor complex with doxepin. *Nature* **2011**, 475, 65-70.

16. Hanson, M. A.; Roth, C. B.; Jo, E.; Griffith, M. T.; Scott, F. L.; Reinhart, G.; Desale, H.; Clemons, B.; Cahalan, S. M.; Schuerer, S. C.; Sanna, M. G.; Han, G. W.; Kuhn, P.; Rosen, H.; Stevens, R. C. Crystal structure of a lipid G protein-coupled receptor. *Science* **2012**, 335, 851-855.
17. Dror, R. O.; Pan, A. C.; Arlow, D. H.; Borhani, D. W.; Maragakis, P.; Shan, Y.; Xu, H.; Shaw, D. E. Pathway and mechanism of drug binding to G-protein-coupled receptors. *Proc. Natl. Acad. Sci. U. S. A.* **2011**, 108, 13118-13123.
18. Mustafi, D.; Palczewski, K. Topology of class A G protein-coupled receptors: insights gained from crystal structures of rhodopsins, adrenergic and adenosine receptors. *Mol. Pharmacol.* **2009**, 75, 1-12.
19. Ballesteros, J. A.; Weinstein, H. [19] Integrated methods for the construction of three-dimensional models and computational probing of structure-function relations in G protein-coupled receptors. In *Methods in Neurosciences*, Stuart, C. S., Ed. Academic Press: 1995; Vol. Volume 25, pp 366-428.
20. Ballesteros, J. A.; Jensen, A. D.; Liapakis, G.; Rasmussen, S. G.; Shi, L.; Gether, U.; Javitch, J. A. Activation of the beta 2-adrenergic receptor involves disruption of an ionic lock between the cytoplasmic ends of transmembrane segments 3 and 6. *J. Biol. Chem.* **2001**, 276, 29171-29177.
21. Jaakola, V. P.; Prilusky, J.; Sussman, J. L.; Goldman, A. G protein-coupled receptors show unusual patterns of intrinsic unfolding. *Protein Eng. Des. Sel.* **2005**, 18, 103-110.
22. Luttrell, L. M. Reviews in molecular biology and biotechnology: transmembrane signaling by G protein-coupled receptors. *Mol. Biotechnol.* **2008**, 39, 239-264.
23. Downes, G. B.; Gautam, N. The G protein subunit gene families. *Genomics* **1999**, 62, 544-552.
24. Cabrera-Vera, T. M.; Vanhauwe, J.; Thomas, T. O.; Medkova, M.; Preininger, A.; Mazzoni, M. R.; Hamm, H. E. Insights into G protein structure, function, and regulation. *Endocr. Rev.* **2003**, 24, 765-781.
25. Dupre, D. J.; Robitaille, M.; Rebois, R. V.; Hebert, T. E. The role of Gbetagamma subunits in the organization, assembly, and function of GPCR signaling complexes. *Annu. Rev. Pharmacol. Toxicol.* **2009**, 49, 31-56.
26. Sunahara, R. K.; Dessauer, C. W.; Gilman, A. G. Complexity and diversity of mammalian adenylyl cyclases. *Annu. Rev. Pharmacol. Toxicol.* **1996**, 36, 461-480.
27. Morris, A. J.; Scarlata, S. Regulation of effectors by G-protein alpha- and beta gamma-subunits. Recent insights from studies of the phospholipase c-beta isoenzymes. *Biochem. Pharmacol.* **1997**, 54, 429-435.
28. Kurose, H. Galpha12 and Galpha13 as key regulatory mediator in signal transduction. *Life Sci.* **2003**, 74, 155-161.
29. Tang, W. J.; Gilman, A. G. Type-specific regulation of adenylyl cyclase by G protein beta gamma subunits. *Science* **1991**, 254, 1500-1503.
30. Jamora, C.; Yamanouye, N.; Van Lint, J.; Laudenslager, J.; Vandenheede, J. R.; Faulkner, D. J.; Malhotra, V. Gbetagamma-mediated regulation of Golgi organization is through the direct activation of protein kinase D. *Cell* **1999**, 98, 59-68.
31. Birnbaumer, L. Expansion of signal transduction by G proteins. The second 15 years or so: from 3 to 16 alpha subunits plus betagamma dimers. *Biochim. Biophys. Acta* **2007**, 1768, 772-793.
32. Seifert, R.; Lushington, G. H.; Mou, T. C.; Gille, A.; Sprang, S. R. Inhibitors of membranous adenylyl cyclases. *Trends Pharmacol. Sci.* **2012**, 33, 64-78.
33. Sassone-Corsi, P. The cyclic AMP pathway. *Cold Spring Harb. Perspect. Biol.* **2012**, 4.

34. Tasken, K.; Skalhegg, B. S.; Tasken, K. A.; Solberg, R.; Knutsen, H. K.; Levy, F. O.; Sandberg, M.; Orstavik, S.; Larsen, T.; Johansen, A. K.; Vang, T.; Schrader, H. P.; Reinton, N. T.; Torgersen, K. M.; Hansson, V.; Jahnsen, T. Structure, function, and regulation of human cAMP-dependent protein kinases. *Adv. Second Messenger Phosphoprotein Res.* **1997**, 31, 191-204.
35. Kadamur, G.; Ross, E. M. Mammalian phospholipase C. *Annu. Rev. Physiol.* **2013**, 75, 127-154.
36. Parys, J. B.; De Smedt, H. Inositol 1,4,5-trisphosphate and its receptors. *Adv. Exp. Med. Biol.* **2012**, 740, 255-279.
37. Berridge, M. J.; Lipp, P.; Bootman, M. D. The versatility and universality of calcium signalling. *Nat. Rev. Mol. Cell Biol.* **2000**, 1, 11-21.
38. Yang, C.; Kazanietz, M. G. Divergence and complexities in DAG signaling: looking beyond PKC. *Trends Pharmacol. Sci.* **2003**, 24, 602-608.
39. Carrasco, S.; Merida, I. Diacylglycerol, when simplicity becomes complex. *Trends Biochem. Sci.* **2007**, 32, 27-36.
40. Kimple, A. J.; Bosch, D. E.; Giguere, P. M.; Siderovski, D. P. Regulators of G-protein signaling and their Galpha substrates: promises and challenges in their use as drug discovery targets. *Pharmacol. Rev.* **2011**, 63, 728-749.
41. Brown, M. D.; Sacks, D. B. Protein scaffolds in MAP kinase signalling. *Cell. Signal.* **2009**, 21, 462-469.
42. Rajagopal, S.; Rajagopal, K.; Lefkowitz, R. J. Teaching old receptors new tricks: biasing seven-transmembrane receptors. *Nat. Rev. Drug Discov.* **2010**, 9, 373-386.
43. Lohse, M. J.; Hoffmann, C. Arrestin interactions with G protein-coupled receptors. *Handb. Exp. Pharmacol.* **2014**, 219, 15-56.
44. Lefkowitz, R. J.; Whalen, E. J. beta-arrestins: traffic cops of cell signaling. *Curr. Opin. Cell Biol.* **2004**, 16, 162-168.
45. Puca, L.; Brou, C. Alpha-arrestins - new players in Notch and GPCR signaling pathways in mammals. *J. Cell Sci.* **2014**, 127, 1359-1367.
46. Han, M.; Gurevich, V. V.; Vishnivetskiy, S. A.; Sigler, P. B.; Schubert, C. Crystal structure of beta-arrestin at 1.9 A: possible mechanism of receptor binding and membrane Translocation. *Structure* **2001**, 9, 869-880.
47. Zhan, X.; Gimenez, L. E.; Gurevich, V. V.; Spiller, B. W. Crystal structure of arrestin-3 reveals the basis of the difference in receptor binding between two non-visual subtypes. *J. Mol. Biol.* **2011**, 406, 467-478.
48. Hirsch, J. A.; Schubert, C.; Gurevich, V. V.; Sigler, P. B. The 2.8 A crystal structure of visual arrestin: a model for arrestin's regulation. *Cell* **1999**, 97, 257-269.
49. Sutton, R. B.; Vishnivetskiy, S. A.; Robert, J.; Hanson, S. M.; Raman, D.; Knox, B. E.; Kono, M.; Navarro, J.; Gurevich, V. V. Crystal structure of cone arrestin at 2.3A: evolution of receptor specificity. *J. Mol. Biol.* **2005**, 354, 1069-1080.
50. Gurevich, V. V.; Gurevich, E. V. The structural basis of arrestin-mediated regulation of G-protein-coupled receptors. *Pharmacol. Ther.* **2006**, 110, 465-502.
51. Shukla, A. K.; Manglik, A.; Kruse, A. C.; Xiao, K.; Reis, R. I.; Tseng, W. C.; Staus, D. P.; Hilger, D.; Uysal, S.; Huang, L. Y.; Paduch, M.; Tripathi-Shukla, P.; Koide, A.; Koide, S.; Weis, W. I.; Kossiakoff, A. A.; Kobilka, B. K.; Lefkowitz, R. J. Structure of active beta-arrestin-1 bound to a G-protein-coupled receptor phosphopeptide. *Nature* **2013**, 497, 137-141.
52. Xiao, K.; Shenoy, S. K.; Nobles, K.; Lefkowitz, R. J. Activation-dependent conformational changes in {beta}-arrestin 2. *J. Biol. Chem.* **2004**, 279, 55744-55753.
53. Gurevich, E. V.; Tesmer, J. J.; Mushegian, A.; Gurevich, V. V. G protein-coupled receptor kinases: more than just kinases and not only for GPCRs. *Pharmacol. Ther.* **2012**, 133, 40-69.

54. Watari, K.; Nakaya, M.; Kurose, H. Multiple functions of G protein-coupled receptor kinases. *J. Mol. Signal.* **2014**, 9, 1.
55. Shenoy, S. K.; Lefkowitz, R. J. beta-Arrestin-mediated receptor trafficking and signal transduction. *Trends Pharmacol. Sci.* **2011**, 32, 521-533.
56. Lohse, M. J.; Andexinger, S.; Pitcher, J.; Trukawinski, S.; Codina, J.; Faure, J. P.; Caron, M. G.; Lefkowitz, R. J. Receptor-specific desensitization with purified proteins. Kinase dependence and receptor specificity of beta-arrestin and arrestin in the beta 2-adrenergic receptor and rhodopsin systems. *J. Biol. Chem.* **1992**, 267, 8558-8564.
57. Perry, S. J.; Baillie, G. S.; Kohout, T. A.; McPhee, I.; Magiera, M. M.; Ang, K. L.; Miller, W. E.; McLean, A. J.; Conti, M.; Houslay, M. D.; Lefkowitz, R. J. Targeting of cyclic AMP degradation to beta 2-adrenergic receptors by beta-arrestins. *Science* **2002**, 298, 834-836.
58. Nelson, C. D.; Perry, S. J.; Regier, D. S.; Prescott, S. M.; Topham, M. K.; Lefkowitz, R. J. Targeting of diacylglycerol degradation to M1 muscarinic receptors by beta-arrestins. *Science* **2007**, 315, 663-666.
59. Goodman, O. B., Jr.; Krupnick, J. G.; Santini, F.; Gurevich, V. V.; Penn, R. B.; Gagnon, A. W.; Keen, J. H.; Benovic, J. L. Beta-arrestin acts as a clathrin adaptor in endocytosis of the beta2-adrenergic receptor. *Nature* **1996**, 383, 447-450.
60. Kim, Y. M.; Benovic, J. L. Differential roles of arrestin-2 interaction with clathrin and adaptor protein 2 in G protein-coupled receptor trafficking. *J. Biol. Chem.* **2002**, 277, 30760-30768.
61. Schmid, E. M.; Ford, M. G.; Burtey, A.; Praefcke, G. J.; Peak-Chew, S. Y.; Mills, I. G.; Benmerah, A.; McMahon, H. T. Role of the AP2 beta-appendage hub in recruiting partners for clathrin-coated vesicle assembly. *PLoS Biol.* **2006**, 4, e262.
62. Oakley, R. H.; Laporte, S. A.; Holt, J. A.; Caron, M. G.; Barak, L. S. Differential affinities of visual arrestin, beta arrestin1, and beta arrestin2 for G protein-coupled receptors delineate two major classes of receptors. *J. Biol. Chem.* **2000**, 275, 17201-17210.
63. Oakley, R. H.; Laporte, S. A.; Holt, J. A.; Barak, L. S.; Caron, M. G. Association of beta-arrestin with G protein-coupled receptors during clathrin-mediated endocytosis dictates the profile of receptor resensitization. *J. Biol. Chem.* **1999**, 274, 32248-32257.
64. Marchese, A.; Trejo, J. Ubiquitin-dependent regulation of G protein-coupled receptor trafficking and signaling. *Cell. Signal.* **2013**, 25, 707-716.
65. Shenoy, S. K. Deubiquitinases and their emerging roles in beta-arrestin-mediated signaling. *Methods Enzymol.* **2014**, 535, 351-370.
66. Nobles, K. N.; Xiao, K.; Ahn, S.; Shukla, A. K.; Lam, C. M.; Rajagopal, S.; Strachan, R. T.; Huang, T. Y.; Bressler, E. A.; Hara, M. R.; Shenoy, S. K.; Gygi, S. P.; Lefkowitz, R. J. Distinct phosphorylation sites on the beta(2)-adrenergic receptor establish a barcode that encodes differential functions of beta-arrestin. *Sci. Signal.* **2011**, 4, ra51.
67. Ren, X. R.; Reiter, E.; Ahn, S.; Kim, J.; Chen, W.; Lefkowitz, R. J. Different G protein-coupled receptor kinases govern G protein and beta-arrestin-mediated signaling of V2 vasopressin receptor. *Proc. Natl. Acad. Sci. U. S. A.* **2005**, 102, 1448-1453.
68. Marchese, A.; Benovic, J. L. Agonist-promoted ubiquitination of the G protein-coupled receptor CXCR4 mediates lysosomal sorting. *J. Biol. Chem.* **2001**, 276, 45509-45512.
69. Girnita, L.; Shenoy, S. K.; Sehat, B.; Vasilcanu, R.; Girnita, A.; Lefkowitz, R. J.; Larsson, O. {beta}-Arrestin is crucial for ubiquitination and down-regulation of the insulin-like growth factor-1 receptor by acting as adaptor for the MDM2 E3 ligase. *J. Biol. Chem.* **2005**, 280, 24412-24419.

70. Shenoy, S. K.; Xiao, K.; Venkataramanan, V.; Snyder, P. M.; Freedman, N. J.; Weissman, A. M. Nedd4 mediates agonist-dependent ubiquitination, lysosomal targeting, and degradation of the beta2-adrenergic receptor. *J. Biol. Chem.* **2008**, 283, 22166-22176.
71. Berthouze, M.; Venkataramanan, V.; Li, Y.; Shenoy, S. K. The deubiquitinases USP33 and USP20 coordinate beta2 adrenergic receptor recycling and resensitization. *EMBO J.* **2009**, 28, 1684-1696.
72. Shenoy, S. K. Arrestin interaction with E3 ubiquitin ligases and deubiquitinases: functional and therapeutic implications. *Handb. Exp. Pharmacol.* **2014**, 219, 187-203.
73. Xiao, K.; McClatchy, D. B.; Shukla, A. K.; Zhao, Y.; Chen, M.; Shenoy, S. K.; Yates, J. R., 3rd; Lefkowitz, R. J. Functional specialization of beta-arrestin interactions revealed by proteomic analysis. *Proc. Natl. Acad. Sci. U. S. A.* **2007**, 104, 12011-12016.
74. Xiao, K.; Sun, J.; Kim, J.; Rajagopal, S.; Zhai, B.; Villen, J.; Haas, W.; Kovacs, J. J.; Shukla, A. K.; Hara, M. R.; Hernandez, M.; Lachmann, A.; Zhao, S.; Lin, Y.; Cheng, Y.; Mizuno, K.; Ma'ayan, A.; Gygi, S. P.; Lefkowitz, R. J. Global phosphorylation analysis of beta-arrestin-mediated signaling downstream of a seven transmembrane receptor (7TMR). *Proc. Natl. Acad. Sci. U. S. A.* **2010**, 107, 15299-15304.
75. Shukla, A. K.; Xiao, K.; Lefkowitz, R. J. Emerging paradigms of beta-arrestin-dependent seven transmembrane receptor signaling. *Trends Biochem. Sci.* **2011**, 36, 457-469.
76. Strungs, E. G.; Luttrell, L. M. Arrestin-dependent activation of ERK and Src family kinases. *Handb. Exp. Pharmacol.* **2014**, 219, 225-257.
77. Burack, W. R.; Shaw, A. S. Signal transduction: hanging on a scaffold. *Curr. Opin. Cell Biol.* **2000**, 12, 211-216.
78. Coffa, S.; Breitman, M.; Hanson, S. M.; Callaway, K.; Kook, S.; Dalby, K. N.; Gurevich, V. V. The effect of arrestin conformation on the recruitment of c-Raf1, MEK1, and ERK1/2 activation. *PLoS One* **2011**, 6, e28723.
79. Luttrell, L. M.; Roudabush, F. L.; Choy, E. W.; Miller, W. E.; Field, M. E.; Pierce, K. L.; Lefkowitz, R. J. Activation and targeting of extracellular signal-regulated kinases by beta-arrestin scaffolds. *Proc. Natl. Acad. Sci. U. S. A.* **2001**, 98, 2449-2454.
80. Tohgo, A.; Choy, E. W.; Gesty-Palmer, D.; Pierce, K. L.; Laporte, S.; Oakley, R. H.; Caron, M. G.; Lefkowitz, R. J.; Luttrell, L. M. The stability of the G protein-coupled receptor-beta-arrestin interaction determines the mechanism and functional consequence of ERK activation. *J. Biol. Chem.* **2003**, 278, 6258-6267.
81. Shenoy, S. K.; Lefkowitz, R. J. Trafficking patterns of beta-arrestin and G protein-coupled receptors determined by the kinetics of beta-arrestin deubiquitination. *J. Biol. Chem.* **2003**, 278, 14498-14506.
82. Luttrell, L. M. 'Location, location, location': activation and targeting of MAP kinases by G protein-coupled receptors. *J. Mol. Endocrinol.* **2003**, 30, 117-126.
83. Morrison, D. K. MAP kinase pathways. *Cold Spring Harb. Perspect. Biol.* **2012**, 4.
84. Tohgo, A.; Pierce, K. L.; Choy, E. W.; Lefkowitz, R. J.; Luttrell, L. M. beta-Arrestin scaffolding of the ERK cascade enhances cytosolic ERK activity but inhibits ERK-mediated transcription following angiotensin AT1a receptor stimulation. *J. Biol. Chem.* **2002**, 277, 9429-9436.
85. Luttrell, L. M.; Gesty-Palmer, D. Beyond desensitization: physiological relevance of arrestin-dependent signaling. *Pharmacol. Rev.* **2010**, 62, 305-330.
86. Luttrell, L. M.; Ferguson, S. S.; Daaka, Y.; Miller, W. E.; Maudsley, S.; Della Rocca, G. J.; Lin, F.; Kawakatsu, H.; Owada, K.; Luttrell, D. K.; Caron, M. G.; Lefkowitz, R. J. Beta-arrestin-dependent formation of beta2 adrenergic receptor-Src protein kinase complexes. *Science* **1999**, 283, 655-661.

87. DeFea, K. A. Stop that cell! Beta-arrestin-dependent chemotaxis: a tale of localized actin assembly and receptor desensitization. *Annu. Rev. Physiol.* **2007**, 69, 535-560.
88. Shonberg, J.; Lopez, L.; Scammells, P. J.; Christopoulos, A.; Capuano, B.; Lane, J. R. Biased Agonism at G Protein-Coupled Receptors: The Promise and the Challenges-A Medicinal Chemistry Perspective. *Med. Res. Rev.* **2014**.
89. Kenakin, T. Functional selectivity and biased receptor signaling. *J. Pharmacol. Exp. Ther.* **2011**, 336, 296-302.
90. Spengler, D.; Waeber, C.; Pantaloni, C.; Holsboer, F.; Bockaert, J.; Seeburg, P. H.; Journot, L. Differential signal transduction by five splice variants of the PACAP receptor. *Nature* **1993**, 365, 170-175.
91. Roth, B. L.; Chuang, D. M. Multiple mechanisms of serotonergic signal transduction. *Life Sci.* **1987**, 41, 1051-1064.
92. Wisler, J. W.; DeWire, S. M.; Whalen, E. J.; Violin, J. D.; Drake, M. T.; Ahn, S.; Shenoy, S. K.; Lefkowitz, R. J. A unique mechanism of beta-blocker action: carvedilol stimulates beta-arrestin signaling. *Proc. Natl. Acad. Sci. U. S. A.* **2007**, 104, 16657-16662.
93. Gay, E. A.; Urban, J. D.; Nichols, D. E.; Oxford, G. S.; Mailman, R. B. Functional selectivity of D2 receptor ligands in a Chinese hamster ovary hD2L cell line: evidence for induction of ligand-specific receptor states. *Mol. Pharmacol.* **2004**, 66, 97-105.
94. Kenakin, T. Functional selectivity through protean and biased agonism: who steers the ship? *Mol. Pharmacol.* **2007**, 72, 1393-1401.
95. Kenakin, T. Ligand-selective receptor conformations revisited: the promise and the problem. *Trends Pharmacol. Sci.* **2003**, 24, 346-354.
96. Galandrin, S.; Bouvier, M. Distinct signaling profiles of beta1 and beta2 adrenergic receptor ligands toward adenylyl cyclase and mitogen-activated protein kinase reveals the pluridimensionality of efficacy. *Mol. Pharmacol.* **2006**, 70, 1575-1584.
97. Kenakin, T. Agonist-receptor efficacy. II. Agonist trafficking of receptor signals. *Trends Pharmacol. Sci.* **1995**, 16, 232-238.
98. Newman-Tancredi, A.; Martel, J. C.; Assie, M. B.; Buritova, J.; Lauressergues, E.; Cosi, C.; Heusler, P.; Bruins Slot, L.; Colpaert, F. C.; Vacher, B.; Cussac, D. Signal transduction and functional selectivity of F15599, a preferential post-synaptic 5-HT1A receptor agonist. *Br. J. Pharmacol.* **2009**, 156, 338-353.
99. Berg, K. A.; Maayani, S.; Goldfarb, J.; Scaramellini, C.; Leff, P.; Clarke, W. P. Effector pathway-dependent relative efficacy at serotonin type 2A and 2C receptors: evidence for agonist-directed trafficking of receptor stimulus. *Mol. Pharmacol.* **1998**, 54, 94-104.
100. DeWire, S. M.; Yamashita, D. S.; Rominger, D. H.; Liu, G.; Cowan, C. L.; Graczyk, T. M.; Chen, X. T.; Pitis, P. M.; Gotchev, D.; Yuan, C.; Koblish, M.; Lark, M. W.; Violin, J. D. A G protein-biased ligand at the mu-opioid receptor is potently analgesic with reduced gastrointestinal and respiratory dysfunction compared with morphine. *J. Pharmacol. Exp. Ther.* **2013**, 344, 708-717.
101. Stallaert, W.; Dorn, J. F.; van der Westhuizen, E.; Audet, M.; Bouvier, M. Impedance responses reveal beta(2)-adrenergic receptor signaling pluridimensionality and allow classification of ligands with distinct signaling profiles. *PLoS One* **2012**, 7, e29420.
102. Kilts, J. D.; Connery, H. S.; Arrington, E. G.; Lewis, M. M.; Lawler, C. P.; Oxford, G. S.; O'Malley, K. L.; Todd, R. D.; Blake, B. L.; Nichols, D. E.; Mailman, R. B. Functional selectivity of dopamine receptor agonists. II. Actions of dihydrexidine in D2L receptor-transfected MN9D cells and pituitary lactotrophs. *J. Pharmacol. Exp. Ther.* **2002**, 301, 1179-1189.
103. Mottola, D. M.; Kilts, J. D.; Lewis, M. M.; Connery, H. S.; Walker, Q. D.; Jones, S. R.; Booth, R. G.; Hyslop, D. K.; Piercey, M.; Wightman, R. M.; Lawler, C. P.; Nichols, D. E.; Mailman,

R. B. Functional selectivity of dopamine receptor agonists. I. Selective activation of postsynaptic dopamine D2 receptors linked to adenylate cyclase. *J. Pharmacol. Exp. Ther.* **2002**, 301, 1166-1178.
104. Ryman-Rasmussen, J. P.; Nichols, D. E.; Mailman, R. B. Differential activation of adenylate cyclase and receptor internalization by novel dopamine D1 receptor agonists. *Mol. Pharmacol.* **2005**, 68, 1039-1048.
105. Ahn, S.; Shenoy, S. K.; Wei, H.; Lefkowitz, R. J. Differential kinetic and spatial patterns of beta-arrestin and G protein-mediated ERK activation by the angiotensin II receptor. *J. Biol. Chem.* **2004**, 279, 35518-35525.
106. Wei, H.; Ahn, S.; Shenoy, S. K.; Karnik, S. S.; Hunyady, L.; Luttrell, L. M.; Lefkowitz, R. J. Independent beta-arrestin 2 and G protein-mediated pathways for angiotensin II activation of extracellular signal-regulated kinases 1 and 2. *Proc. Natl. Acad. Sci. U. S. A.* **2003**, 100, 10782-10787.
107. Boerrigter, G.; Lark, M. W.; Whalen, E. J.; Soergel, D. G.; Violin, J. D.; Burnett, J. C., Jr. Cardiorenal actions of TRV120027, a novel ss-arrestin-biased ligand at the angiotensin II type I receptor, in healthy and heart failure canines: a novel therapeutic strategy for acute heart failure. *Circ. Heart Fail.* **2011**, 4, 770-778.
108. Wisler, J. W.; Xiao, K.; Thomsen, A. R.; Lefkowitz, R. J. Recent developments in biased agonism. *Curr. Opin. Cell Biol.* **2014**, 27, 18-24.
109. Deupi, X.; Kobilka, B. K. Energy landscapes as a tool to integrate GPCR structure, dynamics, and function. *Physiology (Bethesda)* **2010**, 25, 293-303.
110. Kahsai, A. W.; Xiao, K.; Rajagopal, S.; Ahn, S.; Shukla, A. K.; Sun, J.; Oas, T. G.; Lefkowitz, R. J. Multiple ligand-specific conformations of the beta2-adrenergic receptor. *Nat. Chem. Biol.* **2011**, 7, 692-700.
111. Nygaard, R.; Zou, Y.; Dror, R. O.; Mildorf, T. J.; Arlow, D. H.; Manglik, A.; Pan, A. C.; Liu, C. W.; Fung, J. J.; Bokoch, M. P.; Thian, F. S.; Kobilka, T. S.; Shaw, D. E.; Mueller, L.; Prosser, R. S.; Kobilka, B. K. The dynamic process of beta(2)-adrenergic receptor activation. *Cell* **2013**, 152, 532-542.
112. Liu, J. J.; Horst, R.; Katritch, V.; Stevens, R. C.; Wuthrich, K. Biased signaling pathways in beta2-adrenergic receptor characterized by 19F-NMR. *Science* **2012**, 335, 1106-1110.
113. Metra, M.; Cas, L. D.; di Lenarda, A.; Poole-Wilson, P. Beta-blockers in heart failure: are pharmacological differences clinically important? *Heart Fail. Rev.* **2004**, 9, 123-130.
114. Violin, J. D.; DeWire, S. M.; Yamashita, D.; Rominger, D. H.; Nguyen, L.; Schiller, K.; Whalen, E. J.; Gowen, M.; Lark, M. W. Selectively engaging beta-arrestins at the angiotensin II type 1 receptor reduces blood pressure and increases cardiac performance. *J. Pharmacol. Exp. Ther.* **2010**, 335, 572-579.
115. Bohn, L. M.; Lefkowitz, R. J.; Gainetdinov, R. R.; Peppel, K.; Caron, M. G.; Lin, F. T. Enhanced morphine analgesia in mice lacking beta-arrestin 2. *Science* **1999**, 286, 2495-2498.
116. Raehal, K. M.; Walker, J. K.; Bohn, L. M. Morphine side effects in beta-arrestin 2 knockout mice. *J. Pharmacol. Exp. Ther.* **2005**, 314, 1195-1201.

Chapter 2

Scope and Objectives

2. Scope and Objectives

The conformational flexibility and functional selectivity of GPCRs has been a hot topic in pharmacology over the past decade. Although the concept of biased agonism was substantiated by an increasing amount of evidence at many GPCR targets, we are only beginning to understand its physiological consequences and its implications on the drug discovery process.[1-3] Nonetheless, these findings emphasize the necessity to integrate alternate readout systems, addressing non-canonical, G-protein independent signaling pathways, into the ligand characterization process in order to account for the full functional versatility and flexibility of GPCRs.

This thesis aimed at establishing a reliable method to measure arrestin recruitment to selected GPCR targets allowing for the comprehensive characterization of GPCR ligands regarding their functional properties with respect to arrestin activation. Several procedures making use of proximal or distal readouts to access arrestin activation are described in literature.[4] Distal readouts, such as the measurement of arrestin induced ERK phosphorylation, have the advantage of addressing changes in downstream signaling. Unfortunately, differential amplification of the signal and putative crosstalk between convoluted signaling pathways may complicate the interpretation of the results. Alternatively, several cellular assay systems relying on proximal readouts are available, mostly employing fluorescence/bioluminescence resonance energy transfer (FRET/BRET) or enzyme fragment complementation (EFC) techniques using genetically engineered arrestin and receptor fusion constructs. Especially EFC based approaches have proven valuable tools to investigate arrestin activation. Such assays can be easily adapted to multiwell formats enabling high throughput for the screening of large compound libraries. Fusion constructs of receptor and effector at a stoichiometry of 1:1 guarantee a direct proportionality between receptor occupancy and the measured signal. An enzyme fragment complementation assay, using split luciferase fragments from *P. termitilluminans,* developed by Misawa *et al.*, was considered an ideal method to achieve this goal.[5]

Consequently, the generation of HEK293T cells, stably expressing different arrestin and receptor constructs fused to N- and C-terminal fragments of the luciferase, was the initial subject of this dissertation project. These transfectants allowed the measurement of ligand induced arrestin recruitment to representative aminergic and peptidergic receptors in a timely and reliable manner, using bioluminescence in the 96 well format as readout. Due to the chosen modular approach, the assay is easily adaptable to a multitude of GPCRs as drug targets, e.g. for the screening of larger compound libraries.

In our medicinal chemistry department, extensive work has been performed to design, synthesize and investigate new ligands for two prototypic GPCR targets, the histamine receptor family as representative of aminergic GPCRs as well as the neuropeptide Y receptor family as peptidergic receptors.[6,7] The majority of these compounds was characterized by pharmacological techniques such as fluorescence-based or radioligand binding studies and G-protein based functional assays. So far, the functional properties of these ligands in noncanonical signaling pathways, especially concerning

arrestin activation, are elusive. Combining the aforementioned arrestin recruitment assay, established and optimized during this work, with classical G-protein readouts, primarily the thesis aimed at an identification of ligands exhibiting functional bias between arrestin and G-protein activation. For this purpose, a broad variety of structurally diverse ligands of representative GPCRs at hand was considered. For the histamine H_1 and H_2 receptor, the selected compound libraries included several standard ligands, some of them drugs approved for decades, as well as a variety of structurally different compound classes designed and synthesized in our lab. Currently, the H_4R is in the focus of extensive drug development efforts and explored as a potential new target for the therapy of inflammatory diseases. In this context, biased signaling at the H_4R, reported for some ligands, is becoming an issue, also addressed in the thesis. By analogy, argininamide-type antagonists developed as pharmacological tools for the NPY Y_1 and Y_2 receptor were included in view of putative arrestin selectivity, as these compounds exhibit insurmountable antagonism, a phenomenon, explainable by a stabilization of ligand specific receptor conformations.

2.1. References

1. Shonberg, J.; Lopez, L.; Scammells, P. J.; Christopoulos, A.; Capuano, B.; Lane, J. R. Biased Agonism at G Protein-Coupled Receptors: The Promise and the Challenges-A Medicinal Chemistry Perspective. *Med. Res. Rev.* **2014**.
2. Wisler, J. W.; Xiao, K.; Thomsen, A. R.; Lefkowitz, R. J. Recent developments in biased agonism. *Curr. Opin. Cell Biol.* **2014**, 27, 18-24.
3. Kenakin, T. Functional selectivity and biased receptor signaling. *J. Pharmacol. Exp. Ther.* **2011**, 336, 296-302.
4. Rajagopal, S.; Rajagopal, K.; Lefkowitz, R. J. Teaching old receptors new tricks: biasing seven-transmembrane receptors. *Nat. Rev. Drug Discov.* **2010**, 9, 373-386.
5. Misawa, N.; Kafi, A. K.; Hattori, M.; Miura, K.; Masuda, K.; Ozawa, T. Rapid and high-sensitivity cell-based assays of protein-protein interactions using split click beetle luciferase complementation: an approach to the study of G-protein-coupled receptors. *Anal. Chem.* **2010**, 82, 2552-2560.
6. Hill, S. J.; Ganellin, C. R.; Timmerman, H.; Schwartz, J. C.; Shankley, N. P.; Young, J. M.; Schunack, W.; Levi, R.; Haas, H. L. International Union of Pharmacology. XIII. Classification of histamine receptors. *Pharmacol. Rev.* **1997**, 49, 253-278.
7. Michel, M. C.; Beck-Sickinger, A.; Cox, H.; Doods, H. N.; Herzog, H.; Larhammar, D.; Quirion, R.; Schwartz, T.; Westfall, T. XVI. International Union of Pharmacology recommendations for the nomenclature of neuropeptide Y, peptide YY, and pancreatic polypeptide receptors. *Pharmacol. Rev.* **1998**, 50, 143-150.

Chapter 3

Establishing a luciferase complementation assay to quantify arrestin recruitment by GPCRs

3. Establishing a luciferase complementation assay to quantify arrestin recruitment by GPCRs

3.1. Introduction

For the investigation of functional selectivity of 7TM receptors regarding G-protein and arrestin mediated pathways, there was a need to complement the canonical G-protein based readouts routinely used in our lab. For this purpose a reliable method to measure arrestin activation by the GPCR, allowing the characterization of a multitude of receptor ligands in a robust, convenient and cost effective manner, was aimed at.

Therefore, a luciferase complementation assay developed by Misawa *et al.*[1] using fragments of the emerald luciferase (ELuc) from the Brazilian click beetle *Pyrearinus termitilluminans*, was taken into consideration. In comparison to the more widely used firefly luciferase, the emerald luciferase offers an advantage with respect to brightness, i.e. photon counts are roughly 10 times higher, and the emission spectrum is pH independent.[1] In a semirational combinatorial screening, Misawa *et al.* identified a pair of N-terminal (aa 1 – 415) and C-terminal (aa 394 – 542) fragments of the ELuc that yielded excellent signal to noise ratios. Using these fragments, the authors were able to establish an arrestin recruitment assay and adapt it to several GPCRs. Fig. 3-1 illustrates the principle of the luciferase complementation assay. HEK293T cells were genetically engineered to express two fusion constructs, the GPCR of interest, C-terminally fused to the C-terminal fragment

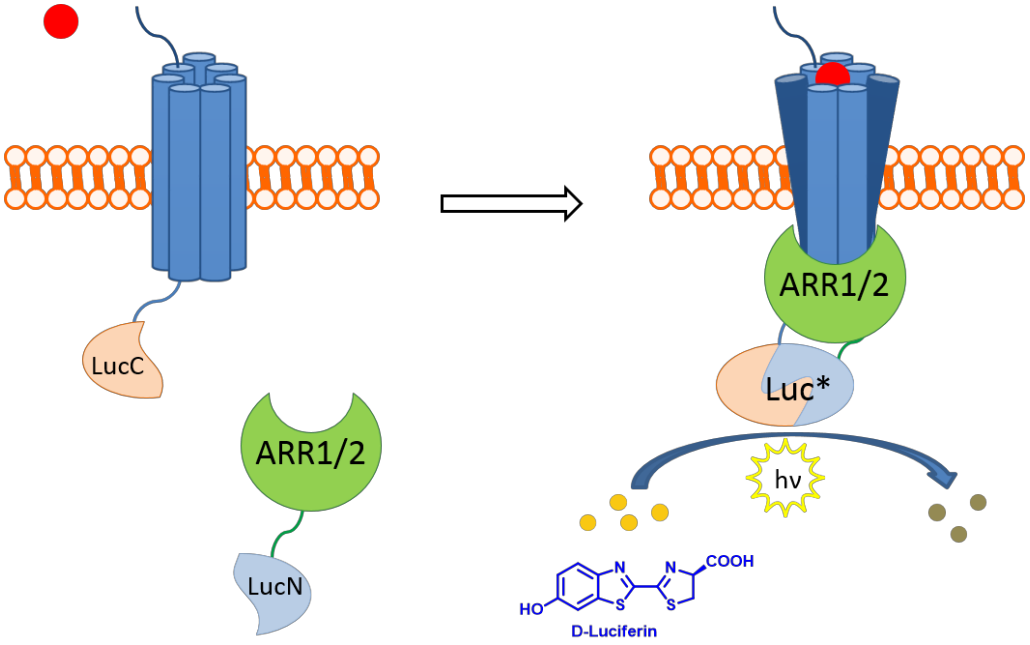

Fig. 3-1: Schematic illustration of the EFC-based β-arrestin recruitment assay

of ELuc, and either β-arrestin 1 or 2, fused to the N-terminal ELuc fragment. Upon agonist binding, conformational changes of the receptor lead to the activation of the signaling

machinery and subsequently induce binding of the arrestin fusion construct. Thereby, the two inactive fragments of ELuc come into close proximity, restoring enzyme activity. The luciferase activity, reflecting the degree of arrestin recruitment to the receptor, can be determined by measuring the bioluminescence emitted upon oxidation of D-luciferin.

3.2. Results and discussion

3.2.1. Generation of stable HEK293T transfectants

In order to achieve maximal versatility of the assay for adaption to different GPCRs, a modular approach was chosen, starting with the generation of the parental cell lines expressing either one of the ELucN-βarrestin isoforms. The plasmid vectors, encoding the arrestin and receptor constructs, were kindly provided by Prof. Dr. Takeaki Ozawa from the University of Tokyo. HEK293T cells were transfected with pcDNA 3.1 HIS-myc B vectors, encoding either the ELucN-βArrestin1 or ELucN-βArrestin2 fusion constructs, using the FugeneHD transfection reagent. The vectors were linearized to facilitate the stable integration into the genome. G418 antibiotic selection afforded stable transfectants after 2 – 3 weeks. These parental cells were subject to a second transfection using the pcDNA 4 V5-HIS B vector encoding the different receptor-ElucC constructs and subsequent antibiotic selection using zeocin.

In case of the βArr1 construct, the first transfection using a FugeneHD/DNA ratio of 9/2 (µl/µg) was successful, giving an appropriate signal after transfection with the H_2R constructs. On the contrary, the βArr2 cells (termed HEK293T βArr2 T1), gave only poor results after H_2R transfection. Therefore, the transfection was repeated using a FugeneHD/DNA ratio of 8/2 (µl/µg), varying the incubation period between the transfection and the start of the antibiotic selection from 24 to 48 h. The transfectants obtained after 24 h of incubation gave the most promising results after transfection with the H_2R (termed HEK293T βArr2 T2).

Using the three different parental cell lines, the arrestin recruitment assay was established for 5 different receptors, namely the H_1, H_2 and H_4 receptor from the histamine receptor family as well as the Y_1 and Y_2 receptor from the NPY receptor family. For the H_1R and H_4R, the cells derived from the βArr2 T1 parental cell lines gave the highest signal intensity, whereas for the H_2R, Y_1R and Y_2R the cells originating from the βArr2 T2 parental cell line were superior.

In total, 24 stable cell lines were generated. The detailed characterization of the transfectants, described below, was only performed in case of the parental cells and the receptor expressing cells used for further investigations.

3.2.2. Expression analysis of the fusion constructs

The expression levels of the ELucN-βArr and receptor-ElucC fusion proteins in the stably transfected HEK293T cells were analyzed using three different methods. Both, the arrestin and the receptor constructs, were investigated by western blot analysis. Furthermore, arrestin expression was analyzed by flow cytometry, whereas receptor expression was confirmed by radioligand saturation binding.

3.2.2.1. Western blot analysis

The stably transfected HEK293T cells were analyzed using an antibody against the c-myc tag of the arrestin fusion constructs and an antibody against the V5 epitope of the receptor fusion constructs. Whole cell extracts of the respective engineered cells and the untransfected HEK293T cells as negative control were prepared in RIPA buffer. For the detection of the arrestin fusion constructs, prior to SDS-PAGE, the samples were prepared according to a standard protocol: addition of Laemmli sample buffer followed by boiling for 5 min. However, in case of the receptor constructs, preliminary experiments revealed that this procedure was inadequate, as a large portion of the receptor constructs formed aggregates and did not migrate into the gel properly. Therefore, the incubation was performed at different temperatures, and urea was added as a chaotropic agent, facilitating the solubilization of the hydrophobic transmembrane domains. The best results were achieved by incubation at RT for 30 min in the presence of 4 M urea.

The theoretical molecular weights of the fusion constructs, calculated from their amino acid sequence, are 97 kDa for ELucN-βArr1 and ElucN-βArr2, 77 kDa for H_1R-ElucC, 62 kDa for H_2R-ElucC, 66 kDa for H_4R-ElucC and Y_1R-ElucC and 64 kDa for the Y_2R-ElucC fusion construct. The samples were analyzed on two separate gels, the first loaded with the extracts of βArr1 and βArr2 T1 parental cells as well as with those of the corresponding H_1R and H_4R expressing cells (Fig. 3-2 **A**, **B**: upper row, samples **2**-**7**). Extracts of the βArr1 and βArr2 T2 parental cells and the corresponding H_2R, Y_1R and Y_2R cells were analyzed in a second gel. (Fig. 3-2 **A**, **B**: lower row, samples **2**, **8**-**14**). Untransfected HEK293T cells were included as negative control (sample **1**). After protein transfer, the membranes were cut in two parts closely above the 50 kDa band of the prestained protein ladder. The upper part was treated with the antibodies recognizing the c-myc or the V5 epitope, while the lower part was developed with a β-actin AB and served as a loading control for the protein samples.

The ELucN-arrestin fusion proteins migrated as sharp, single bands shortly below the 100 kDa band of the biotinylated protein ladder for both, the βArr1 and βArr2 isoform (cf. Fig 3-2), in accordance with the theoretical molecular weight of the constructs. No unspecific binding of the anti c-myc AB was detected in the relevant range of the HEK293T control (**1**). The βArr1 (**2**) and βArr2 T1 (**3**) parental cells revealed comparable expression levels of the fusion proteins, whereas a considerably lower expression was found for the βArr2 T2 cells. The analysis of the receptor expressing cells revealed a drastic impact of the second transfection and the subsequent selection procedure on the expression levels of the arrestin constructs. The βArr1 + H_1R (**4**) and βArr1 + H_2R (**9**) cell lines showed a higher arrestin expression than the corresponding parental cells. By contrast, several other receptor expressing cells exhibited a distinct reduction of the expression level, most pronounced in case of the βArr2 + H_2R (**10**), βArr2 + Y_1R (**12**), and βArr1 + Y_2R cells (**13**). The receptor-ElucC fusion proteins, except for the Y_2R construct, migrated untypically, producing a smear without clearly resolved bands, which complicated the quantification of the signal intensities. In the negative control samples, no unspecific binding of the AB was detected in the relevant size range. However, in preliminary experiments conducted

without β-actin staining as loading control, the AB produced strong unspecific bands at approximately 25 and 45 kDa The H_1R construct (**4** and **5**) showed a strong diffuse band at approximately 90 kDa and two additional feint, faster migrating bands. The expression level was slightly higher in the βArr1 than the βArr2 cell line. The H_4R-ELucC proteins (**6** and **7**) produced a fuzzy band at approximately 70-80 kDa and a faint smear above and below. The expression level was higher in the βArr2 than in the βArr1 cells, but for both considerably

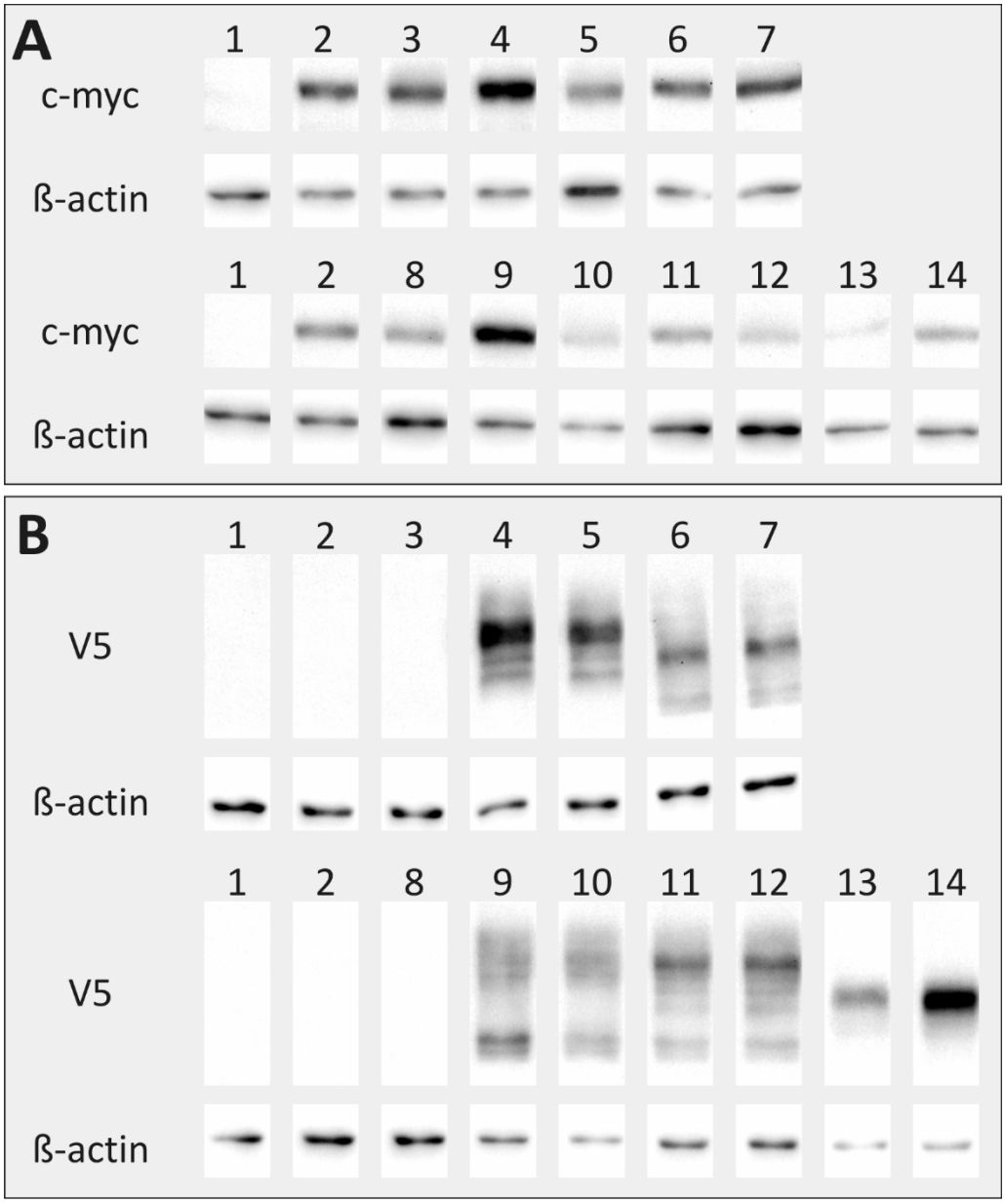

Fig. 3-2: Western blot analysis of the stably transfected HEK293T cell lines. **A**: Immunodetection using a c-myc AB against the ELucN-βArr fusion proteins. **B**: Immunodetection using a V5 AB against the receptor-ELucC fusion proteins. **A** and **B**: The lower part of the blots was developed using a β-actin AB and served as loading control. Whole cell extracts of the following cell lines were analyzed: **1**) HEK293T (untransfected); **2**) HEK293T βArr1; **3**) HEK293T βArr2 T1; **4**) HEK293T βArr1 + H_1R; **5**) HEK293T βArr2 + H_1R; **6**) HEK293T βArr1 + H_4R; **7**) HEK293T βArr2 + H_4R; **8**) HEK293T βArr2 T2; **9**) HEK293T βArr1 + H_2R; **10**) HEK293T βArr2 + H_2R; **11**) HEK293T βArr1 + Y_1R; **12**) HEK293T βArr2 + Y_1R; **13**) HEK293T βArr1 + Y_2R; **14**) HEK293T βArr2 + Y_2R.

lower than in the H_1R expressing cells. The H_2R construct (**9** and **10**) gave a faint smear from ~120-80 kDa and a slightly more distinct band shortly above 60 kDa with slightly higher overall expression in the βArr1 than in the βArr2 cells. The Y_1R-ElucC protein (**11** and **12**) gave a similar picture as the H_2R construct with a clearer band at approx. 90 kDa. The expression levels were comparable for both cell lines. The Y_2R construct (**13** and **14**) was the only one that migrated as a single defined band at ~70 kDa. The signal intensity was several times higher for the βArr2 compared to the βArr1 cells, but for both cell lines, the Y_2R expression was on a high level.

Overall, the detected migration pattern correlated poorly with the theoretical molecular masses of the receptor fusion proteins. The higher molecular masses could be explained by variations in the degree and pattern of glycosylation of the different receptors.[2,3] Moreover, the putative formation of receptor dimers was proposed as an explanation for similar observations.[4]

3.2.2.2. Flow cytometric analysis

Contrary to western blots, flow cytometry allows to analyze the expression of a target protein on a cellular level, enabling the identification of different subpopulations. For the analysis of the arrestin and the receptor fusion proteins the cells were fixed with paraformaldehyde and subsequently permeabilized by means of saponin.

The flow cytometric analysis of the ELucN-arrestin expression was performed using an anti c-myc AB and a secondary R-PE coupled AB. Forward and side scatter gating was applied to exclude cell debris and aggregates (cf. Fig. 3-3 A). The background fluorescence of the stained, untransfected HEK293T cells served as negative control, allowing for setting a cut-off gate in the relevant fluorescence channel to discriminate between positive and negative cell populations (cf. Fig. 3-3 A). The fraction of positive cells and their mean fluorescence as well as the mean fluorescence of the total cell population are given in Table 3-1. The transfected cells revealed a very inhomogeneous picture, as a high portion of negative cells was identified in case of several transfectants, e. g. 54 % of βArr1 parental cells were negative (cf. Fig. 3-3 B). The second transfection and subsequent antibiotic selection had a substantial influence on the ELucN-arrestin expression (cf. Fig. 3-3 B). For the H_1R and Y_1R receptor expressing cells, the fraction of positive cells increased considerably to 89 and 83 %, respectively, whereas for the H_4R and Y_2R expressing cells, the fraction of negative cells remained around 50 %. The mean fluorescence of the positive cell population increased for the H_2R cells, while all other cell lines exhibited a reduction compared to the parental cell line. 62 % of the HEK293T βArr2 T1 parental cells were immunopositive, and the fraction increased upon repeated transfection, giving up to 92 % positive cells with slightly elevated mean fluorescence for the corresponding H_4R cells (cf. Fig 3-3 C). For the βArr2 T2 parental cells, transfection led to an increase in the receptor positive cell population as well as the mean fluorescence thereof for the H_2R and Y_1R cell lines, while the Y_2R cell line showed a lower fraction of positive cells, although with an considerably increased mean fluorescence intensity(cf. Fig 3-3 D).

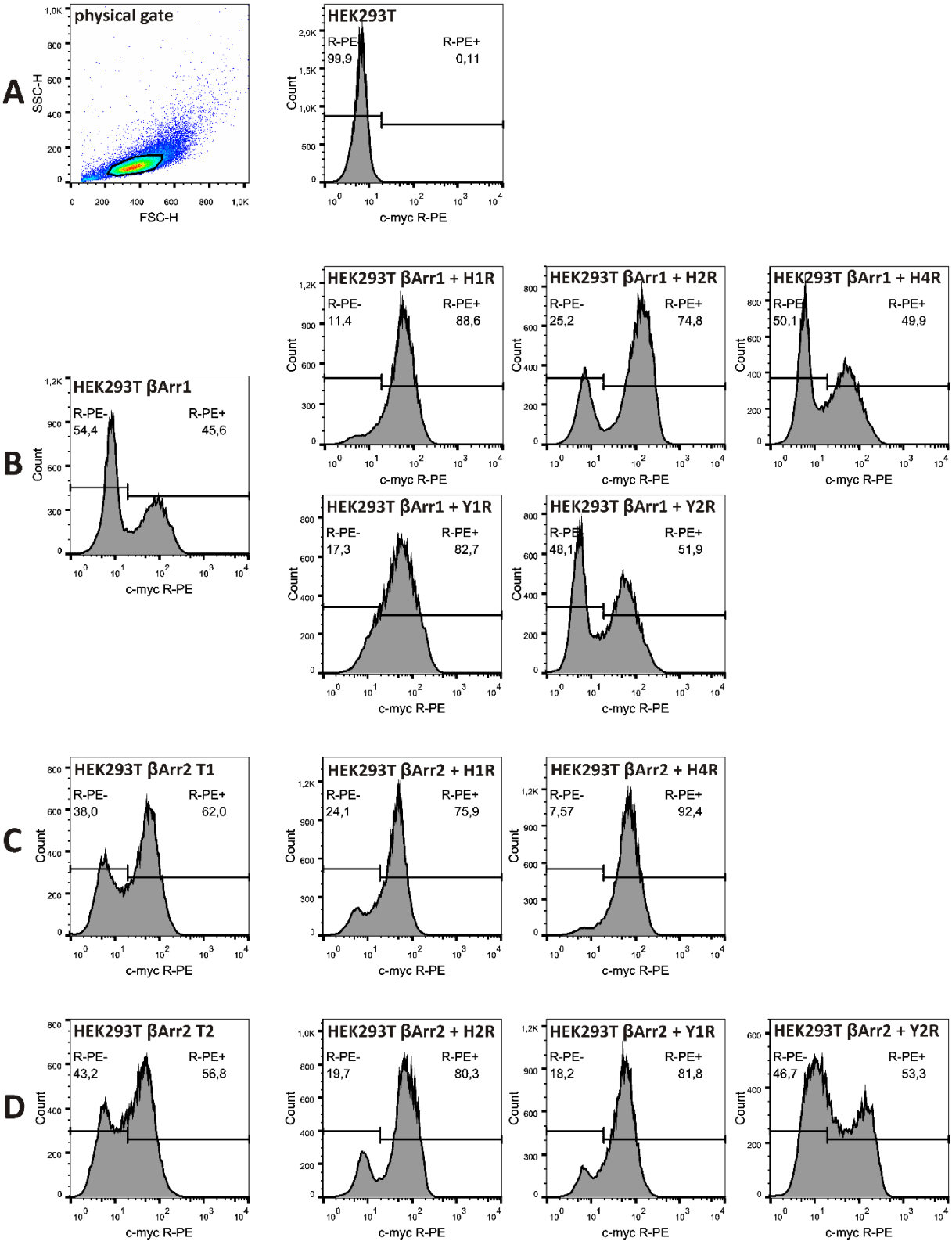

Fig. 3-3: Flow cytometric analysis of ELucN-arrestin expression using the c-myc AB. **A**: Physical gate and background fluorescence of the stained HEK293T negative control. **B**: ELucN-arrestin expression by the HEK293T βArr1 parental cell line and the receptor cell lines derived therefrom. **C**: ELucN-arrestin expression of the HEK293T βArr2 T1 parental cells and the receptor expressing cells derived therefrom. **D**: ELucN-arrestin expression of the HEK293T βArr2 T2 parental cells and the receptor expressing cells derived therefrom.

Table 3-1: Flow cytometric analysis of the ELucN-arrestin expression. The percentage of cells giving a positive R-PE signal as well as the mean fluorescence of the R-PE positive and total cell population is given.

Cell line	% R-PE + cells	mean fluorescence (R-PE + cells)	mean fluorescence (total cells)
HEK293T	0.1		6.9
HEK293T βArr1	45.6	93.0	47.2
HEK293T βArr1 + H_1R	88.6	69.5	62.7
HEK293T βArr1 + H_2R	74.8	142	108
HEK293T βArr1 + H_4R	49.9	71.6	39.5
HEK293T βArr1 + Y_1R	82.7	79.8	68.0
HEK293T βArr1 + Y_2R	51.9	78.3	44.0
HEK293T βArr2 T1	62.0	66.2	44.1
HEK293T βArr2 + H_1R	75.9	51.7	41.5
HEK293T βArr2 + H_4R	92.4	79.4	74.2
HEK293T βArr2 T2	56.8	54.8	34.8
HEK293T βArr2 + H_2R	80.3	84.9	70.0
HEK293T βArr2 + Y_1R	81.8	64.6	54.6
HEK293T βArr2 + Y_2R	53.3	104	59.9

Unfortunately, due to the lack of a suitable antibody, analysis of the receptor-ElucC constructs by analogy with the procedure used for the ElucN-arrestin expression was impossible. Three different anti V5 antibodies were tested in the flow cytometric analysis, all of them revealed very high unspecific binding at the HEK293T cells used as negative control. Reduction of the photomultiplier voltage failed to discriminate between transfected and untransfected cells. In western blot analysis, all three antibodies produced a similar pattern of unspecific bands.

3.2.2.3. [^{3}H]Mepyramine saturation binding at the H_1R expressing cells

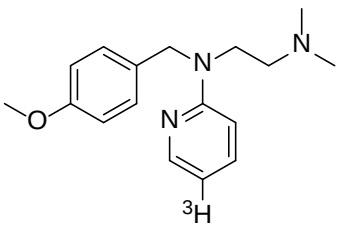

Fig. 3-4: Structure of [^{3}H]mepyramine

[^{3}H]Mepyramine bound in a specific, saturable manner to both the HEK293T βArr1 + H_1R and the HEK293T βArr2 + H_1R cells. Unspecific binding was determined in the presence of 10 µM diphenhydramine and accounted for less than 12 % of total binding at radioligand concentrations up to 80 nM. The determined K_D values for [^{3}H]mepyramine, 4.5 nM at the HEK293T βArr1 + H_1R and 4.4 nM at the HEK293T βArr2 + H_1R cells, are in accordance with data reported in literature.[2,5] The determined B_{max} values allowed the calculation of the number of

specific binding sites per cell, revealing a comparably high receptor expression level for both cell lines, $5.5 \cdot 10^5$ receptors/cell for the HEK293T βArr1 + H_1R and $4.7 \cdot 10^5$ receptors/cell for the HEK293T βArr2 + H_1R cells, respectively.

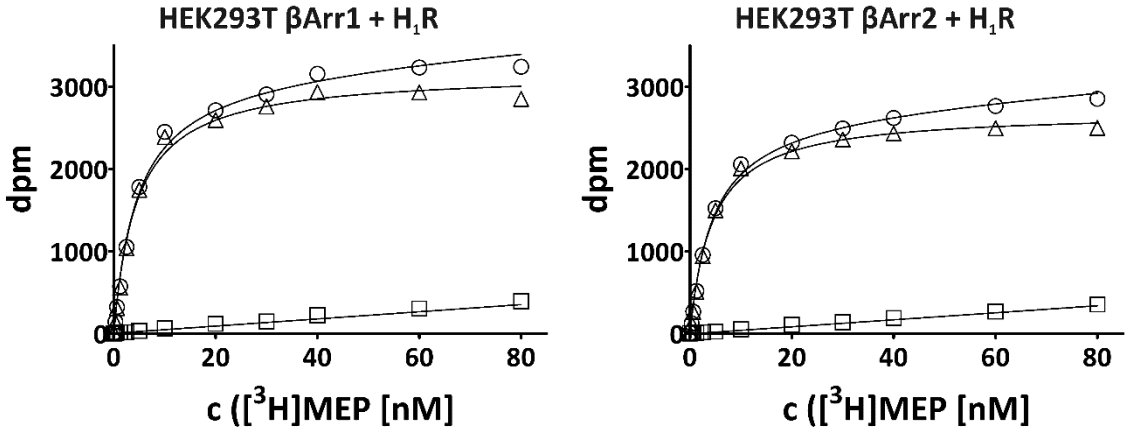

Fig. 3-5: [^{3}H]Mepyramine saturation binding experiments using HEK293T βArr1 + H_1R and HEK293T βArr2 + H_1R cells. Total (circles), specific (triangles) and unspecific (squares) binding was fitted by nonlinear regression to a one site saturation binding model. Unspecific binding was determined in the presence of diphenhydramine (10 µM). Data are mean values ± SEM of a single experiment performed in triplicates.

3.2.2.4. [^{3}H]UR-DE257 saturation binding at the H_2R expressing cells

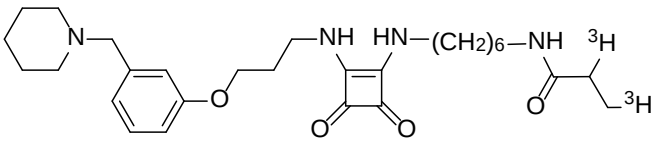

Fig. 3-6: Structure of [^{3}H]UR-DE257

[^{3}H]UR-DE257 bound in a specific, saturable manner to both the HEK293T βArr1 + H_2R and HEK293T βArr2 + H_2R cells. Unspecific binding, determined in the presence of 10 µM famotidine, accounted for up to 48 % of the total binding at a radioligand concentration of 150 nM at the HEK293T βArr2 + H_2R and 31 % at the HEK293T βArr1 + H_2R cells, respectively. The determined K_D value of 17 nM at the βArr2 cells was considerably lower than that at the βArr1 cells (K_D = 44 nM). This discrepancies are probably caused by the high unspecific binding at the βArr2 cells, as the determined K_D value at the HEK293T βArr1 + H_2R cells correlated well with previous findings either using *Sf*9 membranes expressing H_2R-$G_{s\alpha S}$ fusion proteins (K_D = 31 nM) or HEK293T CRE-Luc hH_2R cells (K_D = 55 nM).[6] The calculation of the binding sites yielded an expression level of $4.0 \cdot 10^5$ receptors/cell for the HEK293T βArr1 + H_2R cells and $2.9 \cdot 10^5$ receptors/cell for the HEK293T βArr2 + H_2R cells.

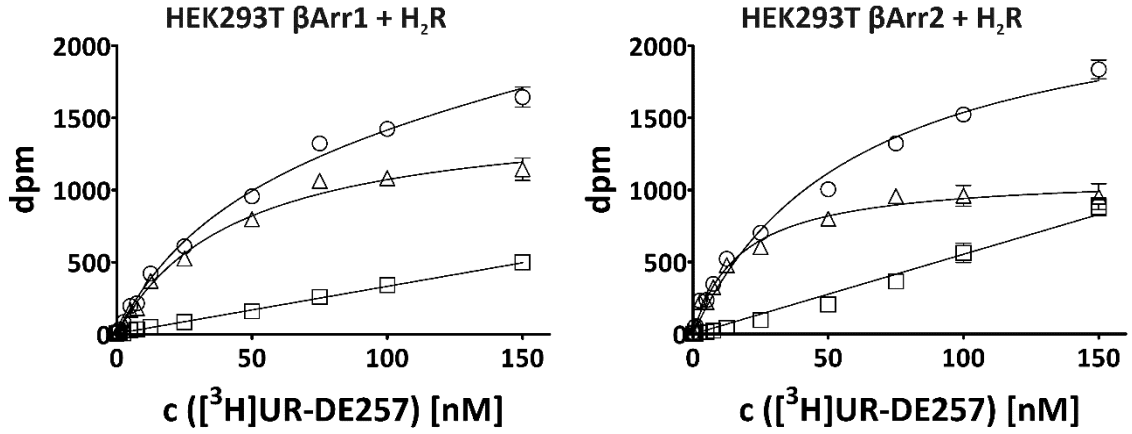

Fig. 3-7: [^{3}H]UR-DE257 saturation binding experiment using the HEK293T βArr1 + H_2R and HEK293T βArr2 + H_2R cell lines. Total (circles), specific (triangles) and unspecific (squares) binding was fitted by nonlinear regression to a one site saturation binding model. Unspecific binding was determined in the presence of famotidine (10 µM). Data are mean values ± SEM of a single experiment performed in triplicates.

3.2.2.5. [^{3}H]Histamine saturation binding at the H_4R expressing cells

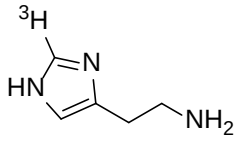

Fig. 3-8: Structure of [^{3}H]histamine

[^{3}H]Histamine bound in a specific, saturable manner to both the HEK293T βArr1 + H_4R and HEK293T βArr2 + H_4R cells. Unspecific binding, determined in the presence of 10 µM thioperamide, was accounted for up to 48 % of the total binding at the HEK293T βArr1 + H_4R and 39 % at the HEK293T βArr2 + H_4R cells. The determined K_D values, 23 nM at the HEK293T βArr1 + H_4R and 39 nM at the HEK293T βArr2 + H_4R cells, were considerably higher than previously reported.[4,7,8] The B_{max} values for the [^{3}H]histamine binding at the H_4R were substantially lower than for the saturation binding experiments at the H_1R and H_2R expressing cells; the

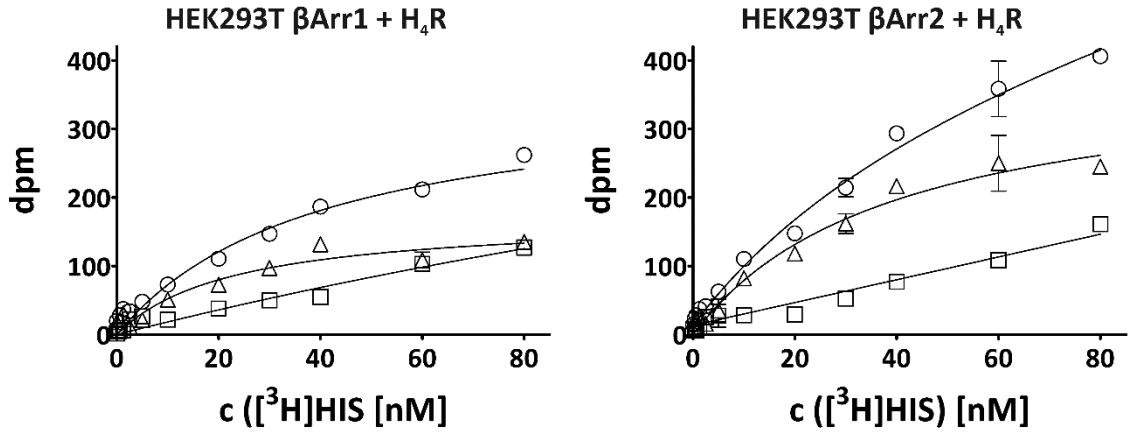

Fig. 3-9: [^{3}H]Histamine saturation binding experiment using the HEK293T βArr1 + H_4R and HEK293T βArr2 + H_4R cells. Total (circles), specific (triangles) and unspecific (squares) binding was fitted by nonlinear regression to a one site saturation binding model. Unspecific binding was determined in the presence of thioperamide (10 µM). Data are mean values ± SEM of a single experiment performed in triplicates.

expression levels amounted to $3.7 \cdot 10^4$ receptors/cell for the HEK293T β-Arr1 + H_4R and $8.1 \cdot 10^4$ receptors/cell for the HEK293T β-Arr2 + H_4R cells.

3.2.2.6. [^{3}H]UR-MK136 saturation binding at the Y_1R expressing cells

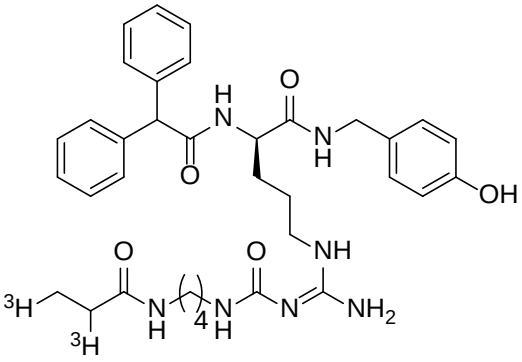

Fig. 3-10: Structure of [^{3}H]UR-MK136

[^{3}H]UR-MK136 bound specifically to both the HEK293T βArr1 + Y_1R and HEK293T βArr2 + Y_1R cells. Unspecific binding was determined in the presence of 1 µM BIBO3304 and was well controlled, accounting for less than 25 % in the used concentration range. [^{3}H]UR-MK136 binding was not saturable at the investigated cells at concentrations up to 8 nM. Unfortunately, higher concentration of the radioligand failed to determine specific binding, a phenomenon often associated with the existence of a second, low affinity binding site for the radioligand. The determined K_D values, 24 nM at the HEK293T βArr1 + Y_1R and 11 nM at the HEK293T βArr2 + Y_1R cells, are considerably higher than previously reported for different cellular backgrounds (2.0 nM at SK-NM-C cells and 6.2 nM at MCF-7-Y_1 cells). The receptor expression calculated from the B_{max} values, $1.4 \cdot 10^5$ receptor/cell at the HEK293T βArr1 + Y_1R and $1.0 \cdot 10^5$ receptor/cell at the HEK293T βArr2 + Y_1R cells, was on an average level. Unfortunately, the reliability of both, the determined K_D and B_{max} values, is challenged by the insufficient concentration range for a saturation binding experiment. Especially the B_{max} values estimated with the GraphPad Prism software were considerably higher as the highest experimentally determined specific binding value.

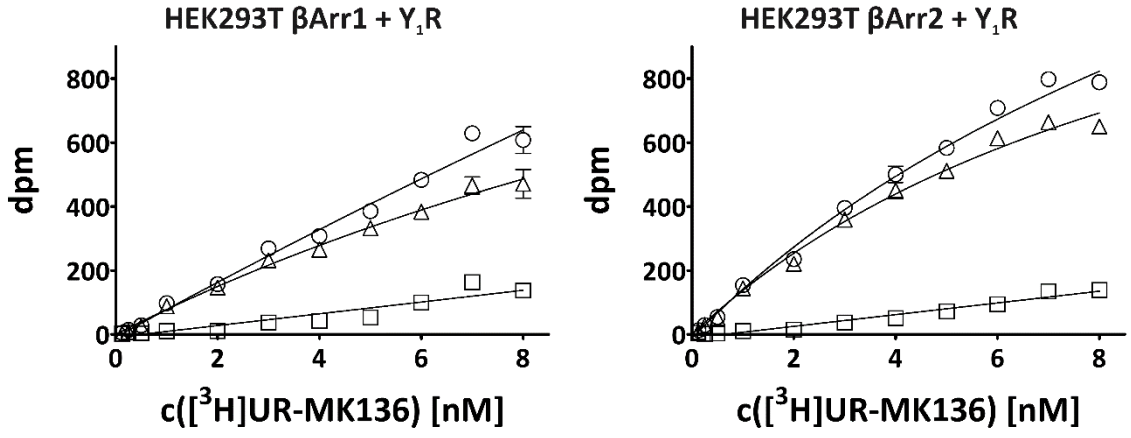

Fig. 3-11: [^{3}H]UR-MK136 saturation binding experiment using the HEK293T βArr1 + Y_1R and HEK293T βArr2 + Y_1R cells. Total (circles), specific (triangles) and unspecific (squares) binding was fitted by nonlinear regression to a one site saturation binding model. Unspecific binding was determined in the presence of BIBO3304 (1 µM). Data are mean values ± SEM of a single experiment performed in triplicates.

3.2.2.7. [^{3}H]UR-PLN187 saturation binding at the Y_2R expressing cells

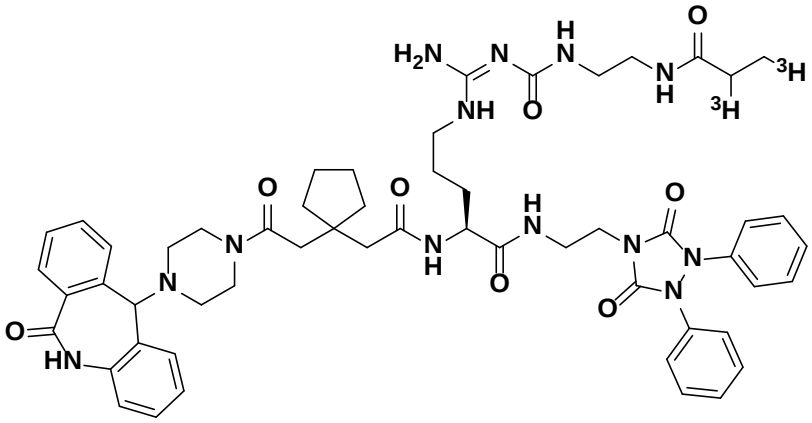

Fig. 3-12: Structure of [^{3}H]UR-PLN187

[^{3}H]UR-PLN187 bound in a specific, saturable manner to both the HEK293T βArr1 + Y_2R and the HEK293T βArr2 + Y_2R cells. Unspecific binding, determined in the presence of 10 µM JNJ31020028, accounted for up to 56 % of the total binding at a radioligand concentration of 90 nM at the HEK293T βArr1 + Y_2R and 32 % at the HEK293T βArr2 + Y_2R cells, respectively. The differences in the determined K_D values, 37 nM at the HEK293T βArr1 + Y_2R and 71 nM at the HEK293T βArr2 + Y_2R cells, are probably caused by the substantially lower specific binding at the HEK293T βArr1 + Y_2R cells and, thus, high portion of unspecific binding. Additionally, the saturation binding experiment could not be carried out at higher radioligand concentrations, as the unspecific binding increased excessively at concentrations above 90 nM, preventing the generation of meaningful binding data. Receptor expression was calculated to $8.3 \cdot 10^5$ receptors/cell for the HEK293T βArr1 + Y_2R and $2.1 \cdot 10^6$ receptors/cell for the HEK293T βArr2 + Y_2R cells, thus showing the highest receptor expression level of all cells investigated in this project, although the reliability is likewise questioned by the insufficient concentration range.

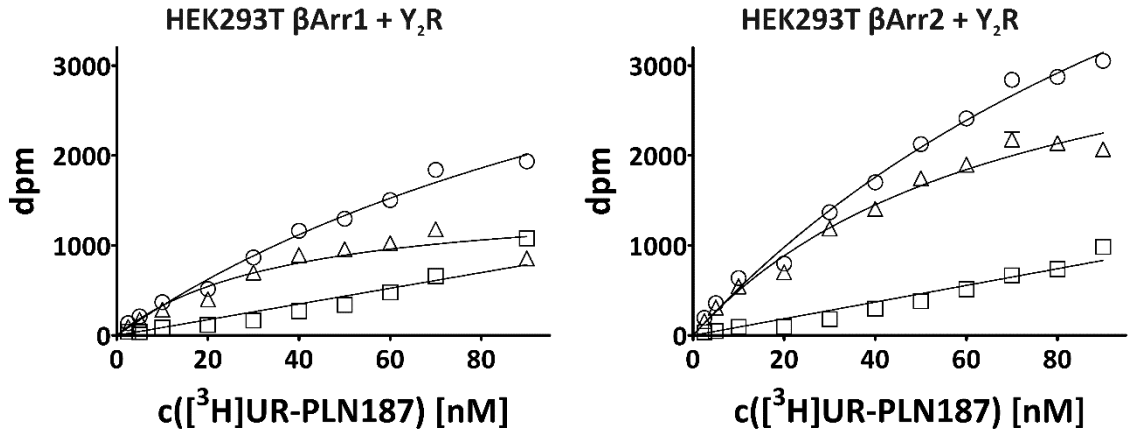

Fig. 3-13: [^{3}H]UR-PLN187 saturation binding experiment using the HEK293T βArr1 + Y_2R and HEK293T βArr2 + Y_2R cells. Total (circles), specific (triangles) and unspecific (squares) binding was fitted by nonlinear regression to a one site saturation binding model. Unspecific binding was determined in the presence of JNJ31020028 (10 µM). Data are mean values ± SEM of a single experiment performed in triplicates.

3.2.2.8. Overview of the receptor expression levels determined by radioligand binding

Table 3-2: receptor expression levels calculated from the B_{max} values

Cell line	receptors/cell (/10^5)
βArr1 + H_1R	5.5
βArr2 + H_1R	4.7
βArr1 + H_2R	4.0
βArr2 + H_2R	2.9
βArr1 + H_4R	0.4
βArr2 + H_4R	0.8
βArr1 + Y_1R	1.4
βArr2 + Y_1R	1.0
βArr1 + Y_2R	8.3
βArr2 + Y_2R	21

The receptor expression levels for the different cell lines, given in Table 3-2 were calculated from the B_{max} values derived from the corresponding saturation binding experiments. The expression levels differed considerably. The lowest expression was found for the H_4R with only 40000, respectively, 80000 receptors/cell, while for the Y_2R, up to 2.1 million receptors/cell were found. Unfortunately, some of the saturation binding experiments could not be performed at sufficiently high radioligand concentration, especially for the Y_1R and Y_2R, thus impairing the reliability of the determined expression levels.

3.2.2.9. Comparison of the expression levels

The expression of the receptor constructs was verified by western blot and radioligand saturation binding. For the 5 different receptors, the results from both analytical methods correlated well. For the H_1R, radioligand binding revealed a higher number of binding sites/cell for the βArr1 compared to the βArr2 cells, coinciding with the corresponding intensities detected in the western blot analysis. A similar correlation was found for the H_2R and Y_1R cells in both readouts. For the H_4R, the lowest receptor expression of all cell lines was determined in radioligand binding and confirmed by the low intensity in the western blot, especially, when the strong bands of the loading control were taken into account. For the Y_2R, by far the highest number of receptors/cell was found in radioligand binding, although the reliability of the determined B_{max} values was questionable due to the insufficient concentration range in the respective saturation binding experiments. However, a high expression level was confirmed in the western blot analysis, where a very strong signal relative to the loading control was found, especially for the βArr2 cells.

The comparison of the expression data for the ELucN-arrestin constructs derived from western blot and flow cytometric analysis was more complicated. Flow cytometric analysis allows to investigate expression levels at a cellular level, enabling the identification of different subpopulations. However, the obtained fluorescence values are difficult to quantify in terms of expression levels. The most suitable measure for flow cytometric quantification of the average expression level is the mean fluorescence of the total cell population, although a rather contrived value for cell lines with different subpopulations.

The mean fluorescence correlated well with the signal intensities in the western blot when comparing the different cell lines for each individual receptor, but globally, much more pronounced differences became obvious from western blot analysis compared to flow cytometry.

3.2.3. Optimization of the assay conditions

3.2.3.1. Influence of DMSO on the assay performance

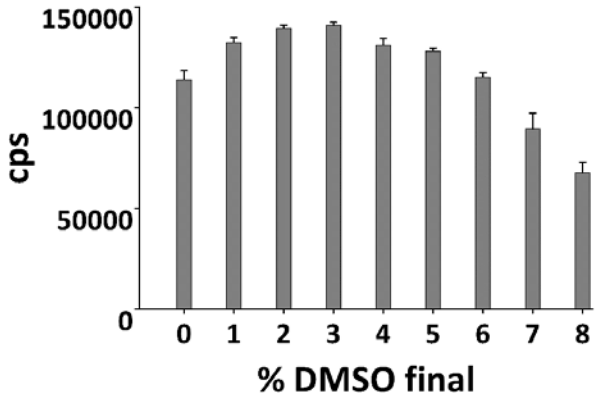

Fig. 3-14: Influence of increasing concentrations of DMSO on the luciferase signal intensity of the β-arrestin recruitment assay. HEK293T βArr1 + H_2R were stimulated by 100 µM histamine and the indicated concentrations of DMSO. Data are mean values ± SEM of quadruplicates.

Many ligands for the histamine and neuropeptide Y receptors are rather lipophilic compounds exhibiting poor solubility in aqueous solutions and therefore require the use of DMSO as solvent for the preparation of higher concentrated stock solutions. As DMSO can strongly influence the performance of cellular assays, the tolerance of the arrestin recruitment assay against DMSO was explored. For this purpose, the HEK293T βArr1 + H_2R cells were stimulated with 100 µM of histamine in the presence of up to 8 % (*v/v*) DMSO. Concentrations of DMSO up to 3 % led to an increase in the luciferase signal intensity and up to 6 % were well tolerated. By contrast, DMSO concentrations exceeding 6 %, resulted in a considerable drop in signal intensity. Therefore, while DMSO at the relevant concentrations did not impair the arrestin recruitment assay, care had to be taken with regard to the normalization of the data. Thus, the raw data for the respective ligands were normalized to the maximal effect induced by the endogenous ligand and the solvent, both containing the corresponding amount of DMSO. Furthermore, the DMSO concentration was kept constant within the dilution series.

3.2.3.2. Time dependence of β-arrestin recruitment

In order to determine the optimal incubation period for the arrestin recruitment assay, the time course of the signal intensity after ligand stimulation was investigated. Hereby, the different receptors in combination with the two arrestin isoforms exhibited rather divergent characteristics. At the H_1R, the recruitment of both βArr1 and βArr2 followed a similar time course with the maximal signal intensity after approximately 60 min. In combination with the H_2R, the two arrestin isoforms differed considerably. The

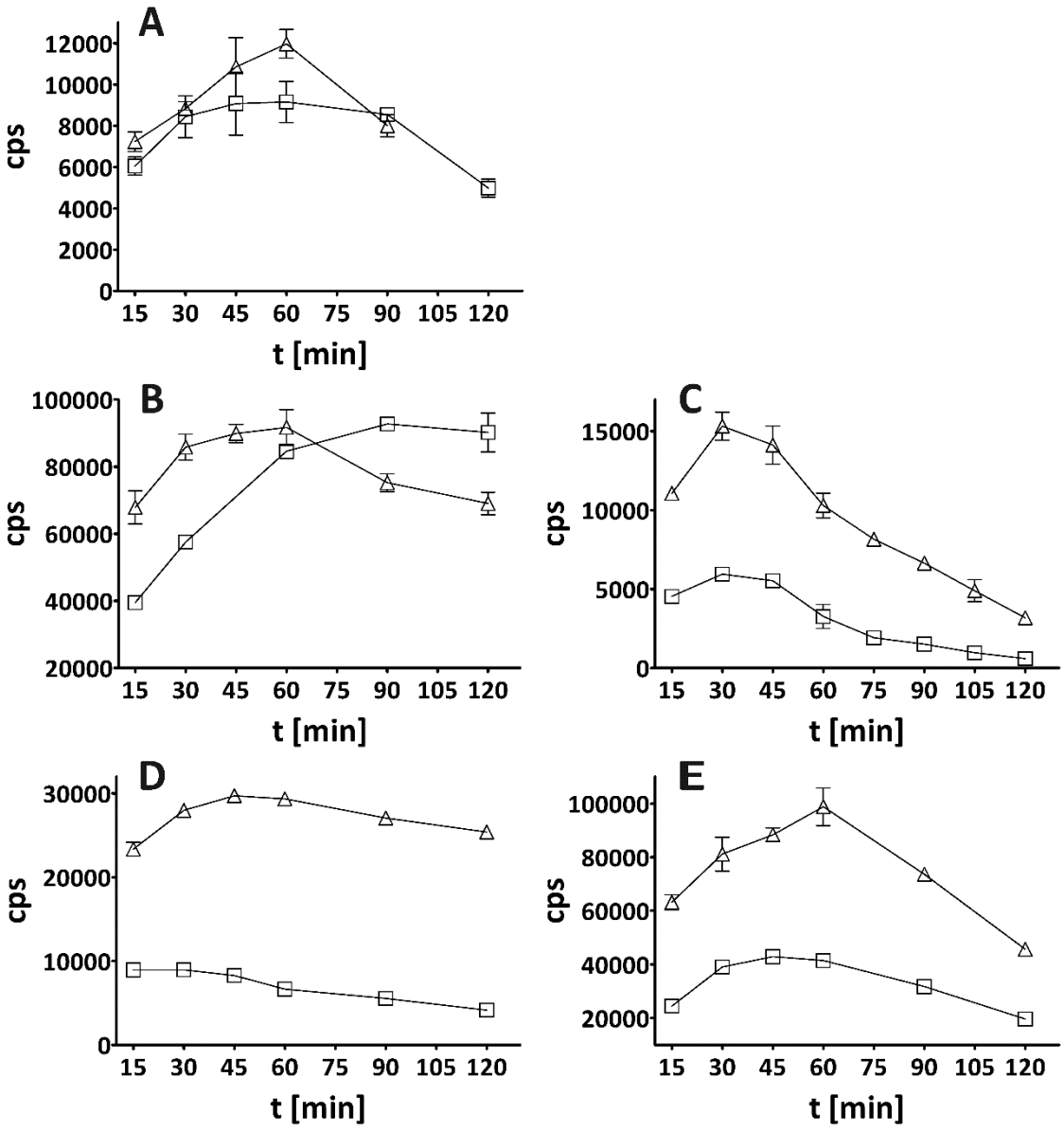

Fig. 3-15: Time dependence of the β-arrestin recruitment assay after stimulation with 100 µM histamine (**A**, **B**, **C**) or 1 µM NPY (**D**, **E**). **A**: Stimulation of the HEK293T βArr1 + H_1R (squares) or HEK293T βArr2 + H_1R (triangles) cells; **B**: Stimulation of the HEK293T βArr1 + H_2R (squares) or HEK293T βArr2 + H_2R (triangles) cells; **C**: Stimulation of the HEK293T βArr1 + H_4R (squares) or HEK293T βArr2 + H_4R (triangles) cells; **D**: Stimulation of the HEK293T βArr1 + Y_1R (squares) or HEK293T βArr2 + Y_1R (triangles) cells; **E**: Stimulation of the HEK293T βArr1 + Y_2R (squares) or HEK293T βArr2 + Y_2R (triangles) cells. Data are mean values ± SEM of a single experiment.

onset of βArr1 recruitment was rather slow, the signal reached maximum intensity only after 90 min and remained constant for up to 120 min. βArr2 recruitment already reached high levels after 30 min with the maximum after 60 min and showed a slow decrease in signal intensity with longer incubation periods. At the H_4R, both isoforms, while differing in absolute signal intensity, showed a similar characteristic. The signal reached maximum intensity already after 30 min and quickly decreased after 45 min. At the Y_1R, βArr2 recruitment gave a maximum signal intensity after 45 min, only slowly degrading with longer incubation time and retaining at more than 80 % of the maximal signal even after 120 min. The βArr1 cell line produced a much lower signal of constant intensity for up to 45 min incubation time, slowly degrading afterwards. At the Y_2R, both isoforms exhibited a similar time course, with the signal intensity reaching a maximum after 45-60 min, followed by a pronounced decline with longer incubation times. The incubation times for the investigation of ligands were adapted accordingly to achieve maximal signal intensity with each of the cell lines.

3.2.3.3. General considerations

The luciferase complementation assay was performed using the BrightGlo luciferase assay reagents from Promega. As the reagent was added to the cells at a 1:1 ratio with respect to the assay mixture, 50 µl were removed from each well prior to BrightGlo addition, giving a final volume of 100 µl. This step had only a marginal effect on the signal intensity, but cut the reagent consumption and thus costs of the assay by 50 %. The adaption of the workup procedure according to a luciferase reporter gene assay established in our lab[9] was not successful, as the self-complemented luciferase was unstable under the harsher assay conditions, so that little to no bioluminescence was detectable. Furthermore, the reconstituted luciferase revealed thermal instability, as incubation at 37 °C after ligand addition completely abolished the bioluminescence signal. Therefore, incubation was carried out using a plate shaker tempered to 25 °C in an air-conditioned laboratory to avoid temperature related variation in assay performance.

3.2.4. Signal intensities and signal-to-noise ratios

Fig. 3-16 gives a summary of the signal intensities achieved in the luciferase complementation assay using the stably transfected HEK293T cells expressing the different receptor constructs in combination with either one of the arrestin fusion proteins. The absolute signal intensities differed tremendously between the individual cell lines, from more than 220 000 cps for the H_2R expressing cells with either arrestin isoform to only about 4000 cps for the βArr1 + H_4R cells. Fortunately, the background noise was well controlled in this assay. In the worst case i. e. with HEK293T βArr2 + H_1R cells, the maximal signal was about 7 fold above the noise level, whereas with HEK293T βArr1 + Y_1R cells a signal-to-noise ratio higher than 200 was achieved.

Table 3-3: Signal-to-noise ratios of the luciferase complementation assay

Cell line	signal/noise ratio
HEK293T βArr1 + H_1R	34
HEK293T βArr2 + H_1R	7
HEK293T βArr1 + H_2R	17
HEK293T βArr2 + H_2R	14
HEK293T βArr1 + H_4R	14
HEK293T βArr2 + H_4R	11
HEK293T βArr1 + Y_1R	277
HEK293T βArr2 + Y_1R	215
HEK293T βArr1 + Y_2R	119
HEK293T βArr2 + Y_2R	57

The differences between the signal intensities in the luciferase complementation assay found for the different receptors cannot be explained by varying expression of the necessary protein constructs. For example, both H_1R expressing cell lines showed comparable or higher expression levels of both, the receptor and arrestin constructs, with those of the corresponding H_2R cell lines, but produced only a fraction of the signal in the arrestin recruitment assay. In case of the Y_1R receptor, the bioluminescence signal was distinctly dependent on the co-expressed arrestin isoform, with an 8-fold higher signal intensity for βArr2 than βArr1 recruitment, despite comparable expression levels of the constructs in both cell lines.

These findings might point towards basal differences in receptor-arrestin interaction inherent for the individual receptors, although the exact nature of these effects remains elusive.

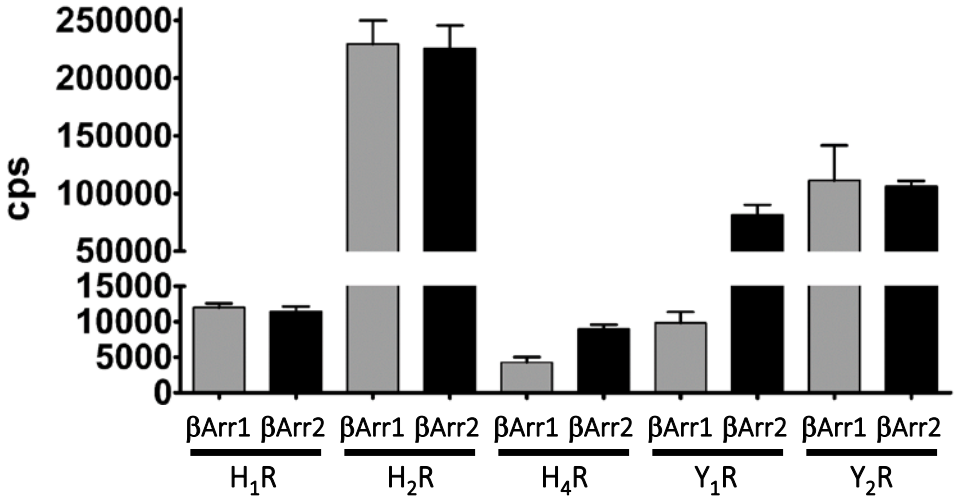

Fig. 3-16: Maximum signal intensities of the different transfectants in the luciferase complementation assay after stimulation with the endogenous ligands, i. e. histamine for the H_xR cells and NPY for the Y_xR cells.

3.3. Summary and conclusions

The luciferase complementation assay proved to be a versatile and reliable method to measure arrestin recruitment to the receptor. Adapted for the investigation of three histamine and two NPY receptor subtypes, the assay worked reliably and with very low noise. The expression of the ELucN-arrestin fusion constructs was verified by western blot and flow cytometry in all transfectants. In addition, the expression of the receptor-ELucC fusion constructs was demonstrated by western blot analysis and saturation binding experiments using radioligands suitable for the individual receptors. The implementation of the 96 well microtiter format provides the throughput necessary to enable the investigation of a multitude of compounds within a short period of time. Furthermore, the employed modular approach will allow for a convenient adaption of the assay to different GPCRs in subsequent projects.

3.4. Materials and methods

3.4.1. Materials

Unless stated otherwise, all chemicals and reagents were from Sigma-Aldrich Chemie (Munich, Germany) or Merck (Darmstadt, Germany). FCS and G418 sulfate were from Biochrom (Berlin, Germany). Zeocin was from Thermo Fisher Scientific (Rockford, IL, USA). PvuI restriction enzyme was from New England Biolabs (Frankfurt a.M., Germany). QIAquick PCR Purification Kit was from Qiagen (Hilden, Germany). Fugene HD transfection reagent was from Roche Diagnostics (Mannheim, Germany). The DC protein assay kit was purchased from Bio-Rad Laboratories (Munich, Germany), BSA (Albumin bovine Fraction V receptor grade) was from Serva Electrophoresis (Heidelberg, Germany). Biotinylated Protein Ladder (9-200 kDa) was from Cell Signaling Technology (Danvers, MA, USA). The precision plus protein dual color standard was from Bio-Rad Laboratories (Munich, Germany). Pierce 9E10 mouse anti c-myc antibody, life technologies mouse anti c-myc mAb, Pierce V5 tag AB (E10/V4RR) from mouse and life technologies mouse anti V5 mAb were from Thermo Fisher Scientific (Rockford, IL, USA). AbD-Serotec mouse anti V5-TAG: DyLight549 was from Bio-Rad Laboratories (Munich, Germany). β-actin (13E5) rabbit mAb was from Cell Signaling Technology (Danvers, MA, USA). Anti mouse IgG HRP conjugated was from Sigma-Aldrich Chemie (Munich, Germany). Donkey anti-rabbit IgG-HRP (sc-2305) was from Santa Cruz Biotechnology (Dallas, TX, USA) Pierce ECL Western Blotting substrate was from Thermo Fisher Scientific (Rockford, IL, USA). [^{3}H]Mepyramine and [^{3}H]histamine were from Hartmann Analytic (Braunschweig, Germany). The radioligands [^{3}H]UR-DE257, [^{3}H]UR-MK136 and [^{3}H]UR-PLN187 were synthesized in our lab.[6,10,11] Diphenhydramine was from Sigma-Aldrich Chemie (Munich, Germany). Famotidine was from Sigma (St Lois, MO, USA). Thioperamide was from Tocris Bioscience (Ellisville, MO, USA). BIBO3304 JNJ31020028 were synthesized in our lab. BrightGlo luciferase assay reagent was from Promega (Mannheim, Germany).

3.4.1.1. Plasmids

The plasmids encoding the arrestin and receptor fusion constructs were kindly provided by Prof. Dr. Takeaki Ozawa from the Department of Chemistry, School of Science, University of Tokyo. Fig. 3-17 gives an overview of the plasmids used in this thesis as well as the utilized expression vectors and the employed cloning strategy. For the expression of the ELucN-arrestin constructs, the pcDNA 3.1 myc-HIS B vector, allowing the expression of the fusion protein under control of the highly active CMV promoter, was used. Furthermore, the vector comprises the neomycin resistance gene, allowing the generation of stable transfectants via G418 antibiotic selection. The receptor-ELucC fusion constructs were cloned into the pcDNA 4 V5 HIS B vector, providing the zeocin resistance gene for antibiotic selection. The arrestin fusion proteins include a c-myc epitope tag for antibody recognition as well as a C-terminal hexahistidine tag for increased proteolytic stability. The

receptor fusion proteins instead were expressed with a V5 epitope tag for antibody recognition and the C-terminal hexahistidine tag.

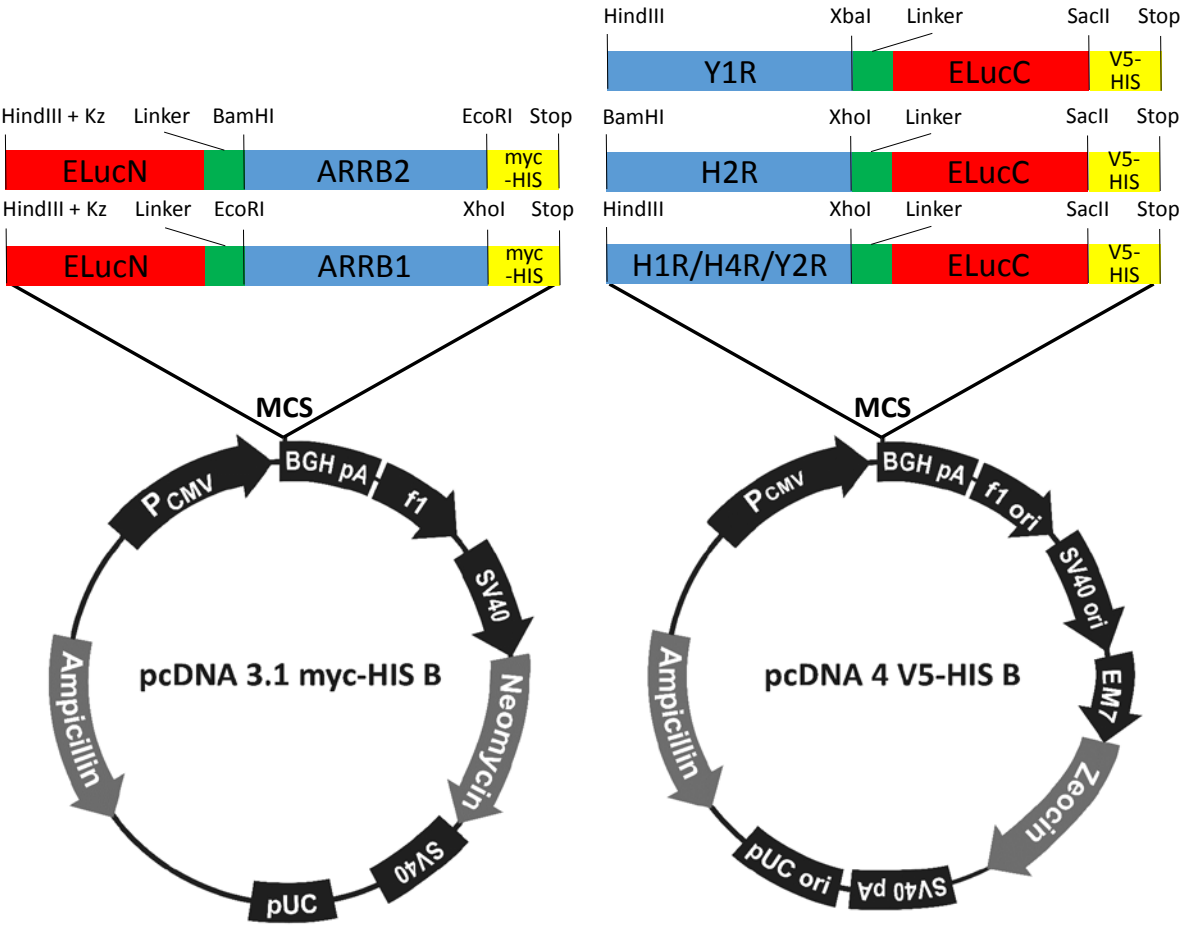

Fig. 3-17: Maps of the used eukaryotic expression vectors pcDNA 3.1 myc-HIS B and pcDNA 4 V5-HIS B including the β-arrestin and receptor fusion constructs. The restriction sites used for cloning are given in the common nomenclature.

3.4.2. Cell culture

HEK293T cells were cultivated in Dulbecco's Modified Eagle Medium containing L-glutamine, 4.5 g/L glucose, 3.7 g/L $NaHCO_3$, 110 mg/L sodium pyruvate (DMEM) and 10 % (v/v) FCS at 37 °C in a water saturated atmosphere containing 5 % CO_2. Whenever necessary, cells were detached by treatment with 0.05 % trypsin, 0.02 % EDTA in PBS (137 mM NaCl, 2.7 mM KCl, 10 mM Na_2HPO_4, 2 mM KH_2PO_4, pH 7,4) and diluted as needed in fresh DMEM + 10 % FCS. For the HEK293T cells transfected with the β-arrestin constructs in the pcDNA 3.1 myc-HIS (B) vector, 600 µg/ml G418 were added to the media. In case of the cells co-transfected with the receptor constructs in the pcDNA 4 V5-HIS (B) vector, 400 µg/ml zeocin were additionally added. For storage, logarithmically growing cells were harvested and resuspended in DMEM + 10 % FCS +10 % (v/v) DMSO. Aliquots were slowly cooled down to -80 °C prior to storage in the vapor phase of liquid nitrogen.

3.4.3. Stable transfection of HEK293T cells

The plasmids for the transfection of the HEK293T cells were linearized prior to use in order to promote integration of the gene constructs into the genome. The plasmids were digested with the restriction enzyme PvuI for 3 h at 37 °C. The mixture contained 40 µg plasmid DNA, 5 µl NEB4 buffer, 0.5 µl 100x BSA, 2 µl PvuI brought to 50 µl with sterile filtered H_2O. Afterwards, the linearized plasmids were purified using the QIAquick PCR Purification Kit according to manufacturer´s instructions. 24 h prior to the transfection, the HEK293T cells were seeded in 2 ml DMEM + 10 % FCS into 6 well plates at a density of 1 mio cells/well. For the transfection, Fugene HD transfection reagent was used. DMEM was added to 2 µg of plasmid DNA to a total volume of 100 µl, and thoroughly mixed before the addition of 6 – 9 µl of Fugene HD transfection reagent. After incubation for 15 min at RT, the transfection mixture was added in a drop wise manner to the cells. The cells were then incubated for 24 or 48 h at 37 °C in a water saturated atmosphere containing 5 % CO_2 before starting with the antibiotic selection. Cells transfected with the pcDNA 3.1 myc-HIS (B) vector were cultivated in the presence of 600 µg/ml G418 for up to 3 weeks until stable growth was observed. For the cells transfected with the pcDNA 4 V5-HIS (B) vector, 400 µg/ml zeocin was used.

3.4.4. Western blot analysis

3.4.4.1. Sample preparation

The HEK293T cells were seeded in 75-cm^2 tissue culture flasks and cultivated for 2 to 3 days in DMEM + 10% FCS to a confluence of about 60-90 %. The cells were then washed 3 times with ice cold PBS and subsequently lysed with 1 ml of RIPA buffer(20 mM Tris/HCl pH 7.8, 200 mM NaCl, 1 mM EGTA, 1 mM, 1 % w/v Triton X-100, 5 mM K_2HPO_4, 1 x protease inhibitor mix (Sigma)). The crude mixture was transferred to 1.5-ml reaction vessels and incubated on ice for 20 min. During this period, the vessels were vigorously vortexed several times. The cell debris was removed by centrifugation (13000 g, 5 min). The supernatant was mixed with 10 % (*v/v*) glycerol, and aliquots were frozen and stored at -80 °C.

The protein content of the samples was determined using the DC protein assay kit (Bio-Rad) according to manufacturer's instructions. The samples were 10-fold diluted with PBS, and a dilutions series of BSA up to 1.5 mg/ml was used to construct a calibration curve. The assay was performed in clear, flat bottom 96-well micro titer plates and the absorbance was measured at a wavelength of 700 nm using the Sunrise remote plate reader (Tecan Austria, Grödig, Austria).

3.4.4.2. SDS-PAGE

The protein samples were analyzed by SDS-PAGE on a 12 % acrylamide gel according to the general procedure established by Laemmli et al.[12] The solution for the preparation of two small 12 % gels was prepared by mixing 5.3 ml of water, 4 ml of buffer A (1.5 M Tris/HCl pH 8.8, 0.4 % (*w/v*) SDS), 6.2 ml of 30 % acrylamide/ bisacrylamide solution (Sigma) and 7 µl of N,N,N',N'-tetramethylethylenediamine (TEMED). The polymerization was started by adding 70 µl of 10 % (*w/v*) ammonium peroxodisulfate (APS) solution. After filling the gel apparatus, the solution was overlaid with water-saturated isobutyl alcohol to support the formation of a smooth gel front. The gel was then allowed to polymerize for at least 30 min, followed by adding the stacking gel, containing 6.5 ml of water, 2.5 ml of buffer B (0.5 M Tris/HCl pH 6.8, 0.4 % (*w/v*) SDS), 1 ml of 30 % acrylamide/bisacrylamide solution, 7 µl of TEMED and 70 µl of 10 % (*w/v*) APS. The gel was then stored at 4 °C overnight to allow complete polymerization.

For gel electrophoresis, 20 µg of protein per sample were loaded onto each lane. The samples for the detection of the V5-tagged receptor fusion constructs were mixed with 1 volume of 2x sample buffer containing 8 M urea and incubated for 30 min at room temperature. The samples for the detection of the c-myc-tagged arrestin fusion constructs were mixed with 1 volume of 2x sample buffer (Sigma) and incubated for 10 min at 98 °C. The precision plus dual color and biotinylated protein ladder were used as molecular weight markers. Electrophoresis was performed at 150 V for approximately 2 h until the bromphenol blue front had migrated completely through the gel.

3.4.4.3. Western blotting

For western blotting, the gels were placed on top of a nitrocellulose membrane between filter papers soaked in blotting buffer (25 mM Tris/HCl pH 8.3, 0.2 M glycine, 20% (v/v) methanol). Blotting was performed for 45 min at 250 mA. Afterwards, the membranes were incubated for at least 1 h in blocking solution (20 mM Tris/HCl pH 7.6, 0.14 M NaCl, 0.1 % (*v/v*) Tween 20, 5 % (*w/v*) fat free milk powder). After blocking, the membranes were cut closely above the 50 kDa band of the prestained protein marker. The lower part of the blots were developed using the anti β-actin antibody, the upper part using the Pierce anti c-myc antibody for detecting the arrestin constructs or the life technologies anti V5 antibody for the receptor constructs, respectively. Incubations with the primary antibodies were performed using a 1:1000 dilution of the respective AB in blocking solution at 4 °C overnight. After 3 washing steps in TBST (20 mM Tris/HCl pH 7.6, 0.14 M NaCl, 0.1 % (*v/v*) Tween 20) for 10 min each, the membranes were incubated with the secondary HRP-coupled antibodies, at a 1:1000 dilution in blocking solution for 1 h at RT. After 3 additional washing steps, the immunoreactive bands were detected using Pierce ECL Western Blotting substrate and the ChemiDoc MP imaging system (Bio-Rad Laboratories, Munich, Germany). The scans of the blots were analyzed using the Image Lab 5.0 software (Bio-Rad Laboratories, Munich, Germany).

3.4.5. Flow cytometry

For the flow cytometric analysis, the corresponding cells were cultivated in a 75- cm^2 cell culture flask in DMEM + 10 % FCS to a confluence of 70 – 90 %. The cells were detached by treatment with 5 ml of 0.05 % trypsin, 0.02 % EDTA in PBS. After addition of 5 ml of PBS + 5 % FCS, the cells were thoroughly singularized and harvested by centrifugation (400 g, 5 min). The cell pellet was resuspended in 2 ml of PBS + 4 % (*w/v*) paraformaldehyde, transferred to 2-ml reaction vessels and incubated on ice for 15 min. After centrifugation (all following centrifugation steps were carried out at 400 g, 5 min and 4 °C), the cells were resuspended in 2 ml of PBS + 0.2 % (*w/v*) saponin and incubated on ice for another 15 min. Then, cells were harvested by centrifugation and resuspended in 2 ml of PBS + 5 % FCS following incubation on ice for 15 min. After centrifugation, cells were resuspended in 1 – 2 ml of PBS + 5 % FCS, depending on the size of the pellet, and 300 µl were transferred to fresh 1.5-ml reaction vessels. After centrifugation, the cells were resuspended in 200 µl of PBS + 5 % FCS containing the respective primary AB at an appropriate concentration (for details see below). Subsequently, the cells were incubated at 4 °C in the dark for 30 min, before addition of 1 ml of PBS + 5 % FCS and centrifugation. The cells were washed once with 1 ml of PBS + 5 % FCS and resuspended in 200 µl of PBS + 5 % FCS containing the secondary goat anti mouse R-PE coupled antibody in a 1:100 dilution. After incubation for 30 min at 4 °C in the dark, 1 ml PBS + 5 % FCS was added, and the cells were harvested by centrifugation. Following a washing step with 1 ml of PBS + 5 % FCS, the cells were resuspended in 300 µl of PBS + 5 % FCS and transferred to FACS tubes.

Flow cytometry was performed using a FACSCalibur cytometer (BD Biosciences, Heidelberg, Germany). The R-PE and DyLight 549 fluorochromes were excited with the 488 nm laser, and emission was measured using the 585/42 BP filter. The photomultiplier voltage was adjusted to the fluorescence of the stained, untransfected HEK293T cells, which served as negative control. Cell debris and viable cells were discriminated using forward (FSC) and side scatter (SSC) gating. The flow rate of the cytometer was adjusted to give less than 1000 events/s. In total, $5 \cdot 10^4$ events were measured per sample.

For the detection of the c-myc epitope tag of the arrestin fusion proteins, the life technologies mouse anti c-myc mAb was used in a 1:500 dilution. For the detection of the V5 epitope tag of the receptor fusion construct, three different antibodies were tested in dilutions from 1:100 to 1:1000, life technologies mouse anti V5, Pierce V5 tag AB (E10/V4RR) from mouse and mouse anti V5 TAG: DyLight549 (AbD-Serotec).

3.4.6. Radioligand saturation binding assays

The radioligand saturation binding assays to determine the receptor expression was performed using whole cells. The HEK293T cells, expressing the respective receptor constructs, were cultivated in DMEM +10 % FCS in a 75-cm^2 cell culture flask to a confluence of about 70 – 90 %. Then, the cells were detached by treatment with 0.05 % trypsin, 0.02 % EDTA in PBS. After addition of 1/10 volume FCS, cells were harvested by centrifugation (400

g, 5 min), subsequently resuspended in Leibovitz L-15 medium + 1 % FCS and adjusted to a cell density of 2 million cells/ml. The binding assay was performed in flat bottom, polypropylene 96-well microtiter plates. The reaction mixture contained 10 µl of the respective radioligand dilution, 55 µl of Leibovitz + 1 % FCS and 25 µl of cell suspension, giving a concentration of 50000 cells/well. The wells for the determination of the total binding contained additional 10 µl of Leibovitz, while, for the unspecific binding, 10 µl of the respective competitor dissolved in Leibovitz were added. The mixture was incubated for 60 to 90 min at RT under shaking at 300 rpm. Afterwards, the cells were harvested by filtration through GF/C filters using a Brandel 96 sample harvester (Brandel, Gaithersburg, MD). After 3 washing steps with ice cold PBS, the filter bound radioactivity was measured by liquid scintillation counting using the Micro Beta^2 1450 scintillation counter (Perkin Elmer, Rodgau, Germany).

Data analysis was performed using GraphPad Prism 5 software (GraphPad Software, La Jolla, CA). Specific binding values were calculated by subtraction of the unspecific binding from the respective total binding values. Data was plotted against the corresponding radioligand concentration and fitted by nonlinear regression using the one site saturation binding model. From the extrapolated B_{max} values, the binding sites per cell were calculated using the specific activity of the corresponding radioligands.

3.4.6.1. [^{3}H]Mepyramine saturation binding at H_1R expressing cells

Saturation binding was performed using [^{3}H]mepyramine at concentrations up to 80 nM. In order to save radioligand, 1 part of [^{3}H]mepyramine was diluted with 1 part of unlabeled mepyramine. Unspecific binding was determined in the presence of 10 µM diphenhydramine.

3.4.6.2. [^{3}H]UR-DE257 saturation binding at H_2R expressing cells

Saturation binding was performed using [^{3}H]UR-DE257 at concentrations up to 150 nM. In order to save radioligand, 1 part of [^{3}H]UR-DE257 was diluted with 3 parts of the corresponding unlabeled compound, UR-DE92 (equivalent to UR-DE257). Unspecific binding was determined in the presence of 10 µM famotidine.

3.4.6.3. [^{3}H]Histamine saturation binding at H_4R expressing cells

Saturation binding was performed using [^{3}H]histamine at concentrations up to 80 nM. Unspecific binding was determined in the presence of 10 µM thioperamide.

3.4.6.4. [^{3}H]UR-MK136 saturation binding at Y_1R expressing cells

Saturation binding was performed using [^{3}H]UR-MK136 at concentrations up to 16 nM. Unspecific binding was determined in the presence of 1 µM BIBO3304.

3.4.6.5. [^{3}H]UR-PLN187 saturation binding at Y_2R expressing cells

Saturation binding was performed using [^{3}H]UR-PLN187 at concentrations up to 160 nM. In order to save radioligand, 1 part of [^{3}H]UR-PLN187 was diluted with 3 parts of unlabeled UR-PLN187. Unspecific binding was determined in the presence of 10 µM JNJ31020028.

3.4.7. Luciferase complementation assay

One day before the experiment, the HEK293T cells expressing the arrestin and receptor fusion constructs were harvested by trypsin treatment (0.05 % trypsin, 0.02 % EDTA in PBS), and subsequent centrifugation (400 g, 5 min). The cells were thoroughly resuspended in DMEM (without phenol red) + 5 % FCS, and 90 µl of the cell suspension were seeded in white, TC treated, flat bottom 96 well micro titer plates at a density of approximately 100000 cells/well. The cells were cultivated at 37 °C overnight in a water saturated atmosphere containing 5 % CO_2. Shortly before the experiment, the cells were removed from the incubator and allowed to equilibrate to RT. The dilutions of the test compounds at the respective concentrations were transferred to a 96 well plate in the desired order to allow for the addition of the compounds to the test plates using a multi-channel pipette in order to reduce the time delay between individual wells. Per well, 10 µl of compound solution were added. After compound addition, the plates were incubated in an air-conditioned room at a plate shaker tempered to 25 °C for the indicated time. Shortly before the end of the incubation period, 50 µl of medium were removed from each well using a multichannel pipette in order to reduce the amount of assay reagent necessary in the next step. To measure luciferase activity, 50 µl of BrightGlo luciferase assay reagent were added to each well, the reagent was prepared according to manufacturer`s instructions and allowed to equilibrate to RT prior to use. Following reagent addition, the plates were incubated under vigorous shaking (800 rpm) for 5 min. Bioluminescence was measured for 1 s per well using the GENios Pro microplate reader (Tecan, Salzburg, Austria).

3.4.7.1. Optimization of the assay conditions

To determine the influence of DMSO, the HEK293T βArr1 + H_2R cell line was used. 1 mM stock solutions of histamine were prepared containing 0 – 80 % DMSO, giving a final concentration of 0 – 8 % DMSO in the assay mixture. The same DMSO solutions without histamine served as background control. Incubation time was set to 60 min. The

background values of the corresponding DMSO concentrations were subtracted from the raw data.

The time dependence of the arrestin recruitment assay was determined for all 5 receptors included in this thesis in combination with either one of the two β-arrestin isoforms. Arrestin recruitment was stimulated for the indicated period of time using the endogenous ligand of the receptor, either histamine at a concentration of 100 µM for the H_1R, H_2R and H_4R or 1 µM of NPY for the Y_1R and Y_2R.

3.5. References

1. Misawa, N.; Kafi, A. K.; Hattori, M.; Miura, K.; Masuda, K.; Ozawa, T. Rapid and high-sensitivity cell-based assays of protein-protein interactions using split click beetle luciferase complementation: an approach to the study of G-protein-coupled receptors. *Anal. Chem.* **2010**, 82, 2552-2560.
2. Strasser, A.; Striegl, B.; Wittmann, H. J.; Seifert, R. Pharmacological profile of histaprodifens at four recombinant histamine H1 receptor species isoforms. *J. Pharmacol. Exp. Ther.* **2008**, 324, 60-71.
3. Seifert, R.; Wenzel-Seifert, K.; Burckstummer, T.; Pertz, H. H.; Schunack, W.; Dove, S.; Buschauer, A.; Elz, S. Multiple differences in agonist and antagonist pharmacology between human and guinea pig histamine H1-receptor. *J. Pharmacol. Exp. Ther.* **2003**, 305, 1104-1115.
4. Schnell, D.; Brunskole, I.; Ladova, K.; Schneider, E. H.; Igel, P.; Dove, S.; Buschauer, A.; Seifert, R. Expression and functional properties of canine, rat, and murine histamine H(4) receptors in Sf9 insect cells. *Naunyn Schmiedebergs Arch. Pharmacol.* **2011**, 383, 457-470.
5. Bruysters, M.; Jongejan, A.; Gillard, M.; van de Manakker, F.; Bakker, R. A.; Chatelain, P.; Leurs, R. Pharmacological differences between human and guinea pig histamine H1 receptors: Asn84 (2.61) as key residue within an additional binding pocket in the H1 receptor. *Mol. Pharmacol.* **2005**, 67, 1045-1052.
6. Baumeister, P.; Erdmann, D.; Biselli, S.; Kagermeier, N.; Elz, S.; Bernhardt, G.; Buschauer, A. [H]UR-DE257: Development of a Tritium-Labeled Squaramide-Type Selective Histamine H Receptor Antagonist. *ChemMedChem* **2014**.
7. Lim, H. D.; van Rijn, R. M.; Ling, P.; Bakker, R. A.; Thurmond, R. L.; Leurs, R. Evaluation of histamine H1-, H2-, and H3-receptor ligands at the human histamine H4 receptor: identification of 4-methylhistamine as the first potent and selective H4 receptor agonist. *J. Pharmacol. Exp. Ther.* **2005**, 314, 1310-1321.
8. Lim, H. D.; de Graaf, C.; Jiang, W.; Sadek, P.; McGovern, P. M.; Istyastono, E. P.; Bakker, R. A.; de Esch, I. J.; Thurmond, R. L.; Leurs, R. Molecular determinants of ligand binding to H4R species variants. *Mol. Pharmacol.* **2010**, 77, 734-743.
9. Nordemann, U.; Wifling, D.; Schnell, D.; Bernhardt, G.; Stark, H.; Seifert, R.; Buschauer, A. Luciferase reporter gene assay on human, murine and rat histamine H4 receptor orthologs: correlations and discrepancies between distal and proximal readouts. *PLoS One* **2013**, 8, e73961.
10. Baumeister, P. Molecular Tools for G-Protein Coupled Receptors: Synthesis, Pharmacological Characterization and [3H]-Labeling of Subtype-selective Ligands for Histamine H4 and NPY Y2 Receptors. University of Regensburg, 2014. http://epub.uni-regensburg.de/30505/.
11. Keller, M.; Bernhardt, G.; Buschauer, A. [(3)H]UR-MK136: a highly potent and selective radioligand for neuropeptide Y Y(1) receptors. *ChemMedChem* **2011**, 6, 1566-1571.
12. Laemmli, U. K. Cleavage of structural proteins during the assembly of the head of bacteriophage T4. *Nature* **1970**, 227, 680-685.

Chapter 4

Investigation of arrestin recruitment at the NPY Y_1 and Y_2 receptors

4. Investigation of arrestin recruitment at the NPY Y_1 and Y_2 receptors

4.1. Introduction

Neuropeptide Y (NPY), peptide YY (PYY) and pancreatic polypeptide (PP) are structurally closely related peptides sharing the same tertiary structure, termed "PP-fold",[1,2] and targeting the same family of GPCRs, the NPY receptors. For humans, the functional expression of four receptor subtypes, the Y_1R, Y_2R, Y_4R and Y_5R, is confirmed and could be verified by molecular cloning of the receptor cDNAs.[3-6] A fifth receptor, the *y*6 receptor, was cloned but is only functional in mice while inactive in most other mammalian species.[2]

The NPY receptor family shares similar signal transduction pathways, coupling to the pertussis toxin sensitive $G_{i/o}$ family of heterotrimeric G-proteins.[2,7] Thus, receptor activation subsequently leads, for example, to inhibition of adenylyl cyclases (ACs) and induction of a Ca^{2+} signal.[7] Furthermore, NPY has been shown to activate alternate, non-canonical signaling pathways.[7] Depending on the tissue or cell type investigated, in a G-protein dependent manner, NPY receptors can activate or block calcium and potassium channel in the cell mebrane[8,9] as well as signal through MAP kinase pathways.[10]

Regarding the interaction of the NPY receptors with β-arrestin, the different subtypes show distinct characteristics. While the Y_1R was shown to exhibit pronounced recruitment of β-arrestin 2 with a fast kinetics of association, the Y_2R and Y_4R gave a much lower signal in the BRET recruitment assay and revealed a slower association rate.[11] These results correlate well with previous findings about the internalization and desensitization behavior of the Y receptors. Whereas the Y_1R was shown to internalize rapidly upon agonist stimulation, the Y_2R exhibited a much slower or no internalization at all.[12,13] The characteristics of arrestin recruitment of the Y_1R and Y_2R were confirmed by confocal microscopy based on bimolecular fluorescence complementation (BiFC).[14] Furthermore, the argininamide-type Y_1R antagonists BIBP3226 and BIBO3304 as well as the peptide antagonist GR231118 were demonstrated to be competitive antagonists regarding arrestin recruitment.[14]

NPY receptor ligands represent potential new therapeutics for the treatment of various disorders, such as obesity and anxiety.[15] Unfortunately, subtype selective, nonpeptidic tracers for the detailed characterization of the receptors *in vivo* and in vitro were unavailable. Therefore, compound libraries based on either the Y_1R selective antagonists BIBP3226 and BIBO3304 or the Y_2R selective antagonist BIIE0246 were synthesized in our lab, aiming at the development of new, subtype selective pharmacological tools. This chapter is dealing with the characterization of selected NPY receptor ligands from these substance libraries, using the established arrestin recruitment assay.

4.1.1. Selected Y_1R antagonists

BIBP3226 (**1**) was the first selective, nonpeptidic antagonist described for the Y_1R.[16] The attachment of acyl, alkoxycarbonyl and carbamoyl substituents to the guanidine of BIBP32226 (Cpd. **2**-**7**) resulted in a series of potent antagonist as potential new radioligands for the Y_1R.[17-19] Furthermore, two triazole derivatives (Cpd. **8**, **9**) and two fluorinated compounds (Cpd. **10**, **11**), representing potential new PET ligands, as well as two bivalent compounds with a free amine function[19] (Cpd. **12** and **13**) were included in the investigation ofY_1R dependent arrestin recruitment. The structures of the selected compounds are given in Fig.4-1.

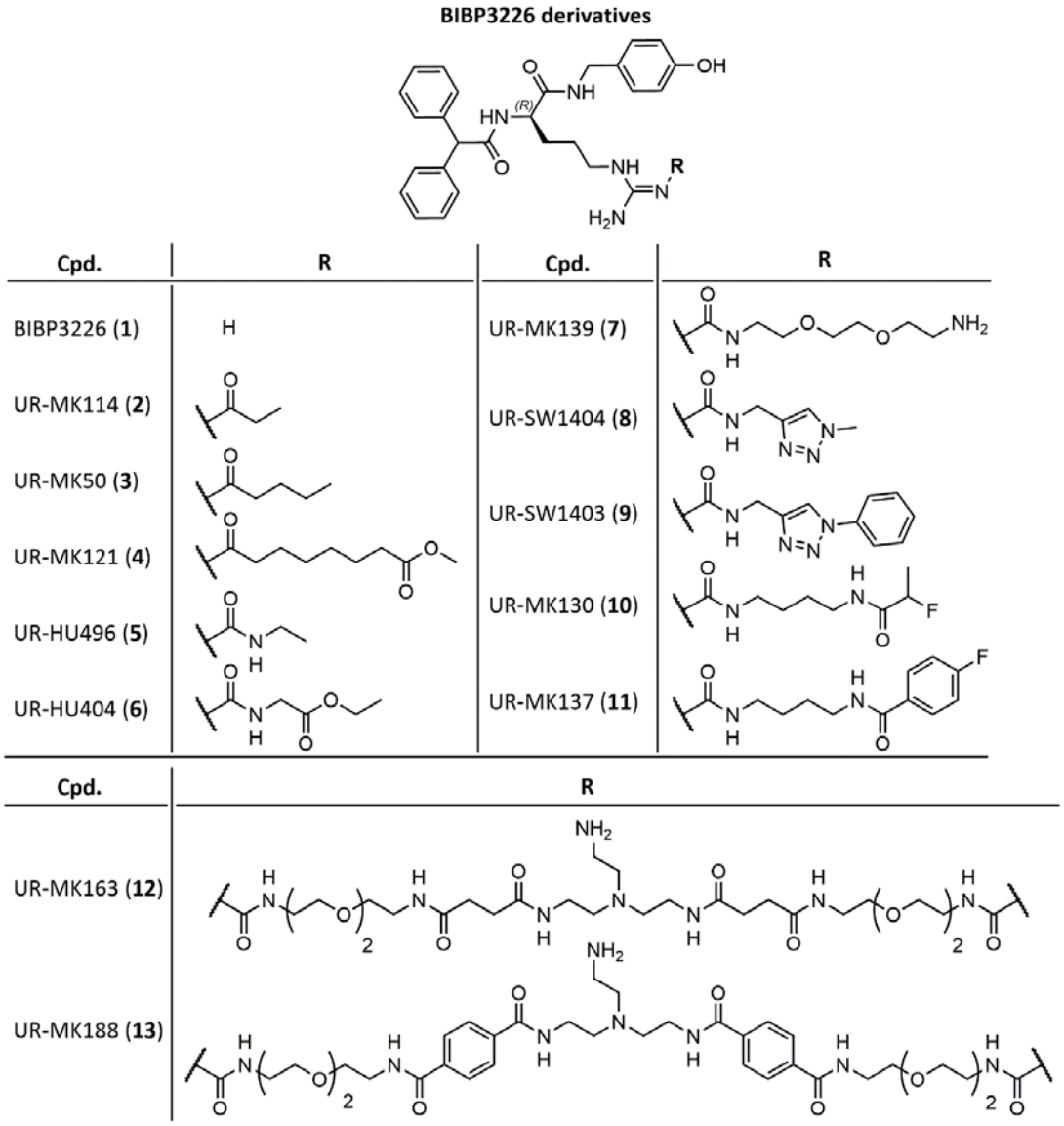

Fig. 4-1: Structures of the selected Y_1R antagonists derived from BIBP3226

BIBO3304 (**14**) is a urea derivative of BIBP3226 with subnanomolar affinity for the Y_1R, originally designed to overcome the CNS toxicity of the latter.[20] Starting from this pharmacophore, several potential new radioligands (Cpd. **15**-**18**) have been designed by introduction of acyl, carbamoyl or alkylamide substituents at either the N^G position of the guanidine or the N^U position of the urea (see Fig. 4-2).[19] Furthermore, the bivalent N^G coupled UR-MK177 (**19**) and the propanoic amide UR-MK280 (**20**) were included in this study. In addition to the BIBP3226 and BIBO3304 derivatives synthesized in our lab, several known, structurally diverse Y_1R antagonists were investigated for functional selectivity including the dihydropyridine BMS 193885 (**21**)[21] and the nitroquinoline PD 160170 (**22**).[22] Besides these nonpeptidic compounds, two known peptide Y_1R antagonists BW1911U90 (**23**) and GR231118 (**24**),[23] were investigated.

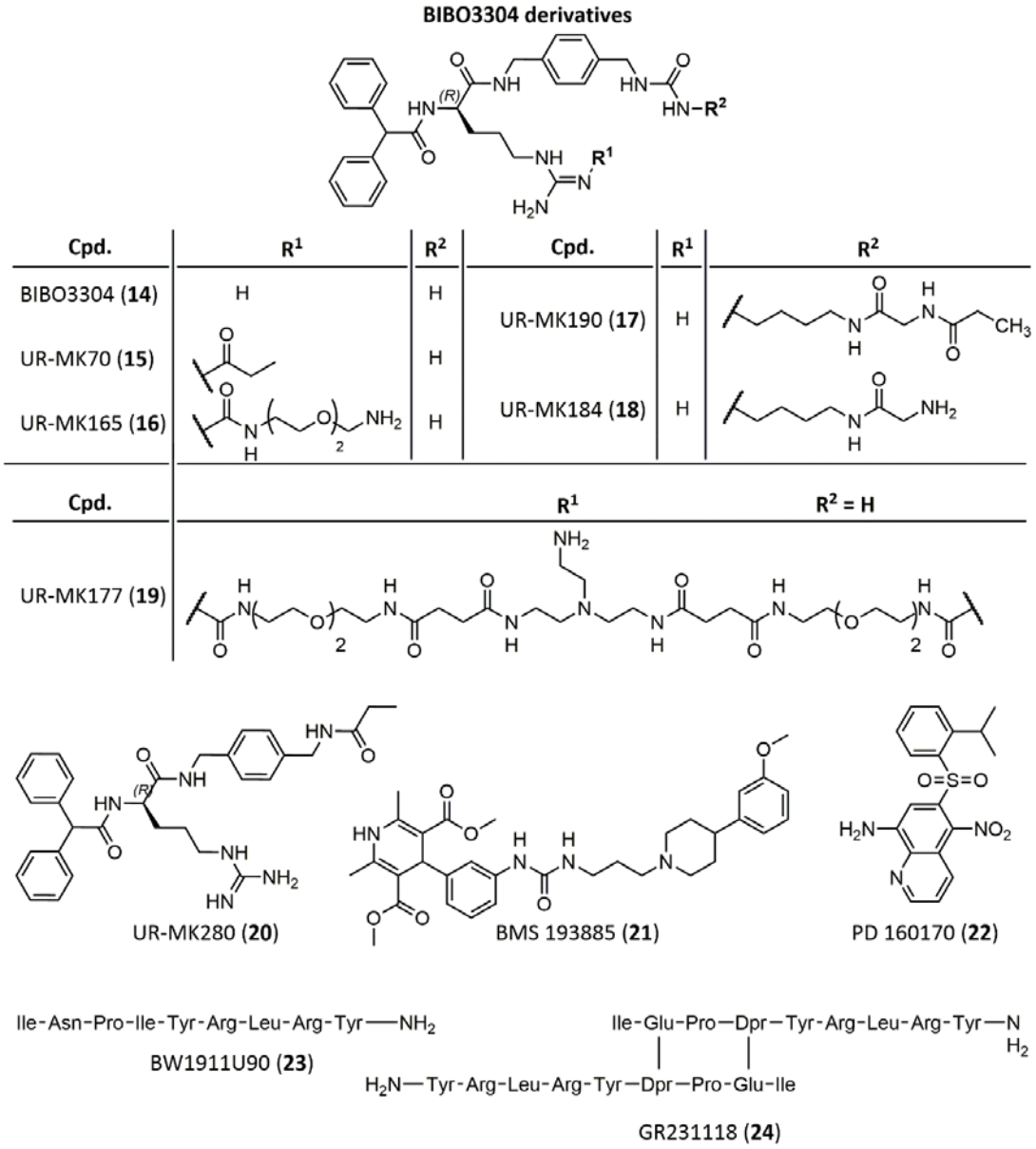

Fig. 4-2: Structures of the selected Y_1R antagonists

4.1.2. Selected Y_2R antagonists

The argininamide BIIE0246 (**25**) was published as high affinity (K_i values of 8 to 15 nM), nonpeptidic antagonist for the Y_2R with selectivity over the other NPY receptor subtypes.[24] Using the BIIE0246 pharmacophore, Pluym *et al.* synthesized a series of potential new radioligands and precursors by introduction of different functionalized acyl or carbamoyl substituents at the N^G position of the guanidine.[25,26] Hereof, several amine precursors as well as the corresponding amides were selected for the screening (Cpd. **26** – **36)**. Furthermore, several fluorinated compounds of this series (Cpd. **37** – **41**), potential new PET ligands, as well as the bivalent ligand UR-PLN176 (**42**) were added (structures see Fig. 4-3).

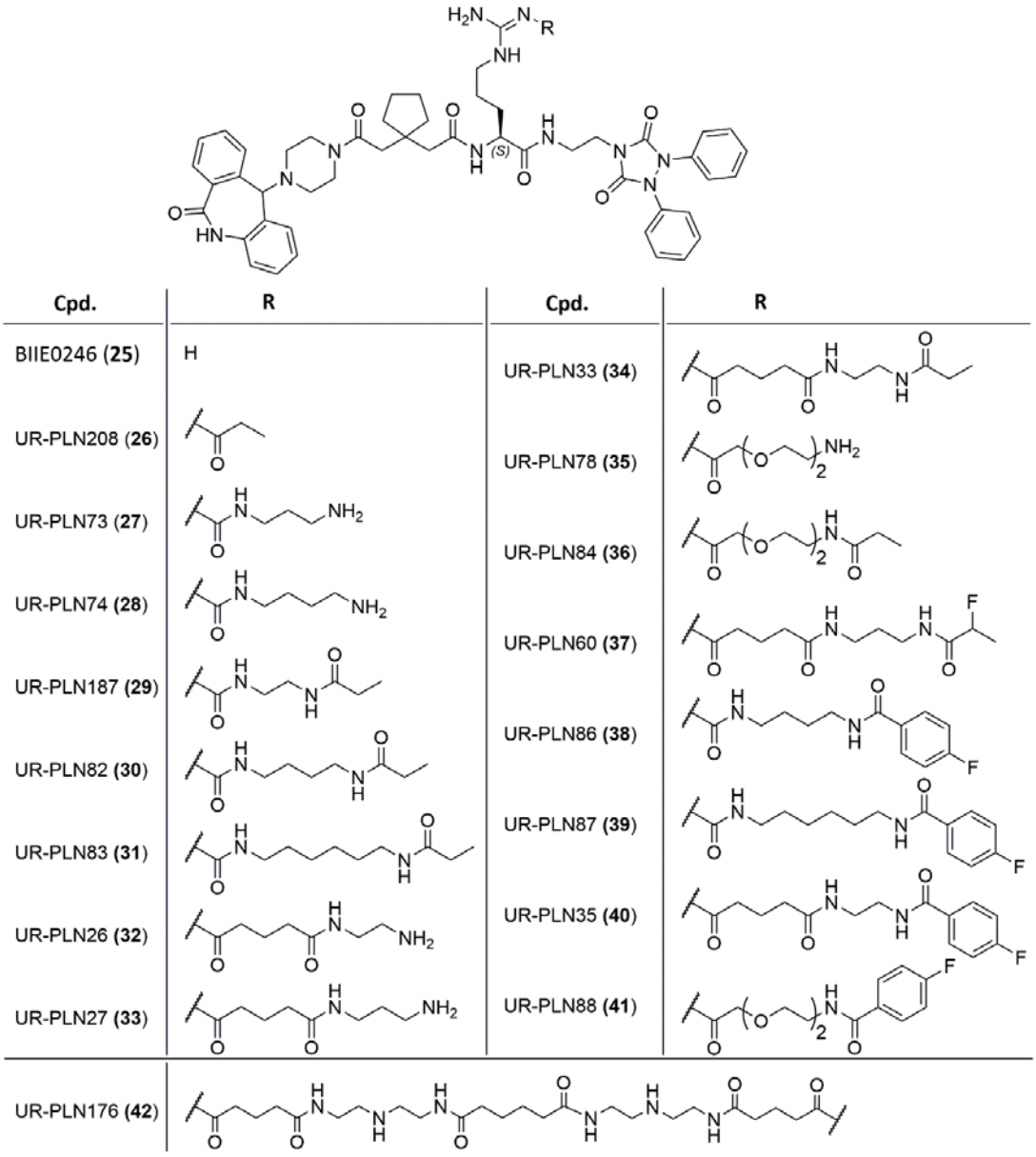

Fig. 4-3: Structures of the selected Y_2R antagonists derived from BIIE0246

In addition to the BIIE0246 derivatives from our lab, several structurally diverse compounds with known affinity for the Y_2R were selected. JNJ5207787 (**43**) was described as neutral antagonist for the Y_2R with over 100 fold selectivity over the other NPY receptor subtypes.[27] SF11 (**44**) was identified as Y_2R ligand in a high throughput screening and published with a K_i value of 1.55 nM in [^{125}I]-PYY competition binding.[28] Unfortunately, **44** was several orders of magnitude less potent when studied in our laboratory in a flow cytometric binding assay using Cy5-pNPY (cf. Tab 4-2). CYM9484 is a derivative of SF11 with strongly improved affinity for the Y_2R (cf. Tab. 4-2).[29] JNJ31020028 (**46**) and the structurally related urea UR-KK51 (**47**) are another class of brain penetrating, high affinity Y_2R antagonists.[30,31] The structures of the selected compounds is given in Fig. 4-4.

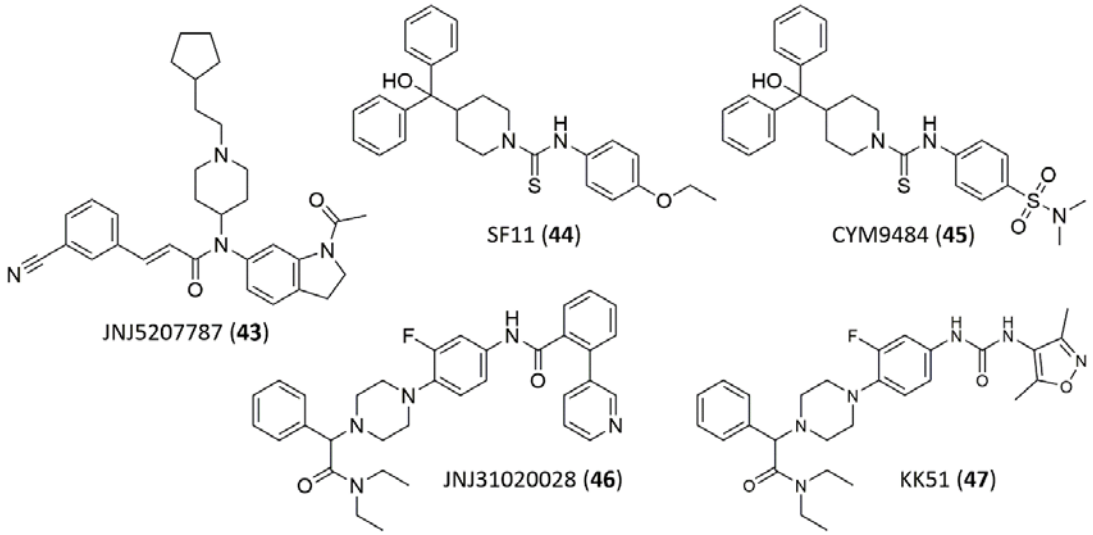

Fig. 4-4: Structures of the selected Y_2R antagonists

4.2. Results and discussion

To determine the functional characteristics of the selected Y_1R and Y_2R ligands regarding receptor-arrestin interaction, all compounds were tested in the established arrestin recruitment assay (cf. Chapter 3). An initial screening using the respective β-arrestin 1 or 2 cell lines, revealed no significant differences between the two arrestin isoforms. Therefore, the following screening was conducted solely with the HEK293T βArr2 + Y_1R and HEK293T βArr2 + Y_2R cells, respectively.

4.2.1. Activity of pNPY in the βArr2 recruitment assay

Instead of the human NPY, which contains a methionine residue in position 17 that is susceptible to oxidation, the porcine analog is used routinely in pharmacological assays.

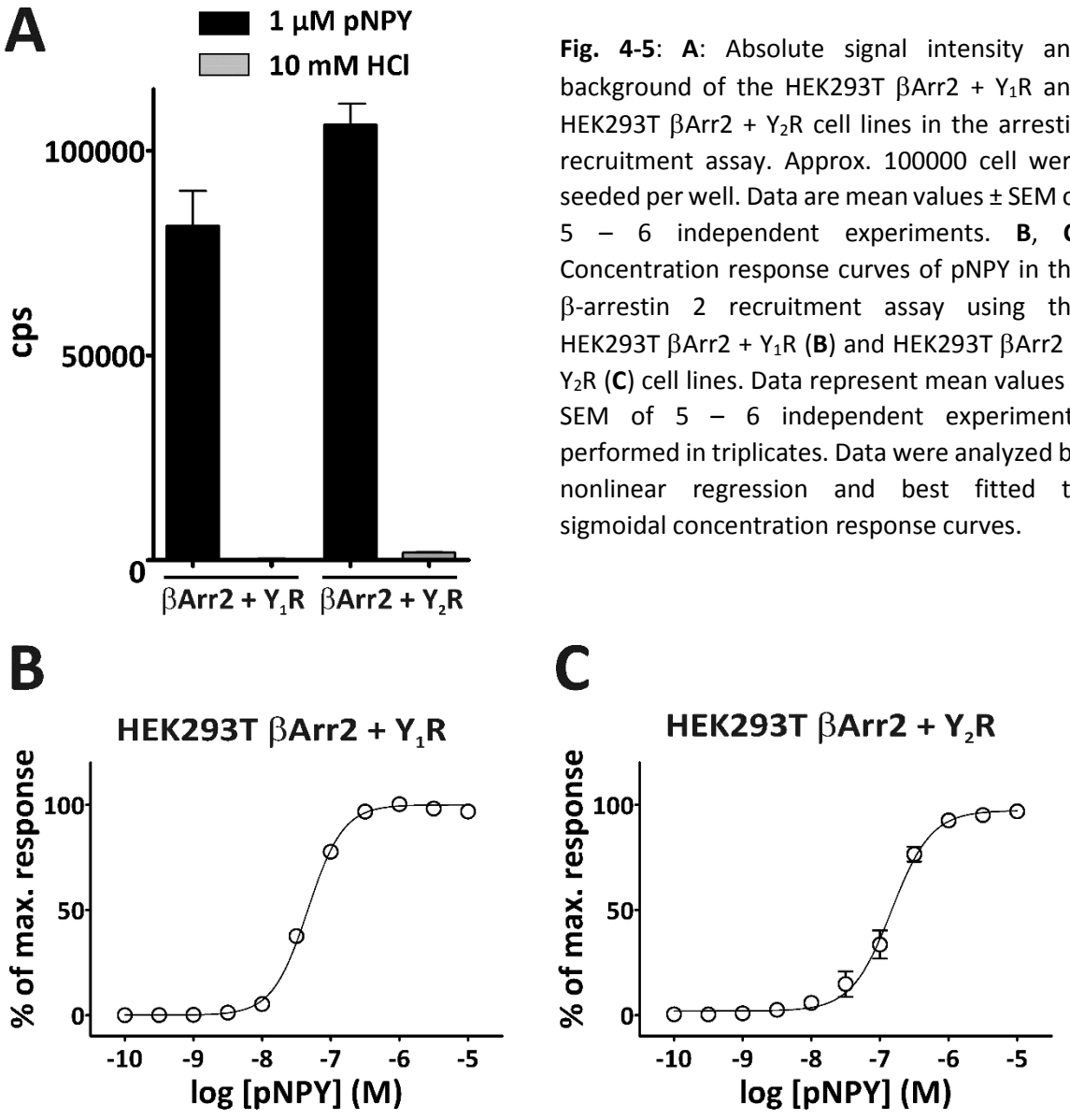

Fig. 4-5: **A**: Absolute signal intensity and background of the HEK293T βArr2 + Y_1R and HEK293T βArr2 + Y_2R cell lines in the arrestin recruitment assay. Approx. 100000 cell were seeded per well. Data are mean values ± SEM of 5 – 6 independent experiments. **B**, **C**: Concentration response curves of pNPY in the β-arrestin 2 recruitment assay using the HEK293T βArr2 + Y_1R (**B**) and HEK293T βArr2 + Y_2R (**C**) cell lines. Data represent mean values ± SEM of 5 – 6 independent experiments performed in triplicates. Data were analyzed by nonlinear regression and best fitted to sigmoidal concentration response curves.

The effect measured in the luciferase complementation assay was normalized to the maximal effect induced by pNPY, as the endogenous ligand is by definition regarded as full, unbiased agonist. As expected, pNPY showed agonistic activity in the arrestin recruitment assay at both, the Y_1R and the Y_2R. Previous findings, where the Y_1R showed a considerably faster and more pronounced recruitment of β-arrestin 2 than the Y_2R,[11] could not be confirmed in our assay system. In the luciferase complementation assay, the Y_2R cells produced a higher absolute signal than the Y_1R cell line (cf. Fig. 4-5), though the far higher expression level of the Y_2R in the corresponding cells has to be taken into account (cf. 3.2.2). At the Y_1R, the potency of pNPY for arrestin recruitment determined in our luciferase complementation was significantly lower than previously reported data gained from BiFC techniques[14] (pEC_{50} (ELuc-Comp.) = 7.36 ± 0.05; pEC_{50} (BIFC) = 8.57 ± 0.05). By contrast, for the Y_2R, the potencies of pNPY determined in the two assay systems were in good agreement (pEC_{50} (ELuc-Comp.) = 6.89 ± 0.12; pEC_{50} (BIFC) = 7.15 ± 0.08[14]). At the Y_1R, the potencies for NPY in G-protein based readouts reported in literature (pEC_{50} = 8.1 – 9.4[32,33]) are considerably higher than in our arrestin recruitment assay. In comparison, the decrease in potency for the Y_2R is much less pronounced (pEC_{50} (G-Protein) = 7.5 – 8.3[32-35]). For the interpretation of the data for pNPY in the arrestin recruitment assay, it has to be taken into consideration that the assay was not optimized for the use of peptidic ligands. It is known that surface adhesion and/or protein binding to the serum albumin present in the assay mixture might influence the effective concentration of the peptide ligand and therefore can significantly affect the detected potencies. Besides physiological differences like variations in signal amplification, such effects might also account at least in part for the huge discrepancies found in the potencies reported for NPY in the different G-protein based readouts. However, a decrease in potency in arrestin recruitment compared to G-protein based readout became also obvious in case of the histamine receptor subtypes, although histamine is uncritical regarding adhesion and protein binding. Thus, the observed differences seem to be inherent to the system. A pNPY concentration of 1 µM was sufficient for full stimulation of arrestin recruitment by both receptors (cf. Fig. 4-5) and was, therefore, used for normalization of the ligand-induced effects in the investigation of antagonists.

4.2.2. Investigation of selected Y_1R antagonists for agonism in the arrestin recruitment assay

The selected Y_1R antagonists were tested at concentrations from 0.1 – 10 µM for their ability to stimulate arrestin recruitment to the Y_1R using the HEK293T βArr2 + Y_1R cell line. The efficacies of the ligands normalized to the maximal effect induced by 1 µM pNPY (100 % value) and solvent (0 % value) as well as the affinities of the selected compounds for the Y_1R are given in Tab. 4-1. Previous findings indicating neutral antagonism of the parent compounds BIBP3226 (**1**) and BIBO3304 (**14**) in arrestin recruitment were confirmed (cf. Tab. 4-1).[14] None of the modifications introduced in Cpd. **2** – **13** and **15** – **20** had significant

Table 4-1: Efficacies in arrestin recruitment assay and Y_1R affinity of the tested Y_1R antagonists

Cpd.	βArr2 recruitment[a]	Y_1R affinity
	E_{max} ± SEM [%]	K_i ± SEM [nM]
BIBP3226 (**1**)	-0.03 ± 0.01	1.3 ± 0.2[b]
UR-MK114 (**2**)	-0.02 ± 0.02	1.2 ± 0.1[c]
UR-MK50 (**3**)	-0.08 ± 0.03	1.6 ± 0.3[d]
UR-MK121 (**4**)	-0.02 ± 0.03	0.94 ± 0.06[e]
UR-HU496 (**5**)	-0.07 ± 0.03	0.17 ± 0.01[d]
UR-HU404 (**6**)	0.04 ± 0.06	0.21 ± 0.05[d]
UR-MK139 (**7**)	-0.05 ± 0.03	7.3 ± 1[f]
UR-SW1404 (**8**)	0.02 ± 0.02	0.56 ± 0.06[d]
UR-SW1403 (**9**)	-0.01 ± 0.02	3.1 ± 0.6[d]
UR-MK130 (**10**)	-0.02 ± 0.00	1.3 ± 0.4[d]
UR-MK137 (**11**)	-0.04 ± 0.00	7.2 ± 2.3[d]
UR-MK163 (**12**)	-0.06 ± 0.01	25 ± 1.7[f]
UR-MK188 (**13**)	-0.05 ± 0.00	24 ± 1.1[f]
BIBO3304 (**14**)	-0.05 ± 0.03	0.25 ± 0.01[b]
UR-MK70 (**15**)	-0.06 ± 0.05	7.8 ± 2.6[d]
UR-MK165 (**16**)	-0.02 ± 0.01	31 ± 1[f]
UR-MK190 (**17**)	-0.07 ± 0.02	73 ± 5.3[f]
UR-MK184 (**18**)	-0.02 ± 0.01	14 ± 1.1[f]
UR-MK177 (**19**)	-0.06 ± 0.00	230 ± 24[f]
UR-MK280 (**20**)	-0.09 ± 0.01	4.2 ± 0.7[g]
BMS 193885 (**21**)	0.18 ± 0.08	3.3 ± 0.17[h]
PD 160170 (**22**)	0.06 ± 0.10	0.05[i]
BW1911U90 (**23**)	-0.02 ± 0.03	8.3 ± 0.0[j]
GR231118 (**24**)	-0.06 ± 0.02	10.2 ± 0.1[j]

[a] Efficacies in arrestin recruitment determined at the HEK293T βArr2 + Y_1R cells as described in 4.3.2
[b], [d], [e], [f]: Determined by competition binding with [^{3}H]UR-MK114 (K_d = 1.2 nM, c = 1.5 nM) on SK-N-MC cells taken from [b] Keller *et al.* 2011[36] [d] Dr. Max Keller, personal communication [e] Keller *et al.* 2009[18] [f] Keller *et al.* 2013[19]
[c] K_D value of [^{3}H]UR-MK114 at SK-N-MC cells[17]
[g] Determined by competition binding with [3H]UR-MK136 on SK-N-MC cells
[h] Determined by competition binding with [^{125}I]PYY on SK-N-MC cell membranes, Poindexter *et al.* 2004[37]
[i] Determined by competition binding with [^{125}I]PYY on SK-N-MC cell membranes, Wielgosz *et al.* 2002[22]
[j] Determined by competition binding with [^{125}I]PYY on CHO-K1 Y_1 cell membranes, Parker *et al.* 1998[23]

influence on their functional characteristics regarding arrestin recruitment, with all determined efficacies comparable to the solvent value. Furthermore, neither the peptidic antagonists (Cpd. **23** and **24**) nor the dihydropyridine BMS 193885 (**21**) and the nitroquinoline PD 160170 (**22**) revealed functional selectivity towards arrestin recruitment.

4.2.3. Investigation of selected Y_2R antagonists for agonism in the arrestin recruitment assay

The selected Y_2R antagonists were tested at concentrations from 0.1 – 10 µM in the arrestin recruitment assay using the HEK293T βArr2 + Y_2R cells. Normalization of the data was performed as described above (cf. 4.2.2). Table 4-1 gives the normalized efficacies of the tested compounds for arrestin recruitment as well as their affinities for the Y_2R. None of the selected BIIE0246 derivatives (Cpd. **25** – **42**) exhibited significant efficacy towards arrestin recruitment (cf. Tab. 4-2). Several ligands of this class, including the parent compound BIIE0246 or the radioligand UR-PLN196 (structurally equivalent to UR-PLN33), were previously described as insurmountable antagonists at the Y_2R exhibiting pseudo-irreversible binding.[26,38] Hereby, the ligands, when preincubated with the receptor, could not be completely displaced by NPY, leading to a depression of the maximal response of the system. Besides possible allosteric modulation, slow ligand dissociation or slow receptor interconversion rates, the stabilization of ligand specific, alternate receptor conformations, as generally associated with functionally biased compounds, explain such a behavior. However, the findings in the arrestin recruitment assay do not support this hypothesis. At least regarding arrestin and the canonical G-protein mediated pathways, the compounds of this class of Y_2R ligands exhibit no functional bias. A similar profile was found for the other tested antagonists, which have scaffolds different from that of BIIE0246 (Cpd. **43** – **47**) and produced signals comparable to the assay background.

Table 4-2: Efficacies in the arrestin recruitment assay and Y_2R affinity of the tested Y_2R antagonists

Cpd.	βArr2 recruitment[a]	Y_2R affinity[b]
	E_{max} ± SEM [%]	K_i ± SEM [nM]
BIIE0246 (**25**)	0.05 ± 0.19	10.2 ± 1.1
UR-PLN208 (**26**)	-0.14 ± 0.02	5.2 ± 1.8
UR-PLN73 (**27**)	-0.04 ± 0.27	2.1 ± 0.3
UR-PLN74 (**28**)	0.23 ± 0.15	3.2 ± 0.3
UR-PLN187 (**29**)	0.33 ± 0.19	64 ± 4
UR-PLN82 (**30**)	0.00 ± 0.12	55 ± 15
UR-PLN83 (**31**)	0.28 ± 0.04	84 ± 64
UR-PLN26 (**32**)	0.18 ± 0.39	3.4 ± 0.1
UR-PLN27 (**33**)	0.14 ± 0.56	2.3 ± 1.4
UR-PLN33 (**34**)	0.29 ± 0.37	9.9 ± 1.0[c]
UR-PLN78 (**35**)	-0.10 ± 0.17	18 ± 1
UR-PLN84 (**36**)	0.39 ± 0.13	15 ± 0.2
UR-PLN60 (**37**)	0.54 ± 0.08	27 ± 4
UR-PLN86 (**38**)	0.09 ± 0.10	68 ± 8
UR-PLN87 (**39**)	-0.05 ± 0.04	82 ± 7
UR-PLN35 (**40**)	-0.09 ± 0.03	8.3 ± 6.4[c]
UR-PLN88 (**41**)	-0.34 ± 0.01	22 ± 9
UR-PLN176 (**42**)	0.18 ± 0.19	21 ± 6
JNJ5207787 (**43**)	0.10 ± 0.34	100 ± 25[d]
SF11 (**44**)	0.00 ± 0.27	1251 ± 348[e]
CYM9484 (**45**)	-0.10 ± 0.33	24 ± 3[e]
JNJ31020028 (**46**)	-0.20 ± 0.32	9.9 ± 0.1[e]
UR-KK51 (**47**)	-0.16 ± 0.41	22 ± 5[e]

[a] Efficacies in arrestin recruitment determined at the HEK293T βArr2 + Y_1R cells as described in 4.3.2
[b] Determined by flow cytometric binding assay using Cy5-pNPY (K_D = 5.2 nM, c = 5 nM) on CHO Y_2 cells[39]
[c] Determined by flow cytometric binding assay using Dy-635-pNPY (K_D = 5.2 nM, c = 5 nM) on CHO Y_2 cells[39]
[d] Determined by competition binding with [^{125}I]PYY on hY_2 KAN-Ts cells, Bonaventure *et al.*[27]
[e] personal communications, Kilian Kuhn

4.3. Materials and methods

4.3.1. Materials

Unless stated otherwise, all chemicals and reagents were purchased from Sigma-Aldrich Chemie (Munich, Germany) or Merck (Darmstadt, Germany). For media and reagents used for the luciferase complementation assay, see Chapter 3.4.

4.3.1.1. Ligands

The porcine NPY (aa sequence: YPSKPDNPGE DAPAEDLARY YSALRHYINL ITRQRY) was used instead of the human peptide in order to avoid problems associated with the oxidation of methionine, as it contains a leucine at position 17 instead of methionine. pNPY and the BIBP3226 and BIBO3304 derivatives (**1 – 20**) were synthesized in our lab.[17-19,36] BMS 193885 (**21**) and PD 160170 (**22**) were purchased from Tocris Bioscience (Ellisville, MO, USA). The peptide ligands BW1911U90 (**23**) and GR231118 (**24**) were kindly provided by Prof. Dr. Chiara Cabrele, University of Salzburg. The BIIE0246 derivatives (**25 – 42**),[25,26,39] JNJ5207787 (**43**), SF11 (**44**), CYM9484 (**45**), JNJ31020028 (**46**) and UR-KK51 (**47**) were synthesized in our lab. For the compounds **1 – 7**, **10 – 15**, **17 – 19**, **21**, **22** and **25 – 47**, 5 mM or 10 mM stock solutions were prepared in DMSO. For the compounds **8**, **9**, **16** and **20**, 10 mM stock solutions were prepared in 50 % MeCN/ 0,05 % TFA. The peptide ligands pNPY, BW1911U90 (**23**) and GR231118 (**24**) were dissolved in 10 mM HCl at suitable concentrations.

4.3.2. Methods

4.3.2.1. Luciferase complementation assay

The luciferase complementation assay was performed as described above (cf. 3.4.7) using the HEK293T-β-Arr2-Y_1R and HEK293T-β-Arr2-Y_2R cells stably expressing either the Y_1R-ElucC or Y_2R-ElucC and the β-Arr2-ElucN fusion constructs (cf. 3.2). For cell culture conditions and media requirements, see 3.4.2. Working solutions for the compounds **1 – 7**, **10 – 15**, **17 – 19**, **21**, **22** and **25 – 47** were prepared in 5 % DMSO / 10 mM TFA. Working solutions for the compounds **8**, **9**, **16** and **20** were prepared in 5 % MeCN / 10 mM TFA. For pNPY, **23** and **24**, the working solutions were prepared in 10 mM HCl.

The cells were stimulated for 45 min with the ligands at concentrations from 0.1 – 10 µM, at least 10- to 100-fold the corresponding K_i value of the ligand. The results were normalized to the maximum effect induced by 1 µM pNPY (100 % value) and solvent (0 % value).

4.3.2.2. Data analysis

The functional data was analyzed using the GraphPad Prism 5 software (GraphPad Software, La Jolla, CA). Concentration response data was best fitted by nonlinear regression to a three parameter sigmoidal function.

4.4. References

1. Larhammar, D. Evolution of neuropeptide Y, peptide YY and pancreatic polypeptide. *Regul. Pept.* **1996**, 62, 1-11.
2. Michel, M. C.; Beck-Sickinger, A.; Cox, H.; Doods, H. N.; Herzog, H.; Larhammar, D.; Quirion, R.; Schwartz, T.; Westfall, T. XVI. International Union of Pharmacology recommendations for the nomenclature of neuropeptide Y, peptide YY, and pancreatic polypeptide receptors. *Pharmacol. Rev.* **1998**, 50, 143-150.
3. Larhammar, D.; Blomqvist, A. G.; Yee, F.; Jazin, E.; Yoo, H.; Wahlested, C. Cloning and functional expression of a human neuropeptide Y/peptide YY receptor of the Y1 type. *J. Biol. Chem.* **1992**, 267, 10935-10938.
4. Rose, P. M.; Fernandes, P.; Lynch, J. S.; Frazier, S. T.; Fisher, S. M.; Kodukula, K.; Kienzle, B.; Seethala, R. Cloning and functional expression of a cDNA encoding a human type 2 neuropeptide Y receptor. *J. Biol. Chem.* **1995**, 270, 29038.
5. Lundell, I.; Blomqvist, A. G.; Berglund, M. M.; Schober, D. A.; Johnson, D.; Statnick, M. A.; Gadski, R. A.; Gehlert, D. R.; Larhammar, D. Cloning of a human receptor of the NPY receptor family with high affinity for pancreatic polypeptide and peptide YY. *J. Biol. Chem.* **1995**, 270, 29123-29128.
6. Weinberg, D. H.; Sirinathsinghji, D. J.; Tan, C. P.; Shiao, L. L.; Morin, N.; Rigby, M. R.; Heavens, R. H.; Rapoport, D. R.; Bayne, M. L.; Cascieri, M. A.; Strader, C. D.; Linemeyer, D. L.; MacNeil, D. J. Cloning and expression of a novel neuropeptide Y receptor. *J. Biol. Chem.* **1996**, 271, 16435-16438.
7. Silva, A. P.; Cavadas, C.; Grouzmann, E. Neuropeptide Y and its receptors as potential therapeutic drug targets. *Clin. Chim. Acta* **2002**, 326, 3-25.
8. Millar, B. C.; Weis, T.; Piper, H. M.; Weber, M.; Borchard, U.; McDermott, B. J.; Balasubramaniam, A. Positive and negative contractile effects of neuropeptide Y on ventricular cardiomyocytes. *Am. J. Physiol.* **1991**, 261, H1727-1733.
9. Xiong, Z.; Cheung, D. W. ATP-Dependent inhibition of Ca2+-activated K+ channels in vascular smooth muscle cells by neuropeptide Y. *Pflugers Arch.* **1995**, 431, 110-116.
10. Keffel, S.; Schmidt, M.; Bischoff, A.; Michel, M. C. Neuropeptide-Y stimulation of extracellular signal-regulated kinases in human erythroleukemia cells. *J. Pharmacol. Exp. Ther.* **1999**, 291, 1172-1178.
11. Berglund, M. M.; Schober, D. A.; Statnick, M. A.; McDonald, P. H.; Gehlert, D. R. The use of bioluminescence resonance energy transfer 2 to study neuropeptide Y receptor agonist-induced beta-arrestin 2 interaction. *J. Pharmacol. Exp. Ther.* **2003**, 306, 147-156.
12. Parker, S. L.; Kane, J. K.; Parker, M. S.; Berglund, M. M.; Lundell, I. A.; Li, M. D. Cloned neuropeptide Y (NPY) Y1 and pancreatic polypeptide Y4 receptors expressed in Chinese hamster ovary cells show considerable agonist-driven internalization, in contrast to the NPY Y2 receptor. *Eur. J. Biochem.* **2001**, 268, 877-886.
13. Gicquiaux, H.; Lecat, S.; Gaire, M.; Dieterlen, A.; Mely, Y.; Takeda, K.; Bucher, B.; Galzi, J. L. Rapid internalization and recycling of the human neuropeptide Y Y(1) receptor. *J. Biol. Chem.* **2002**, 277, 6645-6655.
14. Kilpatrick, L. E.; Briddon, S. J.; Hill, S. J.; Holliday, N. D. Quantitative analysis of neuropeptide Y receptor association with beta-arrestin2 measured by bimolecular fluorescence complementation. *Br. J. Pharmacol.* **2010**, 160, 892-906.
15. Brothers, S. P.; Wahlestedt, C. Therapeutic potential of neuropeptide Y (NPY) receptor ligands. *EMBO Mol. Med.* **2010**, 2, 429-439.

16. Rudolf, K.; Eberlein, W.; Engel, W.; Wieland, H. A.; Willim, K. D.; Entzeroth, M.; Wienen, W.; Beck-Sickinger, A. G.; Doods, H. N. The first highly potent and selective non-peptide neuropeptide Y Y1 receptor antagonist: BIBP3226. *Eur. J. Pharmacol.* **1994**, 271, R11-13.
17. Keller, M.; Pop, N.; Hutzler, C.; Beck-Sickinger, A. G.; Bernhardt, G.; Buschauer, A. Guanidine-acylguanidine bioisosteric approach in the design of radioligands: synthesis of a tritium-labeled N(G)-propionylargininamide ([3H]-UR-MK114) as a highly potent and selective neuropeptide Y Y1 receptor antagonist. *J. Med. Chem.* **2008**, 51, 8168-8172.
18. Keller, M.; Teng, S.; Bernhardt, G.; Buschauer, A. Bivalent argininamide-type neuropeptide y y(1) antagonists do not support the hypothesis of receptor dimerisation. *ChemMedChem* **2009**, 4, 1733-1745.
19. Keller, M.; Kaske, M.; Holzammer, T.; Bernhardt, G.; Buschauer, A. Dimeric argininamide-type neuropeptide Y receptor antagonists: chiral discrimination between Y1 and Y4 receptors. *Bioorg. Med. Chem.* **2013**, 21, 6303-6322.
20. Wieland, H. A.; Engel, W.; Eberlein, W.; Rudolf, K.; Doods, H. N. Subtype selectivity of the novel nonpeptide neuropeptide Y Y1 receptor antagonist BIBO 3304 and its effect on feeding in rodents. *Br. J. Pharmacol.* **1998**, 125, 549-555.
21. Poindexter, G. S.; Bruce, M. A.; LeBoulluec, K. L.; Monkovic, I.; Martin, S. W.; Parker, E. M.; Iben, L. G.; McGovern, R. T.; Ortiz, A. A.; Stanley, J. A.; Mattson, G. K.; Kozlowski, M.; Arcuri, M.; Antal-Zimanyi, I. Dihydropyridine neuropeptide Y Y(1) receptor antagonists. *Bioorg. Med. Chem. Lett.* **2002**, 12, 379-382.
22. Wielgosz-Collin, G.; Duflos, M.; Pinson, P.; Le Baut, G.; Renard, P.; Bennejean, C.; Boutin, J.; Boulanger, M. 8-Amino-5-nitro-6-phenoxyquinolines: potential non-peptidic neuropeptide Y receptor ligands. *J. Enzyme Inhib. Med. Chem.* **2002**, 17, 449-453.
23. Parker, E. M.; Babij, C. K.; Balasubramaniam, A.; Burrier, R. E.; Guzzi, M.; Hamud, F.; Mukhopadhyay, G.; Rudinski, M. S.; Tao, Z.; Tice, M.; Xia, L.; Mullins, D. E.; Salisbury, B. G. GR231118 (1229U91) and other analogues of the C-terminus of neuropeptide Y are potent neuropeptide Y Y1 receptor antagonists and neuropeptide Y Y4 receptor agonists. *Eur. J. Pharmacol.* **1998**, 349, 97-105.
24. Dumont, Y.; Cadieux, A.; Doods, H.; Pheng, L. H.; Abounader, R.; Hamel, E.; Jacques, D.; Regoli, D.; Quirion, R. BIIE0246, a potent and highly selective non-peptide neuropeptide Y Y(2) receptor antagonist. *Br. J. Pharmacol.* **2000**, 129, 1075-1088.
25. Pluym, N.; Brennauer, A.; Keller, M.; Ziemek, R.; Pop, N.; Bernhardt, G.; Buschauer, A. Application of the guanidine-acylguanidine bioisosteric approach to argininamide-type NPY Y(2) receptor antagonists. *ChemMedChem* **2011**, 6, 1727-1738.
26. Pluym, N.; Baumeister, P.; Keller, M.; Bernhardt, G.; Buschauer, A. [(3)H]UR-PLN196: a selective nonpeptide radioligand and insurmountable antagonist for the neuropeptide Y Y(2) receptor. *ChemMedChem* **2013**, 8, 587-593.
27. Bonaventure, P.; Nepomuceno, D.; Mazur, C.; Lord, B.; Rudolph, D. A.; Jablonowski, J. A.; Carruthers, N. I.; Lovenberg, T. W. Characterization of N-(1-Acetyl-2,3-dihydro-1H-indol-6-yl)-3-(3-cyano-phenyl)-N-[1-(2-cyclopentyl-eth yl)-piperidin-4yl]acrylamide (JNJ-5207787), a small molecule antagonist of the neuropeptide Y Y2 receptor. *J. Pharmacol. Exp. Ther.* **2004**, 308, 1130-1137.
28. Brothers, S. P.; Saldanha, S. A.; Spicer, T. P.; Cameron, M.; Mercer, B. A.; Chase, P.; McDonald, P.; Wahlestedt, C.; Hodder, P. S. Selective and brain penetrant neuropeptide y y2 receptor antagonists discovered by whole-cell high-throughput screening. *Mol. Pharmacol.* **2010**, 77, 46-57.

29. Mittapalli, G. K.; Vellucci, D.; Yang, J.; Toussaint, M.; Brothers, S. P.; Wahlestedt, C.; Roberts, E. Synthesis and SAR of selective small molecule neuropeptide Y Y2 receptor antagonists. *Bioorg. Med. Chem. Lett.* **2012**, 22, 3916-3920.
30. Shoblock, J. R.; Welty, N.; Nepomuceno, D.; Lord, B.; Aluisio, L.; Fraser, I.; Motley, S. T.; Sutton, S. W.; Morton, K.; Galici, R.; Atack, J. R.; Dvorak, L.; Swanson, D. M.; Carruthers, N. I.; Dvorak, C.; Lovenberg, T. W.; Bonaventure, P. In vitro and in vivo characterization of JNJ-31020028 (N-(4-{4-[2-(diethylamino)-2-oxo-1-phenylethyl]piperazin-1-yl}-3-fluorophenyl)-2-pyridin-3-ylbenzamide), a selective brain penetrant small molecule antagonist of the neuropeptide Y Y(2) receptor. *Psychopharmacology (Berl).* **2010**, 208, 265-277.
31. Mittapalli, G. K.; Roberts, E. Ligands of the neuropeptide Y Y2 receptor. *Bioorg. Med. Chem. Lett.* **2014**, 24, 430-441.
32. Dautzenberg, F. M.; Higelin, J.; Pflieger, P.; Neidhart, W.; Guba, W. Establishment of robust functional assays for the characterization of neuropeptide Y (NPY) receptors: identification of 3-(5-benzoyl-thiazol-2-ylamino)-benzonitrile as selective NPY type 5 receptor antagonist. *Neuropharmacology* **2005**, 48, 1043-1055.
33. Merten, N.; Lindner, D.; Rabe, N.; Rompler, H.; Morl, K.; Schoneberg, T.; Beck-Sickinger, A. G. Receptor subtype-specific docking of Asp6.59 with C-terminal arginine residues in Y receptor ligands. *J. Biol. Chem.* **2007**, 282, 7543-7551.
34. Ziemek, R.; Brennauer, A.; Schneider, E.; Cabrele, C.; Beck-Sickinger, A. G.; Bernhardt, G.; Buschauer, A. Fluorescence- and luminescence-based methods for the determination of affinity and activity of neuropeptide Y2 receptor ligands. *Eur. J. Pharmacol.* **2006**, 551, 10-18.
35. Pop, N.; Igel, P.; Brennauer, A.; Cabrele, C.; Bernhardt, G. N.; Seifert, R.; Buschauer, A. Functional reconstitution of human neuropeptide Y (NPY) Y(2) and Y(4) receptors in Sf9 insect cells. *J. Recept. Signal Transduct. Res.* **2011**, 31, 271-285.
36. Keller, M.; Erdmann, D.; Pop, N.; Pluym, N.; Teng, S.; Bernhardt, G.; Buschauer, A. Red-fluorescent argininamide-type NPY Y1 receptor antagonists as pharmacological tools. *Bioorg. Med. Chem.* **2011**, 19, 2859-2878.
37. Poindexter, G. S.; Bruce, M. A.; Breitenbucher, J. G.; Higgins, M. A.; Sit, S. Y.; Romine, J. L.; Martin, S. W.; Ward, S. A.; McGovern, R. T.; Clarke, W.; Russell, J.; Antal-Zimanyi, I. Dihydropyridine neuropeptide Y Y1 receptor antagonists 2. bioisosteric urea replacements. *Bioorg. Med. Chem.* **2004**, 12, 507-521.
38. Dautzenberg, F. M.; Neysari, S. Irreversible binding kinetics of neuropeptide Y ligands to Y2 but not to Y1 and Y5 receptors. *Pharmacology* **2005**, 75, 21-29.
39. Pluym, N. Application of the Guanidine–Acylguanidine Bioisosteric Approach to NPY Y2 Receptor Antagonists: Bivalent, Radiolabeled and Fluorescent Pharmacological Tools. University of Regensburg, 2011. http://epub.uni-regensburg.de/22503/.

Chapter 5

Investigation of functional selectivity at the histamine H_1 receptor

5. Investigation of functional selectivity at the histamine H_1 receptor

5.1.1. Introduction

The histamine H_1 receptor is a 487 aa protein and belongs to the class A of rhodopsin-like GPCRs. The term H_1 receptor has been first introduced in 1966, when the findings that several actions of histamine, like the stimulation of gastric acid secretion and the positive chronotropic effect on isolated atria, could not be blocked by low concentrations of antihistamines, suggested the involvement of a second distinct histamine receptor.[1]

Various studies have been performed investigating the distribution pattern of the H_1R in mammalian tissues. Through the use of selective radioligands, like [^{3}H]mepyramine,[2] receptor expression was detected in the brain, the smooth muscles from airways and the gastrointestinal tract, the genitourinary system and the cardiovascular system.[3,4]

The H_1R mediated response has been studied extensively in a variety of these tissues. In the mammalian brain, the histaminergic neurons are gaining attention for their profound involvement in basic brain functions. The H_1R has been shown to regulate the circadian rhythm and has been linked to several neuronal disorders, such as Alzheimer`s disease and schizophrenia,[5] its pathological function yet to be elucidated.[6] The best understood pathophysiological role of the H_1R is its function in allergic reactions (type I) and inflammation.[7] Histamine induced activation of the H_1R leads to vasodilation and bronchoconstriction in the airways and plays a major role in allergic rhinitis.[8] The H_1R is also a key player in the treatment of allergic conjunctivitis,[9] urticaria[10] and atopic dermatitis.[11]

In several different cell types and tissues, the H_1R has been shown to mediate histamine induced activation of phospholipase C (PLC), leading to the hydrolysis of phosphatidylinositol 4,5-bisphosphate (PIP_2) into diacyl glycerol (DAG) and inositol 1,4,5-trisphosphate (IP_3).[3,12] The advent of molecular biology, which in course led to the successful cloning of the cDNAs of several H_1R species orthologs[13-17] in the early 1990s, allowed for the detailed molecular analysis of the receptor signaling profile. The H_1R has been shown to couple primarily to the $G_{q/11}$ family of trimeric G-proteins leading to PLC activation and formation of DAG and IP_3.[18-20] IP_3 subsequently triggers Ca^{2+} release from intracellular stores and the increase in the cytosolic Ca^{2+} concentration leads to various cellular responses, like the activation of calcium-calmodulin dependent protein kinases or nitric oxide (NO) formation.[21] DAG activates protein kinase C (PKC), which in turn phosphorylates a multitude of effector proteins.[22] Furthermore, H_1R exhibited agonist dependent activation of nuclear factor κB (NFκB), a transcription factor involved in inflammation.[23] Interestingly, hereby the H_1R also showed constitutive, $G_{\beta\gamma}$ dependent activation of NFκB. Constitutive activity of the H_1R has been confirmed for inositol phosphate accumulation.[24] H_1R activation induced phosphorylation of mitogen activated protein kinases (MAPKs) in a pertussis toxin sensitive manner.[25] In other recombinant

systems showing high receptor expression levels, histamine activation of the H_1R was also able to induce a cAMP response, albeit with much lower potency than for Ca^{2+} mobilization.[26] Thus, the H_1R seems to be capable of also coupling to G-proteins other than $G_{q/11}$. It remains to be established, weather those findings in recombinant, artificial system are of physiological relevance, especially with regard to constitutive activity, which shows strong dependence on expression levels of the investigated GPCRs.

The H_1R represents a well-established drug target and extensive work has been performed investigating its function on the molecular and physiological level. Despite this fact, knowledge about β-arrestin recruitment and the involvement of arrestin-dependent signaling in the cellular response of the H_1R is still scarce. In human myometrial cells, down regulation of β-arrestin 2 expression, but not β-arrestin 1 down regulation, enhanced and prolonged H_1R-stimulated Ca^{2+} responses and decreased receptor desensitization. Additionally, β-arrestin 2 depletion abolished histamine induced ERK1/2 phosphorylation and increased p38 MAPK phosphorylation.[27]

So far, no pharmacological data is available for H_1R ligands regarding β-arrestin recruitment. In the following, the pharmacological profile of various H_1R ligands, investigated in the established β-arrestin recruitment assay, is described.

5.1.2. Selected H_1 receptor ligands

Except for betahistine, which is used as a drug for the treatment of Menière's disease,[28] H_1R agonists have no clinical relevance but are important tools to decipher receptor function. By now, several different classes of H_1R agonists are known. While the first H_1R selective agonists, like 2-pyridylethylamine, showed reduced potency compared to histamine,[12] the investigation of 2-phenyl-histamine derivatives led the discovery of potent and selective H_1R ligands.[29,30] Replacement of the 2-phenyl substituent by a diphenylpropyl moiety resulted in another class of H_1R agonists, the histaprodifens.[31-33]

For the investigation of β-arrestin recruitment, in addition to the endogenous ligand histamine (**1**), a set of 2-phenylhistamine (**2**-**5**) and histaprodifen derivatives (**6**-**12**) was selected (for chemical structure, see Fig. 5-2).

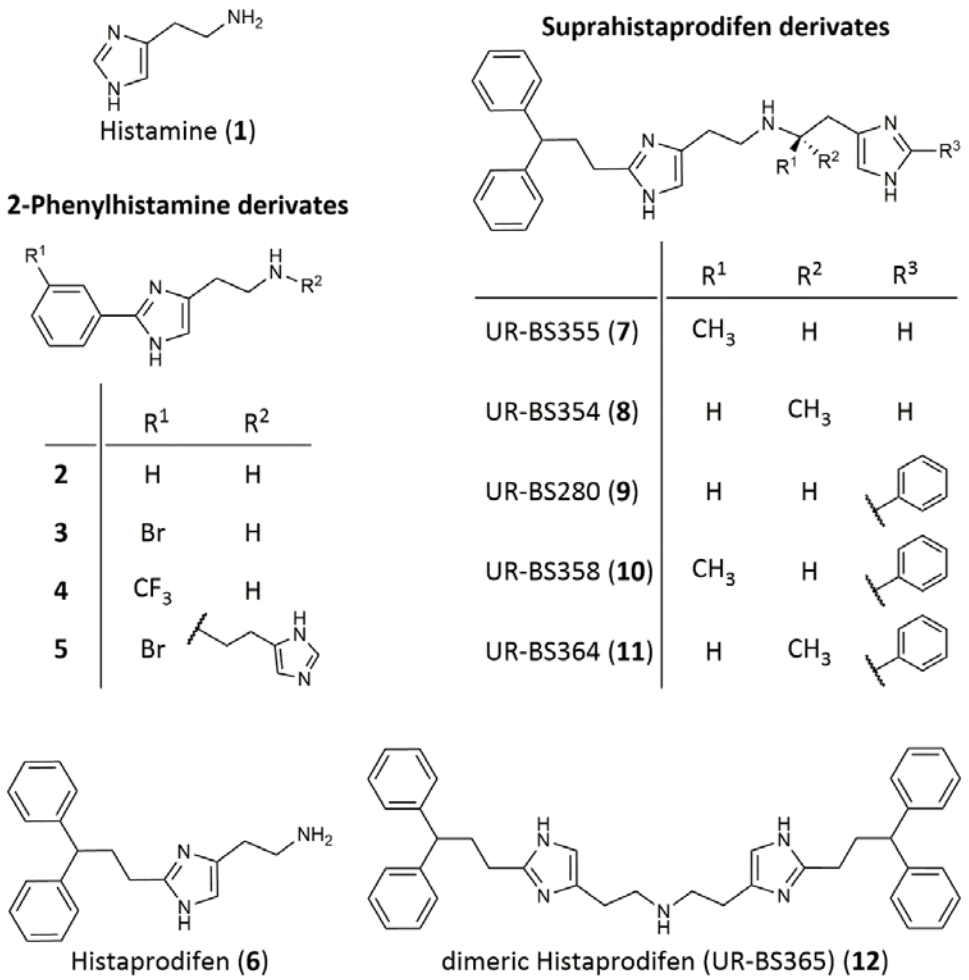

Fig. 5-1: Structures of selected H_1 receptor agonists

Since the discovery of the first antihistamines in the 1930s, the search for selective and potent H_1R antagonists was highly successful. H_1R antagonists have been used for the treatment of allergic conditions for decades, the first generation antihistamines showing side effects like drowsiness and fatigue caused by blocking the H_1R in the brain. Due to their lipophilic character, these compounds easily cross the blood brain barrier. To prevent these undesired drug effects, a second generation of H_1R antagonists was developed, showing strongly reduced CNS availability.[4,34]

For the investigations in the arrestin assays, a set of structurally diverse first and second generation H_1R antagonists was selected. Diphenhydramine (**13**) and mepyramine (**14**) are standard antagonists that have been used extensively to characterize the H_1R in vivo. Clemastine (**16**) and cyproheptadine (**15**) are high affinity H_1R antagonists, the latter still used for the treatment of mental disorders.[35,36] Levocetirizine (**17**), azelastine (**18**), ketotifen (**19**) and terfenadine (**20**) belong to the second generation H_1R antagonists and are widely used for the treatment of allergies.

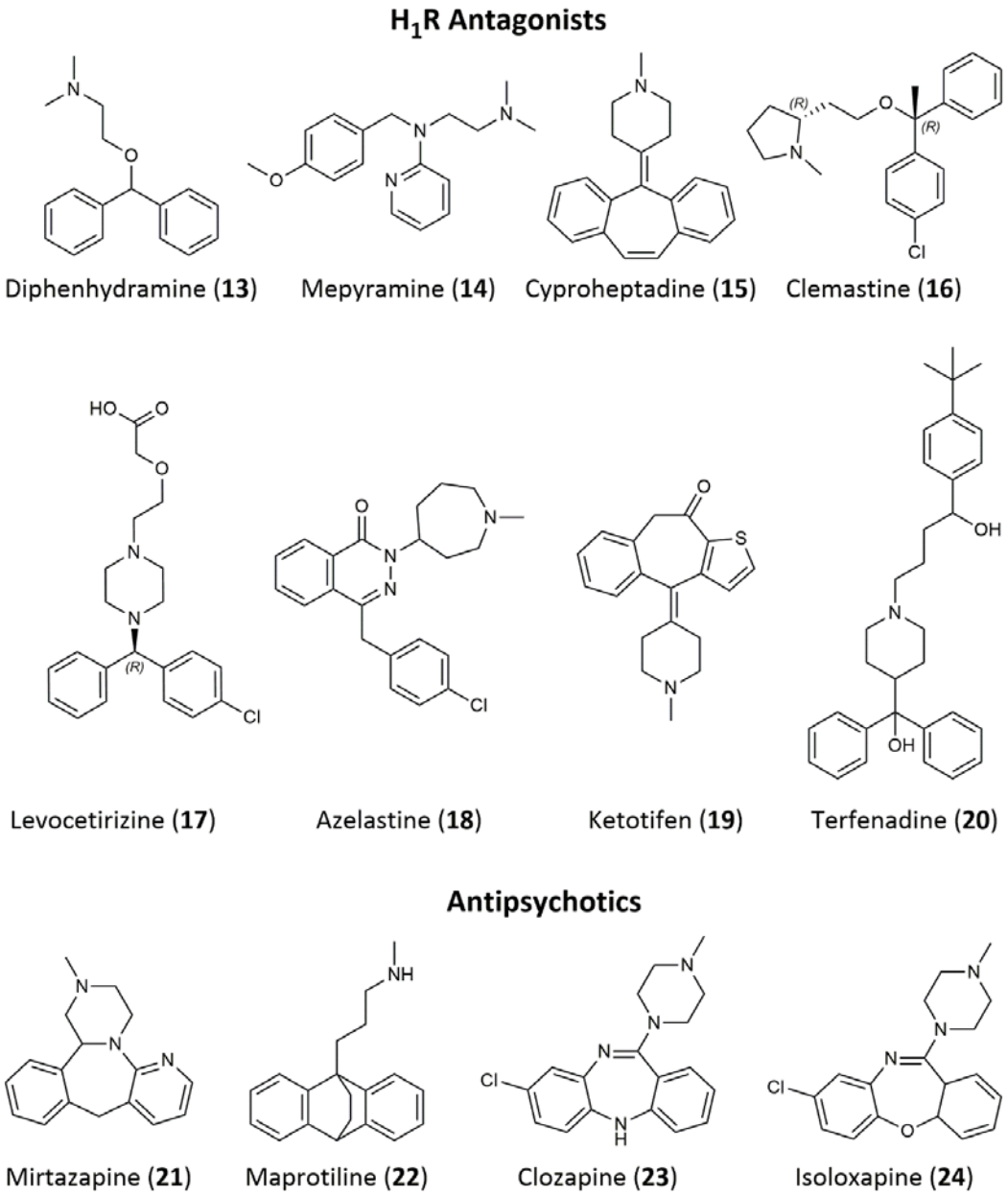

Fig. 5-2: Structures of selected H_1 receptor antagonists and antipsychotics

Besides the dedicated H_1R antagonists, a variety of clinically used antipsychotics and antidepressants have antagonistic or inverse agonistic effects at the H_1R.[37-39] Mirtazapine (**21**) is a noradrenergic and specific serotonergic antidepressant (NaSSA), maprotiline (**22**) belongs to the class of norepinephrine reuptake inhibitor (NRI) and clozapine (**23**) as well as isoloxapine (**24**) represent atypical antipsychotics (AAP). The former three compounds show affinity for the H_1R in the low nanomolar range[37] (for chemical structures of the selected compounds, see Fig. 5-1).

5.2. Results and discussion

To determine functional differences regarding G-protein versus β-arrestin activation, the selected H_1R ligands were investigated in two different assay systems. G-protein activation was determined using the well-established [^{32}P]GTPase assay, measuring ligand induced hydrolysis of [^{32}P] labeled GTP on membranes of *Sf*9 insect cells expressing the H_1R and RGS4 proteins.[40,41] β-Arrestin recruitment to the H_1R was determined in the luciferase complementation assay (for details on the assay system, see chapter 3).

Histamine induced activation of the H_1R stimulated β-arrestin 1 and 2 recruitment with equivalent maximal effects. In both cases the signal-to-noise ratios were sufficiently high, although the β-arrestin 2 expressing cells showed only a 6 fold increase in signal intensity compared to a 30 fold increase for the β-arrestin 1 cell line, due to a 5 fold higher background level (cf. Fig. 5-3). These differences in background intensity cannot be explained by variations in receptor density, as the receptor expression levels were comparable in both transfectants (cf. 3.2.2.3).

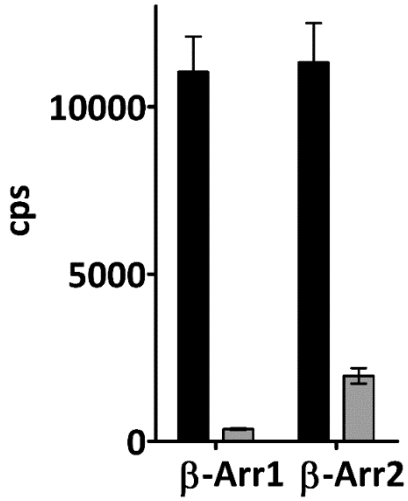

Fig. 5-3: Stimulation of HEK293T cells expressing the H_1R-ELucC and either βArr1-ELucN or βArr2-ELucN fusion constructs by 1 mM histamine (■ black bars) or solvent (■ grey bars). Approximately 100000 cells were seeded per well. Values are given as mean ± 95 % CI (N = 4).

The finding that the H_1R is capable of recruiting both β-arrestin isoforms is contradictory to results from literature, suggesting the involvement of β-arrestin 2, but not β-arrestin 1, in the signal transduction of the H_1R in native cells.[27]

5.2.1. Efficacies of H_1R antagonists in β-arrestin recruitment

All investigated compounds are high affinity ligands for the H_1R and known as antagonists or inverse agonists with regard to G-protein activation.[4,37,38] Information on β-arrestin recruitment was not available so far. Therefore, the compounds were tested at concentrations of 10 and 100 µM for their ability to induce β-arrestin recruitment in the luciferase complementation assay.

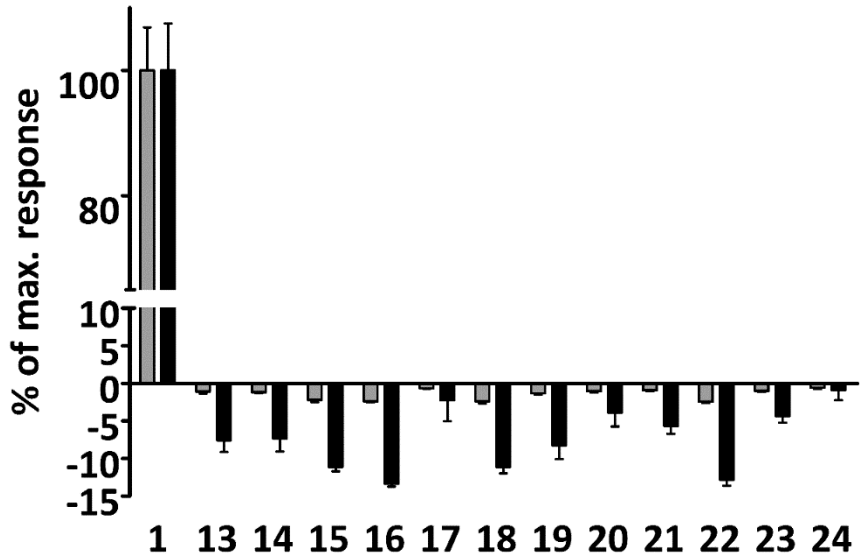

Fig. 5-4: Efficacies of the tested antagonists in the β-arrestin recruitment assay using the β-arrestin 1 (■ grey bars) or β-arrestin 2 (■ black bars) expressing cells. All compounds were investigated at a concentration of 100 µM. The results were normalized to the effect induced by 1 mM histamine (100 % value) and solvent (0 % value). The results are given as mean values ± SEM of 2 to 3 independent experiments performed in triplicate.

Fig. 5-4 summarizes the efficacies of all tested H_1R antagonists regarding β-arrestin 1 or 2 recruitment. Evidently, these compounds did not exhibit agonism in this assay, but rather acted as inverse agonists with varying intrinsic activities. In case of β-arrestin 1 recruitment, the inverse agonistic effects were negligible, between -0.6 and -2.4 % relative to the histamine induced maximal response. By contrast, in the β-arrestin 2 recruitment assay, the compounds exhibited stronger inverse agonistic effects, ranging from -0.8 to -13.3 %. Among the investigated H_1R antagonists, clemastine (**16**) showed the strongest inverse agonistic effect (-13.3 %) in β-arrestin 2 recruitment, while levocetirizine (**17**) had the weakest effect (-2.3 %). Of the tested antipsychotics, maprotiline (**22**) was the strongest inverse agonist (-12.8 % in β-arrestin 2 recruitment). Inverse agonism at the H_1R has been shown in different assay systems for several of those H_1R ligands,[24,38] though strongly depending on the expression levels of the receptor and signal transducer proteins. Except for isoloxapine (**24**), which exhibited neutral behavior both assays, all ligands showed a strong increase in inverse intrinsic activity regarding β-arrestin 2 compared to β-arrestin 1 recruitment. At first glance, these findings may point towards a functional bias of these ligands discriminating between the two arrestin isoforms. However, the extent of inverse agonism is depending on the degree of constitutive activity, that is, the magnitude of the signal background. Therefore, most probably, the difference in H_1R inverse agonism between β-arrestin 2 and β-arrestin 1 cells has to be attributed to the different degrees of constitutive activity rather than a discrimination between arrestin isoforms. Normalization of the effects to the intensity of the background signal extenuates most of these differences, but was relinquished to prevent over-interpretation of minor effects, especially, with regard to the β -arrestin 1 data.

5.2.2. Pharmacological profiling of selected H_1R agonists for G-protein or β-arrestin bias

Comprehensive data on H_1R agonists has been gained from organ pharmacology and recombinant systems relying on G-protein based readouts. By contrast, so far, no information is available regarding ligand biased signaling at the H_1R. In order to investigate selected phenylhistamine- and histaprodifen-type H_1R agonists for functional selectivity, concentration-response curves were determined in the GTPase and the β-arrestin 1 or 2 recruitment assay, respectively.

The potencies and efficacies of the tested ligands in the three different assays are given in Table 5-1. Ligand induced responses were normalized to maximal effect of histamine (100 % value) and the solvent (0 %). Thus, the endogenous ligand histamine (**1**) is defined as unbiased, full agonist (cf. Fig 5-7). Interestingly, while exhibiting comparable potencies in the GTPase and β-arrestin 1 recruitment assay (pEC_{50} (GTPase) = 6.91; pEC_{50} (βArr1) = 7.11), histamine has a significantly increased potency in the β-arrestin 2 assay (pEC_{50} (βArr2) = 7.74; $p < 0.01$). Of all tested compound, UR-KUM530 (**5**) showed the highest potency and acted as a full agonist in all three assays (cf. Fig. 5-5). Compound **5** exhibited the same profile as histamine with the highest potency in β-arrestin 2 recruitment, albeit without significant differences between the assays (cf. Fig. 5-6). The phenylhistamine derivatives **2**-**4** acted as partial agonists in both readout systems and were less potent than histamine. Interestingly, all three compounds revealed a significant

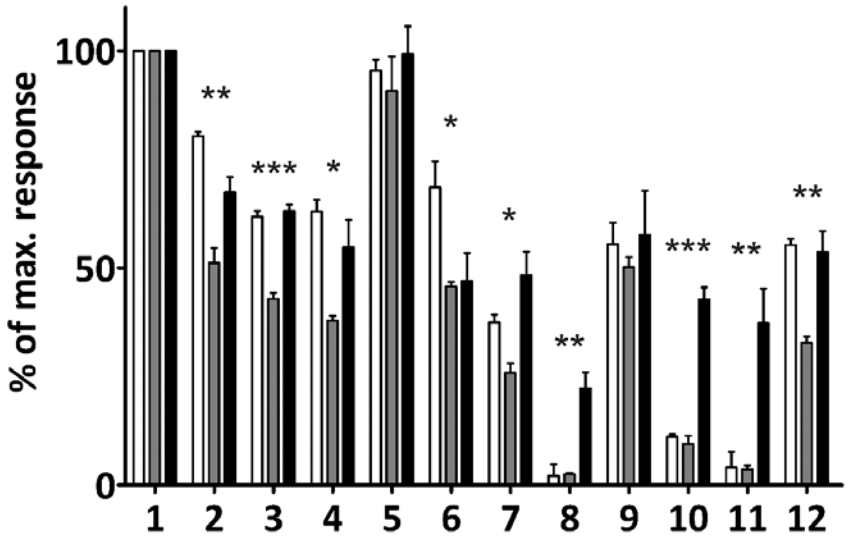

Fig. 5-5: Efficacies of the tested agonists in the [^{32}P]GTPase assay (□ white bars), β-arrestin 1 recruitment assay (■ grey bars) and β-arrestin 2 recruitment assay (■ black bars). The results were normalized to the effect induced by histamine (100 % value) and solvent (0 % value). The results are mean values ± SEM of at 2-4 independent experiments. Statistical analysis was performed using one way ANOVA including Bonferoni`s multiple comparison test ($* \triangleq p < 0.05$; $** \triangleq p < 0.01$; $*** \triangleq p < 0.001$)

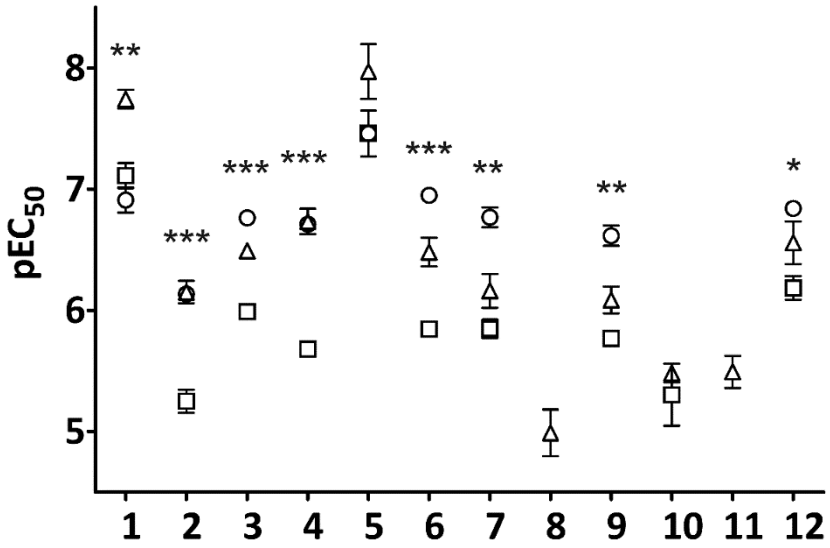

Fig. 5-6: pEC_{50} values of the tested agonists in the [^{32}P]GTPase assay (○ circles), β-arrestin 1 recruitment assay (□ squares) and β-arrestin 2 recruitment assay (△ triangles). The results are mean values ± SEM of 2-4 independent experiments. Lacking efficacy hampered with determining potencies for compounds **8**, **10** and **11** in one or more assays. Statistical analysis was performed using one way ANOVA including Bonferoni`s multiple comparison test ($* \triangleq p < 0.05$; $** \triangleq p < 0.01$; $*** \triangleq p < 0.001$)

reduction in potency and efficacy in β-arrestin 1 recruitment compared to either the G-protein or β-arrestin 2 based readout. Comparing the functional data of 2-(3-bromophenyl)histamine (**3**) to UR-KUM530 (**5**) shows that the introduction of an imidazolylethyl moiety in N^{α} position of the molecule restores full agonistic activity and significantly increases potency. Functional bias, as in case of **3**, was not detectable for **5**.

Histaprodifen (**6**) was previously described as a selective H_1R agonists, equipotent with histamine.[31,32,41] This was confirmed for G-protein activation: the pEC_{50} value for **6** was comparable to that of histamine despite reduced efficacy. However, the β-arrestin recruitment assay revealed a dramatic change. Compound **6** was almost 20-fold less potent than **1** in the β-arrestin 2 assay and 17-fold less potent in β-arrestin 1 recruitment, reflecting a significantly reduced potency and efficacy of **6** in both arrestin recruitment assays compared to the GTPase assay. The chiral suprahistaprodifen derivatives, (*R*)-UR-BS355 (**7**) and (*S*)-UR-BS354 (**8**), exhibited an interesting profile. Whereas the (*R*)-configured compound **7** acted as a partial agonist in all three assay, showing the lowest efficacy in β-arrestin 1 recruitment, the (*S*)-enantiomer **8** was a neutral antagonists in the GTPase and β-arrestin 1 recruitment assay while retaining partial agonism in β-arrestin 2 recruitment. The phenoprodifen derivatives **9**-**11** revealed another interesting effect. Whereas **9** showed comparable efficacies regarding G-protein and arrestin activation, the introduction of a methyl group, resulting in the two stereoisomers (*R*)-UR-BS358 (**10**) and (*S*)-UR-BS364 (**11**), gave a strong bias towards β-arrestin 2 (cf. Fig.5-5). Whereas **10** still showed very weak partial agonism in the GTPase and β-arrestin 1 recruitment assay, the

(*S*)-enantiomer **11** was completely devoid of agonistic activity in those two assays, while still retaining 37 % efficacy in β-arrestin 2 recruitment.

For the chiral histaprodifens exhibiting β-arrestin 2 bias, interesting findings were previously published, regarding their functional behavior at different H_1R species orthologs.[41] Compound **7** acted as partial agonist at all four tested receptor orthologs, whereas **8** activated only the guinea pig H_1R (gpH_1R) and was as a neutral antagonists at the other species, including the human H_1R (hH_1R). Compounds **10** and **11** were antagonists at all investigated H_1R except for the gpH_1R. Surprisingly, this unique switch between agonism and antagonism correlates well with the functional selectivity of these compounds regarding G-protein and β-arrestin activation. Molecular dynamics simulations

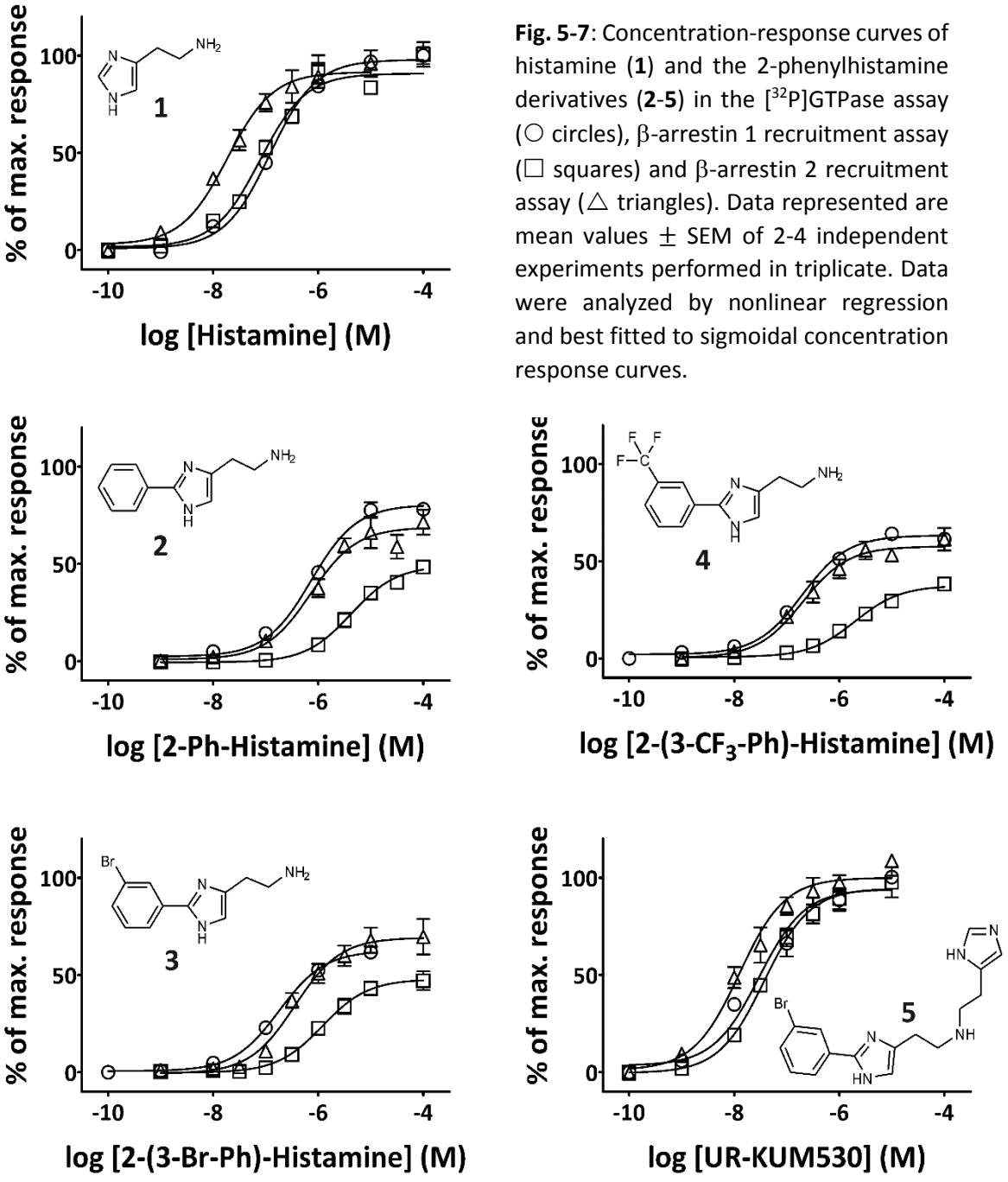

Fig. 5-7: Concentration-response curves of histamine (**1**) and the 2-phenylhistamine derivatives (**2**-**5**) in the [^{32}P]GTPase assay (○ circles), β-arrestin 1 recruitment assay (□ squares) and β-arrestin 2 recruitment assay (△ triangles). Data represented are mean values ± SEM of 2-4 independent experiments performed in triplicate. Data were analyzed by nonlinear regression and best fitted to sigmoidal concentration response curves.

revealed two possible orientations for the binding of the suprahistaprodifen derivatives into the H_1R binding pocket. Only **7** fits well into the binding pocket in both orientations. By contrast one of these orientation is impossible for the (*S*)-configured compound **8** due to a steric clash of the methyl group.[41] Though these findings suggest that different binding modes might be responsible for the functional bias found for these chiral compounds, further molecular modelling studies will be necessary to elucidate the nature of these effects.

Unfortunately the interpretation of these finding is further complicated through the limited structural diversity of the tested compounds. Another problem occurring with several of the histaprodifens were adverse effects when using the compounds at concentrations exceeding 30 µM. At higher concentrations these effects became obvious from a drastic decrease in the detected signal intensity, rendering the generated data useless (data not shown). Most probably, these effects are caused by the amphiphilic nature of the compounds, causing changes in membrane permeability of the cells. These unspecific effects complicated the construction of complete concentration-response curves, especially, for some of the ligands with lower affinity (cf. Fig 5-8).

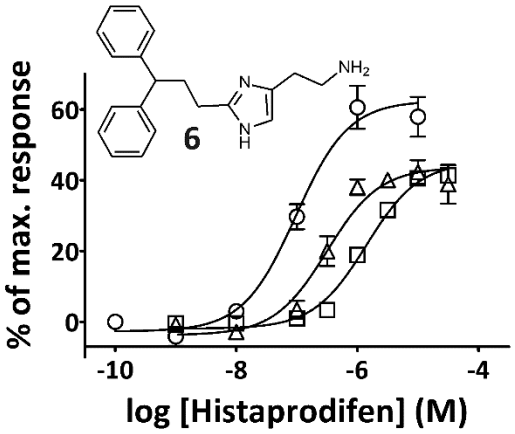

Fig. 5-8: Concentration response curves of the histaprodifen derivatives **6**-**12** in the [^{32}P]GTPase assay (○ circles), β-arrestin 1 recruitment assay (□ squares) and β-arrestin 2 recruitment assay (△ triangles). Data are mean values ± SEM of at least 3 independent experiments performed in triplicate. Data were analyzed by nonlinear regression and best fitted to sigmoidal concentration-response curves.

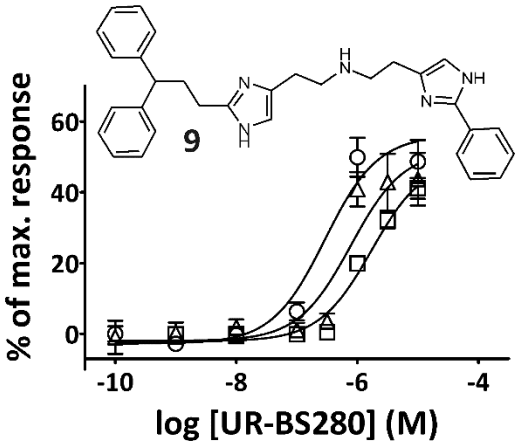

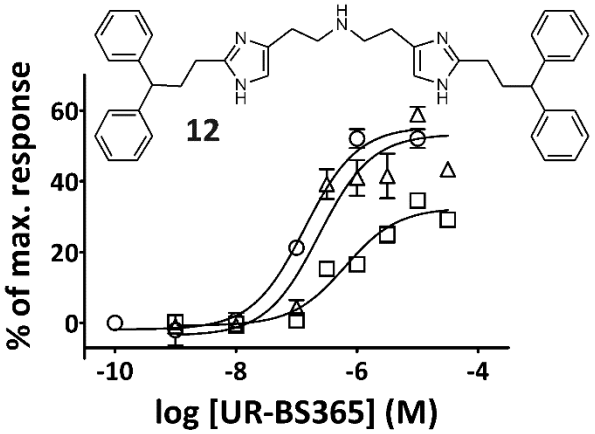

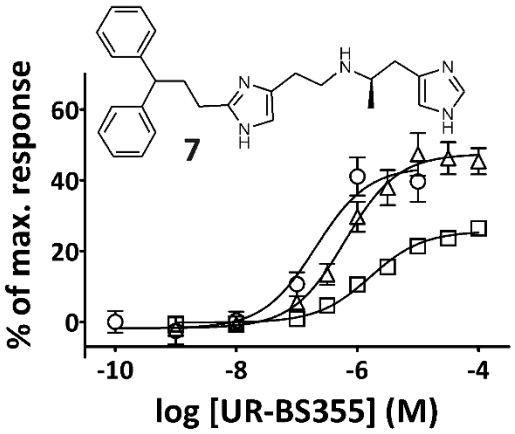

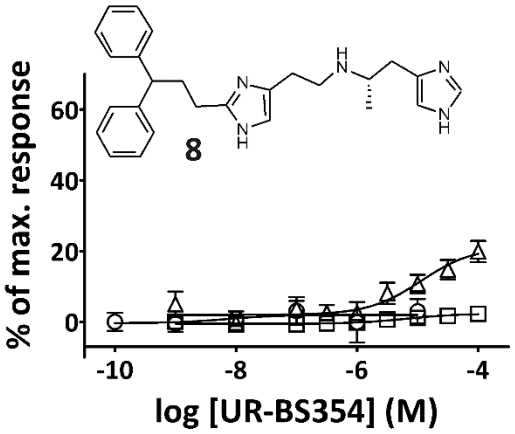

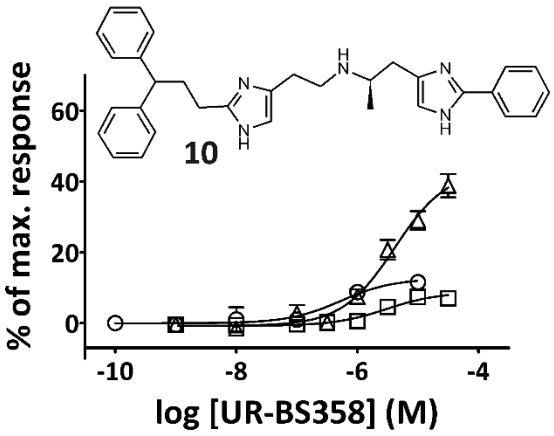

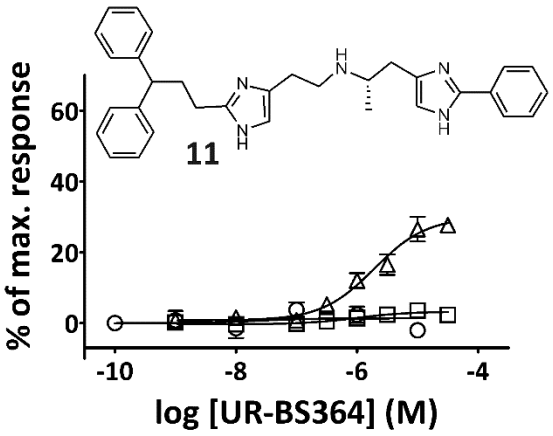

Tab. 5-1: Potencies and efficacies of the tested H_1R agonists in the GTPase and β-arrestin 1 and 2 recruitment assay.

Cpd	GTPase assay			β-arrestin 1 recruitment			β-arrestin 2 recruitment		
	pEC_{50} ± SEM	E_{max} ± SEM	N	pEC_{50} ± SEM	E_{max} ± SEM	N	pEC_{50} ± SEM	E_{max} ± SEM	N
1	6.91 ± 0.10	1.00	4	7.11 ± 0.10	1.00	4	7.74 ± 0.08	1.00	3
2	6.14 ± 0.00	0.80 ± 0.01	3	5.25 ± 0.10	0.51 ± 0.03	3	6.15 ± 0.09	0.67 ± 0.04	3
3	6.76 ± 0.03	0.62 ± 0.01	2	5.99 ± 0.03	0.43 ± 0.01	3	6.49 ± 0.01	0.63 ± 0.02	3
4	6.71 ± 0.04	0.63 ± 0.03	3	5.68 ± 0.06	0.38 ± 0.01	3	6.73 ± 0.10	0.55 ± 0.06	3
5	7.46 ± 0.19	0.95 ± 0.03	3	7.46 ± 0.03	0.91 ± 0.08	3	7.97 ± 0.23	0.99 ± 0.06	3
6	6.95 ± 0.03	0.69 ± 0.06	4	5.85 ± 0.02	0.46 ± 0.01	4	6.48 ± 0.12	0.47 ± 0.06	3
7	6.77 ± 0.08	0.37 ± 0.02	3	5.85 ± 0.07	0.26 ± 0.02	3	6.16 ± 0.14	0.48 ± 0.05	4
8	n.d.	0.02 ± 0.02	3	n.d.	0.03 ± 0.00	3	4.99 ± 0.19	0.22 ± 0.04	4
9	6.61 ± 0.08	0.55 ± 0.05	2	5.77 ± 0.06	0.50 ± 0.02	4	6.01 ± 0.11	0.58 ± 0.10	3
10	n.d.	0.11 ±0.01	3	5.30 ± 0.25	0.09 ± 0.02	3	5.48 ± 0.08	0.43 ± 0.03	4
11	n.d.	0.04 ± 0.03	3	n.d.	0.04 ± 0.01	3	5.49 ± 0.13	0.37 ± 0.08	4
12	6.84 ± 0.05	0.55 ± 0.01	3	6.19 ± 0.10	0.33 ± 0.01	4	6.56 ± 0.18	0.54 ± 0.05	4

5.3. Summary and conclusions

None of the investigated H_1R antagonists exhibited a functional bias. However, varying levels of inverse agonistic effects were detected at the two β-arrestin isoforms. Amongst the phenylhistamine- and histaprodifen-type H_1R agonists, several compounds revealed functional selectivity regarding G-protein versus arrestin activation and exhibited a preference for one of the two β-arrestin isoforms. The phenylhistamines **2**-**4** were biased for G-protein and β-arrestin 2 activation over β-arrestin 1 recruitment, whereas the histaprodifen derivatives **8**, **10** and **11** showed a strong bias for β-arrestin 2. Most studies published on functional selectivity of GPCR ligands were based on just one isoform of β-arrestin, mostly β-arrestin 2, neglecting a possible preference for one of the two variants.

Ligands exhibiting a functional bias are very useful tools for the deconvolution of complex receptor signaling profiles *in vivo* and *in vitro*. Ligands biased for either arrestin isoform could be especially useful to elucidate the complex influence of the two different arrestins on receptor regulation and downstream signaling such as the MAP kinase pathway. Unfortunately, the adverse effects at higher concentrations than 30 µM in combination with the low potency of some of the biased agonists severely limit their suitability as pharmacological tools for investigating arrestin mediated cellular signaling. The characterized compounds might, however, provide a starting point for the development of new biased agonists for the H_1R with higher affinity and improved drug-like properties.

5.4. Materials and methods

5.4.1. Materials

Unless stated otherwise, all chemicals and reagents were purchased from Sigma-Aldrich Chemie (Munich, Germany) or Merck (Darmstadt, Germany). For media and reagents used for the luciferase complementation assay, see Chapter 3.4.

5.4.1.1. H_1 receptor ligands

The chemical structures of the investigated H_1R ligands are shown in Fig. 5-1 and 5-2. Histamine dihydrochloride (**1**) was from Alfa Aesar (Karlsruhe, Germany). The phenylhistamine derivatives **2**-**5** and histaprodifen derivatives **6**-**12** were synthesized in our laboratory.[30,33] Mepyramine maleate (**14**), clemastine fumarate (**16**), ketotifen fumarate (**19**) and terfenadine (**20**) were from Tocris Bioscience (Ellisville, MO, USA). Diphenhydramine (**13**), cyproheptadine hydrochloride (**15**) and azelastine hydrochloride (**18**) were from Sigma-Aldrich Chemie (Munich, Germany). Levocetirizine dihydrochloride (**17**), mirtazapine (**21**) and maprotiline hydrochloride (**22**) were from Biotrend Chemikalien (Cologne, Germany). Clozapine (**23**) was a gift from Novartis Pharma (Nuremberg, Germany). Isoloxapine (**24**) was provided by Prof. Dr. S. Elz, University of Regensburg. Of all compounds, 10 mM stock solutions were prepared in 50 % DMSO.

5.4.2. Methods

5.4.2.1. [^{32}P]GTPase assay

The [^{32}P]GTPase assay was performed as previously described.[40,41] Ligand stimulated G_q-protein catalyzed GTP hydrolysis was measured using membranes of *Sf*9 insect cells expressing the human H_1R and the RGS4 protein. The functional data of the H_1R agonists, determined in the GTPase assay, were kindly provided by Dr. Andrea Strasser.

5.4.2.2. Luciferase complementation assay

The luciferase complementation assay measuring β-arrestin recruitment to the receptor was performed as described above (cf. 3.4.7.) using the HEK293T-βArr1-H_1R and HEK293T-βArr2-H_1R cells stably expressing the H_1R-ElucC and either the βArr1-ElucN or βArr2-ElucN fusion proteins (cf. 3.2.). For cell culture conditions and media requirements, see 3.4.2. The working solutions of all H_1R ligands contained 5 % DMSO, giving a final concentration of 0.5 % DMSO in the assay mixture. The cells were stimulated with the corresponding ligand concentrations for 60 min at RT. The tested H_1R antagonists **13**-**24**

were used at concentrations of 10 µM and 100 µM to stimulate β-arrestin recruitment. For the investigation of the agonists **1**-**12**, dilution series ranging from 100 pM to 100 µM were prepared. The results were normalized to the response induced by 1 mM histamine (100 % value) and the solvent containing 5% DMSO (0 % value).

5.4.2.3. Data analysis

Data analysis was performed as described above (cf. 4.3.2.2). Statistical analysis of variances was performed by one way ANOVA followed by Bonferoni`s multiple comparison test using GraphPad Prism 5 software (GraphPad Software, Inc., La Jolla, CA).

5.5. References

1. Ash, A. S.; Schild, H. O. Receptors mediating some actions of histamine. *B. J. Pharmacol. Chemother.* **1966**, 27, 427-439.
2. Hill, S. J.; Young, J. M.; Marrian, D. H. Specific binding of 3H-mepyramine to histamine H1 receptors in intestinal smooth muscle. *Nature* **1977**, 270, 361-363.
3. Hill, S. J. Distribution, properties, and functional characteristics of three classes of histamine receptor. *Pharmacol. Rev.* **1990**, 42, 45-83.
4. Hill, S. J.; Ganellin, C. R.; Timmerman, H.; Schwartz, J. C.; Shankley, N. P.; Young, J. M.; Schunack, W.; Levi, R.; Haas, H. L. International Union of Pharmacology. XIII. Classification of histamine receptors. *Pharmacol. Rev.* **1997**, 49, 253-278.
5. Yanai, K.; Tashiro, M. The physiological and pathophysiological roles of neuronal histamine: an insight from human positron emission tomography studies. *Pharmacol. Ther.* **2007**, 113, 1-15.
6. Haas, H. L.; Sergeeva, O. A.; Selbach, O. Histamine in the nervous system. *Physiol. Rev.* **2008**, 88, 1183-1241.
7. Thurmond, R. L. Histamine inflammation. Preface. *Adv. Exp. Med. Biol.* **2010**, 709, vii-viii.
8. Taylor-Clark, T. Histamine in allergic rhinitis. *Adv. Exp. Med. Biol.* **2010**, 709, 33-41.
9. Ohbayashi, M.; Manzouri, B.; Morohoshi, K.; Fukuda, K.; Ono, S. J. The role of histamine in ocular allergy. *Adv. Exp. Med. Biol.* **2010**, 709, 43-52.
10. Zuberbier, T.; Maurer, M. Antihistamines in the treatment of urticaria. *Adv. Exp. Med. Biol.* **2010**, 709, 67-72.
11. Buddenkotte, J.; Maurer, M.; Steinhoff, M. Histamine and antihistamines in atopic dermatitis. *Adv. Exp. Med. Biol.* **2010**, 709, 73-80.
12. Leurs, R.; Smit, M. J.; Timmerman, H. Molecular pharmacological aspects of histamine receptors. *Pharmacol. Ther.* **1995**, 66, 413-463.
13. Yamashita, M.; Fukui, H.; Sugama, K.; Horio, Y.; Ito, S.; Mizuguchi, H.; Wada, H. Expression cloning of a cDNA encoding the bovine histamine H1 receptor. *Proc. Natl. Acad. Sci. U. S. A.* **1991**, 88, 11515-11519.
14. De Backer, M. D.; Gommeren, W.; Moereels, H.; Nobels, G.; Van Gompel, P.; Leysen, J. E.; Luyten, W. H. Genomic cloning, heterologous expression and pharmacological characterization of a human histamine H1 receptor. *Biochem. Biophys. Res. Commun.* **1993**, 197, 1601-1608.
15. Fujimoto, K.; Horio, Y.; Sugama, K.; Ito, S.; Liu, Y. Q.; Fukui, H. Genomic cloning of the rat histamine H1 receptor. *Biochem. Biophys. Res. Commun.* **1993**, 190, 294-301.
16. Fukui, H.; Fujimoto, K.; Mizuguchi, H.; Sakamoto, K.; Horio, Y.; Takai, S.; Yamada, K.; Ito, S. Molecular cloning of the human histamine H1 receptor gene. *Biochem. Biophys. Res. Commun.* **1994**, 201, 894-901.
17. Traiffort, E.; Leurs, R.; Arrang, J. M.; Tardivel-Lacombe, J.; Diaz, J.; Schwartz, J. C.; Ruat, M. Guinea pig histamine H1 receptor. I. Gene cloning, characterization, and tissue expression revealed by in situ hybridization. *J. Neurochem.* **1994**, 62, 507-518.
18. Leurs, R.; Traiffort, E.; Arrang, J. M.; Tardivel-Lacombe, J.; Ruat, M.; Schwartz, J. C. Guinea pig histamine H1 receptor. II. Stable expression in Chinese hamster ovary cells reveals the interaction with three major signal transduction pathways. *J. Neurochem.* **1994**, 62, 519-527.

19. Smit, M. J.; Timmerman, H.; Hijzelendoorn, J. C.; Fukui, H.; Leurs, R. Regulation of the human histamine H1 receptor stably expressed in Chinese hamster ovary cells. *Br. J. Pharmacol.* **1996**, 117, 1071-1080.
20. Leopoldt, D.; Harteneck, C.; Nurnberg, B. G proteins endogenously expressed in Sf 9 cells: interactions with mammalian histamine receptors. *Naunyn Schmiedebergs Arch. Pharmacol.* **1997**, 356, 216-224.
21. Berridge, M. J.; Lipp, P.; Bootman, M. D. The versatility and universality of calcium signalling. *Nat. Rev. Mol. Cell Biol.* **2000**, 1, 11-21.
22. Carrasco, S.; Merida, I. Diacylglycerol, when simplicity becomes complex. *Trends Biochem. Sci.* **2007**, 32, 27-36.
23. Bakker, R. A.; Schoonus, S. B.; Smit, M. J.; Timmerman, H.; Leurs, R. Histamine H(1)-receptor activation of nuclear factor-kappa B: roles for G beta gamma- and G alpha(q/11)-subunits in constitutive and agonist-mediated signaling. *Mol. Pharmacol.* **2001**, 60, 1133-1142.
24. Bakker, R. A.; Wieland, K.; Timmerman, H.; Leurs, R. Constitutive activity of the histamine H(1) receptor reveals inverse agonism of histamine H(1) receptor antagonists. *Eur. J. Pharmacol.* **2000**, 387, R5-7.
25. Robinson, A. J.; Dickenson, J. M. Activation of the p38 and p42/p44 mitogen-activated protein kinase families by the histamine H(1) receptor in DDT(1)MF-2 cells. *Br. J. Pharmacol.* **2001**, 133, 1378-1386.
26. Esbenshade, T. A.; Kang, C. H.; Krueger, K. M.; Miller, T. R.; Witte, D. G.; Roch, J. M.; Masters, J. N.; Hancock, A. A. Differential activation of dual signaling responses by human H1 and H2 histamine receptors. *J. Recept. Signal Transduct. Res.* **2003**, 23, 17-31.
27. Brighton, P. J.; Rana, S.; Challiss, R. J.; Konje, J. C.; Willets, J. M. Arrestins differentially regulate histamine- and oxytocin-evoked phospholipase C and mitogen-activated protein kinase signalling in myometrial cells. *Br. J. Pharmacol.* **2011**, 162, 1603-1617.
28. Barak, N. Betahistine: what's new on the agenda? *Expert opin. Investig. Drugs* **2008**, 17, 795-804.
29. Leschke, C.; Elz, S.; Garbarg, M.; Schunack, W. Synthesis and histamine H1 receptor agonist activity of a series of 2-phenylhistamines, 2-heteroarylhistamines, and analogues. *J. Med. Chem.* **1995**, 38, 1287-1294.
30. Kunze, M. Histamin-H1-Rezeptoragonisten vom Suprahistaprodifen- und 2-Phenylhistamin-Typ und 2-substituierte Imidazolylpropan-Derivate als Liganden für H1/H2/H3/H4-Rezeptoren. Neue Synthesestrategien und pharmakologische Testung Dissertation, Universität Regensburg, 2007. http://epub.uni-regensburg.de/10517/.
31. Elz, S.; Kramer, K.; Pertz, H. H.; Detert, H.; ter Laak, A. M.; Kuhne, R.; Schunack, W. Histaprodifens: synthesis, pharmacological in vitro evaluation, and molecular modeling of a new class of highly active and selective histamine H(1)-receptor agonists. *J. Med. Chem.* **2000**, 43, 1071-1084.
32. Elz, S.; Kramer, K.; Leschke, C.; Schunack, W. Ring-substituted histaprodifen analogues as partial agonists for histamine H(1) receptors: synthesis and structure-activity relationships. *Eur. J. Med. Chem.* **2000**, 35, 41-52.
33. Striegl, B. Synthese und funktionelle in-vitro-Pharmakologie neuer Histamin-H1-Rezeptoragonisten aus der Suprahistaprodifen-Reihe. Dissertation, Universität Regensburg, 2007. http://epub.uni-regensburg.de/10494/.
34. Haaksma, E. E.; Leurs, R.; Timmerman, H. Histamine receptors: subclasses and specific ligands. *Pharmacol. Ther.* **1990**, 47, 73-104.

35. Klimek, A. Cyproheptadine (Peritol) in the treatment of migraine and related headache. *Ther. Hung.* **1979**, 27, 93-94.
36. Rijnders, R. J.; Laman, D. M.; Van Diujn, H. Cyproheptadine for posttraumatic nightmares. *Am. J. Psychiatry* **2000**, 157, 1524-1525.
37. Appl, H.; Holzammer, T.; Dove, S.; Haen, E.; Strasser, A.; Seifert, R. Interactions of recombinant human histamine H(1)R, H(2)R, H(3)R, and H(4)R receptors with 34 antidepressants and antipsychotics. *Naunyn Schmiedebergs Arch. Pharmacol.* **2012**, 385, 145-170.
38. Bakker, R. A.; Nicholas, M. W.; Smith, T. T.; Burstein, E. S.; Hacksell, U.; Timmerman, H.; Leurs, R.; Brann, M. R.; Weiner, D. M. In vitro pharmacology of clinically used central nervous system-active drugs as inverse H(1) receptor agonists. *J. Pharmacol. Exp. Ther.* **2007**, 322, 172-179.
39. Richelson, E. Tricyclic antidepressants block histamine H1 receptors of mouse neuroblastoma cells. *Nature* **1978**, 274, 176-177.
40. Seifert, R.; Wenzel-Seifert, K.; Bürckstümmer, T.; Pertz, H. H.; Schunack, W.; Dove, S.; Buschauer, A.; Elz, S. Multiple Differences in Agonist and Antagonist Pharmacology between Human and Guinea Pig Histamine H1-Receptor. *J. Pharmacol. Exp. Ther.* **2003**, 305, 1104-1115.
41. Strasser, A.; Striegl, B.; Wittmann, H. J.; Seifert, R. Pharmacological profile of histaprodifens at four recombinant histamine H1 receptor species isoforms. *J. Pharmacol. Exp. Ther.* **2008**, 324, 60-71.

Chapter 6

Functional selectivity at the H_2 receptor

6. Functional selectivity at the H_2 receptor

6.1. Introduction

The existence of the histamine H_2 receptor, the second addition to the histamine receptor family, was postulated by Ash and Schild in 1966 due to the observation that several actions of histamine could not be blocked by "antihistamines", the H_1R antagonists.[1] The detailed pharmacological characterization of the H_2R by Black and colleagues in the late 1960s led to the discovery of the first selective antagonist burimamide[2] and to the development of cimetidine as a blockbuster antiulcer drug.[3] Another breakthrough in H_2R research was achieved by the successful cloning of the H_2R gene by Gantz and coworkers in 1991.[4]

Detailed analysis of the tissue distribution of the H_2R has been compromised by the lack of suitable radioligands.[5] Even though [^{125}I]iodoaminopotentidine[6] was successfully used to map the H_2R in the brain,[7] most information about H_2R expression patterns is derived from functional studies.[8] These efforts have been greatly facilitated by the development of several selective H_2R agonists (i.e. dimaprit, impromidine, amthamine) and antagonists (i.e. burimamide, cimetidine, famotidine, tiotidine).[9] H_2R mediated cAMP accumulation was demonstrated in gastric parietal cells, where the H_2R plays a crucial role in the regulation of gastric acid secretion.[2,10] Furthermore activation of the H_2R exhibits positive chronotropic and inotropic effects on atrial and ventricular tissue in the heart and leads to relaxation of airway, uterine and vascular smooth muscles.[2,5] H_2R expression has been demonstrated for various cells of the immune system,[5] where it exerts diverse functions like inhibition of histamine release from mast cells and the antibody production of B-cells or modulation of cytokine production from T helper cells.[8,11]

The H_2R is a 359 aa protein and belongs to the class of rhodopsin-like GPCRs.[5] It is now widely accepted, that the H_2R couples primarily to $G_{\alpha s}$ proteins leading to the activation of adenylate cyclases (ACs).[8] The resulting cAMP accumulation leads to the activation of protein kinase A (PKA) and subsequently, for instance, to gene expression via the cAMP response element binding protein (CREB). Although H_2R mediated cAMP accumulation seems to be the main response to H_2R activation,[8] it has been demonstrated for several cell lines and tissues that the H_2R is capable of evoking a Ca^{2+} signal independent of AC activation, though there is controversial evidence, whether this observed rise in intracellular Ca^{2+} is due to influx of extracellular calcium[12] or mobilization from intracellular stores.[13,14] Additionally, H_2R activation was demonstrated to induce $G_{\alpha q}$ mediated PLC activation and incorporation of [^{32}P]GTP azidoanilide into G_q like proteins in different cell lines,[15] while in other systems, G_q coupling of the H_2R could not be confirmed.[16] Collectively, these data suggest that the H_2R is capable of coupling to different G-proteins and that the signal transduction pathways of the H_2R are highly dependent on the cellular background.

So far, only limited information is available on the involvement of β-arrestins on H_2R signaling and regulation. It has been demonstrated, that overexpression of β-arrestin 2, but

not β-arrestin 1, leads to a decrease in the H_2R binding sites at the cell surface and a significant reduction of the amthamine induced cAMP response.[17] Furthermore, down-regulation of β-arrestin 2 by RNA interference abolished agonist-induced internalization of the H_2R as well as subsequent resensitization.[17] This data strongly supports the involvement of β-arrestin 2 in H_2R regulation and trafficking. In a recently published work, Alonso et al. investigated the effect of the standard H_2R antagonists cimetidine (CIM), ranitidine (RAN) and tiotidine (TIO) on receptor desensitization and internalization as well as on $G_{\alpha S}$ protein independent pathways.[18] They demonstrated that treatment with RAN and TIO lead to receptor internalization, which could be suppressed by expression of a dominant negative arrestin mutant. Furthermore, CIM, RAN and TIO induced receptor desensitization and ERK1/2 phosphorylation. Surprisingly, neither effect seemed to be mediated by β-arrestin. ERK phosphorylation of the ligands was rather mediated by the $G_{\beta\gamma}$ subunit of the trimeric G-protein. To date, there is no information available about the functional profiles of various other H_2R ligands regarding the activation of alternate signaling pathways through different receptor conformations, especially, towards arrestin dependent pathways. This chapter will focus on the profiling of a set of H_2R agonists and antagonists for their pharmacological characteristics in β-arrestin activation using the previously introduced arrestin recruitment assay.

6.1.1. Selected H_2R ligands

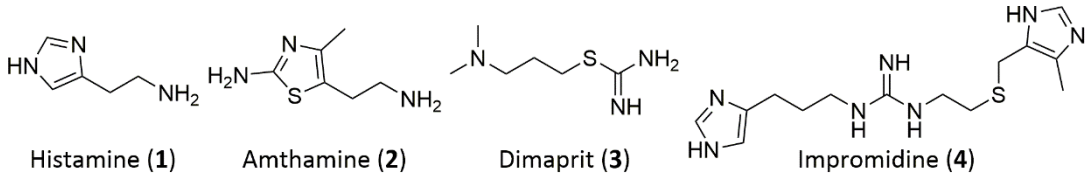

***N^G*-Acylated Imidazoylpropylguanidines**

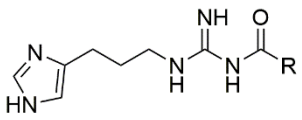

Cpd.	R
UR-AK156 (**5**)	
UR-AK224 (**6**)	(S)
UR-AK437 (**7**)	
UR-AK284 (**8**)	
UR-ML17 (**9**)	
UR-ML22 (**10**)	

***N^G*-Acylated Aminothiazolylpropylguanidines**

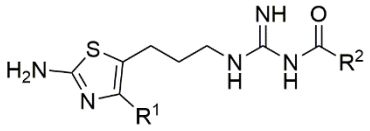

Cpd.	R^1	R^2
UR-AK472 (**11**)	H	
UR-AK477 (**12**)	H	
UR-AK479 (**13**)	H	
UR-BIT336 (**14**)	H	
UR-AK423 (**15**)	CH_3	
UR-BIT24 (**16**)	CH_3	

Fig. 6-1: Structures of the selected H_2R agonists

Since the discovery of the first selective H_2R antagonists burimamide in 1972,[2] a multitude of new H_2R ligands have been reported. Over the past decades, several H_2R agonists such as amthamine (**2**),[19,20] dimaprit (**3**)[21], impromidine (**4**)[22] and arpromidine,[23] have been described. Unfortunately, the lack of selectivity for the H_2R over the H_3R and H_4R[24,25] for some of these compounds, as well as limited oral bioavailability and CNS penetration of guanidine-type agonists such as impromidine and arpromidine considerably reduced their value as pharmacological tools to study H_2R function in vivo. Therefore, in our laboratory much effort has been spent to overcome these limitations, resulting in acylguanidines as bioisosteric replacements of the guanidine-type ligands.[26,27] From these series, a set of compounds, containing either an imidazole (Cpd. **5**-**10**) or amino(methyl)thiazole (Cpd. **11**-**16**) as pharmacophoric entity, was selected for investigation in the arrestin recruitment assay (chemical structures, cf. Fig. 6-1). In addition several bivalent N^G-acylated guanidine type ligands with varying chain lengths were included in this study, due to very high potency at the H_2R[28] (Cpd. **17**-**23**, see Fig. 6-2). Unfortunately, some of the acylguanidine type compounds showed poor stability during storage in aqueous solutions. This stimulated the recent development of bivalent N^G-carbamoylated guanidine type H_2R ligands with improved stability and high potency at the H_2R (Cpd. **24**-**29,** see Fig. 6-2).

Bivalent N^G-Acylated Guanidines

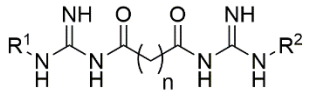

Cpd.	n	R^1=R^2
UR-BIT237 (**17**)	5	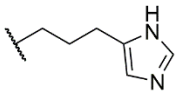
UR-AK480 (**18**)	8	
UR-AK381 (**19**)	8	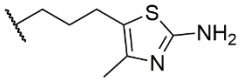
UR-BIT108 (**20**)	6	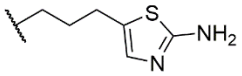
UR-BIT106 (**21**)	8	

Cpd.	n	R^1	R^2
UR-BIT82 (**22**)	8	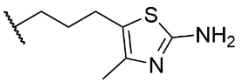	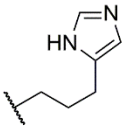
UR-BIT308 (**23**)	8	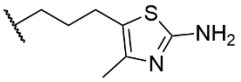	

Bivalent N^G-Carbamoylated Guanidines

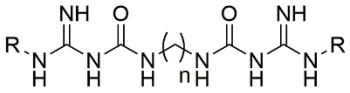

Cpd.	n	R
UR-NK52 (**24**)	4	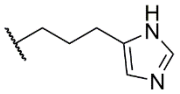
UR-NK3 (**25**)	6	
UR-NK60 (**26**)	8	

Cpd.	n	R
UR-NK41 (**27**)	4	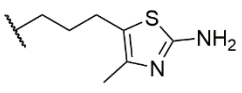
UR-NK22 (**28**)	6	
UR-NK53 (**29**)	7	

Fig 6-2: Structures of the selected bivalent H_2R agonists

H_2R antagonists have been used clinically for decades in the treatment of peptic ulcers and gastrooesophageal reflux disease.[29] Cimetidine (**31**), representing the first clinically used H_2R antagonist, famotidine (**30**) and ranitidine (**32**) are standard H_2R antagonists, which have been used extensively to characterize receptor function *in vivo*.[5] Recently, a series of squaramide derivatives related to the known H_2R antagonist BMY-25368[30] was developed in our lab, representing an interesting starting point for the development of new radiolabeled or fluorescent tool compounds.[31] From this series of compounds, two amine precursors as well as a propionylated (**35**) and a bivalent (**36**) ligand were included in this study (see Fig. 6-3).

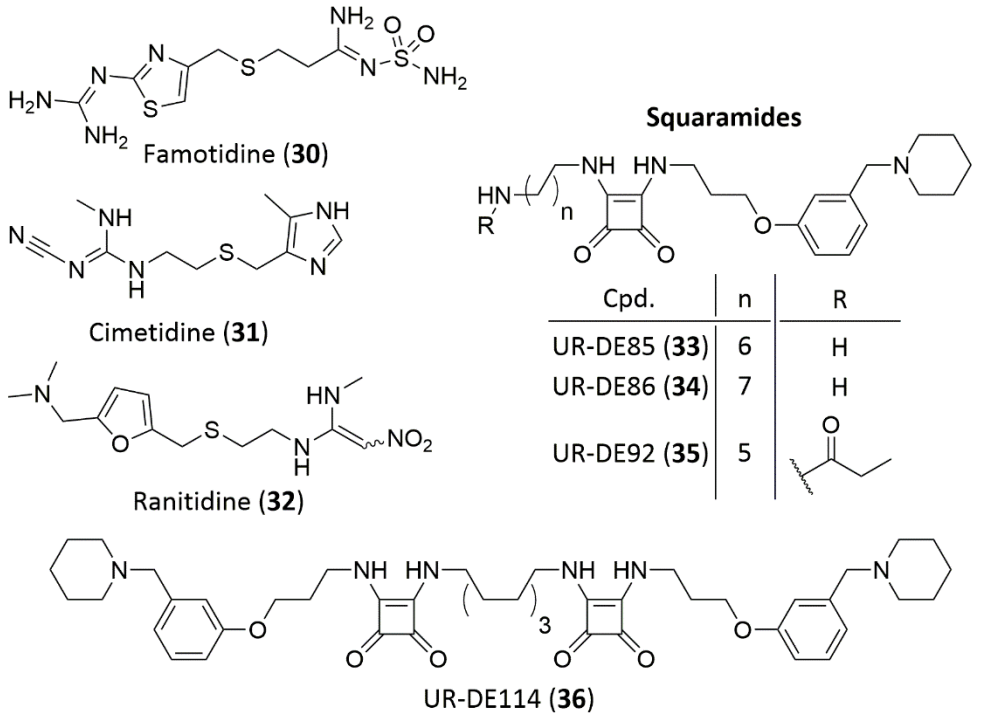

Fig 6-3: Structures of the selected H_2R antagonists

6.2. Results and discussion

In order to address putative functional selectivity of the selected H_2R ligands for G-protein or β-arrestin activation, two assay systems were selected. G-protein activation was determined using the [^{35}S]GTPγS functional binding assay, measuring ligand stimulated binding of nonhydrolysable [^{35}S]GTPγS to *Sf*9 insect cell membranes expressing the H_2R-$G_{s\alpha S}$ fusion protein. β-arrestin recruitment by the H_2R was determined in the luciferase complementation assay (for details on the assay system, see Chapter 3).

Table 6-1 gives an overview of the potencies and efficacies of the selected H_2R ligands in the GTPγS functional binding, β-arrestin 1 recruitment and β-arrestin 2 recruitment assay.

6.2.1. Comparison of the two β-arrestin isoforms

In order to explore, whether the H_2R prefers one of the two arrestin isoforms in a ligand-dependent manner, the selected compounds were investigated at the HEK293T βArr1+H_2R and HEK293T βArr2+H_2R cells. Fig. 6-4 gives a comparison of the potencies and efficacies of the compounds in the recruitment assay for either arrestin isoform.

All compounds exhibited comparable efficacies for the recruitment of both β-arrestin 1 and 2 ($\Delta E_{max} < 0.05$). The comparison of the pEC_{50} values revealed only minor differences between the two isoforms. The largest differences were found for the compounds **9**, **13**

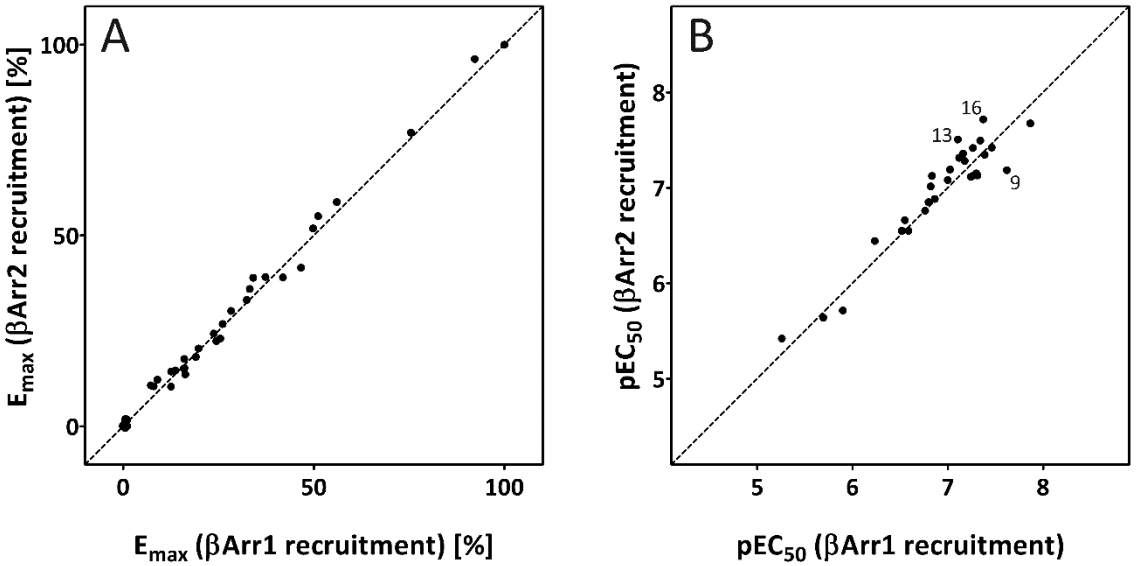

Fig. 6-4: Comparison of β-arrestin 1 and 2 in the luciferase complementation assay. **A**) Dot plot of the efficacies of the selected ligands in βArr1 against βArr2 recruitment. Responses were normalized to the maximal effect induced by histamine (100 %) and solvent (0 %). **B**) pEC_{50} values of the selected agonists in βArr1 against βArr2 recruitment. **A**, **B**) Data are mean values of 2-4 independent experiments.

and **16** ($\Delta pEC_{50} \triangleq 0.34 – 0.43$), however those compounds only exhibited very weak partial agonism in both assays, with efficacies ranging from 0.08 – 0.16, thus strongly impairing the reliability of the determined potencies (Cpd. **9**: $p = 0.043$; Cpd. **13**, **16**: $p > 0.05$).

6.2.2. Functional bias between G-protein and β-arrestin 2

Due to negligible differences between β-arrestin 1 and β-arrestin 2 recruitment, solely the βArr2 data were used for the analysis of functional bias in comparison to G-protein activation. Fig. 6-6 gives a comparison of the potencies and efficacies of all tested compounds in the GTPγS binding and β-arrestin 2 recruitment assay. The responses in both assays were normalized to the maximal effect induced by 1 mM histamine (100 % value) and solvent (0 % value). Thus, histamine (**1**) is defined as a full, unbiased agonist in either readout. Interestingly, **1** exhibits a significantly lower potency in β-arrestin 2 recruitment compared to the GTPγS assay (pEC_{50} (GTPγS) = 6.24; pEC_{50} (βArr2) = 5.42; p = 0.0014). Similarly, the potencies of most of the investigated agonists was lower in the βArr2 recruitment assay (cf. Fig. 6-6: B). The most prominent differences in potency were found for the bivalent agonists UR-BIT108 (**20**) (ΔpEC_{50} = 1.16; p = 0.0046) and UR-NK3 (**25**) (ΔpEC_{50} = 1.21; p < 0.0001), while the monovalent aminothiazoles UR-AK472 (**11**) (ΔpEC_{50} = 0.08) and UR-BIT24 (**16**) (ΔpEC_{50} = 0.05) were equipotent in both assays. Impromidine (**4**) was the only ligand exhibiting a higher potency in βArr2 recruitment than in G-protein activation (ΔpEC_{50} = 0.55; p = 0.006). The systematic shift of the potencies between the

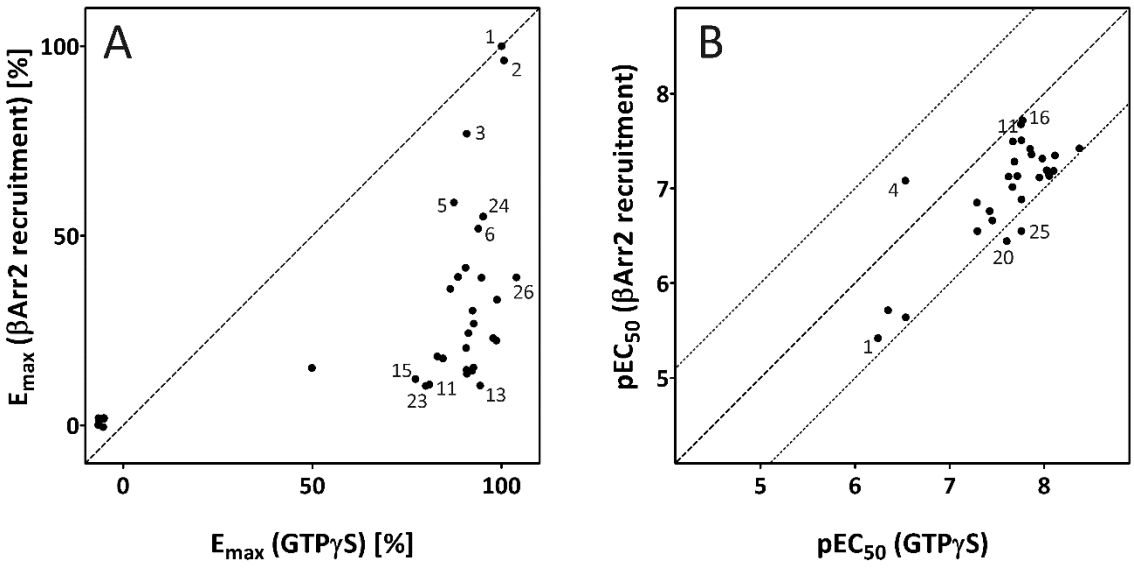

Fig. 6-6: Comparison of [^{35}S]GTPγS and β-arrestin 2 recruitment assay. **A**) The efficacies of the selected ligands in the GTPγS against βArr2 recruitment assay. Responses were normalized to the maximal effect induced by histamine (100 %) and solvent (0 %). **B**) pEC_{50} values of the tested ligands in GTPγS and βArr2 recruitment assay. **A**, **B**) Data are mean values of 2-6 independent experiments.

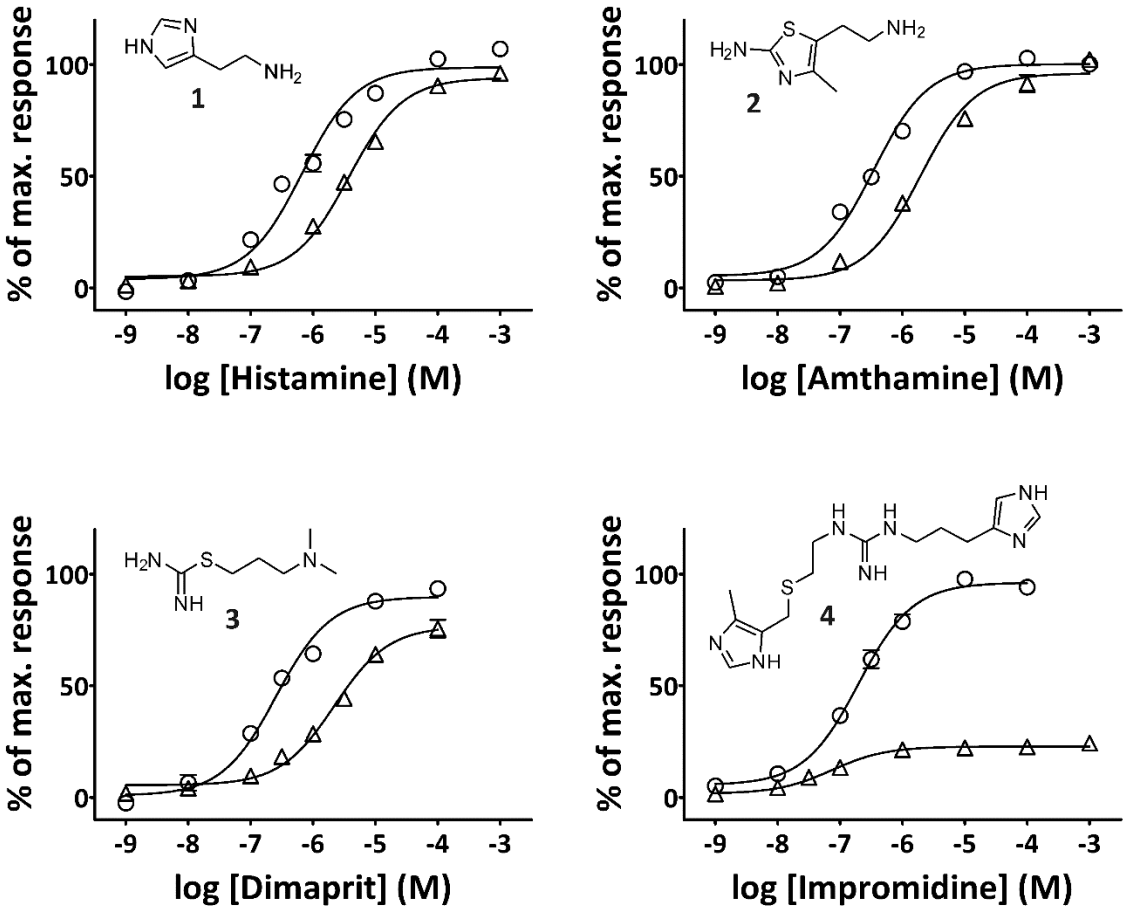

Fig. 6-7: Concentration response curves of the standard H_2R agonists **1**-**4** in the [^{35}S]GTPγS binding (○ circles) and β-arrestin 2 recruitment assay (△ triangles). Data presented are mean ± SEM of 3-4 independent experiments. Data were analyzed by nonlinear regression and best fitted sigmoidal concentration response curves.

two readout systems complicates the use of the determined pEC_{50}-values to address functional selectivity of the tested ligands between G-protein and β-arrestin activation. Similar differences have been reported for G-protein-dependent pathways when using different readouts systems varying in signal amplification or receptor reserve. Furthermore, the validity of the detected differences in potency is affected by the observed decrease in efficacy in βArr2 recruitment for the majority of compounds.

Most of the tested H_2R agonists **1**-**29** were full agonists in the GTPγS binding assay. Interestingly, the published data, obtained using the [^{32}P] GTPase assay at the same H_2R-$G_{s\alpha S}$ fusion construct, revealed discrepancies in the detected efficacies compared to the GTPγS data for several of the ligands.[26-28,32,33] While these differences were rather subtle for most ligands, others exhibited a significant decrease in efficacies in the GTPase assay, for example the bivalent compound UR-AK381 (ΔE_{max} = 0.40) or the monovalent agonist UR-AK477 (ΔE_{max} = 0.26). Collectively, the efficacies of the tested ligands showed a much wider range in the GTPase assay (E_{max} = 0.53 – 1.02) than in the GTPγS binding assay (E_{max} = 0.77 – 0.98) (excluding Cpd. **9**), suggesting the GTPase assay to be more sensitive towards subtle differences in ligand receptor interaction.

Most of the tested compounds revealed a completely different profile in arrestin recruitment. Beside the endogenous ligand histamine (**1**), only amthamine (**2**) acted as full agonists in βArr2 recruitment and, thus, displayed unbiased activity for both pathways (cf. Fig. 6-7). While dimaprit (**3**) showed only a slightly reduced efficacy in βArr2 recruitment (ΔE_{max} = 0.14; p = 0.12), the guanidine-type standard H_2R agonist impromidine (**4**) exhibited

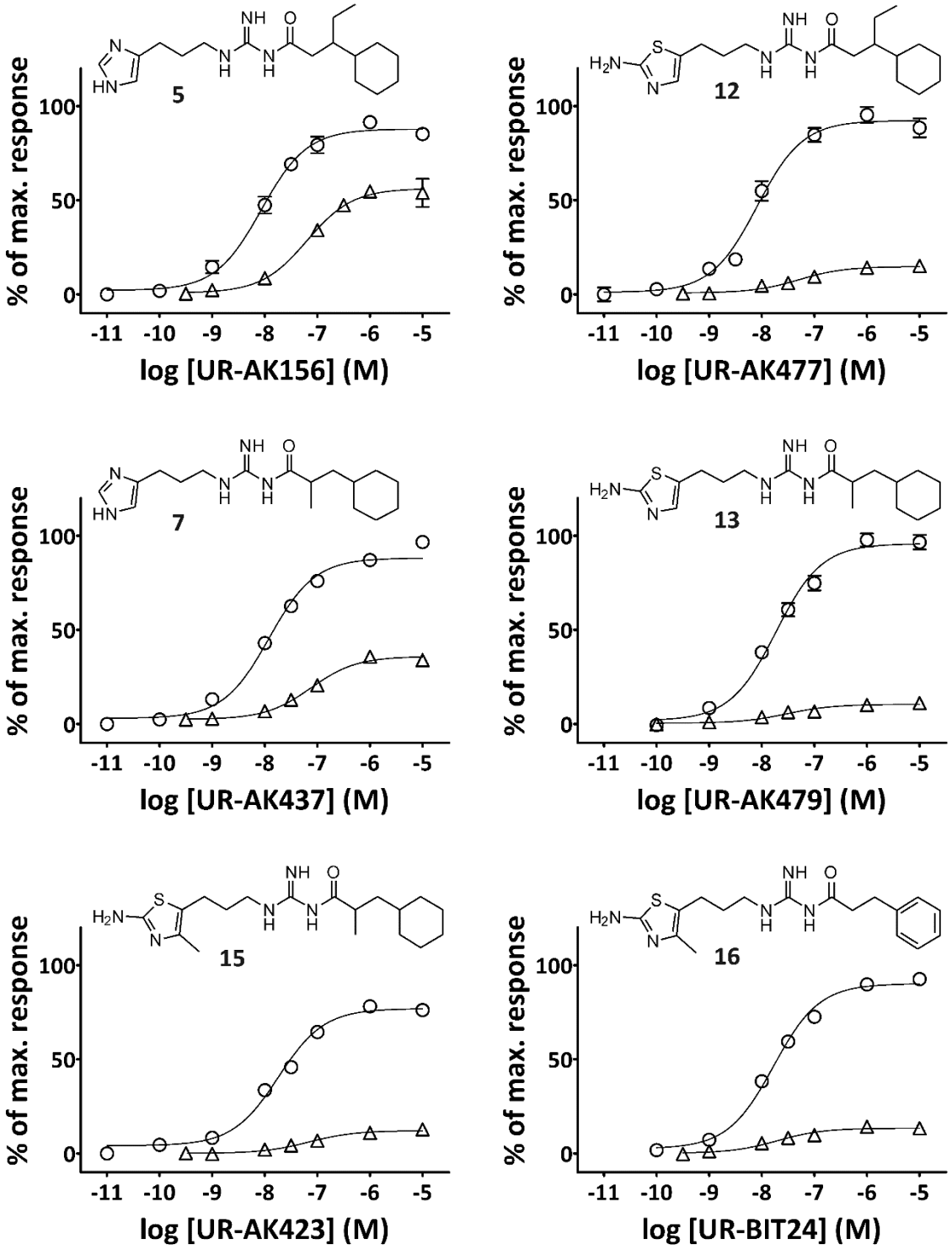

Fig. 6-8: Concentration response curves of selected monovalent N^G-acylated guanidines in the [^{35}S]GTPγS binding (○ circles) and β-arrestin 2 recruitment assay (△ triangles). Data presented are mean values ± SEM of 3-4 independent experiments. Data were analyzed by nonlinear regression and best fitted to sigmoidal concentration-response curves.

a more than 4-fold decrease in efficacy in βArr2 compared to G-protein activation (ΔE_{max} = 0.75; $p < 0.0001$). All tested N^G-acylated or -carbamoylated guanidine-type ligands (**5**-**29**) exhibited a certain degree of bias towards G-protein activation. Except for UR-ML17 (**9**) (E_{max} (GTPγS) = 0.50), the compounds of this class acted as strong partial or full agonists in the GTPγS assay (E_{max} = 0.77-1.04), but were only weak partial agonists in βArr2 recruitment (E_{max} = 0.10-0.59). Amongst the monovalent N^G-acylated guanidines, bias was most striking for the aminothiazole UR-AK479 (Cpd. **13**), which was a full agonist in the GTPγS binding assay (E_{max} = 0.94), while only showing very weak partial agonistic activity in βArr2 recruitment (E_{max} = 0.11). By contrast, the imidazole UR-AK156 (Cpd. **5**) displayed the highest efficacy of all N^G-acylated guanidines regarding arrestin activation (E_{max} = 0.59) (cf. Fig. 6-8). A similar functional profile is evident for all of the tested monovalent N^G-acylated guanidines, with the imidazole containing compounds exhibiting a less pronounced bias for G-protein activation (Cpd. **5-10**; ΔE_{max} = 0.29-0.66) than the aminothiazoles (Cpd. **11-16**; ΔE_{max} = 0.65-0.84). The replacement of the imidazole by an aminothiazole was so far regarded as bioisosteric concerning the function of the ligands at the H_2R, while concurrently procuring selectivity for the H_2R over the H_3R and H_4R.[27] Regarding H_2R arrestin interaction, this assumption has to be challenged, as becomes apparent from the functional profiles of compounds sharing the same substitution pattern of the acyl moiety. While both, **5** and **12**, exhibited comparable efficacies in the GTPγS assay (ΔE_{max} = 0.05; $p > 0.05$), the aminothiazole **12** had a significantly lower intrinsic activity in the βArr2 recruitment assay compared to **5** (ΔE_{max} = 0.44; $p < 0.0001$) (cf. Fig. 7-8). The same phenomenon, although less pronounced, became obvious for **7** and **13** (ΔE_{max} (βArr2) = 0.26; $p < 0.0001$). The addition of a 4-methyl substituent had no major impact on the functional properties of the ligands, despite a slight reduction of efficacy in the GTPγS assay (compare compounds **13** and **15**).

The bivalent ligands (Cpd. **17**-**29**), in general, exhibited a similar characteristic as the monovalent N^G-acylated guanidines, with varying degrees of G-protein bias (ΔE_{max} = 0.40-0.77) (cf. Fig. 6-9). The influence of the imidazole/amino(methyl)thiazole substitution is also observed for these compounds, although less pronounced than for the monovalent ligands. The N^G-carbamoylated imidazolylpropyl guanidine UR-NK52 (**24**) exhibited the highest efficacy in βArr2 recruitment (E_{max} = 0.55), while the aminothiazole UR-BIT308 had the lowest intrinsic activity (E_{max} = 0.10). The carbamoylguanidines containing either an imidazole (**24**-**26**) or aminothiazole moiety (**27**-**29**) revealed a minor influence of the chain length of the linker on the functional properties of the compounds. With increasing chain length, efficacy regarding βArr2 recruitment decreased and, conversely, the bias for G-protein activation increased (**24**-**26**: ΔE_{max} = 0.16; p = 0.0003; **27**-**29**: ΔE_{max} = 0.13; p = 0.0006).

Neither the tested standard H_2R antagonists famotidine (**30**), cimetidine (**31**) and ranitidine (**32**) nor the squaramide derivatives **33**-**36** exhibited functional bias for either pathway. They only exhibited negligible efficacies in arrestin recruitment, while exhibiting minor inverse agonistic effects in the GTPγS binding assay. While an unbiased profile is not uncommon, previous results of investigations for ligand bias using the standard antagonists RAN and CIM suggested a functional selectivity of **32** for β-arrestin recruitment, as it was

shown that RAN induced H_2R depletion depended on β-arrestin 2 function.[18] However, agonistic activity of RAN in β-arrestin recruitment could not be confirmed in our assay system.

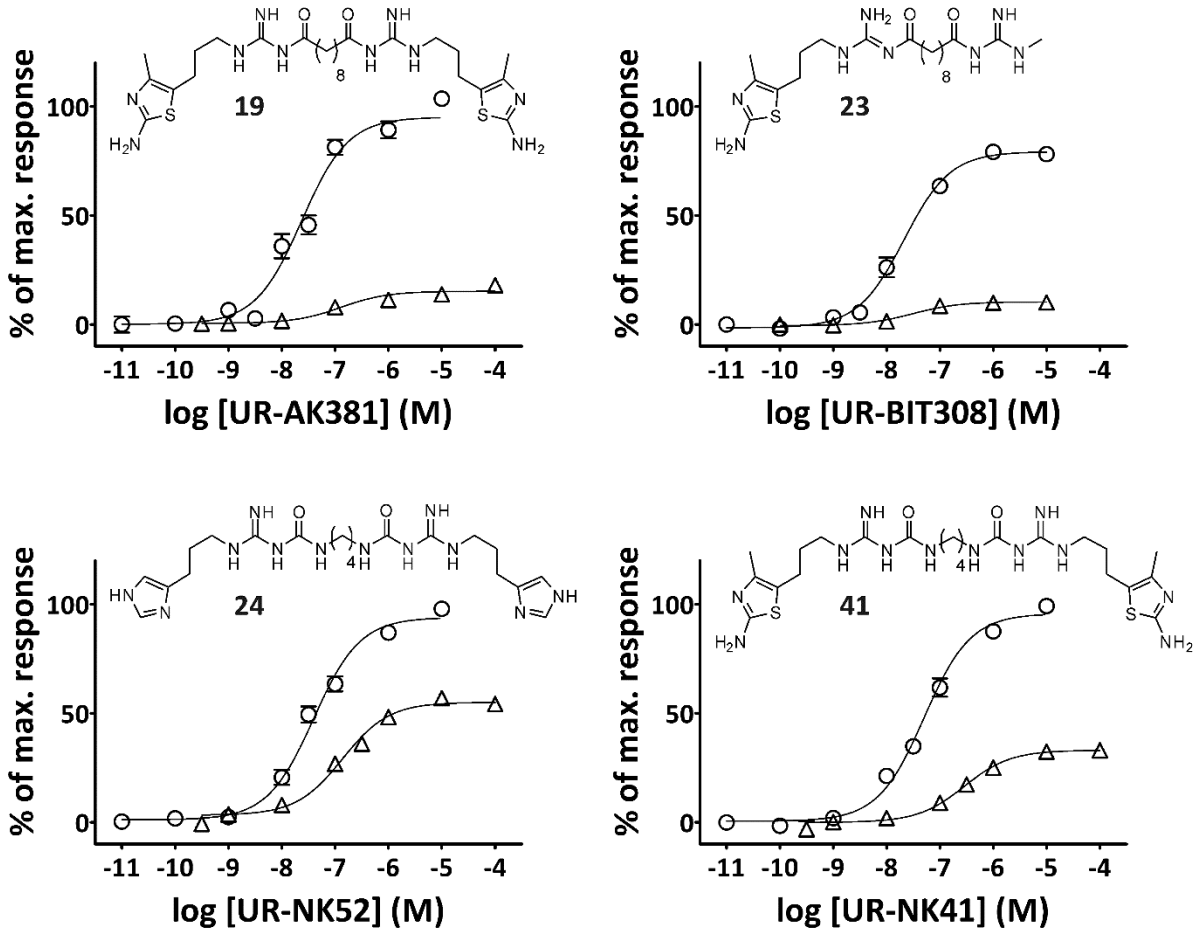

Fig. 6-9: Concentration response curves of selected bivalent H_2R ligands in the [^{35}S]GTPγS binding (○ circles) and β-arrestin 2 recruitment assay (△ triangles). Data presented are mean ± SEM of 3-4 independent experiments. Data were analyzed by nonlinear regression and best fitted sigmoidal concentration response curves.

Tab. 6-1:Potencies and efficacies of the tested H_2R ligands in the [^{35}S]GTPγS binding and β-arrestin 1 and 2 recruitment assay

Cpd.	GTPγS assay			β-arrestin 1 recruitment			β-arrestin 2 recruitment		
	pEC_{50} ± SEM	E_{max} ± SEM	N	pEC_{50} ± SEM	E_{max} ± SEM	N	pEC_{50} ± SEM	E_{max} ± SEM	N
(**1**) HIS	6.24 ± 0.15	1.00	4	5.26 ± 0.03	1.00	5	5.42 ± 0.02	1.00	4
(**2**) AMT	6.35 ± 0.13	1.01 ± 0.02	3	5.90 ± 0.06	0.92 ± 0.01	4	5.71 ± 0.04	0.96 ± 0.02	3
(**3**) DIM	6.54 ± 0.21	0.91 ± 0.03	3	5.69 ± 0.05	0.75 ± 0.03	3	5.64 ± 0.10	0.77 ± 0.06	3
(**4**) IMP	6.53 ± 0.07	0.98 ± 0.02	4	7.00 ± 0.02	0.25 ± 0.01	3	7.08 ± 0.10	0.23 ± 0.01	3
(**5**) UR-AK156	8.05 ± 0.15	0.87 ± 0.05	3	7.27 ± 0.07	0.56 ± 0.03	4	7.13 ± 0.06	0.59 ± 0.02	4
(**6**) UR-AK224	8.05 ± 0.08	0.94 ± 0.04	3	7.30 ± 0.03	0.50 ± 0.06	3	7.15 ± 0.00	0.52 ± 0.01	3
(**7**) UR-AK437	7.95 ± 0.07	0.86 ± 0.04	3	7.24 ± 0.08	0.33 ± 0.05	3	7.12 ± 0.06	0.36 ± 0.02	3
(**8**) UR-AK284	7.66 ± 0.17	0.93 ± 0.05	3	6.82 ± 0.07	0.26 ± 0.02	3	7.02 ± 0.04	0.27 ± 0.01	3
(**9**) UR-ML17	8.10 ± 0.06	0.50 ± 0.05	3	7.62 ± 0.00	0.16 ± 0.01	3	7.18 ± 0.15	0.15 ± 0.01	3
(**10**) UR-ML22	7.42 ± 0.17	0.90 ± 0.06	3	6.76 ± 0.04	0.47 ± 0.03	3	6.76 ± 0.03	0.42 ± 0.03	4
(**11**) UR-AK472	7.75 ± 0.13	0.81 ± 0.02	3	7.87 ± 0.09	0.07 ± 0.01	3	7.68 ± 0.05	0.11 ± 0.01	3
(**12**) UR-AK477	8.11 ± 0.10	0.92 ± 0.08	3	7.39 ± 0.06	0.13 ± 0.01	5	7.35 ± 0.13	0.14 ± 0.01	5
(**13**) UR-AK479	7.76 ± 0.09	0.94 ± 0.09	3	7.10 ± 0.14	0.08 ± 0.01	4	7.51 ± 0.13	0.11 ± 0.01	4
(**14**) UR-BIT336	7.98 ± 0.08	0.91 ± 0.08	4	7.12 ± 0.08	0.14 ± 0.02	3	7.31 ± 0.04	0.15 ± 0.01	3
(**15**) UR-AK423	7.71 ± 0.07	0.77 ± 0.04	3	7.31 ± 0.04	0.09 ± 0.01	3	7.13 ± 0.13	0.12 ± 0.01	3
(**16**) UR-BIT24	7.77 ± 0.10	0.91 ± 0.04	3	7.37 ± 0.07	0.16 ± 0.01	3	7.72 ± 0.11	0.14 ± 0.01	3
(**17**) UR-BIT237	7.45 ± 0.12	0.95 ± 0.03	3	6.55 ± 0.08	0.34 ± 0.02	3	6.66 ± 0.16	0.39 ± 0.02	3
(**18**) UR-AK480	7.85 ± 0.09	0.99 ± 0.03	4	7.26 ± 0.07	0.24 ± 0.01	3	7.42 ± 0.04	0.22 ± 0.01	3
(**19**) UR-AK381	7.76 ± 0.16	0.93 ± 0.04	4	6.86 ± 0.06	0.16 ± 0.01	3	6.88 ± 0.01	0.15 ± 0.00	3

Tab. 6-1 (continued)

Cpd.	GTPγS assay			β-arrestin 1 recruitment			β-arrestin 2 recruitment		
	pEC_{50} ± SEM	E_{max} ± SEM	N	pEC_{50} ± SEM	E_{max} ± SEM	N	pEC_{50} ± SEM	E_{max} ± SEM	N
(**20**) UR-BIT108	7.60 ± 0.24	0.91 ± 0.03	5	6.23 ± 0.13	0.24 ± 0.01	4	6.44 ± 0.06	0.24 ± 0.01	4
(**21**) UR-BIT106	7.62 ± 0.22	0.84 ± 0.02	3	6.83 ± 0.03	0.16 ± 0.02	3	7.12 ± 0.03	0.18 ± 0.00	3
(**22**) UR-BIT82	7.86 ± 0.16	0.83 ± 0.08	3	7.16 ± 0.17	0.19 ± 0.01	3	7.36 ± 0.03	0.18 ± 0.01	3
(**23**) UR-BIT308	7.67 ± 0.20	0.80 ± 0.02	3	7.34 ± 0.06	0.13 ± 0.01	2	7.49 ± 0.09	0.10 ± 0.01	3
(**24**) UR-NK52	7.29 ± 0.08	0.95 ± 0.03	6	6.80 ± 0.07	0.51 ± 0.02	3	6.85 ± 0.09	0.55 ± 0.00	3
(**25**) UR-NK3	7.76 ± 0.03	0.88 ± 0.03	2	6.59 ± 0.03	0.37 ± 0.01	3	6.55 ± 0.01	0.39 ± 0.01	3
(**26**) UR-NK60	8.37 ± 0.10	1.04 ± 0.05	4	7.46 ± 0.01	0.42 ± 0.01	3	7.42 ± 0.06	0.39 ± 0.02	4
(**27**) UR-NK41	7.29 ± 0.13	0.99 ± 0.04	5	6.52 ± 0.04	0.32 ± 0.02	3	6.55 ± 0.09	0.33 ± 0.01	3
(**28**) UR-NK22	8.03 ± 0.02	0.92 ± 0.01	2	7.02 ± 0.03	0.28 ± 0.01	3	7.19 ± 0.09	0.30 ± 0.02	3
(**29**) UR-NK53	7.68 ± 0.08	0.91 ± 0.05	6	7.18 ± 0.02	0.20 ± 0.01	3	7.28 ± 0.05	0.20 ± 0.01	4
(**30**) FAM	n.d.	-0.05 ± 0.01	2	n.d.	0.01 ± 0.01	2	n.d.	0.02 ± 0.01	2
(**31**) CIM	n.d.	-0.07 ± 0.01	2	n.d.	0.01 ± 0.01	2	n.d.	0.02 ± 0.01	2
(**32**) RAN	n.d.	-0.05 ± 0.01	2	n.d.	0.01 ± 0.01	2	n.d.	0.02 ± 0.00	2
(**33**) UR-DE85	n.d.	-0.05 ± 0.01	2	n.d.	0.00 ± 0.00	2	n.d.	0.00 ± 0.00	2
(**34**) UR-DE86	n.d.	-0.06 ± 0.02	2	n.d.	0.01 ± 0.01	2	n.d.	0.00 ± 0.00	2
(**35**) UR-DE92	n.d.	-0.06 ± 0.02	2	n.d.	0.00 ± 0.00	2	n.d.	0.01 ± 0.01	2
(**36**) UR-DE114	n.d.	-0.07 ± 0.02	2	n.d.	0.00 ± 0.00	2	n.d.	0.00 ± 0.00	2

6.2.3. Quantifying stimulus bias using the operational model

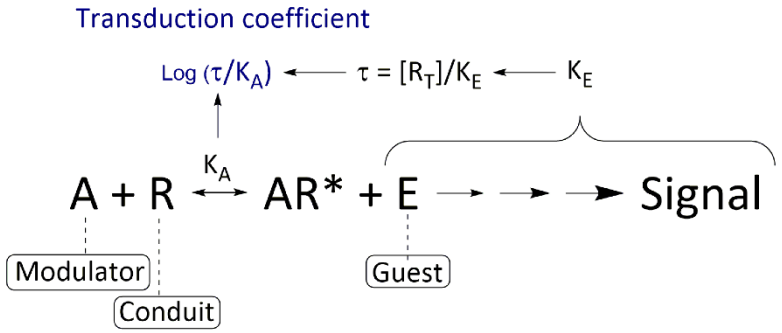

Fig 6-10: Schematic diagram for the use of the operational model of agonism[33] to characterize agonist function. (Adapted from Kenakin et al., 2012[34])

With the general acceptance that GPCR ligands can produce a response biased for one pathway over another, the necessity arose to quantify this functional selectivity in order to allow for the analysis of structure-activity relationships (SAR) to guide the development of biased agonists. Unfortunately, the use of ligand potencies and efficacies as classically derived from concentration-response curves proved inadequate in many cases, as the comparison of rank orders of potency fails to discriminate between full and partial agonists, while the use of ligand efficacies cannot account for changes in potency between different pathways. Furthermore, a systematic bias between two different readout systems, as described above for the potencies of H_2R agonists, can complicate the data interpretation.

Several recent publications recommend the use of the operational model of agonism[34] to overcome these limitations.[35,36] Fig. 6-10 gives a schematic overview of the model. Here receptor agonism is defined as an allosteric system comprised of a modulator (agonist), operating on a protein conduit (receptor) to a protein guest (signaling molecule).[35] The use of the operational model gives access to the 2 parameters, intrinsic efficacy and potency, defining the agonistic potential of the test compound. The equilibrium dissociation constant (K_A) of the ligand receptor complex provides a measure for the ligand affinity and the τ value, derived from $[R_T]/K_E$, describes the agonists efficacy. Hereby, R_T is the receptor density and K_E describes the coupling efficiency of the ligand receptor complex to the respective downstream effector.[35] From these two parameters, the so called "transduction coefficient" log (τ/K_A) is derived, a composite parameter sufficient to describe agonism for a given pathway.[37] The transduction coefficients for the tested compounds can be normalized to the log (τ/K_A) of the endogenous ligand, thereby cancelling out potential systematic bias generated by differences in the cellular background and/or signal amplification of the chosen readout systems. The comparison of the normalized transduction coefficients of a ligand for different signaling pathways then allows for the quantification of the ligand bias.

The functional data of the H_2R agonists from either the GTPγS binding or arrestin recruitment assay were fitted to the operational model as described in 6.2.4.2. Tab. 6-2

gives the absolute and normalized transduction coefficients for either readout as well as the bias factors $\Delta\Delta\log(\tau/K_A)$ of the ligands between the G-protein and arrestin pathway. The determined bias factors allowed for the quantification of the functional selectivity evident in the functional data of the tested acyl- and carbamoylguanidine-type ligands. For most of the test compounds, the determined bias factors correlated well with the differences identified by simply comparing the potencies and efficacies. UR-AK156 (**5**), for example, showed only a moderate degree of G-protein bias with a $\Delta\Delta\log(\tau/K_A)$ of 0.44, which can be explained by the moderate decrease in efficacy in βArr2 recruitment compared to G-protein activation (cf. Tab. 6-1). The acylguanidines exhibiting the strongest bias, with $\Delta\Delta\log(\tau/K_A)$ values from 1.27 to 1.38 (cf. Fig. 6-11), revealed pronounced differences in potency and/or efficacy between the two readouts. UR-BIT108 (**20**) exhibited the highest bias factor (cf. Fig. 6-12), and while not showing the highest of all differences in efficacy, the major decrease in potency found for arrestin recruitment accounts for the increased bias. Other compounds showing a strong bias, such as UR-AK381 (**19**) or UR-

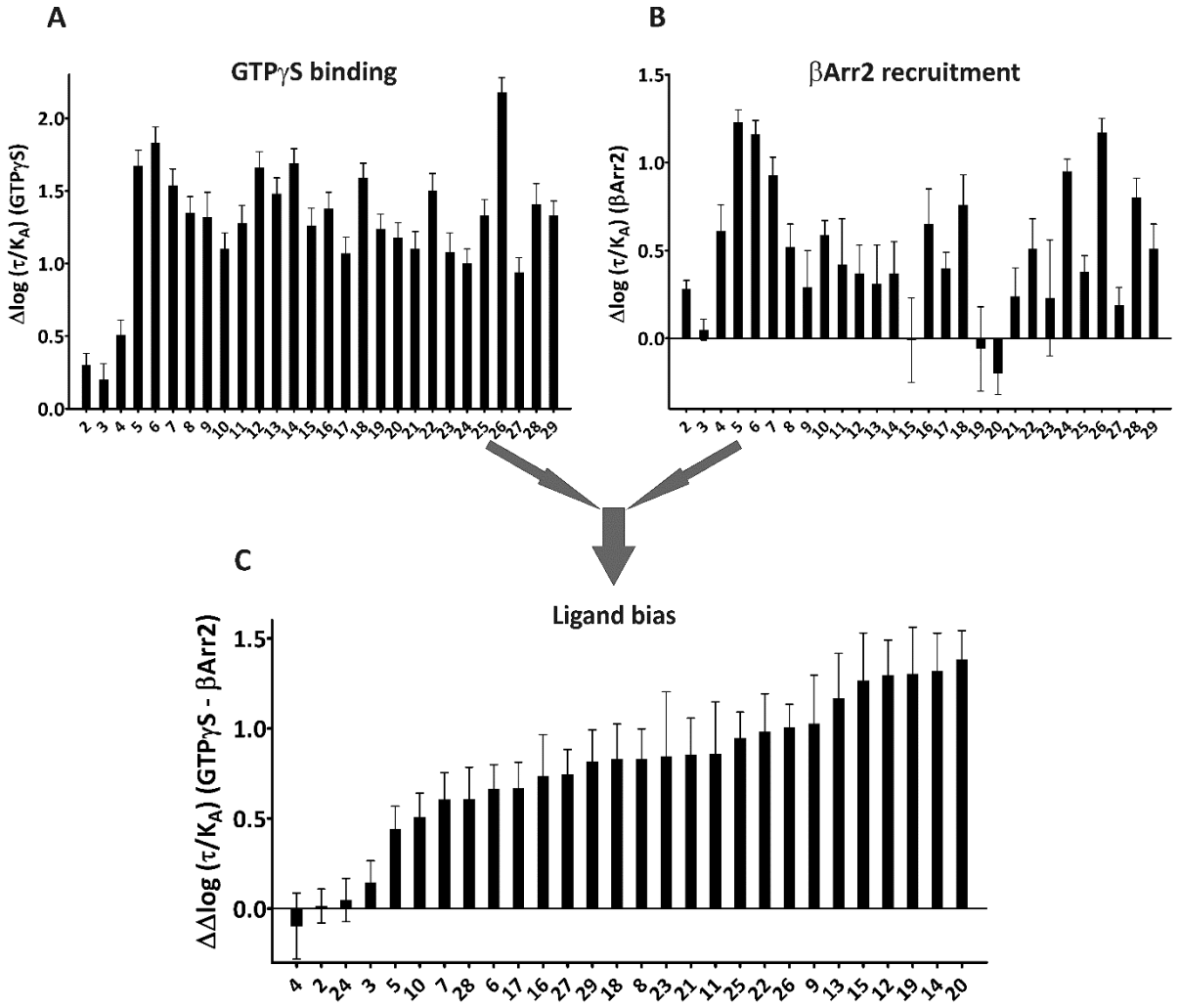

Fig. 6-11: Quantification of the functional bias of the tested H_2R agonists between the GTPγS binding and the arrestin recruitment assay. The normalized $\Delta\log(\tau/K_A)$ values for the G-protein (A) and arrestin (B) pathway were calculated as described in 6.4.2.4 Eq. 2. Subtraction of the $\Delta\log(\tau/K_A)$ values of the arrestin recruitment assay from the GTPγS binding yielded the bias factors $\Delta\Delta\log(\tau/K_A)$ (C) for the tested compounds.

AK477 (**12**), were amongst the compounds with the most pronounced decrease in efficacy in arrestin recruitment. Applying the model to the data of the neutral agonist amthamine (**2**) revealed the effectiveness of the data normalization. Amthamine acted as a full agonist in both assays, revealing a shift in potency comparable to histamine between the two readouts. The difference in the transduction coefficients log (τ/K_A) for the individual readouts is cancelled out through the normalization, giving a bias factor around zero. Some

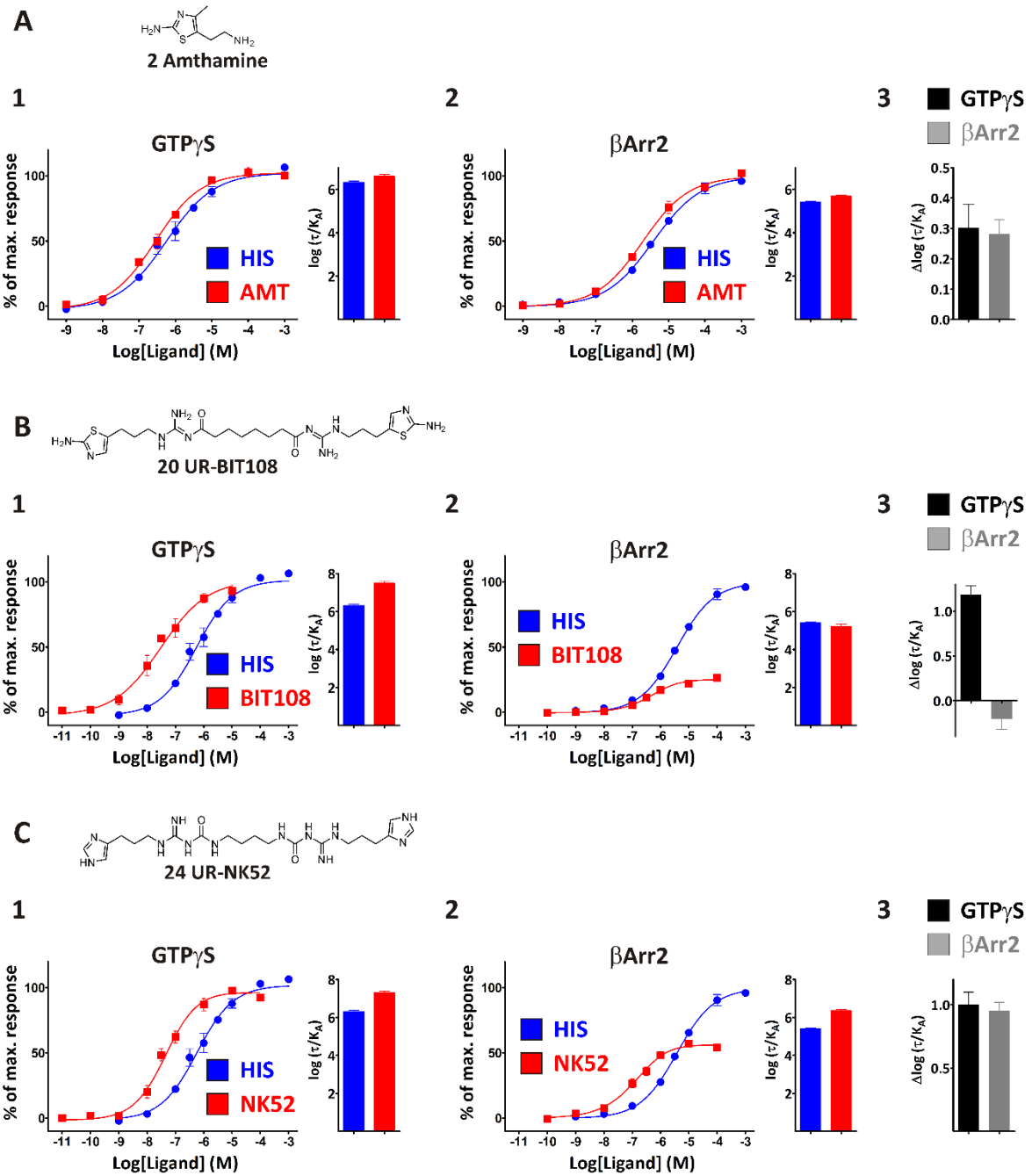

Fig. 6-12: Concentration-response curves of selected H_2R ligands in comparison with the endogenous ligand histamine fitted with the operational model of agonism as described in 6.4.2.4 and the corresponding transduction coefficients log (τ/K_A) for the GTPγS binding (1) and arrestin recruitment assay (2). Thereof, the normalized transduction coefficients Δlog (τ/K_A) (3) for each assay were derived. Data shown are mean values ± SEM calculated as described in 6.4.2.4 for amthamine (A), UR-BIT108 (B) and UR-NK52 (C).

other compounds showed a neutral, unbiased characteristic in the operational model, which was not expected from the concentration-response curves. Both impromidine (**4**) and the carbamoylguanidine UR-NK52 (cf. Fig 6-12 C) exhibited a decreased efficacy in arrestin recruitment but showed $\Delta\Delta\log(\tau/K_A)$ values around zero. In both cases, an increased potency in arrestin recruitment compared to the endogenous ligand histamine compensated for the loss in efficacy and resulted in comparable normalized transduction coefficients in both readouts. Whether those findings really imply a neutral agonistic behavior of these compounds under physiological conditions remains elusive.

Tab. 6-2: Transduction coefficients log (τ/K_A) and normalized transduction coefficients Δlog (τ/K_A) in the GTPγS and arrestin recruitment assay and the bias factors $\Delta\Delta$log (τ/K_A) of the tested H_2R agonists.

Cpd.	GTPγS		βArr2		$\Delta\Delta$log (τ/K_A) (G-Arr)
	log (τ/K_A)	Δlog (τ/K_A)	log (τ/K_A)	Δlog (τ/K_A)	
(**1**) HIS	6.32 ± 0.07		5.41 ± 0.03		
(**2**) AMT	6.61 ± 0.08	0.30 ± 0.08	5.69 ± 0.04	0.28 ± 0.05	0.01 ± 0.09
(**3**) DIM	6.52 ± 0.08	0.20 ± 0.11	5.46 ± 0.05	0.05 ± 0.06	0.15 ± 0.12
(**4**) IMP	6.83 ± 0.08	0.51 ± 0.10	6.01 ± 0.15	0.61 ± 0.15	-0.10 ± 0.18
(**5**) UR-AK156	7.99 ± 0.08	1.67 ± 0.11	6.63 ± 0.06	1.23 ± 0.07	0.44 ± 0.13
(**6**) UR-AK224	8.15 ± 0.09	1.83 ± 0.11	6.57 ± 0.07	1.16 ± 0.08	0.66 ± 0.14
(**7**) UR-AK437	7.85 ± 0.08	1.54 ± 0.11	6.34 ± 0.10	0.93 ± 0.10	0.61 ± 0.15
(**8**) UR-AK284	7.67 ± 0.08	1.35 ± 0.11	5.93 ± 0.12	0.52 ± 0.13	0.83 ± 0.17
(**9**) UR-ML17	7.64 ± 0.15	1.32 ± 0.17	5.70 ± 0.21	0.29 ± 0.21	1.03 ± 0.27
(**10**) UR-ML22	7.41 ± 0.08	1.10 ± 0.11	5.99 ± 0.07	0.59 ± 0.08	0.51 ± 0.13
(**11**) UR-AK472	7.59 ± 0.09	1.28 ± 0.12	5.82 ± 0.26	0.42 ± 0.26	0.86 ± 0.29
(**12**) UR-AK477	7.98 ± 0.08	1.66 ± 0.11	5.77 ± 0.16	0.37 ± 0.16	1.30 ± 0.20
(**13**) UR-AK479	7.79 ± 0.08	1.48 ± 0.11	5.71 ± 0.22	0.31 ± 0.22	1.17 ± 0.25
(**14**) UR-BIT336	8.00 ± 0.08	1.69 ± 0.10	5.77 ± 0.18	0.37 ± 0.18	1.32 ± 0.21
(**15**) UR-AK423	7.58 ± 0.10	1.26 ± 0.12	5.40 ± 0.23	-0.01 ± 0.24	1.27 ± 0.27
(**16**) UR-BIT24	7.70 ± 0.08	1.38 ± 0.11	6.05 ± 0.20	0.65 ± 0.20	0.74 ± 0.23
(**17**) UR-BIT237	7.39 ± 0.09	1.07 ± 0.11	5.81 ± 0.09	0.40 ± 0.09	0.67 ± 0.15
(**18**) UR-AK480	7.91 ± 0.07	1.59 ± 0.10	6.17 ± 0.16	0.76 ± 0.17	0.83 ± 0.19
(**19**) UR-AK381	7.56 ± 0.07	1.24 ± 0.10	5.35 ± 0.24	-0.06 ± 0.24	1.30 ± 0.26
(**20**) UR-BIT108	7.50 ± 0.08	1.18 ± 0.10	5.21 ± 0.12	-0.20 ± 0.12	1.38 ± 0.16
(**21**) UR-BIT106	7.42 ± 0.10	1.10 ± 0.12	5.65 ± 0.16	0.24 ± 0.16	0.85 ± 0.20
(**22**) UR-BIT82	7.81 ± 0.10	1.50 ± 0.12	5.92 ± 0.17	0.51 ± 0.17	0.98 ± 0.21
(**23**) UR-BIT308	7.40 ± 0.11	1.08 ± 0.13	5.64 ± 0.33	0.23 ± 0.33	0.85 ± 0.36
(**24**) UR-NK52	7.32 ± 0.07	1.00 ± 0.10	6.36 ± 0.06	0.95 ± 0.07	0.05 ± 0.12
(**25**) UR-NK3	7.65 ± 0.09	1.33 ± 0.11	5.79 ± 0.08	0.38 ± 0.09	0.95 ± 0.14
(**26**) UR-NK60	8.50 ± 0.07	2.18 ± 0.10	6.58 ± 0.07	1.17 ± 0.08	1.00 ± 0.13
(**27**) UR-NK41	7.26 ± 0.07	0.94 ± 0.10	5.60 ± 0.09	0.19 ± 0.10	0.74 ± 0.14
(**28**) UR-NK22	7.73 ± 0.12	1.41 ± 0.14	6.21 ± 0.11	0.80 ± 0.11	0.61 ± 0.18
(**29**) UR-NK53	7.65 ± 0.07	1.33 ± 0.10	5.92 ± 0.14	0.51 ± 0.14	0.82 ± 0.18

The transduction coefficients log (τ/K_A) were derived from pooled functional data of 2 – 6 independent experiments fitted to the operational model of agonism as described in 6.4.2.4. Data are given as mean values ± SEM calculated as described in 6.4.2.4.

6.3. Summary and conclusions

All of the investigated H_2R antagonists exhibited a neutral, unbiased characteristic in the arrestin and G-protein readout. Amongst the H_2R agonists, the acyl- and carbamoylguanidines revealed varying degrees of G-protein bias; most compounds being strong or full agonists in the GTPγS assay, while only producing weak partial agonistic effects in arrestin recruitment. None of the tested compounds exhibited functional selectivity towards arrestin activation. Furthermore, no significant differences were detectable regarding the recruitment of the two arrestin isoforms, except for minor variations in potency for some of the compounds with low efficacy. The application of the operational model of agonism enabled the calculation of a bias factor to quantify the functional selectivity between the two pathways. A method for the quantification of ligand bias is crucial for the analysis of structure-activity relationships to guide the development of new biased ligands.

In the case of the H_2R, selective agonists came into focus as potential new drug candidates for the treatment of acute myeloid leukemia. For AML patients, histamine in combination with interleukin IL-2 (Ceplene®)[38] is available as post consolidation therapy and has shown to prolong leukemia free survival compared to the standard therapy.[39] The putative mode of action for histamine hereby is the inhibition of ROS-induced apoptosis of T- and NK-cells via H_2R-mediated inhibition of NADPH oxidase in myeloid cells.[40,41] Hereby, the substitution of histamine by selective H_2R agonists could prevent several severe side effects caused by the activation of H_XR subtypes other than H_2R, in particular H_1R and H_4R.[41] A recent study investigating the pharmacological profile of several known H_2R agonists on native monocytes identified several compounds exhibiting functional selectivity between the induction of cAMP production and the inhibition of fMLP stimulated ROS generation,[41] thus emphasizing the necessity to fully characterize the functional profile of potential drug candidates regarding non-canonical signaling pathways. Besides the unknown implications on receptor signaling, treatment with G-protein biased agonists could be beneficial compared to neutral agonists in reducing adverse effect associated with arrestin mediated processes such as receptor down-regulation and drug resistance.

6.4. Materials and methods

6.4.1. Materials

Unless stated otherwise, all chemicals and reagents were purchased from Sigma-Aldrich Chemie (Munich, Germany) or Merck (Darmstadt, Germany). Insect-Xpress medium was from Lonza (Verviers, Belgium), FCS was from Biochrom (Berlin, Germany). The DC protein assay kit was purchased from Bio-Rad Laboratories (München, Germany), BSA (Albumin bovine Fraction V receptor grade) was from Serva Electrophoresis (Heidelberg, Germany). [^{35}S]GTPγS was purchased from Hartmann Analytic (Braunschweig, Germany), guanosine diphosphate (GDP) was from Sigma-Aldrich Chemie (Munich, Germany), unlabeled GTPγS was from Roche (Mannheim, Germany). GF/C glass fiber filter were from Whatman International (Maidstone, UK). Rotiscint eco plus scintillation cocktail was from Roth Carl (Karlsruhe, Germany). For media and reagents used for the luciferase complementation assay, see 3.4.

6.4.1.1. H_2R ligands

Histamine dihydrochloride (**1**) was from Alfa Aesar (Karlsruhe, Germany). Amthamine dihydrobromide (**2**) and dimaprit dihydrochloride (**3**) were from Tocris Bioscience (Ellisville, MO, USA). The compounds **4**-**29** and **33**-**36** were synthesized in our laboratory.[27,28,32,33,42] Famotidine (**30**) and ranitidine (**32**) were from Sigma (St. Louis, USA). Cimetidine (**31**) was from Tocris Bioscience (Ellisville, USA). Stock solutions (10 mM) of compounds **1**-**4** and **30**-**32** were prepared with distilled water. In case of compounds **5**-**29** and **33**-**36**, stock solutions (10 mM) were prepared with 10 mM TFA.

6.4.2. Methods

6.4.2.1. *Sf*9 insect cell membrane preparation

*Sf*9 membranes were prepared as previously described[43,44] using a baculovirus transfection system. The *Sf*9 insect cells (*Spodoptera frugiperda* ovary cells) and the stock solution of the baculovirus encoding the human H_2R-$G_{s\alpha S}$ fusion construct were kindly provided by Prof. Dr. Roland Seifert (Institute of Pharmacology, Medical School of Hannover, Germany). *Sf*9 cells were seeded at a density of 3 million cells/ml in Insect express medium supplemented with 5 % FCS and infected with a 1:100 titer of the virus stock. After incubation for 48 h at 28 °C under shaking, membranes were prepared as described.[43] Membranes were resuspended in binding buffer (12.5 mM $MgCl_2$, 1 mM EDTA and 75 mM Tris/HCl, pH 7.4) and aliquots were stored at -80 °C until use. The protein content of the membranes was determined using the DC protein assay kit (BioRad) according to manufacturer`s instructions. A BSA dilution series served as reference.

6.4.2.2. [^{35}S]GTPγS functional binding assay

[^{35}S]GTPγS functional binding assay was performed as previously described.[16,44] The *Sf*9 membranes expressing the hH_2R-$G_{s\alpha S}$ fusion protein were thawed, sedimented by centrifugation at 16000 g for 10 min at 4 °C and thoroughly resuspended in ice cold binding buffer. The assay was performed in a 96 well polypropylene plate. Each well contained *Sf*9 membranes (10 µg protein/well), 1 µM GDP, 0.05 % BSA, 0.2 nM [^{35}S]GTPγS and the corresponding ligands in varying concentrations, brought to a total volume of 100 µl with binding buffer. The plates were incubated for 90 min under shaking at RT. Subsequently, the membranes were harvested by filtration through GF/C filters using a Brandel 96 sample harvester (Brandel, Gaithersburg, MD). After 3 washing steps with ice cold binding buffer, the membrane bound radioactivity was measured by liquid scintillation counting using the Micro Beta^2 1450 scintillation counter (Perkin Elmer, Rodgau, Germany).

6.4.2.3. Luciferase complementation assay

The luciferase complementation assay was performed as described above (cf. 3.4.7) using the HEK293T-βArr1-H_2R and HEK293T-βArr2-H_2R cell lines stably expressing the H_2R-ElucC and either the βArr1-ElucN or βArr2-ElucN fusion constructs (cf. 3.2). For cell culture conditions and media requirements, see 3.4.2. Dilution series of the tested compounds were prepared with the same solvent as the stock solutions (cf. 6.4.1.1). The cells were stimulated for 60 min with varying concentrations of the ligands. The results were normalized to the maximum effect induced by 1 mM histamine (100 % value) and solvent (0 % value). Concentration-response curves determined for histamine, using either distilled water or 10 mM TFA as solvent, revealed no significant differences.

6.4.2.4. Data analysis

Data analysis was performed as described above (cf. 4.3.2.2). Statistical analysis of the variances was performed either by unpaired T test for comparing 2 sets of values or by one way ANOVA followed by Bonferoni`s multiple comparison test for multiple sets of values. The analysis was performed using GraphPad Prism 5 software (GraphPad Software, La Jolla, CA, USA).

To allow for the quantification of functional bias, the concentration-response curves of the ligands producing agonistic effects in both readouts were fitted to the operational model of agonism[34] as previously described[35,37] using the following equation:

$$Y = basal + \frac{(E_m - basal)\left(\frac{\tau}{K_A}\right)^n [A]^n}{[A]^n \left(\frac{\tau}{K_A}\right)^n + \left(1 + \frac{[A]}{K_A}\right)^n} \quad (1)$$

where E_m is the maximal response of the system, basal is the background level of the response, K_A is the equilibrium dissociation constant of the ligand A, τ is a measure of the signaling efficacy of the agonist and is defined as R_T/K_E, where R_T is the total receptor number and K_E is the coupling efficacy of the ligand-receptor complex to the downstream effector, and n is the slope of the transducer function that links occupancy to response.[37] It is assumed, that the maximal response of the system (E_m) and the transduction machinery used for a specific pathway are identical for all agonists, such that the E_m and transducer slope (n) are shared between agonists.[37] The pooled data for all ligands for a given readout was fitted globally to determine the log (τ/K_A) ratio using an implementation for GraphPad Prism kindly provided by Dr. J. Robert Lane from the Monash University, Australia. The transduction coefficient log (τ/K_A) is an excellent parameter to describe bias between two given pathways, as bias can either originate from a different affinity (K_A) of a ligand for different receptor conformations and/or different coupling efficacies of the ligand-receptor complex to the respective downstream effectors.[37]

In order to mitigate the influence of a possible systematic bias between the two different readout systems, the log (τ/K_A) values for each ligand were normalized to that of the endogenous ligand histamine for the given pathway as follows

$$\Delta log\left(\frac{\tau}{K_A}\right) = log\left(\frac{\tau}{K_A}\right)_{cpd} - log\left(\frac{\tau}{K_A}\right)_{HIS} \quad (2)$$

Using the normalized Δlog (τ/K_A) values, a bias factor can be calculated for each ligand for the G-protein over the β-arrestin mediated pathway as follows

$$\Delta\Delta log\left(\frac{\tau}{K_A}\right)_{G-Arr} = \Delta log\left(\frac{\tau}{K_A}\right)_{G} - \Delta log\left(\frac{\tau}{K_A}\right)_{Arr} \quad (3)$$

An unbiased response of given ligand for the two investigated pathways would result in a bias factor $\Delta\Delta$log (τ/K_A) around 0, while positive or negative values indicate a bias for the G-protein or arrestin pathway, respectively.

The propagation of the error when employing equation (2) and (3) was addressed using the following equation

$$SEM = \sqrt{(SEM_i)^2 + (SEM_j)^2}$$

6.5. References

1. Ash, A. S.; Schild, H. O. Receptors mediating some actions of histamine. *Br J Pharmacol Chemother* **1966**, 27, 427-439.
2. Black, J. W.; Duncan, W. A.; Durant, C. J.; Ganellin, C. R.; Parsons, E. M. Definition and antagonism of histamine H 2 -receptors. *Nature* **1972**, 236, 385-390.
3. Brimblecombe, R. W.; Duncan, W. A.; Durant, G. J.; Ganellin, C. R.; Parsons, M. E.; Black, J. W. The pharmacology of cimetidine, a new histamine H2-receptor antagonist. *Br. J. Pharmacol.* **1975**, 53, 435P-436P.
4. Gantz, I.; Munzert, G.; Tashiro, T.; Schaffer, M.; Wang, L.; DelValle, J.; Yamada, T. Molecular cloning of the human histamine H2 receptor. *Biochem. Biophys. Res. Commun.* **1991**, 178, 1386-1392.
5. Hill, S. J.; Ganellin, C. R.; Timmerman, H.; Schwartz, J. C.; Shankley, N. P.; Young, J. M.; Schunack, W.; Levi, R.; Haas, H. L. International Union of Pharmacology. XIII. Classification of histamine receptors. *Pharmacol. Rev.* **1997**, 49, 253-278.
6. Hirschfeld, J.; Buschauer, A.; Elz, S.; Schunack, W.; Ruat, M.; Traiffort, E.; Schwartz, J. C. Iodoaminopotentidine and related compounds: a new class of ligands with high affinity and selectivity for the histamine H2 receptor. *J. Med. Chem.* **1992**, 35, 2231-2238.
7. Ruat, M.; Traiffort, E.; Bouthenet, M. L.; Schwartz, J. C.; Hirschfeld, J.; Buschauer, A.; Schunack, W. Reversible and irreversible labeling and autoradiographic localization of the cerebral histamine H2 receptor using [125I]iodinated probes. *Proc. Natl. Acad. Sci. U. S. A.* **1990**, 87, 1658-1662.
8. Hill, S. J. Distribution, properties, and functional characteristics of three classes of histamine receptor. *Pharmacol. Rev.* **1990**, 42, 45-83.
9. Del Valle, J.; Gantz, I. Novel insights into histamine H2 receptor biology. *Am. J. Physiol.* **1997**, 273, G987-996.
10. Black, J. W.; Shankley, N. P. The isolated stomach preparation of the mouse: a physiological unit for pharmacological analysis. *Br. J. Pharmacol.* **1985**, 86, 571-579.
11. Schneider, E.; Rolli-Derkinderen, M.; Arock, M.; Dy, M. Trends in histamine research: new functions during immune responses and hematopoiesis. *Trends Immunol* **2002**, 23, 255-263.
12. Seifert, R.; Hoer, A.; Schwaner, I.; Buschauer, A. Histamine increases cytosolic Ca2+ in HL-60 promyelocytes predominantly via H2 receptors with an unique agonist/antagonist profile and induces functional differentiation. *Mol. Pharmacol.* **1992**, 42, 235-241.
13. Mitsuhashi, M.; Mitsuhashi, T.; Payan, D. G. Multiple signaling pathways of histamine H2 receptors. Identification of an H2 receptor-dependent Ca2+ mobilization pathway in human HL-60 promyelocytic leukemia cells. *J. Biol. Chem.* **1989**, 264, 18356-18362.
14. Negulescu, P. A.; Machen, T. E. Intracellular Ca regulation during secretagogue stimulation of the parietal cell. *Am. J. Physiol.* **1988**, 254, C130-140.
15. Kuhn, B.; Schmid, A.; Harteneck, C.; Gudermann, T.; Schultz, G. G proteins of the Gq family couple the H2 histamine receptor to phospholipase C. *Mol. Endocrinol.* **1996**, 10, 1697-1707.
16. Houston, C.; Wenzel-Seifert, K.; Burckstummer, T.; Seifert, R. The human histamine H2-receptor couples more efficiently to Sf9 insect cell Gs-proteins than to insect cell Gq-proteins: limitations of Sf9 cells for the analysis of receptor/Gq-protein coupling. *J. Neurochem.* **2002**, 80, 678-696.

17. Fernandez, N.; Monczor, F.; Baldi, A.; Davio, C.; Shayo, C. Histamine H2 receptor trafficking: role of arrestin, dynamin, and clathrin in histamine H2 receptor internalization. *Mol. Pharmacol.* **2008**, 74, 1109-1118.
18. Alonso, N.; Monczor, F.; Echeverria, E.; Davio, C.; Shayo, C.; Fernandez, N. Signal transduction mechanism of biased ligands at histamine H2 receptors. *Biochem. J.* **2014**, 459, 117-126.
19. Coruzzi, G.; Timmerman, H.; Adami, M.; Bertaccini, G. The new potent and selective histamine H2 receptor agonist amthamine as a tool to study gastric secretion. *Naunyn Schmiedebergs Arch. Pharmacol.* **1993**, 348, 77-81.
20. Eriks, J. C.; van der Goot, H.; Sterk, G. J.; Timmerman, H. Histamine H2-receptor agonists. Synthesis, in vitro pharmacology, and qualitative structure-activity relationships of substituted 4- and 5-(2-aminoethyl)thiazoles. *J. Med. Chem.* **1992**, 35, 3239-3246.
21. Parsons, M. E.; Owen, D. A.; Ganellin, C. R.; Durant, G. J. Dimaprit -(S-[3-(N,N-dimethylamino)prophyl]isothiourea) - a highly specific histamine H2 -receptor agonist. Part 1. Pharmacology. *Agents Actions* **1977**, 7, 31-37.
22. Durant, G. J.; Ganellin, C. R.; Hills, D. W.; Miles, P. D.; Parsons, M. E.; Pepper, E. S.; White, G. R. The histamine H2 receptor agonist impromidine: synthesis and structure-activity considerations. *J. Med. Chem.* **1985**, 28, 1414-1422.
23. Buschauer, A. Synthesis and in vitro pharmacology of arpromidine and related phenyl(pyridylalkyl)guanidines, a potential new class of positive inotropic drugs. *J. Med. Chem.* **1989**, 32, 1963-1970.
24. Lim, H. D.; van Rijn, R. M.; Ling, P.; Bakker, R. A.; Thurmond, R. L.; Leurs, R. Evaluation of histamine H1-, H2-, and H3-receptor ligands at the human histamine H4 receptor: identification of 4-methylhistamine as the first potent and selective H4 receptor agonist. *J. Pharmacol. Exp. Ther.* **2005**, 314, 1310-1321.
25. Igel, P.; Schneider, E.; Schnell, D.; Elz, S.; Seifert, R.; Buschauer, A. N(G)-acylated imidazolylpropylguanidines as potent histamine H4 receptor agonists: selectivity by variation of the N(G)-substituent. *J. Med. Chem.* **2009**, 52, 2623-2627.
26. Ghorai, P.; Kraus, A.; Keller, M.; Gotte, C.; Igel, P.; Schneider, E.; Schnell, D.; Bernhardt, G.; Dove, S.; Zabel, M.; Elz, S.; Seifert, R.; Buschauer, A. Acylguanidines as bioisosteres of guanidines: NG-acylated imidazolylpropylguanidines, a new class of histamine H2 receptor agonists. *J. Med. Chem.* **2008**, 51, 7193-7204.
27. Kraus, A.; Ghorai, P.; Birnkammer, T.; Schnell, D.; Elz, S.; Seifert, R.; Dove, S.; Bernhardt, G.; Buschauer, A. N(G)-acylated aminothiazolylpropylguanidines as potent and selective histamine H(2) receptor agonists. *ChemMedChem* **2009**, 4, 232-240.
28. Birnkammer, T.; Spickenreither, A.; Brunskole, I.; Lopuch, M.; Kagermeier, N.; Bernhardt, G.; Dove, S.; Seifert, R.; Elz, S.; Buschauer, A. The bivalent ligand approach leads to highly potent and selective acylguanidine-type histamine H(2) receptor agonists. *J. Med. Chem.* **2012**, 55, 1147-1160.
29. Parsons, M. E.; Ganellin, C. R. Histamine and its receptors. *Br. J. Pharmacol.* **2006**, 147 Suppl 1, S127-135.
30. Cavanagh, R. L.; Buyniski, J. P. Effect of BMY-25368, a potent and long-acting histamine H2-receptor antagonist, on gastric secretion and aspirin-induced gastric lesions in the dog. *Aliment. Pharmacol. Ther.* **1989**, 3, 299-313.
31. Erdmann, D. Histamine H2 and H3 Receptor Antagonists: Synthesis and Characterization of Radiolabelled and Fluorescent Pharmacological Tools. University of Regensburg, 2010. http://epub.uni-regensburg.de/19062/.

32. Kraus, A. Highly Potent, Selective Acylguanidine-Type Histamine H2 Receptor Agonists: Synthesis and Structure-Activity Relationships. University of Regensburg, 2007. http://epub.uni-regensburg.de/10699/.
33. Birnkammer, T. Highly potent and selective acylguanidinetype histamine H2 receptor agonists: synthesis and structure-activity relationships of mono- and bivalent ligands. University of Regensburg, 2011. http://epub.uni-regensburg.de/22237/.
34. Black, J. W.; Leff, P. Operational models of pharmacological agonism. *Proc. R. Soc. Lond. B. Biol. Sci.* **1983**, 220, 141-162.
35. Kenakin, T.; Watson, C.; Muniz-Medina, V.; Christopoulos, A.; Novick, S. A simple method for quantifying functional selectivity and agonist bias. *ACS Chem. Neurosci.* **2012**, 3, 193-203.
36. Rajagopal, S.; Ahn, S.; Rominger, D. H.; Gowen-MacDonald, W.; Lam, C. M.; Dewire, S. M.; Violin, J. D.; Lefkowitz, R. J. Quantifying ligand bias at seven-transmembrane receptors. *Mol. Pharmacol.* **2011**, 80, 367-377.
37. Shonberg, J.; Herenbrink, C. K.; Lopez, L.; Christopoulos, A.; Scammells, P. J.; Capuano, B.; Lane, J. R. A structure-activity analysis of biased agonism at the dopamine D2 receptor. *J. Med. Chem.* **2013**, 56, 9199-9221.
38. Committee for Orphan Medicinal, P.; the European, M.; Westermark, K.; Holm, B. B.; Soderholm, M.; Llinares-Garcia, J.; Riviere, F.; Aarum, S.; Butlen-Ducuing, F.; Tsigkos, S.; Wilk-Kachlicka, A.; N'Diamoi, C.; Borvendeg, J.; Lyons, D.; Sepodes, B.; Bloechl-Daum, B.; Lhoir, A.; Todorova, M.; Kkolos, I.; Kubackova, K.; Bosch-Traberg, H.; Tillmann, V.; Saano, V.; Heron, E.; Elbers, R.; Siouti, M.; Eggenhofer, J.; Salmon, P.; Clementi, M.; Krievins, D.; Matuleviciene, A.; Metz, H.; Vincenti, A. C.; Voordouw, A.; Dembowska-Baginska, B.; Nunes, A. C.; Saleh, F. M.; Foltanova, T.; Mozina, M.; Torrent i Farnell, J.; Beerman, B.; Mariz, S.; Evers, M. P.; Greene, L.; Thorsteinsson, S.; Gramstad, L.; Mavris, M.; Bignami, F.; Lorence, A.; Belorgey, C. European regulation on orphan medicinal products: 10 years of experience and future perspectives. *Nat. Rev. Drug Discov.* **2011**, 10, 341-349.
39. Brune, M.; Castaigne, S.; Catalano, J.; Gehlsen, K.; Ho, A. D.; Hofmann, W. K.; Hogge, D. E.; Nilsson, B.; Or, R.; Romero, A. I.; Rowe, J. M.; Simonsson, B.; Spearing, R.; Stadtmauer, E. A.; Szer, J.; Wallhult, E.; Hellstrand, K. Improved leukemia-free survival after postconsolidation immunotherapy with histamine dihydrochloride and interleukin-2 in acute myeloid leukemia: results of a randomized phase 3 trial. *Blood* **2006**, 108, 88-96.
40. Thoren, F. B.; Romero, A. I.; Brune, M.; Hellstrand, K. Histamine dihydrochloride and low-dose interleukin-2 as post-consolidation immunotherapy in acute myeloid leukemia. *Expert Opin. Biol. Ther.* **2009**, 9, 1217-1223.
41. Werner, K.; Neumann, D.; Seifert, R. Analysis of the histamine H-receptor in human monocytes. *Biochem. Pharmacol.* **2014**.
42. Baumeister, P.; Erdmann, D.; Biselli, S.; Kagermeier, N.; Elz, S.; Bernhardt, G.; Buschauer, A. [H]UR-DE257: Development of a Tritium-Labeled Squaramide-Type Selective Histamine H Receptor Antagonist. *ChemMedChem* **2014**.
43. Seifert, R.; Lee, T. W.; Lam, V. T.; Kobilka, B. K. Reconstitution of beta2-adrenoceptor-GTP-binding-protein interaction in Sf9 cells--high coupling efficiency in a beta2-adrenoceptor-G(s alpha) fusion protein. *Eur. J. Biochem.* **1998**, 255, 369-382.
44. Wenzel-Seifert, K.; Kelley, M. T.; Buschauer, A.; Seifert, R. Similar apparent constitutive activity of human histamine H(2)-receptor fused to long and short splice variants of G(salpha). *J. Pharmacol. Exp. Ther.* **2001**, 299, 1013-1020.

Chapter 7

Analysis of functional selectivity at the histamine H_4 receptor

7. Analysis of functional selectivity at the histamine H_4 receptor

7.1. Introduction

The histamine H_4 receptor represents the newest addition to the histamine receptor family. Its existence was first postulated by Raible *et al.* in 1994, triggered by the finding that human eosinophils express a histamine receptor with a pharmacological profile distinct from that of the three other histamine receptor subtypes.[1] However, it was not until after the successful cloning of the histamine H_3 receptor in 1999[2] that the H_4R was identified with the aid of genomic databases due its high homology with the H_3R. In the years 2000 and 2001, independent of each other, several research groups reported the cloning of the H_4R.[3-9]

The analysis of the expression pattern of the H_4R in humans and mice has been performed mostly by using reverse transcriptase PCR (RT-PCR) techniques detecting transcription levels of the corresponding mRNA transcripts in the different tissues.[10,11] Hereby, H_4R expression was detected in spleen, lung, liver, thymus, bone marrow, small intestines and colon as well as in several cells of the hematopoietic lineage.[3,8,9,11,12] Reports about H_4R expression in the brain have so far been inconclusive, as RT-PCR techniques are prone to contamination and detailed expression analysis on the protein level has so far been hampered by the lack of suitable, specific H_4R antibodies or radioligands for autoradiography studies.[13-15]

The predominant expression of the H_4R in hematopoietic cells, including neutrophils, mast cells, eosinophils, basophils, dendritic cells and T cells,[11] suggest a broad involvement of the H_4R in immune modulation and inflamation.[16] It has been demonstrated that the H_4R is involved in the chemotaxis of eosinophils through induction of actin rearrangement and upregulation of certain adhesion proteins.[1,16,17] In mast cells, H_4R activation induces chemotaxis without triggering degranulation and thereby might be crucial for the development of chronic allergic inflammation.[12,16] Furthermore, the H_4R plays a role in the activation of dendritic cells and the release of interleukins from T lymphocytes.[16,18] Therefore, the H_4R is considered as a promising new target for the treatment of allergic and inflammatory disorders, like asthma, pruritus and allergic rhinitis, and several H_4R antagonists are currently under investigation in clinical trials.[19-23]

The full length H_4R is a 390 aa protein belonging to the class A, rhodopsin-like GPCRs. The coding sequence of the H_4R gene is separated by two large intron sequences, theoretically allowing for multiple alternative splice variants of the gene transcript.[3] So far only two truncated variants of the H_4R have been identified, $H_4R_{(67)}$ and $H_4R_{(302)}$, neither exhibiting GPCR-like functions on their one, but rather playing a role in regulation of the full length H_4R.[11,24] The H_4R couples to pertussis toxin (PTX) sensitive $G_{\alpha i/0}$ proteins leading to inhibition of the ACs and, thus, a decrease in intracellular cAMP levels, thereby inhibiting

transcription of genes under control of the CRE promoter.[5,8,11] Furthermore H_4R stimulation induced a PTX sensitive activation of downstream MAPK pathways.[5] In addition to $G_{\alpha i/0}$ activation, the H_4R couples to PLC dependent pathways via the $G_{\alpha 15/16}$ proteins,[5,8] which are exclusively expressed in hematopoietic cells.[25] In most recombinant systems, the H_4R exhibited constitutive activity, susceptible to inhibition by different inverse agonists.[11] In mast cells endogenously expressing the H_4R, histamine stimulation induced a Ca^{2+} signal, which was inhibited by PTX and the PLC inhibitor U73122.[12]

In 2011, the functional versatility of the H_4R came into focus, when Rosethorne *et al.* identified the indole derivative JNJ7777120, previously regarded as a standard antagonist for the H_4R, as a biased agonist, inducing H_4R-mediated β-arrestin recruitment.[26,27] The authors reported that JNJ7777120, while being an antagonist in a [^{35}S]GTPγS binding assay, exhibited strong partial agonistic activity in a β-arrestin recruitment assay and that the observed stimulation by JNJ7777120 was insensitive to the treatment with PTX.[26] Furthermore, JNJ7777120 induced ERK1/2 phosphorylation in a time course significantly prolonged in comparison to the corresponding histamine effect,[26] as generally expected for G-protein versus β-arrestin mediated signaling.[28] Following this initial discovery, a variety of known H_4R ligands were investigated for functional selectivity, and several compounds of different chemical classes were identified as either G-protein or β-arrestin biased ligands at the H_4R.[29]

Due to the reported discrimination between G protein and arrestin signaling, the H_4R is an especially interesting target to study functional selectivity and to evaluate the enzyme fragment complementation based β-arrestin recruitment assay established as part of this doctoral project. In addition to several reference compounds previously tested for biased agonism in other laboratories, new classes of H_4R ligands synthesized in our department[30-32] were selected for pharmacological characterization in the β-arrestin recruitment assay.

7.1.1. H_4R ligands selected for the functional selectivity screening

The pharmacological investigations were performed with a set of 29 structurally diverse H_4R ligands (chemical structures, cf. Fig. 7-1). This selection included the endogenous ligand histamine (**1**) as well as several methylhistamine derivatives (**2**-**5**) with known affinity for the H_4R, including 4(5)-methylhistamine (**5**), the first potent and selective agonist for the H_4R.[33] Furthermore, several imidazole containing compounds, originally designed as H_3R agonists, but also exhibiting H_4R affinity, were included (**6**-**10**).[33] The same holds for the thiourea derivative thioperamide (**11**), a known inverse agonist at the H_3R and H_4R, and the isothiourea-type H_3R antagonists clobenpropit (**12**) and iodophenpropit (**13**). Similar to 4(5)-methylhistamine, VUF8430 (**14**)[33,34] as well as the acylguanidine UR-AK51 (**15**) were initially designed as H_2R agonist, but found to be potent H_4R agonists. UR-AK51 triggered the development of UR-PI294 (**16**), a potent full agonist at the H_4R with strong selectivity over the H_1R and H_2R and low efficacy at the H_3R.[30] The atypical antipsychotic dibenzodiazepine derivative clozapine (**17**) and its structural analog isoloxapine (**18**) are known to possess affinity to the H_1R and H_4R.[33] The aminopyrimidines A943931 (**19**) and

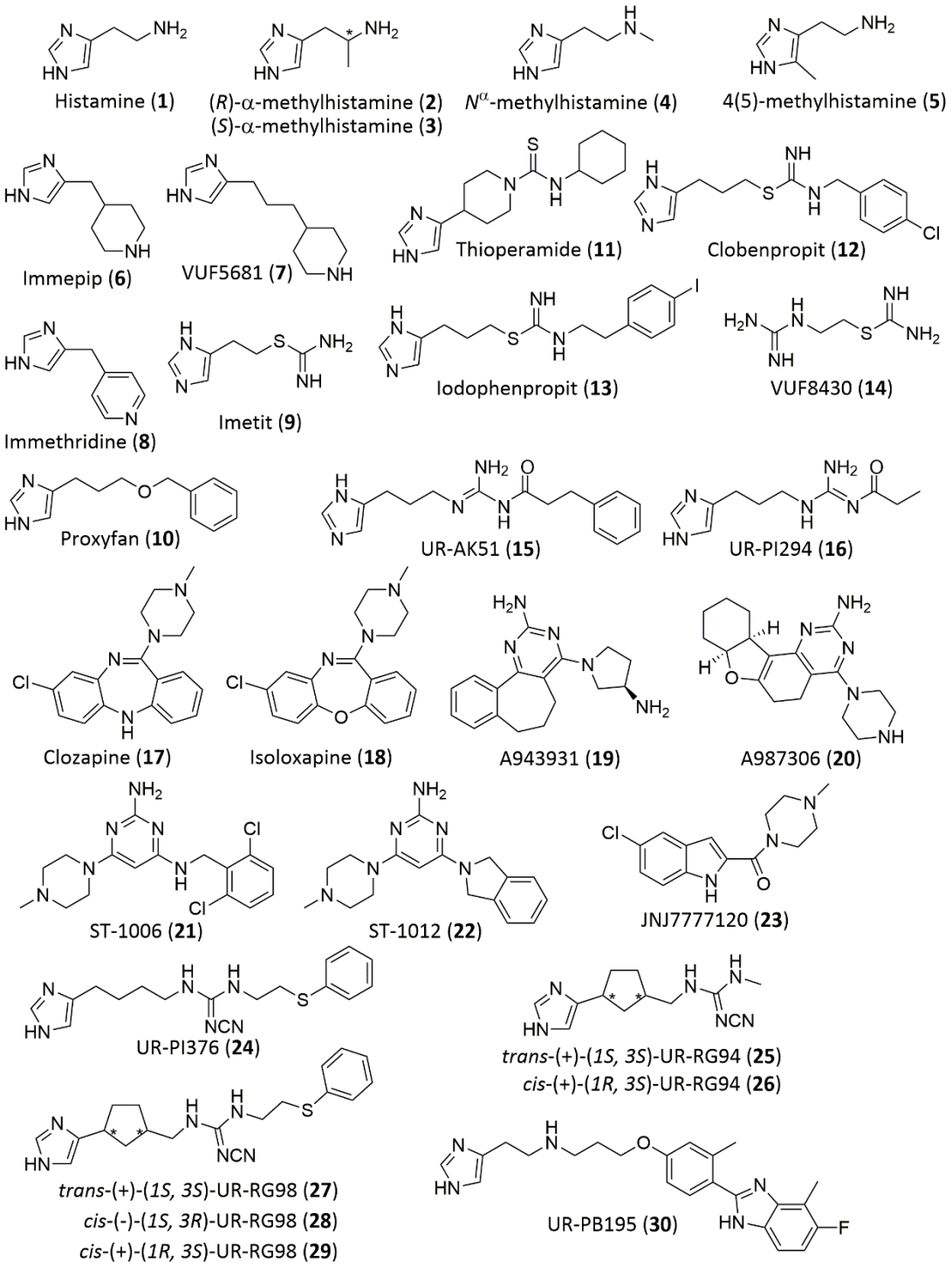

Fig. 7-1: Structures of the selected H_4R ligands

A987306 (**20**) were described as new potent and selective H_4R antagonists with anti-inflammatory and pain blocking efficacy in mice.[35,36] Independently, Sanders *et al.* developed another set of aminopyrimidines and identified ST-1006 (**21**) and ST-1012 (**22**) as high affinity H_4R ligands.[37] Interestingly, while **22** acted as inverse agonist at the H_4R, **21** exhibited partial agonistic activity.[37] As mentioned above, JNJ7777120 was the first β-arrestin biased ligand at the H_4R described in the literature and, therefore, included as reference compound.[29] The cyanoguanidine UR-PI376 (**24**) was developed from the N^G-

acylated guanidines (cf. **15** and **16**) to improve subtype selectivity for the H_4R.[38] Aiming at a further improvement of the selectivity over the H_3R, the introduction of a cyclopentane-1,3-diyl linker resulted in a set of four chiral compounds with interesting selectivity profiles depending on the stereochemistry (**25**-**29**).[39] The 2-aryl-benzimidazole **30** (UR-PB195) was described as a full agonist with subnanomolar affinity for the H_4R and excellent selectivity over the other histamine receptor subtypes.[40]

7.2. Results and discussion

The selected H_4R ligands were studied for functional selectivity using two different assay systems. H_4R-dependent G-protein activation was determined in a reporter gene assay, measuring the $G_{\alpha i}$ mediated inhibition of forskolin stimulated expression of a firefly luciferase under control of the cAMP response element.[41] β-Arrestin recruitment to the H_4R was measured in the established luciferase complementation assay. In an initial screening, all ligands were tested for functional differences in recruitment of the two β-arrestin isoforms. As no major differences became obvious, further investigations were performed solely with the β-arrestin 2 expressing cells.

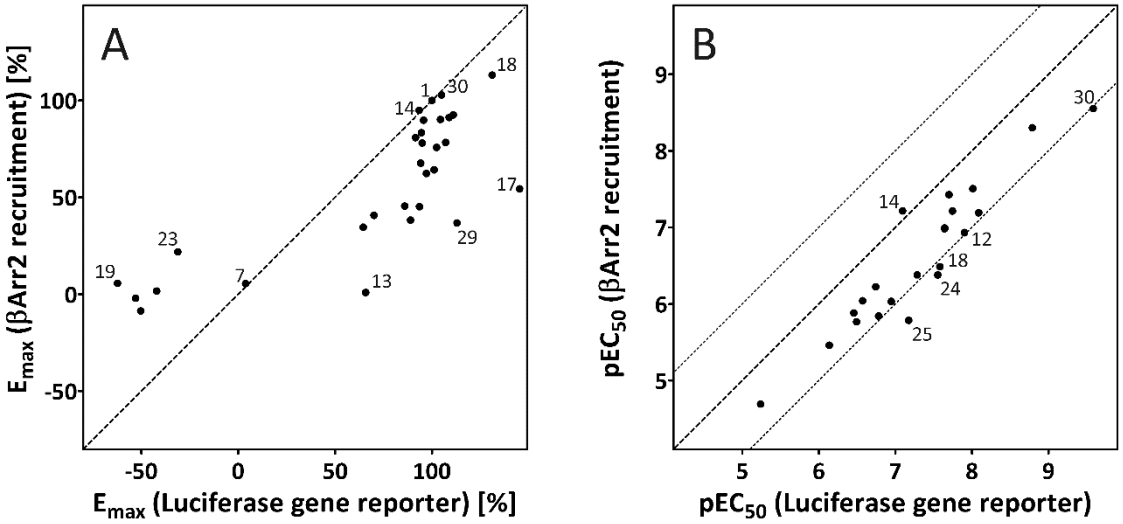

Fig. 7-2: Comparison of the luciferase gene reporter and β-arrestin 2 recruitment assay. **A**) The efficacies of the selected ligands in the luciferase gene reporter against βArr2 recruitment assay. Responses were normalized to the maximal effect induced by histamine (100 %) and solvent (0 %). **B**) pEC_{50} values of the tested ligands in the luciferase gene reporter and βArr2 recruitment assay. **A**, **B**) Data are mean values of 2-7 independent experiments.

Table 7-1 gives a summary of the potencies and efficacies of the tested ligands in the CRE-luciferase and the β-arrestin 2 recruitment assay. The responses in both assays were normalized to the maximum effect induced by 1 mM histamine (100 % value) and solvent (0 % value). Therefore, the endogenous ligand histamine (**1**) is defined as a full, unbiased agonist in both assays (cf. Fig. 7-3). Generally, the determined potencies were higher in the reporter gene assay compared to the arrestin recruitment assay (cf. Fig. 7-2). Except for VUF8430 (**14**) (ΔpEC_{50} = -0.12) and imetit (**9**) (ΔpEC_{50} =0.27), which were equipotent in both readouts, all agonists exhibited a considerably lower potency regarding β-arrestin 2 recruitment (ΔpEC_{50} = 0.49 – 1.39). These results are consistent with previously published data, showing a similar systematic shift between an enzyme fragment complementation (EFC)-based arrestin recruitment assay and the CRE luciferase assay.[29] In theory, such differences can be attributed to the signal amplification occurring in the distal, second messenger based CRE-luciferase assay compared to the proximal EFC-based arrestin

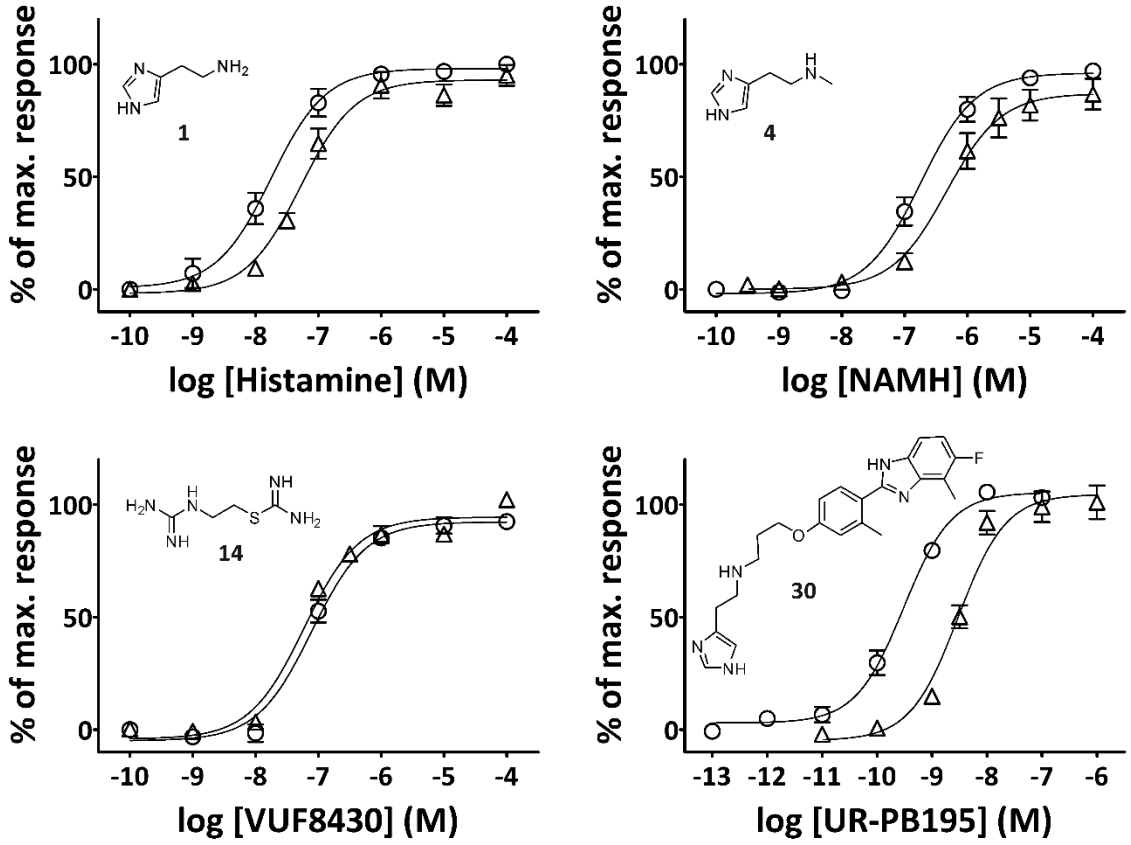

Fig. 7-3: Concentration-response curves of selected full H_4R agonists in the luciferase gene reporter (○ circles) and β-arrestin 2 recruitment assay (△ triangles). Data presented are mean ± SEM of 2-4 independent experiments. Data were analyzed by nonlinear regression and best fitted to sigmoidal concentration-response curves.

recruitment assay. A similar decrease in potency was evident for arrestin recruitment compared to G-protein activation in case of the H_2R (cf. Chapter 6), even though the GTPγS binding assay was performed with membranes expressing H_2R-$G_{s\alpha S}$ fusion ensuring a 1:1 stoichiometry of receptor and effector protein as in the EFC-based arrestin recruitment assay, thus annihilating presumed differences in signal amplification.

Fig. 7-3 gives the concentration response curves of compounds acting as full agonists in both assays, thus exhibiting no bias with regard to the intrinsic activities of the compounds. The potencies of the compounds, however, show a completely different picture. While histamine (**1**) and N^{α}-methyl-histamine (**4**) exhibited only a minor shift towards lower potencies in arrestin recruitment (ΔpEC_{50} (**1**) = 0.53; ΔpEC_{50} (**4**) = 0.52), the benzimidazole UR-PB195 showed a pronounced decrease (ΔpEC_{50} = 1.03; p = 0.0014). The isothiourea VUF8430 on the other hand displays equal potencies in either readout (ΔpEC_{50} = -0.12; p = 0.35). These differences imply that, despite comparable response to all four ligands, **30** induces a G-protein biased response (ΔE (1 nM UR-PB195) = 0.57) at submaximal concentrations, in contrast to **14**, which produces unbiased effects over the whole concentration range. Whether such a bias in the detected potencies implies distinct, ligand specific receptor conformations and different physiological responses to the corresponding compounds, remains to be determined.

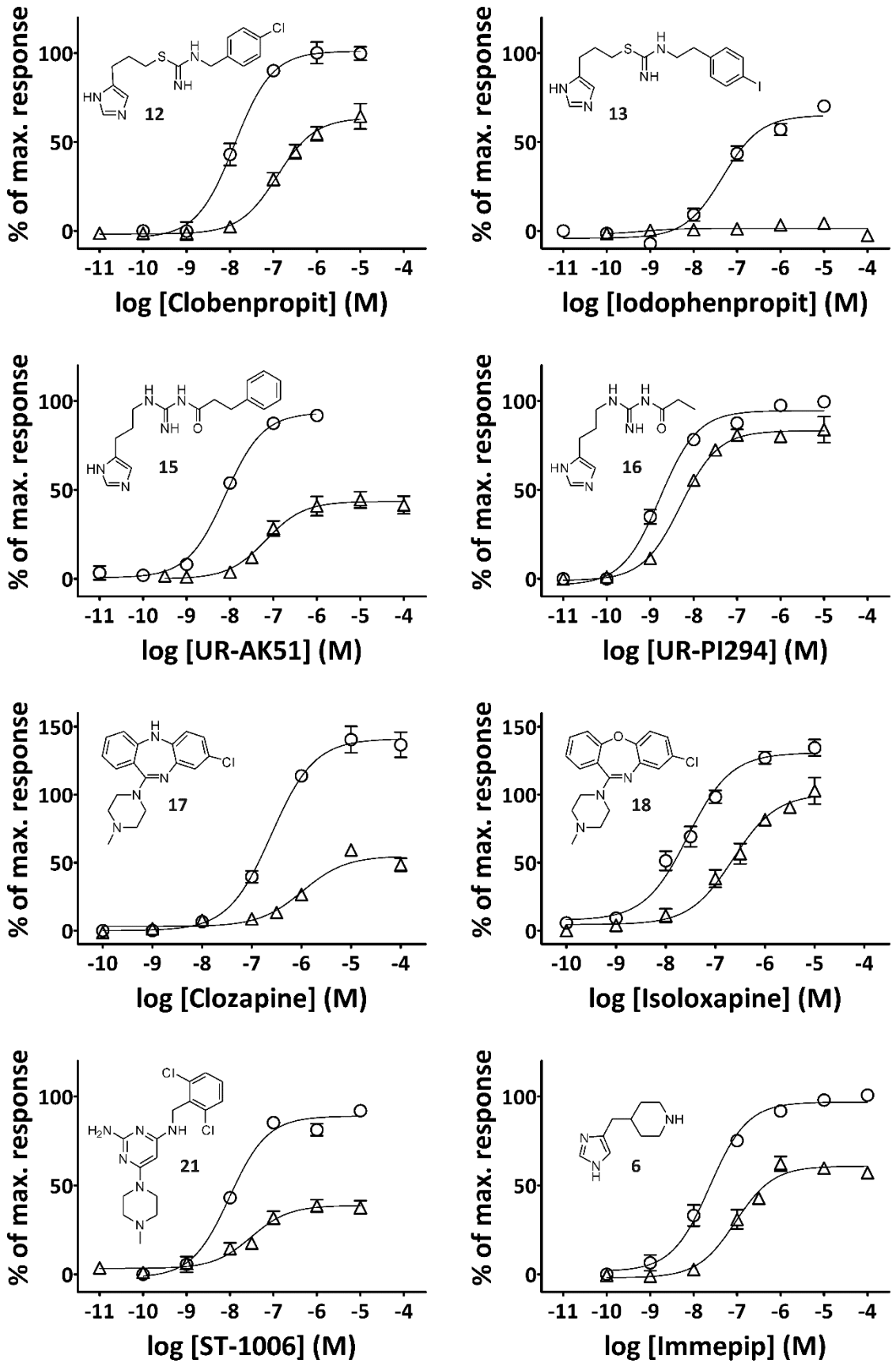

Fig. 7-4: Concentration- response curves of selected H_4R ligands in the luciferase gene reporter (○ circles) and β-arrestin 2 recruitment assay (△ triangles). Data presented are mean ± SEM of 2-6 independent experiments. Data were analyzed by nonlinear regression and best fitted to sigmoidal concentration-response curves.

Of the tested methyl-histamine derivatives (**2**-**5**) only **4** acted as full agonist in both assays, the other three compounds revealed a moderate decrease in efficacy in arrestin recruitment (ΔE_{max} = 0.16 – 0.27). Of the enantiomers **2** and **3**, (*R*)-α-methylhistamine was the eutomer in both pathways. Immepip (**6**) exhibited a higher potency and efficacy than its pyridine analog immethridine (**8**) in both readouts, while both compounds revealed a decrease in potency as well as efficacy in β-arrestin compared to G-protein activation.

Several structurally related compounds exhibited interesting functional profiles (cf. Fig. 7-4). Clobenpropit (**12**) displayed a significant bias towards G-protein activation, acting as full agonist in the luciferase gene reporter assay, while exhibiting significantly lower potency and efficacy in arrestin recruitment (ΔE_{max} = 0.37, p = 0.0115; ΔpEC_{50} = 0.97, p = 0.0002). In contrast to full agonism in the luciferase assay, **12** was reported to be a partial agonists in the GTPγS functional binding assay at H_4R expressing *Sf*9 cell membranes.[42] The homologization of the linker between the phenyl and isothiourea moiety and the replacement of the chlorine by iodine (cf. iodophenpropit, **13**), had a considerable impact on the pharmacological properties of the compound. In the G-protein based readout, **13** still displayed partial agonism, though at lower levels of potency and efficacy compared to **12**. By contrast, **13** was completely devoid of intrinsic activity in the β-arrestin recruitment assay. Although such a profile suggests a strong bias of **13** for G-protein over arrestin activation, these results have to be interpreted with caution, as controversial results on the pharmacology of **13** at the H_4R have been reported. For example, **13** was a neutral H_4R antagonist in a CRE-β-galactosidase gene reporter assay in SK-N-MC cells[33] and in the GTPγS functional binding assay at *Sf*9 membranes (David Wifling, personal communications), but a H_4R partial agonist in HEK293T cells in the CRE-luciferase assay[41] as well as in a Ca^{2+} mobilization assay, when the H_4R was co-expressed with the chimeric G_{iq5} protein.[9] Additionally, **13** showed different pharmacological properties depending on H_4R species orthologs, exhibiting partial agonism at the human H_4R but neutral antagonism at the rodent receptor orthologs.[41] So far, it cannot be ruled out that the observed effects of **13** in the CRE based luciferase assay are, at least in part, mediated by mechanisms distinct from the $G_{\alpha i}$ pathway.

The acylguanidine UR-AK51 (**15**), originally developed as H_2R agonist, revealed functional selectivity for G-protein activation at the H_4R. Acting as highly potent nearly full agonist in the CRE-luciferase assay (pEC_{50} = 8.09; E_{max} = 0.93), **15** only exhibited partial agonism at a significantly lower potency in β-arrestin recruitment (pEC_{50} = 7.19; E_{max} = 0.45). Interestingly, this functional characteristic closely resembles the bias of structurally related acylguanidine-type ligands containing imidazole moieties, when tested for agonism at the H_2R (cf. Chapter 6.2; compds. **5**-**10**). The structurally closely related UR-PI294 (**16**), devoid of a phenyl substituent as in **15**, showed a significantly increased potency compared to **15** in both assay system. Additionally, **16** is devoid of functional bias for either pathway. This suggests that, in addition to generally reducing the H_4R affinity,[30] the bulky phenyl substituent in **15** impedes the receptor from adapting conformation(s) required for arrestin binding.

Both the benzodiazepine clozapine (**17**) and its benzoxazepine analog isoloxapine (**18**) gave superagonistic responses in the CRE-luciferase assay, exceeding the maximal

histamine induced effect (E_{max} (**17**) = 1.45; E_{max} (**18**) =1.31). However, while **18** also acted as full agonist in arrestin recruitment (E_{max} = 1.13), though with lower potency compared to the G-protein readout, **17** showed an almost 3-fold reduction in efficacy in the arrestin pathway (E_{max} = 0.54). Comparing these two readouts suggests a strong bias of **17** for G-protein activation. However, it should be stressed that the exceedingly high efficacy of these two compounds could not be confirmed in other G-protein based functional assays. For example, in the GTPγS functional binding assay on membranes of *Sf*9 insect cells expressing the H_4R, **17** and **18** exhibited partial agonism instead of superagonism,[42] questioning the interpretation of data from different assay systems as functional bias.

Among the four tested aminopyrimidines, as expected from the published data, only ST-1006 (**21**) showed H_4R agonism.[35-37] Compared to arrestin recruitment, the CRE-luciferase data revealed a significant bias for G-protein over arrestin activation (ΔE_{max} = 0.51, p = 0.0001; ΔpEC_{50} = 0.51, p = 0,038). Again, considerably lower efficacies of **21** in the proximal GTPγS binding assay[37] compared to the gene reporter assay have to be taken into consideration with respect to interpretation of data as functional selectivity.

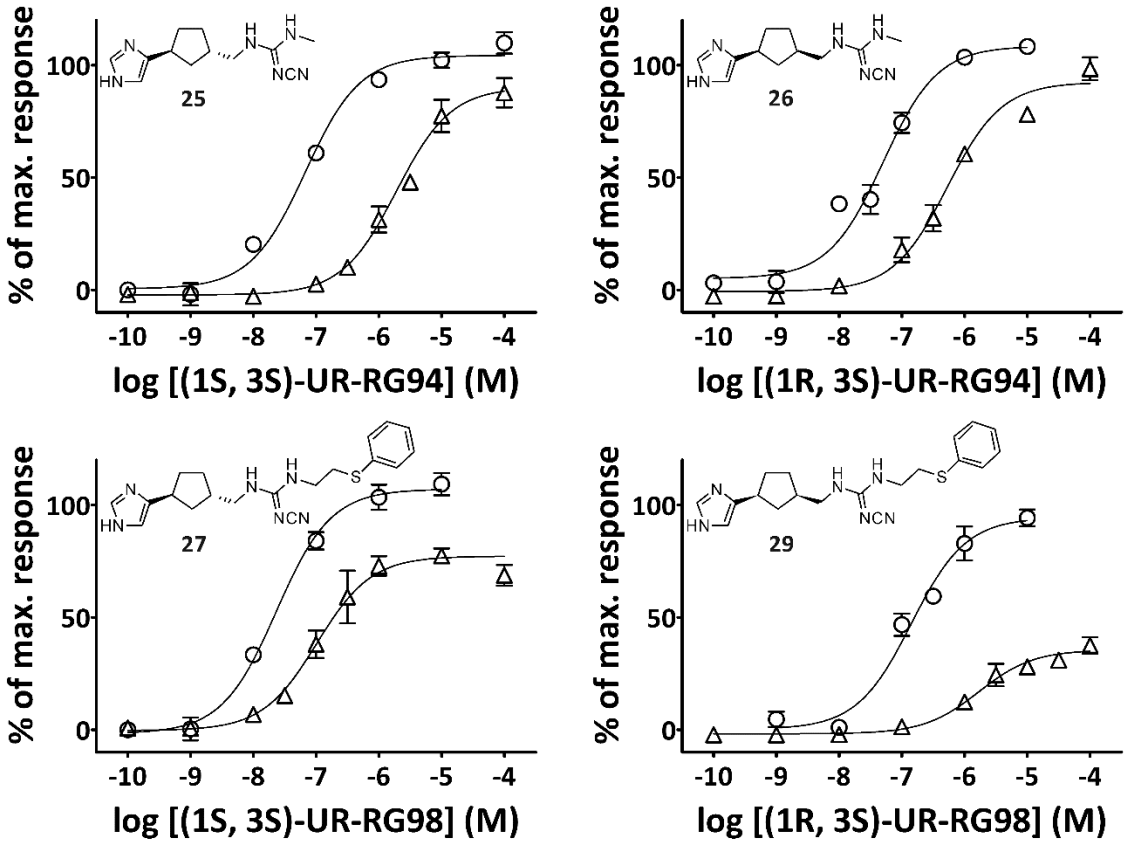

Fig. 7-5: Concentration-response curves of the stereoisomers of the conformationally constrained cyanoguanidines **25-27** and **29** in the luciferase gene reporter (○ circles) and β-arrestin 2 recruitment assay (△ triangles). Data presented are mean ± SEM of 2-4 independent experiments. Data were analyzed by nonlinear regression and best fitted to sigmoidal concentration-response curves.

The chiral cyanoguanidines containing a cylopentane-1,3-diyl-linker (**25**-**29**) reveal an interesting relationship between their functional characteristic and their absolute

configuration (cf. Fig. 7-5). From each group of compounds, the methyl- and the phenylsulfanylethyl-substituted cyanoguanidines, several stereoisomers were selected, namely those possessing highest H_4R agonist potency in the GTPγS assay.[39] For UR-RG94, both, the *trans*-(*1S,3S*)- (**25**) and the *cis*-(*1R,3S*)-configured (**26**) diastereomers, were full agonists with comparable potencies in the CRE gene reporter assay (pEC_{50} (**25**) = 7.17; pEC_{50} (**26**) = 7.28). In arrestin recruitment both diastereomers showed nearly full maximal response, but revealed a remarkable drop in potency (ΔpEC_{50} (**25**) = 1.39, p = 0.0003; ΔpEC_{50} (**26**) = 0.91, p = 0.043) compared to the data from the luciferase assay. In case of UR-RG98 (**27**-**29**), bearing the bulkier phenylsulfanylethyl moiety, the configuration of the stereoisomers had a more pronounced effect on the pharmacological properties. While the three tested diastereomers exhibited comparable efficacies in the G-protein readout (ΔE_{max} < 0.21, *p* = 0.21), the cis-configured compounds, *cis*-(*1S,3R*) (**28**) and *cis*-(*1R,3S*) (**29**), induced significantly lower maximal responses in arrestin recruitment than *trans*-(*1S,3S*)-UR-RG98 (**27**), revealing a significant bias for G-protein activation. These data suggest that that in case of the bulky substituents *cis*-configuration of the ligand disfavors receptor conformation(s) enabling arrestin recruitment, whereas a methyl group is still tolerated. In contrast to **27-29**, the flexible parent compound UR-PI376 (**24**) was an unbiased full agonist in both readouts. Unfortunately, as for other compounds, differing efficacies for these cyanoguanidines have been reported in the GTPγS binding assay.[39]

The discrepancies between the efficacies of several compounds in assays based on distal and proximal G-protein dependent readouts challenge whether the apparent functional bias is truly mediated by ligand-specific receptor conformations or rather caused by an amplification of the signal by the effector cascade downstream of G-protein activation. The agonism/antagonism switch in case of **13**, evident in CRE-based reporter gene assays depending on the cellular background,[33,41] further indicates, that these processes are highly susceptible to variations in the expression patterns of signal effector proteins. In the functional GTPγS binding assay, the human H_4R was reported to exhibit very high constitutive activity, thus producing unfavorable signal-to-noise ratios, limiting the reliability of the assay for the detection of variation in the intrinsic activity of related compounds, further complicating the interpretation of the aforementioned discrepancies.

The H_4R ligands selected for the investigations for functional selectivity included several compounds that were previously described as inverse agonists or neutral antagonists at the H_4R (cf. Fig. 7-6). For the indole derivative JNJ7777120 (**23**), the first biased H_4R ligand reported in the literature,[26,29] functional selectivity for β-arrestin recruitment could be confirmed. Compound **23** acted as inverse agonist in the luciferase gene reporter assay (E_{max} = -0.31) while exhibiting partial agonism in arrestin recruitment (E_{max} = 0.22). VUF5681 (**7**) was the only compound displaying neutral behavior in both assays, all other "antagonists" revealed inverse agonistic activity in at least one assay. Thioperamide (**11**) was an inverse agonist in both readouts (E_{max} (G-protein) = -0.50, E_{max} (βArr2) = -0.09), the aminopyrimidines A987306 (**20**) and ST-1012 (**22**) behaved as neutral antagonists in arrestin recruitment, while exhibiting inverse agonistic effects comparable to **11** in the CRE luciferase assay. This functional characteristic is most pronounced for A943931 (**19**), which showed the strongest inverse efficacy of all compounds in G-protein

activation (E_{max} = -0.62), while revealing even slight agonistic effect in arrestin recruitment (E_{max} = 0.06). Though this increasing difference for **19** compared to **11,** regarding the efficacies for either readout, suggest a functional bias for the compounds, the interpretation of these findings, as mentioned in previous chapters (cf. 5.2.1.), is complicated as the detectability of inverse agonism depends on the level of constitutive activity of the receptor of interest in the respective assay.

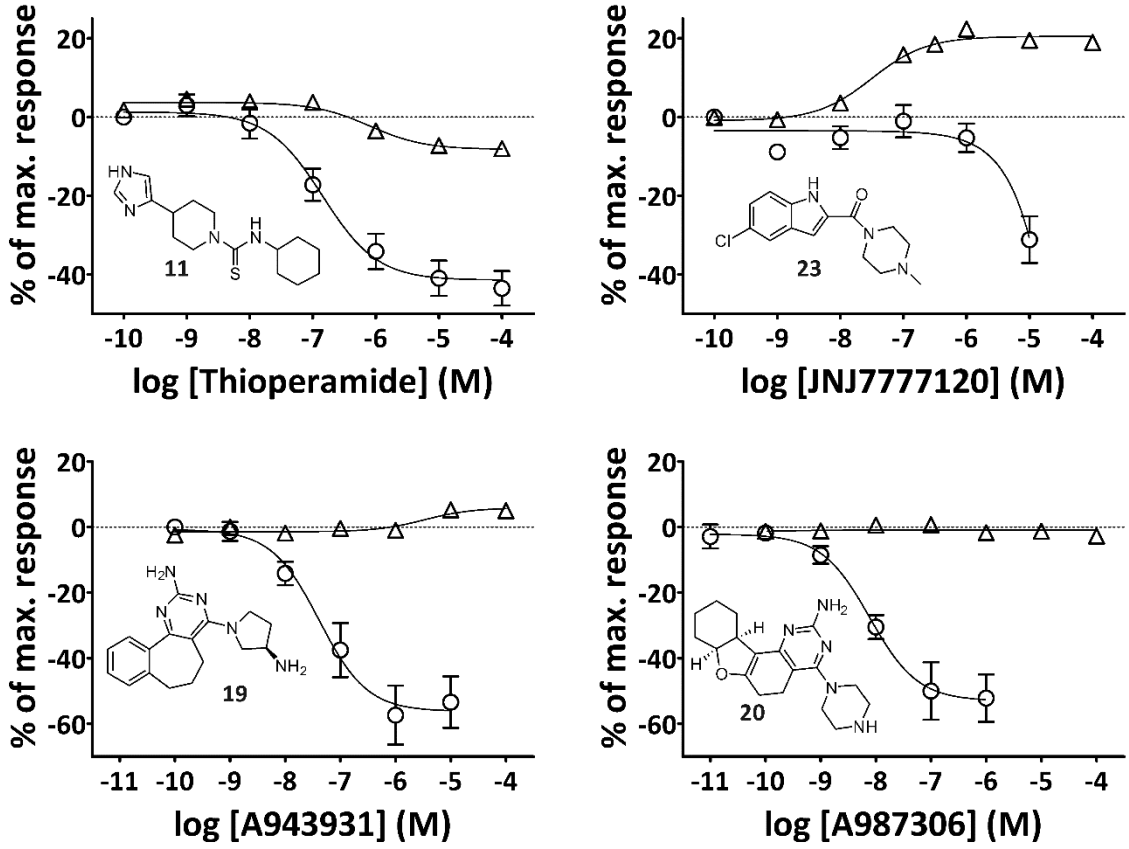

Fig. 7-6: Concentration-response curves of the selected H_4R antagonists or inverse agonists in the luciferase gene reporter (○ circles) and β-arrestin 2 recruitment assay (△ triangles). Data presented are mean ± SEM of 2-6 independent experiments. Data were analyzed by nonlinear regression and best fitted to sigmoidal concentration-response curves.

Tab. 7-1: Potencies and efficacies of the tested H_4R ligands in the CRE luciferase gene reporter and β-arrestin 2 recruitment assay

Compd.	CRE luciferase gene reporter			β-arrestin 2 recruitment		
	pEC_{50}	E_{max}	N	pEC_{50}	E_{max}	N
1 Histamine	7.75 ± 0.15	1.00	6	7.21 ± 0.07	1.00	4
2 (*R*)-α-Methylhistamine	6.46 ± 0.08	1.02 ± 0.03	5	5.88 ± 0.19	0.76 ± 0.05	4
3 (*S*)-α-Methylhistamine	5.24 ± 0.08	0.94 ± 0.06	5	4.69 ± 0.26	0.68 ± 0.01	4
4 N^{α}-Methylhistamine	6.74 ± 0.12	0.96 ± 0.03	4	6.22 ± 0.22	0.90 ± 0.08	4
5 5-Methylhistamine	7.25 ± 0.05	0.95 ± 0.02	3	6.60 ± 0.03	0.78 ± 0.04	3
6 Immepip	7.64 ± 0.12	0.97 ± 0.00	5	6.98 ± 0.15	0.62 ± 0.03	3
7 VUF5681	n.d.	0.04 ± 0.01	2	n.d.	0.06 ± 0.01	3
8 Immethridine	6.14 ± 0.19	0.65 ± 0.06	3	5.46 ± 0.08	0.35 ± 0.04	3
9 Imetit	7.70 ± 0.16	0.91 ± 0.03	6	7.43 ± 0.08	0.81 ± 0.12	4
10 Proxyfan	6.95 ± 0.07	0.70 ± 0.06	4	6.03 ± 0.10	0.41 ± 0.05	3
11 Thioperamide	n.d.	-0.50 ± 0.11	5	n.d.	-0.09 ± 0.02	3
12 Clobenpropit	7.90 ± 0.07	1.01 ± 0.03	3	6.93 ± 0.04	0.64 ± 0.08	3
13 Iodophenpropit	7.32 ± 0.11	0.66 ± 0.01	4	n.d.	0.01 ± 0.01	3
14 VUF8430	7.09 ± 0.09	0.93 ± 0.02	4	7.21 ± 0.07	0.95 ± 0.02	3
15 UR-AK51	8.09 ± 0.06	0.93 ± 0.06	3	7.19 ± 0.09	0.45 ± 0.10	3
16 UR-PI294	8.79 ± 0.10	0.95 ± 0.02	6	8.30 ± 0.06	0.83 ± 0.02	2
17 Clozapine	6.57 ± 0.08	1.45 ± 0.09	4	6.04 ± 0.12	0.54 ± 0.04	4
18 Isoloxapine	7.58 ± 0.15	1.31 ± 0.12	3	6.49 ± 0.20	1.13 ± 0.14	3
19 A943931	7.19 ± 0.08	-0.62 ± 0.10	4	n.d.	0.06 ± 0.04	2
20 A987306	8.15 ± 0.06	-0.53 ± 0.08	4	n.d.	-0.02 ± 0.00	2
21 ST-1006	8.01 ± 0.04	0.89 ± 0.01	3	7.51 ± 0.15	0.38 ± 0.04	4
22 ST-1012	n.d.	-0.42 ± 0.06	3	n.d.	0.02 ± 0.02	3
23 JNJ7777120	n.d.	-0.31 ± 0.06	6	7.40 ± 0.14	0.22 ± 0.03	4
24 UR-PI376	7.55 ± 0.08	1.11 ± 0.05	7	6.38 ± 0.14	0.92 ± 0.13	3
25 *trans*-(*1S,3S*)-UR-RG94	7.17 ± 0.04	1.04 ± 0.04	4	5.79 ± 0.18	0.90 ± 0.07	3
26 *cis*-(*1R,3S*)-UR-RG94	7.28 ± 0.18	1.09 ± 0.01	2	6.38 ± 0.18	0.91 ± 0.06	3
27 *trans*-(*1S,3S*)-UR-RG98	7.64 ± 0.04	1.07 ± 0.06	4	6.99 ± 0.19	0.78 ± 0.03	3
28 *cis*-(*1S,3R*)-UR-RG98	6.78 ± 0.26	0.86 ± 0.04	2	5.84 ± 0.07	0.45 ± 0.05	3
29 *cis*-(*1R,3S*)-UR-RG98	6.89 ± 0.09	0.92 ± 0.10	3	5.77 ± 0.11	0.37 ± 0.04	4
30 UR-PB195	9.59 ± 0.17	1.05 ± 0.04	3	8.55 ± 0.06	1.03 ± 0.04	4

7.2.1. Quantification of functional bias by use of the operational model

To allow for a quantification of the ligand bias, the operational model, as described in 6.2.3, was applied to the functional data from the CRE luciferase and arrestin recruitment assay for all ligands producing agonistic effects in both readouts. The absolute and normalized transduction coefficients for either readout as well as the bias factors $\Delta\Delta\log(\tau/K_A)$ of the ligands between the G-protein and arrestin pathway are given in Tab. 7-2. The negative bias factors determined for some of the compounds indicate a bias towards β-arrestin that was not immediately obvious from the concentration response

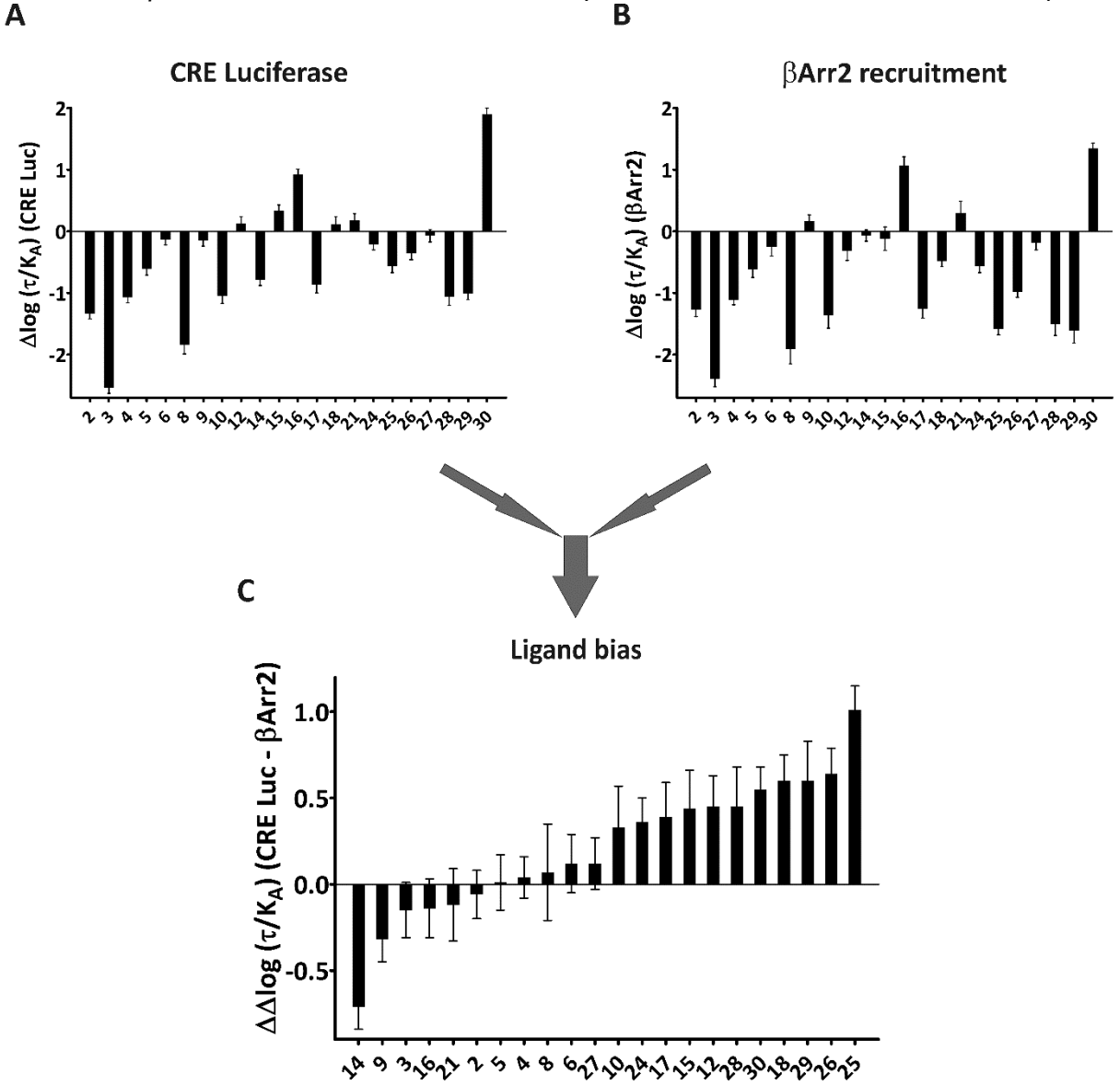

Fig. 7-7: Quantification of the functional bias of the tested H_4R agonists comparing the CRE Luciferase and the arrestin recruitment assay. The normalized $\Delta\log(\tau/K_A)$ values for the G-protein (**A**) and arrestin (**B**) pathway were calculated as described in 6.4.2.4 Eq. 2. Subtraction of the $\Delta\log(\tau/K_A)$ values determined in the CRE luciferase and the arrestin recruitment assay, respectively, yields the bias factors $\Delta\Delta\log(\tau/K_A)$ (**C**) for the tested compounds.

data. The isothiourea VUF8430 (**14**) showed the lowest bias factor ($\Delta\Delta\log(\tau(K_A)$ = -0.71), despite reaching full agonism in both assays (cf. Fig. 7-8). In this case, the determined arrestin bias is caused by a lower potency of **14** in the CRE luciferase compared to histamine, while both ligands are equipotent in arrestin recruitment. Therefore, the normalized transduction coefficient of **14** is significantly lower in the CRE luciferase than in the arrestin recruitment assay. The same effects account for the arrestin bias detected for

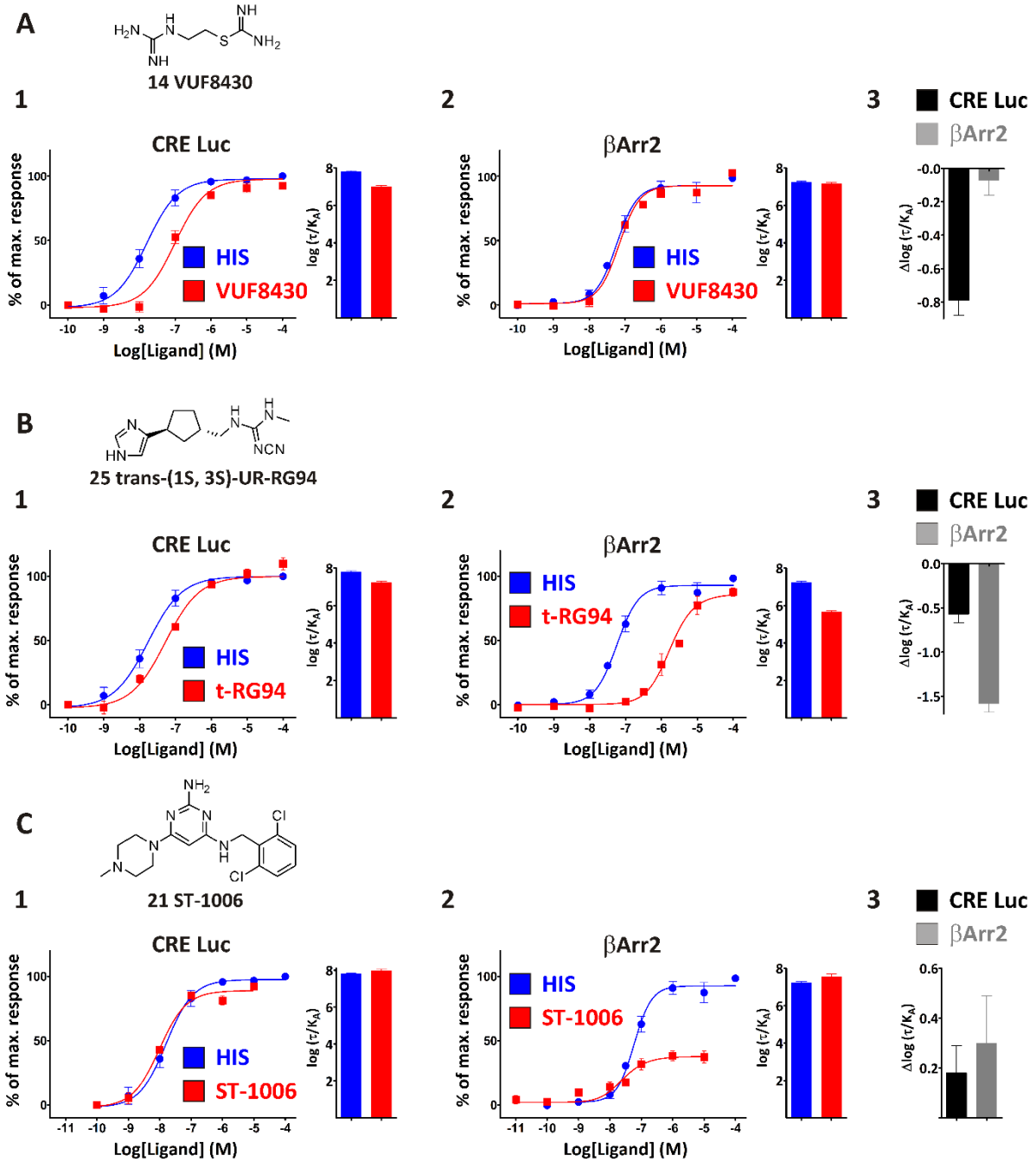

Fig. 7-8: Concentration-response curves of selected H_4R ligands in comparison with the endogenous ligand histamine fitted according to the operational model of agonism as described in 6.4.2.4 and the corresponding transduction coefficients log (τ/K_A) for the CRE luciferase (1) and arrestin recruitment assay (2). Thereof, the normalized transduction coefficients Δlog (τ/K_A) (3) for each assay were derived. Data shown are mean ± SEM calculated as described in 6.4.2.4 for VUF8430 (A), trans-(1S, 3S)-UR-RG94 (B) and ST1006 (C).

imetit (**9**). From the compounds exhibiting G-protein bias, the cyanoguanidine *trans*-(*1S,3S*)-UR-RG94 (**25**) has the highest bias factor ($\Delta\Delta\log(\tau/K_A)$ =1.01). Hereby, as with the arrestin biased compounds, the bias factor is driven by large differences in the detected potency between the two pathways rather than by (insignificant) changes in intrinsic activity, as **25** shows the most pronounced shift towards lower potencies in arrestin recruitment of all tested agonists. The same is true for the compounds **26** and **30**, which showed only minor differences in efficacy. Even so, most of the compounds exhibiting a pronounced bias in the detected efficacies, foremost clozapine (**17**) and *cis*-(*1R,3S*)-UR-RG98 (**29**), showed biased transduction coefficients, too. An exception was ST-1006 (**21**), which showed a clearly reduced efficacy in arrestin recruitment, while the data analysis using the operational model gave comparable $\Delta\log(\tau/K_A)$ values for both readouts. This effect is caused by an increase in potency relative to histamine in the arrestin recruitment assay compensating for the loss in efficacy. Similar effects were registered for some ligands at the H_2R.

Collectively, the results obtained according to the operational model indicate that the chosen method might overrate the contribution of changes in potency to bias. So far, there is no absolute method to quantify functional bias between two distinct signaling pathways, and while the above findings advice caution in interpreting results from the operational model, it offers the possibility to compensate for systematic bias between the different readouts and thus can facilitate the interpretation of bias studies.

Tab. 7-2: Transduction coefficients log (τ/K_A) and normalized transduction coefficients Δlog (τ/K_A) in the CRE luciferase and arrestin recruitment assay and the bias factors $\Delta\Delta$log (τ/K_A) of the tested H_2R agonists.

Cpd.	CRE Luc		βArr2		ΔΔlog (τ/K_A) (G-Arr)
	log (τ/K_A)	Δlog (τ/K_A)	log (τ/K_A)	Δlog (τ/K_A)	
1 Histamine	7.79 ± 0.06		7.23 ± 0.06		
2 (*R*)-α-methylhistamine	6.46 ± 0.07	-1.33 ± 0.09	5.96 ± 0.10	-1.27 ± 0.11	-0.06 ± 0.14
3 (*S*)-α-methylhistamine	5.25 ± 0.07	-2.54 ± 0.09	4.84 ± 0.11	-2.39 ± 0.13	-0.15 ± 0.16
4 N^{α}-methylhistamine	6.72 ± 0.07	-1.07 ± 0.09	6.12 ± 0.06	-1.11 ± 0.08	0.04 ± 0.12
5 5-methylhistamine	7.18 ± 0.08	-0.61 ± 0.10	6.62 ± 0.11	-0.62 ± 0.13	0.01 ± 0.16
6 Immepip	7.66 ± 0.07	-0.13 ± 0.09	6.98 ± 0.13	-0.25 ± 0.15	0.12 ± 0.17
8 Immethridine	5.95 ± 0.14	-1.84 ± 0.15	5.33 ± 0.23	-1.91 ± 0.24	0.07 ± 0.28
9 Imetit	7.64 ± 0.07	-0.15 ± 0.09	7.40 ± 0.08	0.17 ± 0.10	-0.32 ± 0.13
10 Proxyfan	6.75 ± 0.11	-1.04 ± 0.13	5.87 ± 0.20	-1.36 ± 0.21	0.33 ± 0.24
12 Clobenprobit	7.92 ± 0.09	0.13 ± 0.11	6.92 ± 0.13	-0.32 ± 0.15	0.45 ± 0.18
14 VUF8430	7.00 ± 0.07	-0.79 ± 0.09	7.16 ± 0.07	-0.07 ± 0.09	-0.71 ± 0.13
15 UR-AK51	8.12 ± 0.08	0.33 ± 0.10	7.12 ± 0.18	-0.12 ± 0.19	0.44 ± 0.22
16 UR-PI294	8.72 ± 0.06	0.93 ± 0.08	8.30 ± 0.13	1.07 ± 0.14	-0.14 ± 0.17
17 Clozapine	6.92 ± 0.11	-0.87 ± 0.13	5.97 ± 0.14	-1.26 ± 0.15	0.39 ± 0.20
18 Isoloxapine	7.91 ± 0.11	0.12 ± 0.12	6.75 ± 0.07	-0.48 ± 0.09	0.60 ± 0.15
21 ST-1006	7.97 ± 0.09	0.18 ± 0.11	7.53 ± 0.18	0.30 ± 0.19	-0.12 ± 0.21
24 UR-PI376	7.58 ± 0.07	-0.21 ± 0.09	6.67 ± 0.10	-0.56 ± 0.11	0.36 ± 0.14
25 *trans*-(*1S, 3S*)-UR-RG94	7.22 ± 0.08	-0.57 ± 0.10	5.66 ± 0.08	-1.58 ± 0.10	1.01 ± 0.14
26 *cis*-(*1R, 3S*)-UR-RG94	7.44 ± 0.09	-0.35 ± 0.11	6.25 ± 0.08	-0.98 ± 0.09	0.64 ± 0.15
27 *trans*-(*1S, 3S*)-UR-RG98	7.72 ± 0.09	-0.07 ± 0.10	7.04 ± 0.09	-0.19 ± 0.11	0.12 ± 0.15
28 *cis*-(*1S, 3R*)-UR-RG98	6.73 ± 0.13	-1.06 ± 0.14	5.73 ± 0.17	-1.51 ± 0.18	0.45 ± 0.23
29 *cis*-(*1R, 3S*)-UR-RG98	6.78 ± 0.08	-1.01 ± 0.10	5.63 ± 0.20	-1.61 ± 0.20	0.60 ± 0.23
30 UR-PB195	9.69 ± 0.08	1.90 ± 0.10	8.58 ± 0.05	1.35 ± 0.08	0.55 ± 0.13

The transduction coefficients log (τ/K_A) were derived from pooled functional data of 2 – 6 independent experiments fitted to the operational model of agonism as described in 6.4.2.4. Data are given as mean ± SEM calculated as described in 6.4.2.4.

7.2.2. Comparison of the luciferase complementation and the PathHunter assay for measuring arrestin recruitment

Previous publications addressing functional selectivity at the H_4R employed the so-called PathHunter assay (DiscoverX Corp., Fremont, CA, USA) to measure β-arrestin 2 recruitment to the receptor.[26,29] This assay, like the luciferase complementation assay established in our lab, is based on enzyme fragment complementation. Both assays rely on fusion constructs between the enzyme fragments and arrestin and the receptor respectively, providing a 1:1 receptor:effector stoichiometry and eliminating possible effects of variations in signal amplification. The main differences between the two assays are the reporter enzyme, β-galactosidase instead of luciferase, and the cell background, an osteosarcoma cell line (U2OS) instead of HEK293T cells, respectively.

Fig. 7-9 gives a comparison of the potencies and efficacies of ligands tested in both assay systems (data for the PathHunter assay taken from Nijmeijer *et. al.*[29]). Although the detected maximal effects were comparable for most compounds, there was a tendency towards higher efficacies in the PathHunter assay. This was most pronounced for the biased agonist JNJ7777120 (**23**), which exhibited almost 3-fold higher efficacies in the PathHunter assay. The potencies of histamine (**1**) were nearly identical in the two assays, whereas minor differences became obvious for the other compounds. The potencies determined in the luciferase complementation assay were lower than in the PathHunter assay for all ligands except VUF8430 (**14**). Nevertheless, the reported results for the PathHunter assay were in good agreement with the data determined in the luciferase complementation assay in our laboratory. Most importantly, we were able to confirm the previously reported functional characteristics of the tested compounds in the arrestin and G-protein readout.

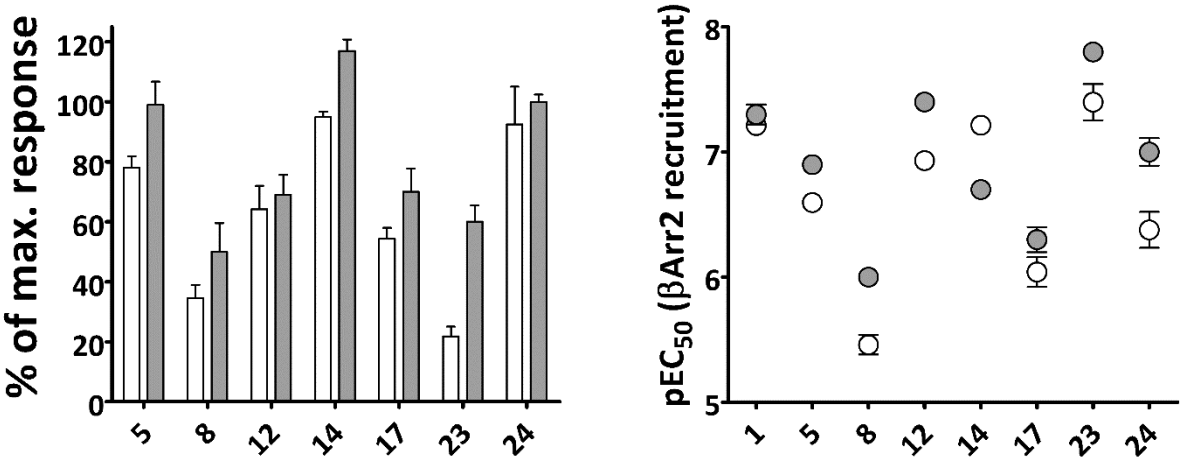

Fig. 7-9: Potencies and efficacies of selected H_4R ligands determined using the Luciferase complementation assay (white) or the PathHunter assay from DiscoverX (grey). Data for the PathHunter assay was reported by Nijmeijer *et al.*[29] Data represent mean ± SEM.

7.3. Summary and conclusions

A set of 30 structurally diverse ligands with known affinity for the H_4R was investigated for functional selectivity regarding G-protein- and β-arrestin-mediated signaling pathways. Therefore, a CRE luciferase reporter gene assay and the established arrestin recruitment assay were employed. Several structurally different H_4R ligands exhibited a functional bias towards G-protein activation, including the isothiourea iodophenpropit, the acylguanidine UR-AK51, the benzodiazepine clozapine and the cyanoguanidine *cis*-(*1R,3S*)-UR-RG98. As for β-arrestin bias, previous findings for the indole derivative JNJ7777120 could be confirmed. Moreover, variations in inverse agonistic efficacy between the two pathways were detected for several H_4R antagonists. However, conclusion from these findings should be drawn with caution, due to discrepancies between intrinsic activities in G-protein based assays, depending on proximal or distal readouts, respectively.[33,41,42] Apart from the discrepancies in ligand efficacy, several compounds revealed pronounced differences in potencies in the two assays, thus, while exhibiting unbiased intrinsic activities, mediating a concentration dependent functional bias. The use of an operational model to quantify the ligand bias supports functional selectivity for those compounds.

The H_4R is a promising target for the development of new drugs for the treatment of various allergic and inflammatory disorders. For the profound interpretation of results from *in vivo* studies, a detailed knowledge of the molecular pharmacological properties of the administered compounds is mandatory, especially, with regard to alternate signaling pathways. In combination with G-protein based readouts, the luciferase complementation assay proved to be a valuable method for the pharmacological characterization of H_4R ligands, therefore aiding in the development of new ligands with distinct functional selectivity as valuable pharmacological tools to decipher complex receptor signaling profiles *in vivo* and *in vitro*.

7.4. Materials and methods

7.4.1. Materials

Unless stated otherwise, all chemicals and reagents were from Sigma-Aldrich Chemie (Munich, Germany) or Merck (Darmstadt, Germany). Hygromycin B was from A.G scientific (San Diego, CA, USA). Forskolin was from Sigma-Aldrich Chemie (Munich, Germany). D-luciferin potassium salt was from Synchem (Felsberg, Germany). For media and reagents used for cell culture of the HEK293T cells as well as for the luciferase complementation assay, see 3.4.1.

7.4.1.1. H_4R ligands

Histamine (**1**) was from Alfa Aesar (Karlsruhe, Germany). (*R*)-α-Methylhistamine (**2**), (*S*)-α-methylhistamine (**3**), N^{α}-methylhistamine (**4**), 4(5)-methylhistamine (**5**), immepip (**6**), VUF5681 (**7**), Immethridine (**8**), imetit (**9**), proxyfan (**10**), thioperamide (**11**), clobenpropit (**12**), iodophenpropit (**13**), A943931 (**19**) and A987306 (**20**) were purchased from Tocris Bioscience (Ellisville, MO, USA). Clozapine (**17**) was a gift from Novartis Pharma (Nuremberg, Germany). ST-1006 (**21**) and ST-1012 (**22**) were kindly provided by Prof. Dr. Holger Stark (Institute of Pharmaceutical and Medicinal Chemistry, Heinrich Heine University, Düsseldorf, Germany). VUF8430 (**14**), UR-AK51 (**15**), UR-PI294 (**16**), Isoloxapine (**18**), JNJ7777120 (**23**), the cyanoguanidines **24**-**29** and UR-PB195 (**30**) were synthesized in our lab.[30,32,38,39,43] 10 mM stock solutions for all compounds were prepared with the following solvents: **1**-**10**, **12**-**14** and **23**: distilled water; **11**, **17**, **19**-**22** and **24**-**29**: 50 % DMSO; **15**, **16** and **30**: 10 mM TFA; **18**: 100 % DMSO.

7.4.2. Methods

7.4.2.1. CRE Luciferase reporter gene assay

The luciferase reporter gene assay was performed as previously described,[41] using the HEK293T-SF-hH_4R-His_6-CRE-Luc cell line, expressing the human H_4R as well as the firefly luciferase under control of the inducible CRE promoter. The cells were cultivated in DMEM with 10 % FCS, 600 µg/ml G418 and 200 µg/ml hygromycin at 37 °C in a water saturated atmosphere containing 5 % CO_2. Dilution series of **1**-**10**, **12**-**16**, **23** and **30** were prepared in DMEM + 10 % (*v/v*) FCS; of **17**-**22** and **24**-**29** in DMEM + 10 % (*v/v*) FCS + 10 % DMSO, giving a final concentration of 1 % DMSO in the assay mixture. 24 h prior to the experiment, cells were seeded in DMEM + 10 % FCS in flat bottom 96 well plates at a density of approximately $2*10^5$ cells/well and cultivated at 37 °C in a water saturated atmosphere containing 5 % CO_2. The following day, the cells were stimulated by the addition of 0.4 µM forskolin and the corresponding ligands at varying concentrations. After incubation for 5 h, the cells were

washed once with 100 µl PBS and afterwards lysed by addition of 40 µl lysis buffer (25 mM Tricine pH 7.8, 10 % (*v/v*) glycerol, 2 mM EGTA, 1 % (*v/v*) Triton X-100, 5 mM $MgSO_4$, 1 mM DTT) and shaking for 45 min at 200 rpm. 20 µl of the lysate were transferred to white, flat bottom 96 well plates. Luminescence was induced by the injection of 80 µl luciferase assay buffer (15 mM KH_2PO_4 pH 7.8, 25 mM Gly-Gly, 15 mM $MgSO_4$, 4 mM EGTA, 2 mM ATP, 2 mM DTT, 0.2 mg/ml D-luciferin potassium salt) using the GENios Pro microplate reader (Tecan, Salzburg, Austria) immediately before the measurement. RLU (relative light units) were measured for 10 s. The raw data was normalized to the maximal effect induced by 1 mM histamine (100 % value) and solvent (0 % value).The functional data for the compounds **1**-**14**, **16**, **17**, **19**-**25** and **27** were kindly provided by Dr. Uwe Nordemann.[41]

7.4.2.2. Luciferase complementation assay

The luciferase complementation assay was performed as described above (cf. 3.4.7) using the HEK293T-β-Arr2-H_4R cells stably expressing the H_4R-ElucC and the ß-Arr2-ElucN fusion constructs (cf. 3.2). For cell culture conditions and media requirements, see 3.4.2. Dilution series of **1**-**10**, **12**-**14** and **23** were prepared in distilled water, for **11**, **17**, **18** and **24**-**29** in 10 % DMSO, giving a final concentration of 1 % DMSO in the assay mixture, and for **15**, **16** and **30** in 10 mM TFA. The cells were stimulated for 45 min with varying concentrations of the ligands. The results were normalized to the maximum effect induced by 1 mM histamine, in the corresponding solvent, (100 % value) and solvent (0 % value).

7.4.2.3. Data analysis

Data analysis was performed as described above (cf. 4.3.2.2). Statistical analysis of the variances was performed either by unpaired T test for comparing two sets of values or by one way ANOVA followed by Bonferoni`s multiple comparison test for multiple sets of values. The analysis was performed using GraphPad Prism 5 software (GraphPad Software, Inc., La Jolla, CA, USA). Quantification of the stimulus bias using the operational model was performed as described in 6.4.2.4.

7.5. References

1. Raible, D. G.; Lenahan, T.; Fayvilevich, Y.; Kosinski, R.; Schulman, E. S. Pharmacologic characterization of a novel histamine receptor on human eosinophils. *Am. J. Respir. Crit. Care Med.* **1994**, 149, 1506-1511.
2. Lovenberg, T. W.; Roland, B. L.; Wilson, S. J.; Jiang, X.; Pyati, J.; Huvar, A.; Jackson, M. R.; Erlander, M. G. Cloning and functional expression of the human histamine H3 receptor. *Mol. Pharmacol.* **1999**, 55, 1101-1107.
3. Coge, F.; Guenin, S. P.; Rique, H.; Boutin, J. A.; Galizzi, J. P. Structure and expression of the human histamine H4-receptor gene. *Biochem. Biophys. Res. Commun.* **2001**, 284, 301-309.
4. Liu, C.; Ma, X.; Jiang, X.; Wilson, S. J.; Hofstra, C. L.; Blevitt, J.; Pyati, J.; Li, X.; Chai, W.; Carruthers, N.; Lovenberg, T. W. Cloning and pharmacological characterization of a fourth histamine receptor (H(4)) expressed in bone marrow. *Mol. Pharmacol.* **2001**, 59, 420-426.
5. Morse, K. L.; Behan, J.; Laz, T. M.; West, R. E., Jr.; Greenfeder, S. A.; Anthes, J. C.; Umland, S.; Wan, Y.; Hipkin, R. W.; Gonsiorek, W.; Shin, N.; Gustafson, E. L.; Qiao, X.; Wang, S.; Hedrick, J. A.; Greene, J.; Bayne, M.; Monsma, F. J., Jr. Cloning and characterization of a novel human histamine receptor. *J. Pharmacol. Exp. Ther.* **2001**, 296, 1058-1066.
6. Nakamura, T.; Itadani, H.; Hidaka, Y.; Ohta, M.; Tanaka, K. Molecular cloning and characterization of a new human histamine receptor, HH4R. *Biochem. Biophys. Res. Commun.* **2000**, 279, 615-620.
7. Nguyen, T.; Shapiro, D. A.; George, S. R.; Setola, V.; Lee, D. K.; Cheng, R.; Rauser, L.; Lee, S. P.; Lynch, K. R.; Roth, B. L.; O'Dowd, B. F. Discovery of a novel member of the histamine receptor family. *Mol. Pharmacol.* **2001**, 59, 427-433.
8. Oda, T.; Morikawa, N.; Saito, Y.; Masuho, Y.; Matsumoto, S. Molecular cloning and characterization of a novel type of histamine receptor preferentially expressed in leukocytes. *J. Biol. Chem.* **2000**, 275, 36781-36786.
9. Zhu, Y.; Michalovich, D.; Wu, H.; Tan, K. B.; Dytko, G. M.; Mannan, I. J.; Boyce, R.; Alston, J.; Tierney, L. A.; Li, X.; Herrity, N. C.; Vawter, L.; Sarau, H. M.; Ames, R. S.; Davenport, C. M.; Hieble, J. P.; Wilson, S.; Bergsma, D. J.; Fitzgerald, L. R. Cloning, expression, and pharmacological characterization of a novel human histamine receptor. *Mol. Pharmacol.* **2001**, 59, 434-441.
10. de Esch, I. J.; Thurmond, R. L.; Jongejan, A.; Leurs, R. The histamine H4 receptor as a new therapeutic target for inflammation. *Trends Pharmacol. Sci.* **2005**, 26, 462-469.
11. Leurs, R.; Chazot, P. L.; Shenton, F. C.; Lim, H. D.; de Esch, I. J. Molecular and biochemical pharmacology of the histamine H4 receptor. *Br. J. Pharmacol.* **2009**, 157, 14-23.
12. Hofstra, C. L.; Desai, P. J.; Thurmond, R. L.; Fung-Leung, W. P. Histamine H4 receptor mediates chemotaxis and calcium mobilization of mast cells. *J. Pharmacol. Exp. Ther.* **2003**, 305, 1212-1221.
13. Beermann, S.; Seifert, R.; Neumann, D. Commercially available antibodies against human and murine histamine H(4)-receptor lack specificity. *Naunyn Schmiedebergs Arch. Pharmacol.* **2012**, 385, 125-135.
14. Feliszek, M.; Speckmann, V.; Schacht, D.; von Lehe, M.; Stark, H.; Schlicker, E. A search for functional histamine H receptors in the human, guinea pig and mouse brain. *Naunyn Schmiedebergs Arch. Pharmacol.* **2014**.
15. Seifert, R.; Strasser, A.; Schneider, E. H.; Neumann, D.; Dove, S.; Buschauer, A. Molecular and cellular analysis of human histamine receptor subtypes. *Trends Pharmacol. Sci.* **2013**, 34, 33-58.

16. Zampeli, E.; Tiligada, E. The role of histamine H4 receptor in immune and inflammatory disorders. *Br. J. Pharmacol.* **2009**, 157, 24-33.
17. Buckland, K. F.; Williams, T. J.; Conroy, D. M. Histamine induces cytoskeletal changes in human eosinophils via the H(4) receptor. *Br. J. Pharmacol.* **2003**, 140, 1117-1127.
18. Gantner, F.; Sakai, K.; Tusche, M. W.; Cruikshank, W. W.; Center, D. M.; Bacon, K. B. Histamine h(4) and h(2) receptors control histamine-induced interleukin-16 release from human CD8(+) T cells. *J. Pharmacol. Exp. Ther.* **2002**, 303, 300-307.
19. Salcedo, C.; Pontes, C.; Merlos, M. Is the H4 receptor a new drug target for allergies and asthma? *Front. Biosci.* **2013**, 5, 178-187.
20. Thurmond, R. L.; Chen, B.; Dunford, P. J.; Greenspan, A. J.; Karlsson, L.; La, D.; Ward, P.; Xu, X. L. Clinical and preclinical characterization of the histamine H(4) receptor antagonist JNJ-39758979. *J. Pharmacol. Exp. Ther.* **2014**, 349, 176-184.
21. Kollmeier, A.; Francke, K.; Chen, B.; Dunford, P. J.; Greenspan, A. J.; Xia, Y.; Xu, X. L.; Zhou, B.; Thurmond, R. L. The histamine H(4) receptor antagonist, JNJ 39758979, is effective in reducing histamine-induced pruritus in a randomized clinical study in healthy subjects. *J. Pharmacol. Exp. Ther.* **2014**, 350, 181-187.
22. Leurs, R.; Vischer, H. F.; Wijtmans, M.; de Esch, I. J. En route to new blockbuster anti-histamines: surveying the offspring of the expanding histamine receptor family. *Trends Pharmacol. Sci.* **2011**, 32, 250-257.
23. Kiss, R.; Keseru, G. M. Novel histamine H4 receptor ligands and their potential therapeutic applications: an update. *Expert Opin. Ther. Pat.* **2014**, 24, 1185-1197.
24. van Rijn, R. M.; van Marle, A.; Chazot, P. L.; Langemeijer, E.; Qin, Y.; Shenton, F. C.; Lim, H. D.; Zuiderveld, O. P.; Sansuk, K.; Dy, M.; Smit, M. J.; Tensen, C. P.; Bakker, R. A.; Leurs, R. Cloning and characterization of dominant negative splice variants of the human histamine H4 receptor. *Biochem. J.* **2008**, 414, 121-131.
25. Offermanns, S.; Simon, M. I. G alpha 15 and G alpha 16 couple a wide variety of receptors to phospholipase C. *J. Biol. Chem.* **1995**, 270, 15175-15180.
26. Rosethorne, E. M.; Charlton, S. J. Agonist-biased signaling at the histamine H4 receptor: JNJ7777120 recruits beta-arrestin without activating G proteins. *Mol. Pharmacol.* **2011**, 79, 749-757.
27. Seifert, R.; Schneider, E. H.; Dove, S.; Brunskole, I.; Neumann, D.; Strasser, A.; Buschauer, A. Paradoxical stimulatory effects of the "standard" histamine H4-receptor antagonist JNJ7777120: the H4 receptor joins the club of 7 transmembrane domain receptors exhibiting functional selectivity. *Mol. Pharmacol.* **2011**, 79, 631-638.
28. Luttrell, L. M.; Gesty-Palmer, D. Beyond desensitization: physiological relevance of arrestin-dependent signaling. *Pharmacol. Rev.* **2010**, 62, 305-330.
29. Nijmeijer, S.; Vischer, H. F.; Rosethorne, E. M.; Charlton, S. J.; Leurs, R. Analysis of multiple histamine H(4) receptor compound classes uncovers Galphai protein- and beta-arrestin2-biased ligands. *Mol. Pharmacol.* **2012**, 82, 1174-1182.
30. Igel, P.; Schneider, E.; Schnell, D.; Elz, S.; Seifert, R.; Buschauer, A. N(G)-acylated imidazolylpropylguanidines as potent histamine H4 receptor agonists: selectivity by variation of the N(G)-substituent. *J. Med. Chem.* **2009**, 52, 2623-2627.
31. Geyer, R.; Buschauer, A. Synthesis and histamine H(3) and H(4) receptor activity of conformationally restricted cyanoguanidines related to UR-PI376. *Arch. Pharm. (Weinheim).* **2011**, 344, 775-785.
32. Baumeister, P. Molecular Tools for G-Protein Coupled Receptors: Synthesis, Pharmacological Characterization and [3H]-Labeling of Subtype-selective Ligands for

Histamine H4 and NPY Y2 Receptors. University of Regensburg, 2014. http://epub.uni-regensburg.de/30505/.
33. Lim, H. D.; van Rijn, R. M.; Ling, P.; Bakker, R. A.; Thurmond, R. L.; Leurs, R. Evaluation of histamine H1-, H2-, and H3-receptor ligands at the human histamine H4 receptor: identification of 4-methylhistamine as the first potent and selective H4 receptor agonist. *J. Pharmacol. Exp. Ther.* **2005**, 314, 1310-1321.
34. Lim, H. D.; Smits, R. A.; Bakker, R. A.; van Dam, C. M.; de Esch, I. J.; Leurs, R. Discovery of S-(2-guanidylethyl)-isothiourea (VUF 8430) as a potent nonimidazole histamine H4 receptor agonist. *J. Med. Chem.* **2006**, 49, 6650-6651.
35. Cowart, M. D.; Altenbach, R. J.; Liu, H.; Hsieh, G. C.; Drizin, I.; Milicic, I.; Miller, T. R.; Witte, D. G.; Wishart, N.; Fix-Stenzel, S. R.; McPherson, M. J.; Adair, R. M.; Wetter, J. M.; Bettencourt, B. M.; Marsh, K. C.; Sullivan, J. P.; Honore, P.; Esbenshade, T. A.; Brioni, J. D. Rotationally constrained 2,4-diamino-5,6-disubstituted pyrimidines: a new class of histamine H4 receptor antagonists with improved druglikeness and in vivo efficacy in pain and inflammation models. *J. Med. Chem.* **2008**, 51, 6547-6557.
36. Liu, H.; Altenbach, R. J.; Carr, T. L.; Chandran, P.; Hsieh, G. C.; Lewis, L. G.; Manelli, A. M.; Milicic, I.; Marsh, K. C.; Miller, T. R.; Strakhova, M. I.; Vortherms, T. A.; Wakefield, B. D.; Wetter, J. M.; Witte, D. G.; Honore, P.; Esbenshade, T. A.; Brioni, J. D.; Cowart, M. D. cis-4-(Piperazin-1-yl)-5,6,7a,8,9,10,11,11a-octahydrobenzofuro[2,3-h]quinazolin-2 -amine (A-987306), a new histamine H4R antagonist that blocks pain responses against carrageenan-induced hyperalgesia. *J. Med. Chem.* **2008**, 51, 7094-7098.
37. Sander, K.; Kottke, T.; Tanrikulu, Y.; Proschak, E.; Weizel, L.; Schneider, E. H.; Seifert, R.; Schneider, G.; Stark, H. 2,4-Diaminopyrimidines as histamine H4 receptor ligands--Scaffold optimization and pharmacological characterization. *Bioorg. Med. Chem.* **2009**, 17, 7186-7196.
38. Igel, P.; Geyer, R.; Strasser, A.; Dove, S.; Seifert, R.; Buschauer, A. Synthesis and structure-activity relationships of cyanoguanidine-type and structurally related histamine H4 receptor agonists. *J. Med. Chem.* **2009**, 52, 6297-6313.
39. Geyer, R. Hetarylalkyl(aryl)cyanoguanidines as histamine H4 receptor ligands: Synthesis, chiral separation, pharmacological characterization, structure-activity and -selectivity relationships University of Regensburg, 2011. http://epub.uni-regensburg.de/22958/.
40. Savall, B. M.; Edwards, J. P.; Venable, J. D.; Buzard, D. J.; Thurmond, R.; Hack, M.; McGovern, P. Agonist/antagonist modulation in a series of 2-aryl benzimidazole H4 receptor ligands. *Bioorg. Med. Chem. Lett.* **2010**, 20, 3367-3371.
41. Nordemann, U.; Wifling, D.; Schnell, D.; Bernhardt, G.; Stark, H.; Seifert, R.; Buschauer, A. Luciferase reporter gene assay on human, murine and rat histamine H4 receptor orthologs: correlations and discrepancies between distal and proximal readouts. *PLoS One* **2013**, 8, e73961.
42. Wifling, D.; Loffel, K.; Nordemann, U.; Strasser, A.; Bernhardt, G.; Dove, S.; Seifert, R.; Buschauer, A. Molecular determinants for the high constitutive activity of the human histamine H receptor: Functional studies on orthologs and mutants. *Br. J. Pharmacol.* **2014**.
43. Kraus, A. Highly Potent, Selective Acylguanidine-Type Histamine H2 Receptor Agonists: Synthesis and Structure-Activity Relationships. University of Regensburg, 2007. http://epub.uni-regensburg.de/10699/.

Chapter 8

Summary

8. Summary

The advances in our understanding of GPCRs and the functional versatility of these signal transduction machineries require an extension of the methodology used for ligand characterization to account for alternate signaling pathways. This thesis aimed at the establishment of an arrestin recruitment assay to allow the comprehensive characterization of newly developed ligand classes with respect to alternate, arrestin mediated signaling pathways.

The optimized luciferase complementation assay proofed a fast and reliable method to investigate ligand induced arrestin recruitment to GPCRs. Through the chosen modular approach, the assay can be easily adapted to a plethora of GPCR targets. This thesis demonstrated the feasibility of an EFC based arrestin recruitment assay at five distinct receptor species, the H_1R, H_2R and H_4R from the histamine receptor family, and additionally, the NPY Y_1R and Y_2R. For all receptors, HEK293T cell lines were generated, stably expressing the receptor-ELucC and either the ELucN-βArr1 or ELucN-βArr2 fusion construct, respectively. All five receptors coupled to both arrestin isoforms, although the absolute signal intensity differed considerably for the different receptors. All cell lines produced an excellent signal-to noise ratio in the luciferase complementation assay, thus providing a suitable platform for the characterization of compound libraries to identify functional selective ligands.

Of the NPY receptor family, this thesis covered the Y_1R and Y_2R, for which a selection of subtypspecific, nonpeptidic ligands, including several structurally divers antagonists described in literature as well as a set of argininamide type antagonists were available. At the Y_1R, neither the commercially available antagonists, nor the argininamide type BIBP3226 or BIBO3304 derivatives exhibited significant efficacy regarding arrestin recruitment. Concerning arrestin and G-protein mediated pathways, none of these compounds exhibited a functional bias. Likewise, none of the selected Y_2R antagonists revealed functional selectivity towards arrestin recruitment. Therefore, these results do not support the assumption that the insurmountable antagonism previously reported for this compound class, is due to ligand specific receptor conformations.

In case of the histamine H_1R, the ligand selection comprised a set of structurally divers H_1R antagonists, amongst them several approved drugs for the treatment of allergic or psychological disorders, and additionally, several phenylhistamine and histaprodifen type agonists. While none of the antagonists exhibited functional bias, several chiral histaprodifen derivatives were identified as arrestin biased ligands. Interestingly, these compounds also discriminated between the two arrestin isoforms, with a preference for β-arrestin 2. Functional screening for selectivity at the H_2R identified a set of acyl- or carbamoylguanidine type ligands as G-protein biased agonists. Several of these compounds behaved as full agonists in the G-protein readout, whereas their efficacy was markedly lower in the arrestin recruitment assay. At the H_4R a set of 30 structurally diverse ligands was investigated. Regarding their efficacy, several of these compounds exhibited G-protein bias. On the contrary, arrestin bias was only confirmed in case of the known, functionally

selective, ligand JNJ7777120. The findings at the H_2R and H_4R were verified using a bias quantification approach based on the operational model of agonism. This method allows the integration of both efficacy and potency information derived from the concentration response data into a single bias value, thereby enabling the elucidation of structure activity relationship to guide the development of biased ligands.

With increasing insight into the physiological implications of arrestin mediated signaling, biased agonism has gained interest as a new means to fine-tune drug action towards a desired outcome. The findings in this thesis emphasize the necessity to fully characterize newly designed compounds classes with regard to their functional behavior towards alternate pathways. The established arrestin recruitment assay, in combination with various G-protein based readouts and holistic, label free assay systems, established in our research group, should allow the comprehensive exploration of the impact of putative signaling outcome.

Abbreviations

95% CI	95% confidence interval
aa	amino acid
AAP	atypical antipsychotics
AB	antibody
AC	adenylate cyclase
AC	adenylate cyclase
ARRDC	arrestin domain containing protein
βArr1	β-arrestin 1
βArr2	β-arrestin 2
BIFC	bimolecular fluorescence complementation
CAM	calmodulin
cAMP	cyclic adenosine monophosphate
CCP	clathrin coated pit
CRE	cAMP response element
CREB	cAMP response element binding protein
DAG	diacyl glycerol
DMEM	Dulbecco's Modified Eagle Medium
DMSO	dimethyl sulfoxide
DTT	dithiotreitol
ECL	extracellular loop
EFC	enzyme fragment complementation
EGTA	ethyleneglycoltetraacetic acid
ERK	extracellular signal-regulated kinase
ERK	endoplasmatic reticulum
ERK	extracellular regulated kinase
GDI	guanine nucleotide dissociation inhibitor
GEF	guanine-nucleotide exchange factor
GPCR	G-protein coupled receptor
GRK	G-protein receptor kinase
GTP	guanosine triphosphate
H_1R	histamine H_1 receptor
H_2R	histamine H_2 receptor
H_3R	histamine H_3 receptor
H_4R	histamine H_4 receptor
ICL	intracellular loop
IP_3	inositol 1,4,5-trisphosphate
MAPK	mitogen-activated protein kinases
mRNA	messenger ribonucleic acid
NaSSA	noradrenergic and specific serotonergic antidepressant
NFκB	nuclear factor κB

NO	nitric oxide
NPY	neuropeptide Y
NRI	norepinephrine reuptake inhibitor
PBS	Phosphate buffered saline
PDE	phosphodiesterase
PIP_2	phosphatidylinositol 4,5-bisphosphate
PKA	protein kinase A
PKC	protein kinase C
PKD	protein kinase D
PLC	phospholipase C
PP	pancreatic polypeptide
PTX	pertussis toxin
PYY	peptide YY
RGS	regulator of G-protein signaling
ROS	reactive oxygen species
RT	room temperature
RT-PCR	reverse transcriptase polymerase chain reaction
TM	transmembrane helix
Y_1R	neuropeptide Y receptor 1
Y_2R	neuropeptide Y receptor 2